UNDERSTANDING THE MOLECULAR MECHANISMS OF SPINAL CORD CAVITATION AFTER SPINAL CORD INJURY

by

SARINA SUREY

A thesis submitted to the University of Birmingham for the degree of DOCTOR OF PHILOSOPHY

Neurotrauma and Neurodegeneration

School of Clinical and Experimental Medicine

College of Medical and Dental Sciences

University of Birmingham

June 2014

Abstract

Spinal cord injury (SCI) is a debilitating neurodegenerative disease that affects many people worldwide. Those that are unfortunate to experience SCI also experience a reduced quality of life due to partial or complete paralysis. Whilst there is no cure to date much of the SCI research in animal models is centred on axon regeneration and preservation in an aim to cure paralysis. Whilst many animal models are used to imitate SCI, mice and rats are widely studied and experienced models. The vascular disruption, blood vessel loss and cavitation that occur at SCI epicentres in humans are known to be different in mice and rats. This study investigates acute SCI responses and documents angiogenic and inflammatory factors and matrix deposition in both species. Although cavitation was absent in mice, the lesion site in rats was 21- and 27-fold larger at 8 and 15 days post lesion (dpl), respectively, compared to intact controls. Absence of cavitation in mice correlated with increased levels of immunoreactive pro-angiogenic/wound healing factors, e.g. laminin, matrix metalloproteinase-1 (MMP-1) and vascular endothelial growth factor-A (VEGF-A) within the wound, which were 6.0-, 2.9-, and 2.8-fold, respectively, higher in mice compared to rats at 8 dpl. Increased axonal sparing was observed after dorsal column (DC) injury, detected by higher levels of PKC-γ and NF200 immunoreactivity in the DC of mice compared to rats at both T7 and T9 spinal segments. Despite similar post SCI deficits in plantar heat tests at 2 hours after injury (1.4- and 1.6-fold lower than control mice and rats, respectively), by 7 days the magnitude of these responses were comparable to sham-treated controls in both species. Microarray analysis revealed angiogenic/wound healing-related genes such as, protein kinase C eta (PRKCH), retinoic acid receptor beta (RARβ) and metallothionein 1H (MT1H) to

be differentially regulated in mice and rats after sub-acute SCI. Furthermore, inducing inflammation directly after injury using zymosan in our model demonstrated distinct inflammatory-induced angiogenic responses between mice and rats at 8 dpl that further contribute to tissue damage and micro-cavities in the CNS microenvironment of mice and rats. In conclusion the robust angiogenic/wound healing response in the mouse attenuates post-injury wound cavitation, and may protect against secondary axon damage, creating an environment more conducive to axon sprouting/regeneration. These results suggest the potential therapeutic utility of manipulating the angiogenic and inflammatory response after human SCI.

Dedication

I dedicate this thesis to my dad, Pary Kundi, without him this thesis would not have been written nor would I have continued with higher education and found my love for science.

“Just give it a go you never know you might like it”

Acknowledgments

I would firstly like to thank my two supervisors, Dr Zubair Ahmed and Professor Roy Bicknell for seeing potential in me and giving me the opportunity to undertake my PhD at University of Birmingham. Zubair has not only been an amazing supervisor throughout my time at Birmingham but he has provided me with endless support and drive to not only complete my PhD but also (without completely admitting it) enjoy doing it and make me feel passionate about my research.

I would like to acknowledge members of the Neurotrauma and Neurodegeneration group, firstly Ann Logan for the use of her lab, guidance, support and her expert knowledge with in the field. Martin Berry, a true example of someone who is still passionate about science, has provided me with endless guidance, support and expert knowledge within the field. Ana Maria Gonzalez, Debbie Gordon, Vasanthy Vigneswara, Hannah Botfield, Richard Blanch, Jenna O'Neill, Ben Mead, Lisa Hill, Pete Morgan-Warren and Carolyn Jones and anyone else who is a member of the N&N group, all of whom have provided me with training, support, feedback but more importantly reminded me that science is not all about positive results and it's ok to relax once in a while!

My amazing husband, Sandeep Surey, has provided me with much needed laughter, endless love and support (and hugs) and kept me sane (which he would disagree) during my final months of my PhD. I would also I to thank my family, Pary, Gurdip, Parminder and Aman for their endless love, support, encouragement, cake and

chocolate! It definitely made the 3 years easier. I would like to thank my in-laws Kalvinder, Amardeep, Anup and Mandeep who welcomed me with open arms into their family a year ago, for their support and endless tea! Lastly, I would like to thank my two besties; Harpreet and Madhvi, you have provided me with laughter and endless experiences that has strengthened our friendship.

Table of Contents

List of Figures

List of Tables

Table of abbreviations

Abbreviation	Full name
AAV	Adeno-associated vector
ALS	Amyotrophic lateral sclerosis
AML	Acute myeloid leukaemia
ANG	Angiopoietins
ANG-1	Angiopoietin 1
ANG-2	Angiopoietin 2
ANOVA	Analysis of variance
ANXA3	Annexin A3
ARNT	Aryl hydrocarbon nuclear translocator
ASC	Adipose derived stem cells
ASIA	American Spinal Injury Association
α2B-AR	Alpha-2adrenergic receptor beta
BBB	Basso, Beattie and Bresnahan locomotor score
BBB	Blood brain barrier
BMSC	Bone marrow mesenchymal stem cells
BSCB	Blood spinal cord barrier
C	Cervical
CA10	Carbonic anhydrase 10
CBS	Corticobasal syndrome
CD13	Cluster of differentiation 13
CD31	Cluster of differentiation 31
CD4	Cluster of differentiation 4
CD43	Cluster of differentiation 43
CD45	Cluster of differentiation 45
CD47	Cluster of differentiation 47
CD8	Cluster of differentiation 8
CD68 (ED1)	Cluster of differentiation 68
CD11b	Cluster of differentiation 11b
CD95L	CD95 ligand
CNS	Central Nervous System
Co	Coccygeal
Col-1	Collagen-1
CoMTB	Conditioned medium from *myobacterium tuberculosis* monocytes
cRNA	Complementary ribonucleic acid
CSF	Cerebral spinal fluid
CSF-1	Cytokine colony stimulating factor-1
CSPG	Chondroitin sulphate proteoglycans
CST	Corticospinal tract
Cy3	Cyanine 3
Cy5	Cyanine 5
DAP1	4', 6-diamino-2-phenylindole
DC	Dorsal column
DF	Dorsal funiculus
DNA	Deoxyribonucleic acid

Dpl	Days post lesion
DRG	Dorsal root ganglion
DRGN	Dorsal root ganglion neurone
DVT	Deep vein thrombosis
EAA	Excitatory amino acid
EAE	Experimental autoimmune encephalomyelitis
ECL	Enhanced chemiluminescence
ECM	Extracellular Matrix
EDTA	Ethylenediaminetetraacetic acid
EGFR	Epidermal growth factor receptor
EGTA	Ethylene glycol tetra acetic acid
FDR	False discovery rate
FGF	Fibroblast growth factor
FGF2	Fibroblast growth factor 2
FGFR	Fibroblast growth factor receptor
FGR	Fetal growth restriction
GBM	Glioblastoma multiforme
GFAP	Glial fibrillary acidic protein
GLA	Glial limitans accessoria
GLE	Glial limitans externa
GM	Grey matter
GP1bα	Glycoprotein 1bα
HAND	HIV-associated neurological disorder
HCL	Hydrochloride
HCV-MC	Hepatitis C virus infection-associated mixed cryoglobulinemia
HDAC	Histone deactylase
HDACi	Histone deactylase inhibitors
HGF	Hepatocyte growth factor
HIF	Hypoxia inducible factor
HIF-1α	Hypoxia inducible factor 1 alpha
HIF-1β	Hypoxia inducible factor 1 beta
HLX1	H2.0-like homeobox 1
HRE	Hypoxia response element
HRP	Horseradish peroxidase
HSPG	Heparin sulphate proteoglycans
HUVEC	Human umbilical endothelial cells
H+E	Haematoxylin and Eosin
IR plantar heat	Infra-Red plantar heat test
IPA analysis	Ingenuity pathway analysis
ITGβ2	Integrin beta2
L	Lumbar
LAD1	Leukocyte adhesion deficiency type 1
LCS	Lumbar spinal canal stenosis
LIMA	Linear models for microarray data
LN	Laminin
LRP2	megalin
MAG	Myelin associate glycoprotein
MAP	Molecule activity predictor

MAPC	Multipotent adult progenitor cells
MAPK	Mitogen-activated protein kinase
miRNA	Micro ribonucleic acid
mRNA	Messenger ribonucleic acid
MMPs	Matrix metalloproteinase
MMP-1	Matrix metalloproteinase-1
MMP-2	Matrix metalloproteinase-2
MMP-9	Matrix metalloproteinase-9
MP	Methylprednisolone
MRI	Magnetic resonance imaging
mRNA	Messenger ribonucleic acid
MS	Multiple sclerosis
MSA	Multiple system atrophy
MT	Metallothionein
MT1	Metallothionein 1
MT1F	Metallothionein 1F
MT1G	Metallothionein 1G
MT1H	Metallothionein 1H
MT1M	Metallothionein 1M
MT1X	Metallothionein 1X
MT2	Metallothionein 2
MT2A	Metallothionein 2A
MT3	Metallothionein 3
MT4	Metallothionein 4
Multiscribe RT	Multiscribe reverse transcriptase
NaCl	Sodium chloride
NF-$_k$B	Nuclear factor kappa beta
NF200	Neurofilament 200
NGF	Nerve growth factor
NG2	NG2 chondroitin sulphate proteoglycan
NPC	Neural progenitor cell
NP1	Neuropilin-1
NP2	Neuropilin-2
NP-40	Nonyl phenoxypolyethoxylethanol
Nrf2	Nuclear factor erythroid 2-related factor 2
NS	Nervous System
NSPC	Neural stem progenitor cells
NSCISC	National Spinal Cord Injury Statistical Center
NT-3	Neurotrophin-3
OECs	Olfactory ensheathing cells
OMgp	Oligodendrocyte-derived myelin glycoprotein
OPC	Oligodendrocyte progenitor cells
PAN	Polyarteritis nodosa
PBS	Phosphate buffered saline
PD	Parkinson’s disease
PDGF	Platelet-derived growth factor
PDGF-AA	Platelet-derived growth factor-AA
PDGF-BB	Platelet-derived growth factor-BB

PDGF-CC	Platelet-derived growth factor-CC
PDGF-DD	Platelet-derived growth factor-DD
PGDFRα	Platelet-derived growth factor receptor alpha
PDGFRβ	Platelet-derived growth factor receptor beta
rPDGF-BB	Recombinant platelet-derived growth factor beta
PECAM1	Platelet endothelial cell adhesion molecule 1
PFA	Paraformaldehyde
PGF	Placental growth factor
PI3K	Phosphoinositide 3-kinse
PKB	Protein kinase B
PKC	Protein kinase C
PKC-γ	Protein kinase C gamma
PNS	Peripheral Nervous System
PRKCH	Protein kinase C eta
PRP	PDGF responsive neural precursors
PSP	Progressive supranuclear palsy
pVHL	Von Hippel-Lindau protein
PVDF	Immunobilon-P polyvinylidene fluoride
q-PCR	Real time quantitative polymerase chain reaction
RARβ	Retinoic acid receptor beta
RARβ1	Retinoic acid receptor beta 1
RARβ2	Retinoic acid receptor beta 2
RARβ3	Retinoic acid receptor beta 3
RARβ4	Retinoic acid receptor beta 4
RECA-1	Rat endothelial cell antigen
RGC	Retinal ganglion cells
RIN	RNA integrity number
RNA	Ribonucleic acid
ROS	Reactive oxygen species
RT	Room temperature
RT buffer	Reverse transcriptase buffer
rt-PCR	Real time polymerase chain reaction
S	Sacral
SAM	Statistical analysis of microarray
SCI	Spinal Cord Injury
SDS-PAGE	Sodium dodecyl sulphate polyacrylamide gel electrophoresis
SEM	Standard error of the mean
Sema 3a	Semaphorin 3A
siRNA	Small interfering ribonucleic acid
SM171	Endothelial barrier antigen
Smad-2	Mothers against decapentaplegic homolog-2
Smad-4	Mothers against decapentaplegic homolog-4
SNP	Single nucleotide polymorphisms
T	Thoracic
T8	Thoracic 8
TB	Tuberculosis
TBST	Tris buffered saline with Tween 20
TGFβ	Transforming growth factor beta

TGFβ-1	Transforming growth factor beta-1
TGFβ-2	Transforming growth factor beta-2
TGFβ-3	Transforming growth factor beta-3
TGFβR1	Transforming growth factor beta receptor 1
Tie-1	Tyrosine kinase immunoglobulin-like and EGF-like domains 1
Tie-2	Tyrosine kinase immunoglobulin-like and EGF-like domains 2
TIMP	Tissue inhibitor of matrix metalloproteinases
TIMP-1	Tissue inhibitor of matrix metalloproteinases-1
TIMP-2	Tissue inhibitor of matrix metalloproteinases-2
TIMP-3	Tissue inhibitor of matrix metalloproteinases-3
TMP-4	Tissue inhibitor of matrix metalloproteinases-4
TNF-α	Tumor necrosis factor alpha
VEGF	Vascular endothelial growth factor
VEGF-A	Vascular endothelial growth factor-A
VEGF-R	Vascular endothelial growth factor-receptor
vWF	Von Willebrand Factor
UK	United Kingdom
USA	United States of America
WM	White matter
ZFP	Zinc finger protein
3DCM-ASCs	Three-dimensional cell mass of adipose derived stem cells

CHAPTER 1

INTRODUCTION

Sections of the introduction are published in the following reviews:

Kundi S., Bicknell R., Ahmed Z. (2013). The role of angiogenic and wound-healing factors after spinal cord injury in mammals. Neuroscience Research. 76, 1-9.

Kundi S., Bicknell R., Ahmed Z. (2013). Spinal cord injury: Current mammalian models. American Journal of Neuroscience. 4 (1), 1-12.

1.1 Overview of SCI

To date spinal cord injury (SCI) is defined as 'damage or trauma to the spinal cord that results in a loss or impaired function causing reduced mobility or feeling' (Apparelyzed.com). SCI can be sub-divided into two main categories; complete and incomplete injury (Figure 1.1). According to the ASIA neurological classification complete SCI refers to 'no preservation of motor and/or sensory function that exists more than three segments below the level of injury', whereas incomplete SCI refers to 'some preservation of motor and/or sensory function existing more than three segments below the level of the injury' (American Association of Spinal Cord Injury, 2004).

Although advances have been made through research, there are currently no fully restorative therapy for SCI and therefore, safety measures especially in the sports industry have been put in place to reduce the risk of developing new cases (Thuret et al., 2006). SCI can lead to devastating long term effects and Methylprednisolone; the only treatment for acute human SCI, helps to reduce inflammation and pain for the individual (Akhtar et al., 2008, Turner et al., 2001, Balazy, 1992). The life expectancy of an individual diagnosed with SCI can be significantly reduced, impacting on their quality of life which results in income loss if

the severity of the condition worsens (Hagg and Oudega, 2006, Krassioukov et al., 2003, Rintala et al., 1998, Cairns et al., 1996, Segatore, 1994). This further impact's on the economic burden along with the high costs associated with primary care of the individual (Talac et al., 2004, Nakae et al., 2011).

After SCI, pathological changes at the lesion site ultimately play a part in nerve conduction loss and prolonged demyelination. These changes include increased inflammation, disruption of blood-spinal cord barrier (BSCB) and extensive haemorrhage, along with an increase in necrosis, apoptosis, cavitation and ischemia (James et al., 2011, Byrnes et al., 2010, Benton et al., 2009, Benton et al., 2008, Carmeliet, 2005, Whetstone et al., 2003, Sroga et al., 2003, Segal et al., 1997). An upregulation of all these factors results in detrimental effects on axon regeneration after injury.

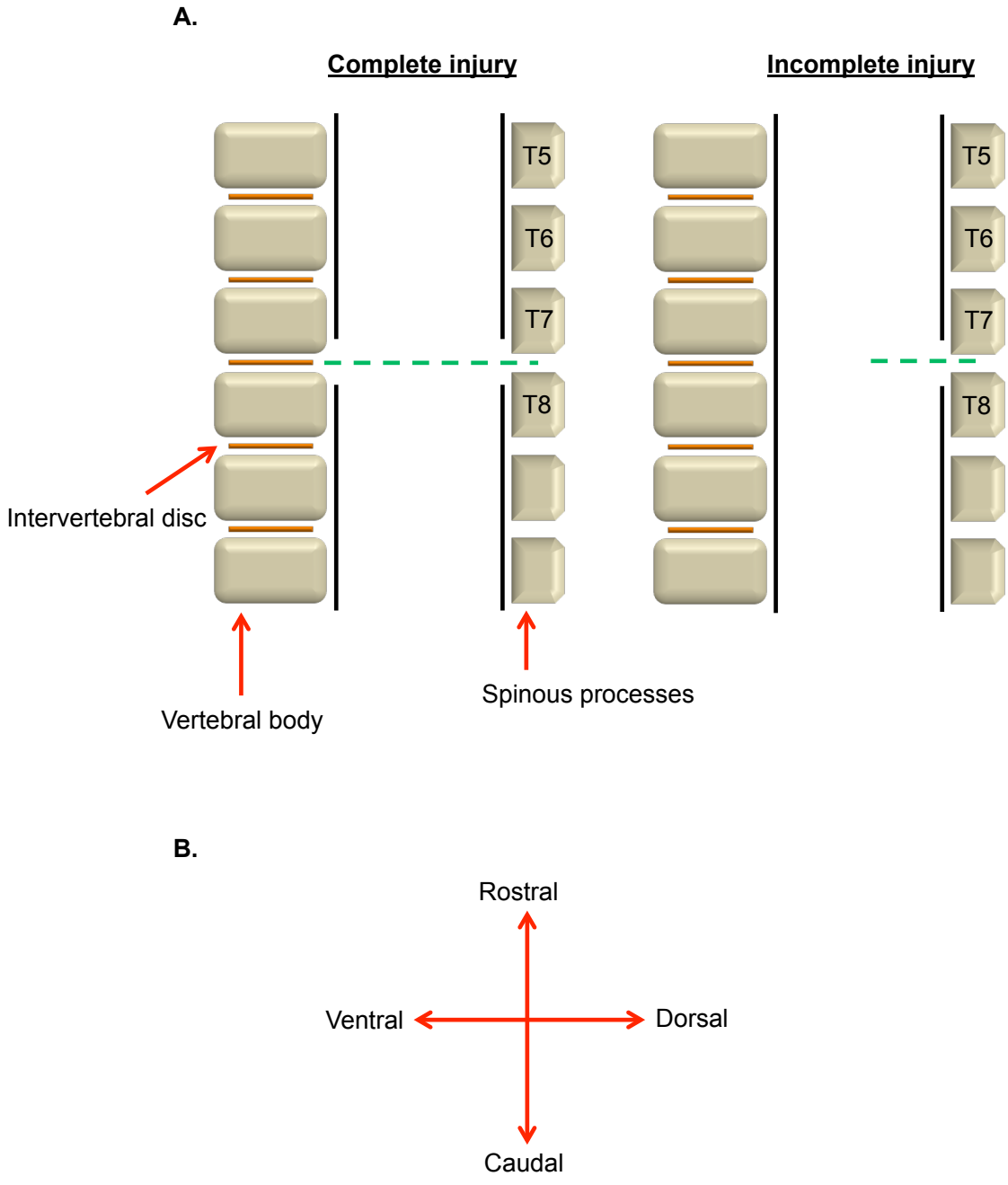

Figure 1.1 A diagrammatic illustration demonstrating complete vs. incomplete SCI. Complete injury transects the whole of the spinal cord resulting in complete loss of sensory and/or motor function **(A)**. Whilst incomplete injury only transects part of the spinal cord resulting in reduced sensory and/or motor function. The orientation of the spinal cord **(B)**.

1.2 Prevalence and demographics of SCI

The prevalence and incidence of SCI is increasing over recent years as a result of car accidents, sports injuries and trips and falls, particularly in developing countries due to the large amounts of manual labour (Singh et al., 2003). In the US, it is estimated that 273,000 people are living with SCI and 12,000 new cases occur annually with road accidents being the major cause accounting for 46% (Bernhard et al., 2005, Burke et al., 2001, NSCISC, 2013, Sekhon and Fehlings, 2001). 80% of spinal cord injured patients are also reported to be male which could be a consequence of sport related injures (Beers and Porter, 2006, Bernhard et al., 2005, Jackson et al., 2004, NSCISC, 2013, Sekhon and Fehlings, 2001, Strauss et al., 2006). Most new cases occur in the younger generation with an estimated 50%-70% of those aged between 15-35 years (Bernhard et al., 2005). The estimated racial and ethnic distribution of SCI patients reported is 77% Caucasian, 25% African American, 8% Hispanic and 2% other (NSCISC, 2013). However, in UK and Ireland there are approximately 1,000 new cases each year with road accidents being the major contributor (Spinal Research, 2011).

SCI affects more than 2.5 million people worldwide and 130,000 new cases are reported each year (International Campaign for Cures of Spinal Cord Injury Paralysis). Recent reports have shown that the global incidence rate in 2007 was 179,312 cases per annum/ 23 cases per million extracted from regional data (Lee et al., 2014). Whilst a systemic review reported that global incidence varies between 8-246 cases per million and the global prevalence is 236-1,298 cases per million (Furlan et al., 2013). These results show the huge variation in incidence and prevalence and one of the key factors that could affect the reported cases of SCI is

the unreported cases. This in particular is seen in developing countries where lifting large heavy loads results in injures to the back (Singh et al., 2003).

1.3 Complex systems in the human body

The human body is a complex organism functioning under numerous intricate systems enabling us to perform simple gestures such as thinking, moving and talking. Amongst some of the major systems like the cardiovascular and respiratory systems, the nervous system acts as a central control system for the entire body regulating voluntary and involuntary actions. Information received from a stimulus, such as; pain, taste or smell, is processed to bring about a response through other organ systems. The nervous system is further subdivided into two categories that include the central nervous system (CNS) and peripheral nervous system (PNS). The current research under taken concentrates on the CNS and in particular the spinal cord and the effects on the microvasculature after injury in an aim to translate research efforts for clinical outcomes.

1.4 Spinal cord anatomy

The spinal cord is a major component of the CNS, playing an essential role in relaying information between the brain and the body. The spinal cord is surrounded by cerebral spinal fluid (CSF), encased within a vertebral column and, like the brain, is encapsulated by three CNS membranes known as the meninges; pia mater, arachnoid and dura mater. The dura mater is the tough outer sheath and directly beneath it is the arachnoid and then the pia mater is the innermost layer that adheres to the surface of the spinal cord (Nogradi and Vrbova, 2000). The human spinal cord

is made up of 31 segments that are subdivided into 5 groups; cervical, thoracic, lumbar, sacral and coccygeal. There are 8 cervical (C) segments, 12 thoracic (T), 5 lumbar (L), 5 sacral (S) and 1 coccygeal (Co). The spinal cord consists of three main components; white matter (WM), grey matter (GM) and a small central canal filled with CSF that runs along the entire length (Figure 1.2). However, it is important to note that the ratio between the WM and GM varies depending on the level of the spinal cord. The WM that surrounds the GM mainly contains myelinated and unmyelinated nerve fibres, and is divided into three sectional areas known as the dorsal (posterior), lateral and ventral (anterior) columns, that contain both ascending and descending axon fibre tracts (Figure 1.2). Whilst, the GM, characteristically shaped like a 'butterfly', contains mainly cell bodies of neurones and glia.

There are entry and exit sites at each level of the spinal cord that harbour the spinal nerves; sensory and motor nerve roots, which are named in accordance to the site of their emergence. C1-8 spinal nerves contribute largely to motor control in the head, neck and upper extremities. Whilst T9-T20 provides control for the abdominal musculature and the lumbar and sacral segments of the spinal cord provide control to the lower extremities. The ascending tracts relay sensory information via the dorsal root ganglion (DRG) from the sensory receptors to the brain, whilst the descending tract carries information via the ventral root from the brain to the target organ, muscle or cell.

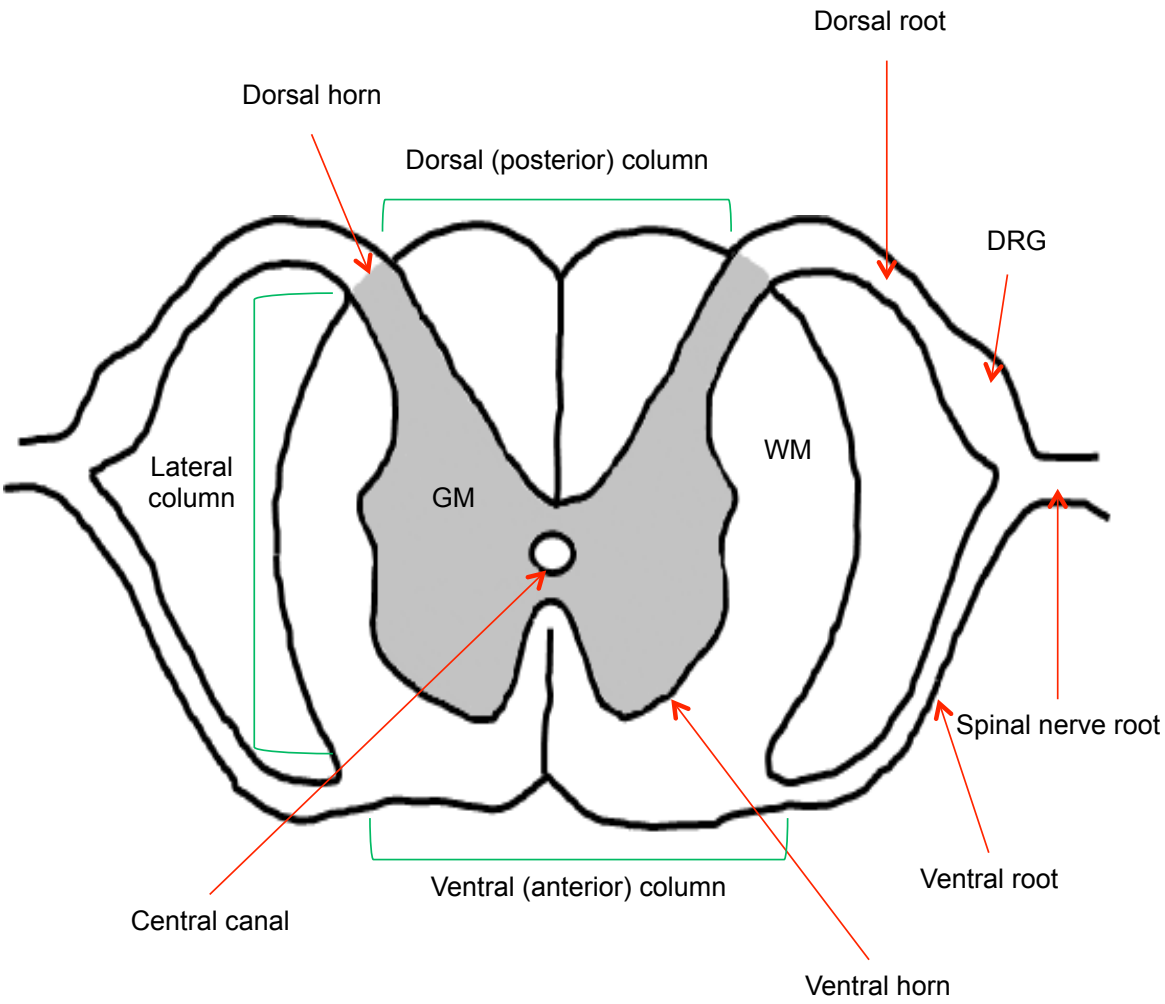

Figure 1.2 A diagrammatic illustration of the components of the spinal cord (Adapted from Mautes et al., 2000). The white matter (WM) largely surrounds the grey matter (GM) with a small central canal containing the cerebral spinal fluid (CSF). The spinal cord is divided into three main areas; dorsal, lateral and ventral, in which the anatomical structures are named after to understand the orientation (DRG = dorsal root ganglion).

1.5 Vascular supply to the uninjured spinal cord

The blood supply to the spinal cord arises from extrinsic and intrinsic arterial supply, and in the thoracic region the extrinsic blood supply arises from the intercostal artery that enters via the intervertebral foramen. The spinal artery then divides into three branches; the anterior and posterior spinal canal arteries and the radicular arteries (Crock and Yoshizawa, 1977) (Figure 1.3). The radicular artery further divides into the anterior radicular artery and the posterior radicular artery that penetrates the dura mater and joins three major arteries on the surface of the spinal cord; right and left posterolateral longitudinal spinal arteries and the anterior median longitudinal spinal artery (Dommisse, 1975). Among these arteries is a branching network of small arteries called the arterial vasocorona. The vasocorona and central arteries, originating from the anterior median longitudinal spinal artery, make up the intrinsic arterial blood supply to the spinal cord (Figure 1.4). The vasocorona connects the anterior and posterior spinal arteries on the surface of the spinal cord allowing an uninterrupted blood supply to the entire length through the pia mater. Both systems are characterised by different blood flow directions in an aim to supply the whole length of the spinal cord. But regions arise that may not receive a direct blood supply referred to as the ‘watershed zone’ that are dependent on the overlapping vascular fields and thus may be prone to vulnerability (Mautes et al., 2000). In the thoracic region the blood is largely supplied by the anterior radicular artery and in a CNS injury model occlusion to the artery results in ischemia (Zivin and DeGirolami, 1980).

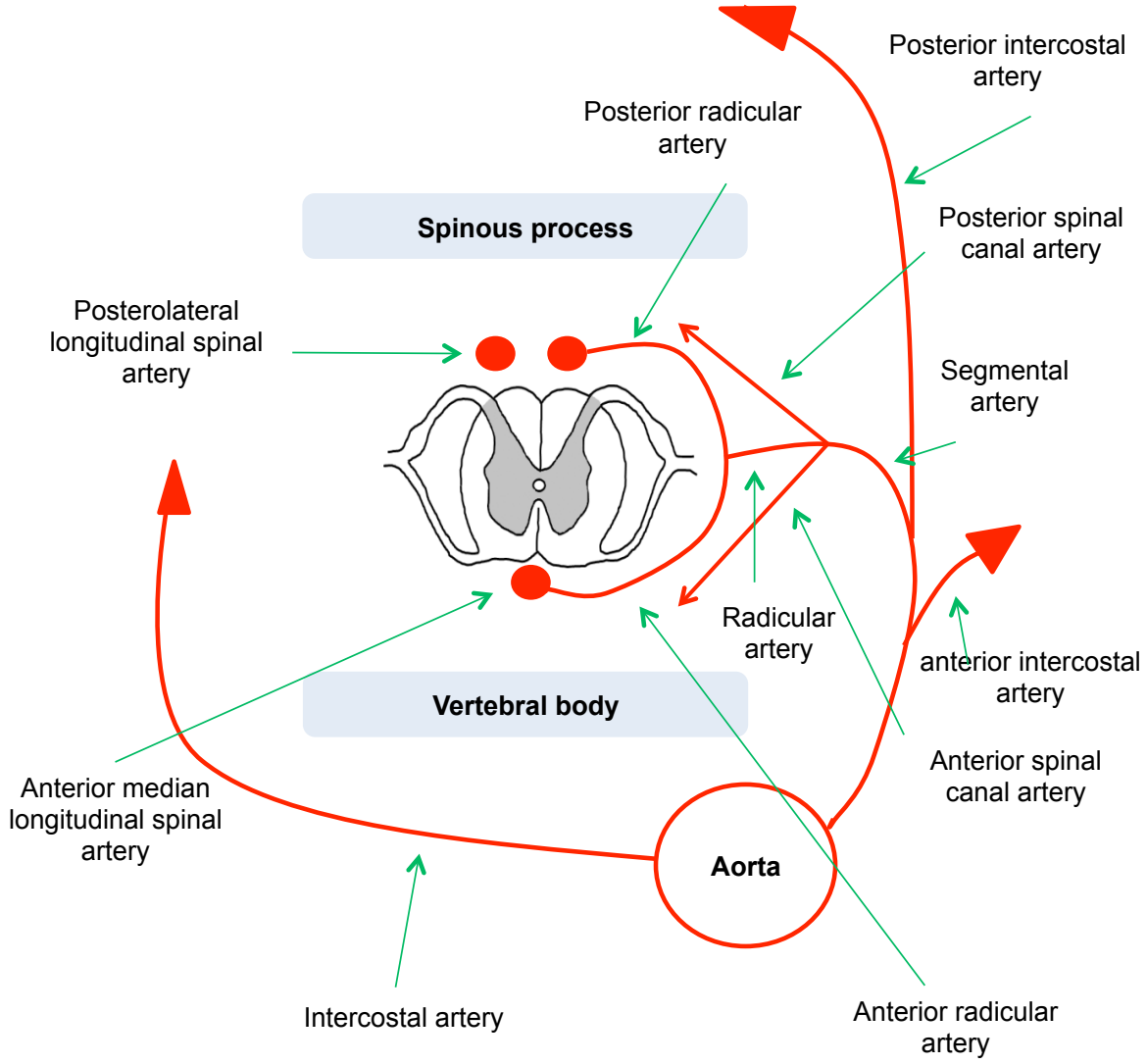

Figure 1.3 A diagrammatic illustration of the extrinsic blood supply to the spinal cord to the thoracic region (Adapted from Mautes et al., 2000). The incoming intercostal artery divides into three branches: the radicular artery and the anterior and posterior spinal canal arteries, which aid in the extrinsic blood supply. The radicular artery travels along the nerve root to further divide into the anterior and posterior radicular arteries.

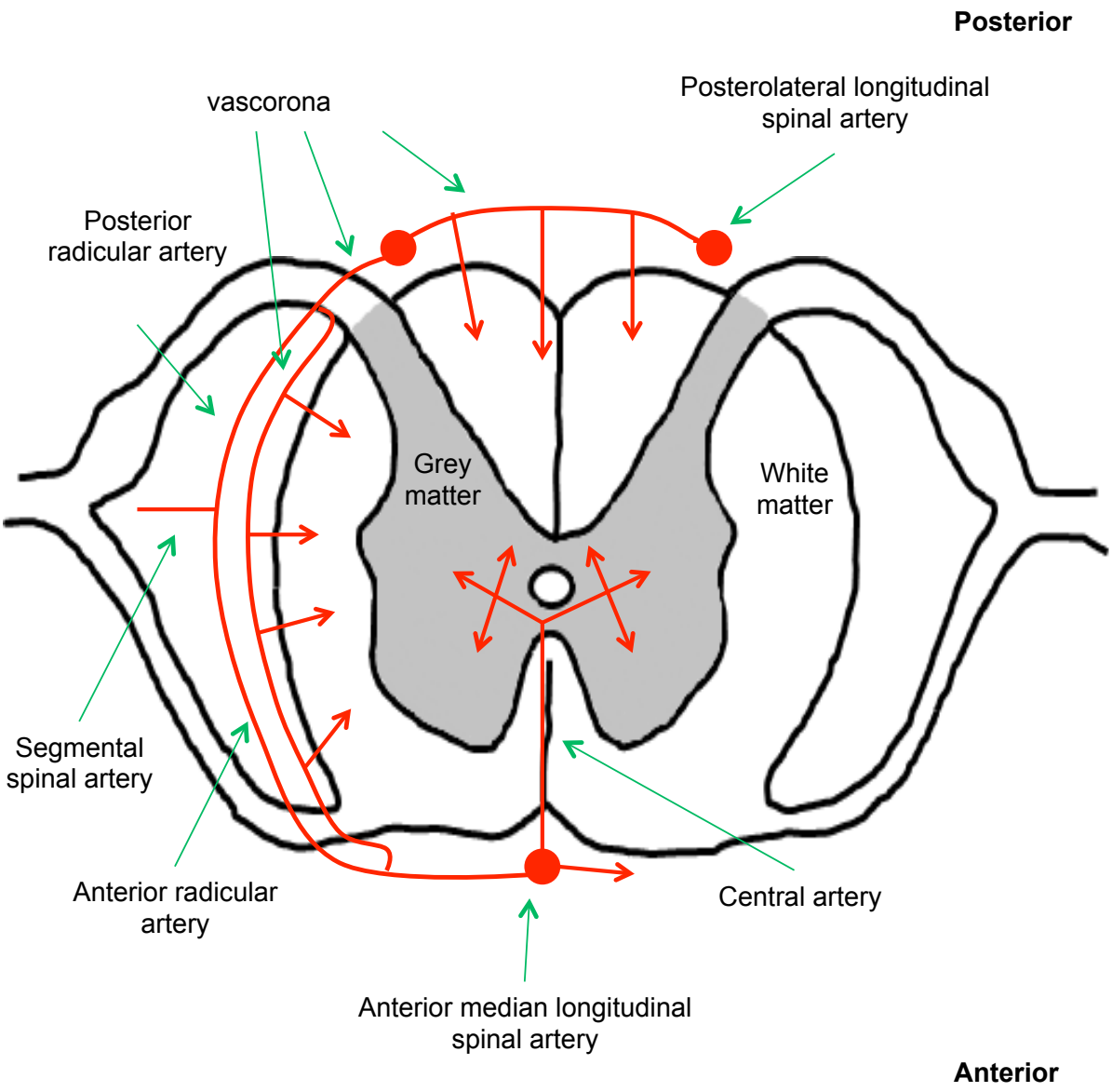

Figure 1.4 A diagrammatic illustration of the intrinsic blood supply to the spinal cord (Adapted from Mautes et al., 2000). The central artery and the vasocorona are the main intrinsic systems that supply the blood to the spinal cord. Note the different blood flow directions within the cord itself.

1.5.1 Vascular supply after SCI

After SCI it is known that the primary injury results in the deleterious secondary consequences, such as haemorrhage, as a result to injured blood vessels in the spinal cord coinciding with cavity development (Noble and Wrathall, 1989a, Noble and Wrathall, 1989b). Blood can be toxic to the CNS due to the disruption of blood vessels form the primary injury playing a role in the secondary pathogenesis of SCI (Mautes et al., 2000). In the spinal cord the blood flow is not unidirectional and therefore can reverse in some of the vessels known as 'partial blood flow theory', where ascending and descending blood flow currents exist in the radicular arteries resulting in the multidirectional flow (Adamkiewicz, 1882, Thron, 1988). This multidirectional flow may serve as protection to the spinal cord after injury when local blood vessels are damaged and incapable of supporting the surrounding tissue (Mautes et al., 2000).

After SCI the highly vascularised central GM undergoes immediate vasospasm of the superficial vessels and haemorrhage (Ducker and Assenmacher, 1969). These superficial vessels are subject to shear stress and stretching and thus impairing microcirculation and perfusion that results in reduced spinal cord blood supply and the impairment of autoregulatory systems (Young et al., 1981, Senter and Venes, 1978, Dohrmann et al., 1972). The extent of haemorrhage is directly proportional to the severity of the injury (Noble and Wrathall, 1989a, Noble and Wrathall, 1989b, Noble and Wrathall, 1985). This haemorrhage is dominant at the site of injury in both the WM and GM, extending to distant sites in the rostral and caudal segments of the cord away from the injury epicentre. Haemorrhage can further exacerbate the damage in the CNS contributing to cavity development and

cell damage (Bullock and Fujisawa, 1992, Noble and Wrathall, 1989a, Noble and Wrathall, 1989b).

1.5.2 Cellular responses to SCI

One phenomenon that has received attention after SCI is cavitation (Figure 1.5). Cavities are fluid-filled cysts that form around the injury site after SCI and occur as a result of lysosomal spinal cord autotomy (Kao et al., 1977). Experimentally, spinal cord cavitation occurs after intraspinal injection of quiscolic acid; a known excitatory amino acid (EAA) agonist that causes cell death (Bhatoe, 2009). Inflammation is also a key regulator in activating a cascade of events that leads to secondary damage, progressive cavitation and glial scarring in the CNS (Singh et al., 2012, Fitch et al., 1999). Cavitation can also occur in regions of chronic ischemia of vascular origin (Sherk et al., 1984).

SCI is a two-step process marked by distinct changes during the primary and secondary injury phases. 'Primary injury refers to damage sustained by the neural elements at the time of trauma through shear forces to axons or blood vessels and results in irreversible injury (Cadotte and Fehlings, 2011). The secondary injury phase refers to the body's response to the primary injury and involves a host of cellular processes that occur immediately after injury and persists for months to years' (Cadotte and Fehlings, 2011). The primary injury produces the cyst, which is a characteristic cumulative effect that brings about the secondary injury causing the progression of the initial lesion. Initiation of the secondary injury is brought about when the injured site becomes infiltrated with immune cells, such as, monocytes and macrophages. This occurs within the first few hours after the initial injury and over the

next few days or weeks the lesion site becomes enlarged causing the formation of a glial scar lining the cavity (Fitch et al., 1999) (Figure 1.5 and 1.6). The cyst contains extracellular connective tissue matrix (ECM) proteins such as collagen type 1, 2 and 3, laminin, fibronectin and chondroitin sulphate proteoglycans (CSPGs) that become fluid-filled (Sroga et al., 2003). These cysts are located in and around the lesion epicentre, preventing re-growth of damaged axons. Demyelination is the loss of oligodendrocytes, the myelin forming cells of the CNS (Guest et al., 2005). Prolonged demyelination of the spared axons can lead to degeneration resulting in the loss of nerve conduction in the spinal cord. In an attempt to remyelinate axons, cells that produce oligodendrocytes (oligodendrocyte progenitor cells (OPC)) which are located in the spinal cord migrate towards the site of demyelination.

After SCI, astrocytes become reactive, up-regulating the expression of glial fibrillary acidic protein (GFAP) which increases the flow of ions and neurotransmitters from neurons to the extracellular fluid (Faulkner et al., 2004). The astrocytes divide and fill the vacant spaces with glial scar tissue, where the axons of pre-injury neurons are occupied; this is where regenerating axons would be located prior to the injury, thus resulting in regenerative failure (Thuret et al., 2006). Glial scarring is the bodies' mechanism to protect and begin the healing process in the CNS.

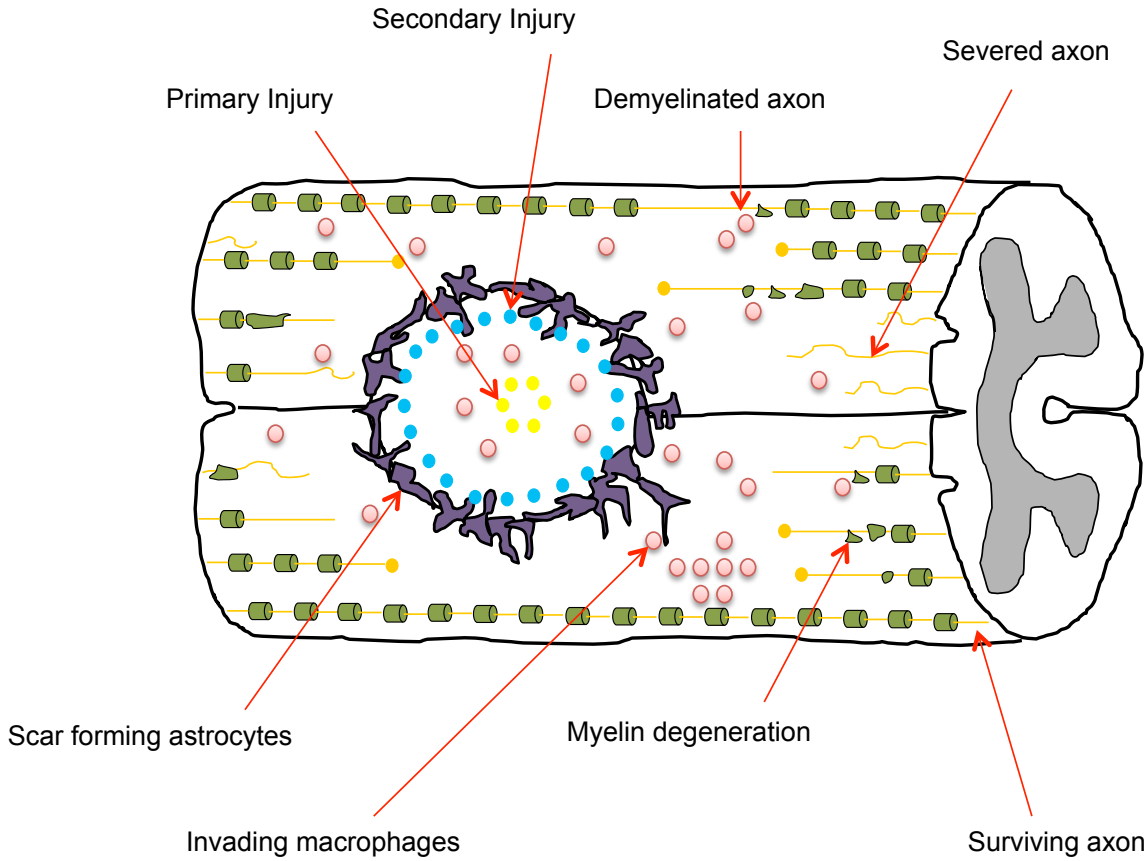

Figure 1.5 A diagrammatic representation of the formation of fluid-filled cysts after SCI. (Adapted from Springer Images). The primary injury is the initial lesion sustained to the cord causing an influx of immune cells and macrophages into the lesion site. It is the constant influx of these invading immune cells that leads to the formation of fluid-filled cysts or cavities, which bring about the secondary injury, causing the up-regulation of reactive astrocytes that divide and fill the vacant spaces with glial scar tissue lining the cavity. The glial scar then acts as an inhibitory factor leading to myelin degradation, and nerve conduction loss.

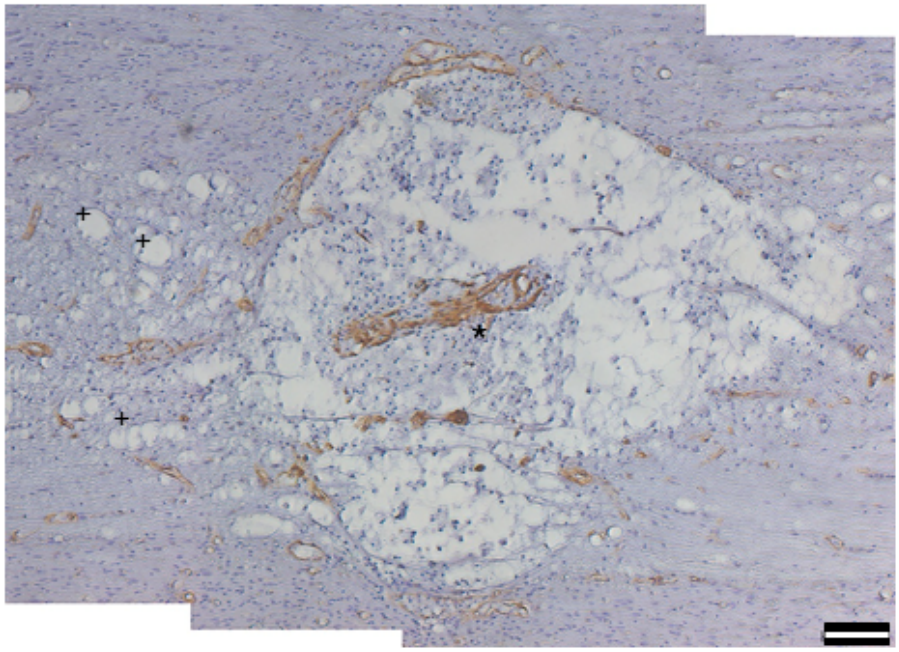

Figure 1.6 Longitudinal section from a T8 dorsal column crush injured rat demonstrating laminin immunostaining at 8 days post lesion (dpl) (counterstained with Haematoxylin) and the extent of the cavitation at the lesion site. A large cavity is observed at the epicentre of the lesion (*) while smaller cavities are observed in adjacent areas (+). These cavities lead to destruction of axon and eventual loss of function. Scale bar = 100μm.

Although the glial scar has a beneficial effect such as stimulating neovascularisation of blood capillaries to increase the support of the nervous tissue, it can also have a detrimental effect on the CNS such as preventing neuronal re-growth by acting like a physical barrier. Following demyelination there is also an increase in apoptosis, necrosis and secretion of inhibitory molecules such as ephrins, semaphorins, oligodendrocyte-derived myelin glycoprotein (OMgp), Nogo and myelin associate glycoprotein (MAG) that inhibit axon regeneration (Vourc'h and Andres, 2004, Hamill et al., 2005). Therefore, suppressing or arresting the development of secondary

damage will provide a more conducive environment for the growth of regenerating axons through the SCI sites (Kundi et al., 2013).

After SCI, the lesioned area contains cavities that are subdivided into two categories; Type I and II cavities. These are classified on the basis of their cellular and ECM content and lining (Lagord et al., 2002). Type I cavities contain ECM proteins including laminin and collagen and are in continuity with the subarachnoid space, whereas Type II cavities contain mainly inflammatory cells with no ECM proteins and no continuity with the subarachnoid space (Fitch et al., 1999). Typically mice develop small Type I cavities after SCI whereas in the rat, Type II cavities predominate.

The condition present in humans that results in cavitation after SCI is known as post-traumatic Syringomyelia, affecting approximately 40,000 people in the UK (The Back-up Trust.org.uk). This condition can cause progressive pain, headaches and loss of upper extremity function, which can be life-threatening and potentially disastrous complication of SCI if the syrinx extends rostrally into the brain stem and interferes with the nerve impulses (Edgar and Quail, 1994, Biyani and el Masry, 1994). Symptoms do not develop at a specific time but can manifest soon after injury or later in life. Due to the availability of MRI for diagnosis and follow-up, Syringomyelia is increasingly being recognised as an important cause of delayed neurological deterioration after SCI. Management of the condition involves drainage of the syrinx with a thecal shunt and correction of deformity allowing relief from the sensory symptoms (Lam et al., 2008).

1.5.3 Angiogenesis and cavitation

Angiogenesis is a multistep process requiring the interaction of the ECM and its component cells that is primarily triggered by tissue hypoxia after injury (Chung et al., 2010). After an angiogenic stimulus, endothelial cells adopt a proteolytic phenotype losing their contact with the vascular basement membrane and causing the basement membrane to be degraded by matrix metalloproteinases (MMPs) (Hughes, 2008, Haas, 2005). The pro-angiogenic factor, vascular endothelial growth factor (VEGF)-A, stimulates the outgrowth of endothelial tip-cells and proliferation of stalk cells allowing new vessels to sprout at the basement membrane along with pericyte detachment (Gerhardt et al., 2003, Ruhrberg et al., 2002). When endothelial cells and the basement membrane re-establish contact, tissue inhibitors of metalloproteinases (TIMP)-2 switch off the proteolytic phenotype of endothelial cells allowing cell migration and proliferation to occur in response to activated pro-angiogenic proteins such as VEGF, basic fibroblast growth factor (FGF2) and MMPs (Saunders et al., 2006). As vessels mature, endothelial cells align, aided by platelet-derived growth factor (PDGF), MMPs, and angiopoietins recruiting pericytes. Pericyte/endothelial cell/vascular smooth muscle cell association is essential for the maturation of endothelial tubes into blood vessels (Chung et al., 2010).

In humans, inhibited angiogenesis occurs after suppressing VEGF and its receptor: VEGF-R whilst VEGF-R alone has shown to induce cavitation in lung and non-small-cell lung tumours (Johnson et al., 2004, Marom et al., 2008, Crabb et al., 2009). Cavitation in the rat SCI lesion site is associated with vascular regression and endothelial cell loss at the lesion epicentre that causes ischemia, haemorrhage and blood spinal cord barrier (BSCB) disruption (Loy et al., 2002, Casella et al., 2006).

Such vascular dysfunction after SCI is an important contributor to the ensuing neurological deficits (Fassbender et al., 2011).

1.6 Current mammalian models of SCI

Animal models have been developed with the aim of recreating features of either complete or incomplete SCI allowing understanding of the anatomical and biological consequences of SCI to be investigated. Animal models have several obvious advantages over their human counterpart: for example, the specified tissue needed can be used and processed for histological purposes to investigate co-localisation of proteins of interest, mRNA analysis (microarray) to give expression levels of genes, and protein analysis (western blotting) to give levels of protein. Rat models are most widely used to study SCI since they are inexpensive, have few surgical infections, are easy to care for and can be studied in large numbers but increasingly mouse models have also been implemented in SCI research (Talac et al., 2004). Larger mammals such as dogs and cats are also used but less established models in SCI research, requiring expensive after care and housing as well as stringent ethical considerations (Kundi et al., 2013).

Currently there are range of models that are used by researchers (Table 1.1) that include contusion, compression and transection-based models amongst others. The limitation of these different animal models is that they can never truly express the clinical characteristics of the human condition (Davoody et al., 2011), but the real question is ‘have animal models contributed to actual therapies?’. The only actual therapy for the treatment of acute SCI in humans is Methylprednisolone (MP), and even though it has shown a significant benefit in animal models the benefits on

human SCI remain unproven and is not considered a regulatory treatment for SCI (Akhtar et al., 2008, Hugenholtz, 2003, Hurlbert, 2000, Blight, 2000, Hall, 1992, Hall and Braughler, 1982). This review aims to establish the current animal models that are used to study SCI and the advantages and disadvantages of the techniques and therefore the potential outcomes in relation to the human condition.

Model	Description	Advantages/Disadvantages	
Contusion	• Induced with an impactor i.e. weight-drop from a specified height (Allen, 1911), thoracic contusion is most commonly used (Jakeman et al., 2000, Behrmann et al., 1993)	• Impact from contusion can be difficult to assess pain behaviour due to variation of distance	• Dogs, rats and mice
Clip Compression	• Induced with clips calibrated to exert a force of 50/35g- 50g=severe response and 35g=moderate response • The clip is closed over the entire cord for 1 minute (Bruce et al., 2002)	• Allows for precise control of injury • Does not resemble injury seen in humans	• Rats only
Balloon Compression	• Uses different volumes of balloon inflation and different durations of expression to create contusion (Lim et al., 2007)	• Controlled environment • Non-invasive method of creating SCI	• Dogs and monkeys
Computer Controlled Contusion	• Uses an animal trap that delivers a set weight to the exposed spinal cord; the computer monitors the impact (Stokes and Jakeman, 2002)	• Reproducible, controlled environment • But equipment is expensive	• Mice only
Spinal Cord Displacement	• Attempts to regulate trauma impact by controlling displacement length of the	• Controlled displacement and monitoring of biochemical	• Mice and rats

	spinal cord (Nakae et al., 2011)	parameters at the time of impact helps reduce outcome variability- controlled environment	
Transection	• Complete spinal transection, performed using spring scissors (Nakae et al., 2011, Kang et al., 2011)	• Widely used to asses regeneration (Talac et al., 2004) but it's clinically irrelevant (Poon et al., 2007)	• Rats only
Photochemical	• The use of a dye induces the photochemical reaction by activating an argon laser to produce single oxygen molecules on the endothelial surface of spinal cord vessels (Watson et al., 1986)	• Reliable and reproducible • Does not induce mechanical trauma to the cord • Extent of injury is difficult to control	• Rat and mouse
Excitotoxic	• Intraspinal/intrathecally injection of excitotoxins e.g. quiscolic acid (Bhatoe, 2009)	• Long-lasting spontaneous pain, thermal hyperalgesia and mechanical allodynia (Fairbanks et al., 2000, Yezierski et al., 1998) • Has ability to correlate specific areas of tissue damage	• Rats only

Spinothalamic Tract Lesions	• Lesions core pain pathway; spinothalamic tract area using tungsten microelectrode (Nakae et al., 2011, Zeilig et al., 2011)	• Resembles allodynia and hyperalgesia • Provides useful and novel insights into the underlying biological mechanisms of SCI	• Rats only
Canal Stenosis	• Is entrapment of the cauda equine and/or lumber nerve roots by hypertrophy of osseous and soft tissue structures surrounding the lumber spinal cord that reduces blood flow (Sekido et al., 2012)	• This model helps clarify pathophysiology of chronic, light pressure to the spinal cord (Sekiguchi et al., 2004)	• Rats only

Table 1.1 Summary of the current SCI animal models that are used in research to mimic the clinical human SCI. These animal models are used to assess pain, behaviour, histology and genetic alterations following SCI, but more importantly to assess neural and molecular outcomes. These models are more frequently developed on rat and mice and less frequently on larger animals such as cats and dogs.

1.6.1 Contusion Models

The vast majority of human SCI are caused as a result of motor vehicle accidents, falls and sporting injuries involving a sudden compression of the spinal cord. This results in vertebral damage that allows the bone or vertebral disc to encroach on the spinal canal space. Other instances include laceration of the spinal cord, bullet wounds and slow compression injuries that can result from tumour growth. The contusion model is the most widely used animal model that relies on an impactor device, such as weight-drop from a specified height. The impact of the weight can vary depending on the distance moved by the weight. The first tightly controlled contusion model of SCI was described by Allen (1911), in which a specified weight could be dropped from a defined height, delivering a defined amount of energy to the exposed spinal cord in canine. This caused injury to the spinal cord as a result of compression and displacement and was used to study the effects of myelotomy on the outcome of SCI (Allen, 1911). Later, a modification to this model was introduced in the form of the New York University Impactor developed in rats (Gruner, 1992). More recently the Ohio State University Spinal Cord Research Centre has produced a weight-drop device controlled by a computer to closely control a particular level of spinal cord compression in mice and rats (Stokes et al., 1992, Behrmann et al., 1993, Jakeman et al., 2000). A variety of slow rapid compression models have been used but it is the extent of the cord displacement that determines the severity of the injury. However, the clinical relevance of such contusion models has not been established.

Nonetheless, the contusion model has been used in a variety of studies that include: (1), the use of CM101, a polysaccharide derived from group B streptococcus

which inhibited inflammatory angiogenesis, protecting axons from Wallerian degeneration and improving functional outcome in mice (Wamil et al., 1998, Nanney et al., 2001) (2), suppression of CD47, an inhibitor of angiogenesis improved functional outcomes in knockout mice (Myers et al., 2011a, Myers et al., 2011b) (3), the use of human CNS stem cells grown as neurospheres that were isolated from brain tissue and were implanted after a moderate contusion injury improving locomotor recovery in mice (Hooshmand et al., 2009); and (4), transplantation of bone marrow mesenchymal stem cells (BMSCs) also increased motor function in rats by upregulation of VEGF expression and induced angiogenesis (Yu et al., 2011).

However, this initial model has been modified to use other devices that bring about compression to injure the cord; such as clip compression, balloon compression, computer controlled contusion and spinal cord displacement. These are all examples that bring about incomplete SCI.

1.6.1.1 Clip Compression

The clip compression model in some ways resembles the contusion model as the injury is caused by pressure to the cord. The injury is induced using clips calibrated to exert a specific force. A force of 50g is normally used to produce an outcome that would have a severe response and a force of 35g is used to produce an outcome that would have a moderate response. The clip is then closed over the cord for 1 minute allowing precise control over the pressure exerted and the time that the pressure is used for, but this model does not truly mimic the injury seen in humans (Bruce et al., 2002). Despite this the model is reproducible in rats at the thoracic level (Poon et al., 2007).

The clip compression model has also been applied to the cervical region of the cord in rats to evaluate the efficacy of antagonising the Fas receptor using a soluble Fas receptor post-injury (Fehlings and Robins-Steele, 2012). This study showed behavioural recovery along with enhanced cell survival, tissue sparing and integrity of descending fibre tracts when soluble Fas was administrated via an intrathecal catheter either 8 or 24 hours post-injury. Clip compression has also been applied to the cord at the thoracic level in rats to test if neutralization of nerve growth factor (NGF) with a fusion protein to Trk-A blocked the development of autonomic dysreflexia, a life-threatening condition caused by aberrant primary afferent sprouting in the dorsal horn that is NGF-dependent (Marsh et al., 2002). The model has also been used to carry out kinematic studies to assess locomotor recovery following spinal cord clip compression in adult rats, suggesting that kinematic parameters (e.g. daily training on a treadmill over a six week period) should be taken into account when looking at new strategies to improve locomotor function after SCI (Alluin et al., 2011).

1.6.1.2 Balloon Compression

The Balloon Compression model was first described by Tarlov in 1953 and has been modified since then. The method uses different volumes and durations of balloon inflation to induce injuries at varying severities, allowing for a controlled environment (Lim et al., 2007). In an initial description of the balloon compression model, an embelectomy catheter was inserted into the epidural space through a hemilaminectomy hole at the vertebral arches and balloons were then inflated with varying amounts of contrast agents, causing direct compression to the spinal cord

(Lim et al., 2007). This method was further adapted and improved such that hemilaminectomy was not required, but that balloons were inserted through the lumbosacral space into the epidural space, where balloons were then inflated (Lee et al., 2008). A variety of different species from canine to monkeys have been assessed through this model to gain a controlled compression model of SCI (Guizar-Sahagun et al., 2011).

1.6.1.3 Computer controlled contusion

A computer controlled contusion model consists of an animal trap that reproducibly delivers a defined weight to the exposed spinal cord, with a computer monitoring the dynamics of the impact (Stokes et al., 1992, Stokes and Jakeman, 2002). The device allows the researcher to take control of the degree of the injury produced and demonstrates that a well-controlled contusion injury can be observed in mice (Jakeman et al., 2000). This is because it reduces the variability of the experiment and allows monitoring of biochemical parameters as well as assessments of behavioural and histological outcomes following contusion injury (Ma et al., 2001).

1.6.1.4 Spinal cord displacement

Spinal cord displacement allows the cord to be exposed to a single rapid and calibrated displacement at the site of a laminectomy. The injury is initiated at the tip of a vertical shaft driven by an electromagnetic shaker. Transducers are arranged in series with the shaft recording the patterns of displacement and force during the impact in mice (Jakeman et al., 2000). The results demonstrate that the electromagnetic device can be used to produce a well-controlled contusion injury.

The model attempts to regulate trauma impact by controlling displacement length of the spinal cord and therefore helps to reduce outcome variability (Nakae et al., 2011).

Sensory testing after SCI in rats has been carried out, and it is thought that SCI injury impairs sensory systems causing allodynia, showing that early detection of this provoked pain pathway can identify mechanisms that are responsible for its development (Detloff et al., 2010). Hypothermia improves mobility in rodents and experiments have reported the preservation of neurons immediately after injury and a faster rate of recovery occurs after cervical displacement when hyperthermia is implemented (Lo et al., 2009).

1.6.2 Transection Models

The transection model is referred to as a complete spinal transection which is performed using spring scissors following laminectomy, producing a laceration to the cord. This model may reflect complete SCI in patients but this type of injury is rarely seen in the clinic (Nakae et al., 2011, Poon et al., 2007, Talac et al., 2004). However, partial transection (hemisection) is also modelled and has become popular for studies in the mechanisms of pain. Transection models are also increasingly used to model the effects of scaffolds and biomaterials on axon regeneration after injury. For example, a polymer scaffold with rat bone marrow stem cells has been used to promote plasticity and limited regeneration in spinal cords after injury (Kang et al., 2011). Combinatorial therapies have also been used where neurotrophic factors have been combined with biomaterials after complete transection of the spinal cord in rats (Fan et al., 2011). Enhancing axonal regrowth appears to be a promising therapeutic approach to repair the injured spinal cord. To allow for regeneration, sterile gel foams

have been placed between the two ends of transected cords with variable degree of success (Nakae et al., 2011). Particularly, after complete transection sterile gel foams were implanted with neurotrophic factors administered exogenously via a minipump. Results demonstrated that host axons are able to grow into the transplant. Furthermore, there was an increase in motor function recovery and regeneration from supraspinal pathways (Coumans et al., 2001).

Neurotrophic factors have also been used in studies by García-Alías *et al* (2011) after a lateral hemisection to the spinal cord, combining NT-3 with Chondroitinase ABC treatment as it restores plasticity in the adult CNS. They found that these animals displayed inter-limb coordination and improved body stability. Furthermore, neural stem/progenitor cells (NSPCs) have been used to deliver soluble Nogo66 receptor protein (blocks the inhibitory effects of myelin-based inhibitors) and growth factors to rat spinal cord following complete transection (Guo et al., 2012). Results show an increase in survival of transplanted NSPCs while soluble Nogo66 enhanced axonal regeneration, although no effect on functional recovery was observed, since a small number of descending corticospinal tract axons grew into the central portions of the bridges. Nogo-66 has been discussed previously by Wei *et al* (2010) following hemisection in rats to show the effects of using hyaluronic acid hydrogels modified with Nogo66 receptor antibodies in supporting angiogenesis and inhibiting the glial scar at the lesion site (Wei et al., 2010). Despite the fact that transection is rarely seen in the clinic patients with this type of injury would be considered for clinical trial. But this is very much dependant on the type of trial instigated. However, these models have served useful purposes in allowing the use of biomaterials, stem cells and neural progenitor cells to show that some of these

therapies, when used in combination can restore some degree of function through mainly plasticity-related changes to the spinal circuits.

1.6.3 Photochemical Models

This method was first developed by Watson *et al* (1986), which showed a photochemical-based rat model of SCI, and is now widely used to study neurotrauma (Gaviria et al., 2002, Watson et al., 1986). To bring about the injury, a dye is used to induce the photochemical reaction by activating an argon laser to produce single oxygen molecules on the endothelial surface of spinal cord vessels. This causes intense platelet responses, vessel occlusion and damage to parenchymal tissues (Hao et al., 1991). The model is reliable and reproducible and does not require mechanical trauma and therefore there is no need for a laminectomy since the injury is caused purely by ischemia. Once the injury has been induced, behavioural studies can be performed.

The model reproduces the phenomenon of secondary lesions such as; cavitation that is seen after SCI. Using this model, motor recovery after photochemical SCI, induced before or after intrathecal injection of bupivacaine (an anaesthetic drug belonging to an amino amide group that blocks sodium channels and therefore prevents the influx of sodium and thus depolarisation) resulted in improved motor recovery in rats (Lopez et al., 2004). The model has also been successfully adapted in the mouse showing that it is reproducible and reliable (Piao et al., 2009, Gaviria et al., 2002). Different exposures to a cold light source correlated with the extent and severity of the injury, while histopathological analysis showed cavity formation in the ischemic environment. How these models relate to the human

condition needs further investigation but these studies can model some of the features of the secondary injury phase and thus may be beneficial.

1.6.4 Excitotoxic Models

An excitotoxic model is induced via intraspinal/intrathecal injection of excitotoxins such as, quiscolic acid. The use of excitotoxins produces long-lasting spontaneous pain, thermal hyperalgesia and mechanical allodynia but also produce cavity formation, neuronal loss and astrocytic scaring (glial scar tissue which correlates with the general environment observed after SCI). The advantage of this model is that it has the ability to correlate specific areas of tissue damage with behavioural changes (Nakae et al., 2011). Animals that are exposed to SCI using this method do exhibit pain that is much greater than any other model due to the excitotoxic injury inducing spontaneous and/or evoked pain behaviours that are associated with chronic neuropathic pain (Yezierski et al., 1998). Yezierski *et al* injected AMPA-metabatrophic receptor agonist quiscolic acid to stimulate injury, resembling ischemic events and cavitation observed after SCI, characteristic of the clinical condition known as post-traumatic Syringomyelia. Intraspinal injection of quiscolic acid has also been used to induce excitotoxic SCI in rats demonstrating pathological changes that correlate with clinical SCI; such as, neuronal loss, haemorrhage and cavitation (Bhatoe, 2009, Berens et al., 2005, Schwartz et al., 1999). Although the excitotoxic model is a non-traumatic model it displays the characteristic pathological differences that would be seen after clip compression and contusion models that are more commonly used. Therefore, the model is useful in investigating excitotoxic-mediated changes after SCI.

1.6.5 Spinothalamic Tract Model

This model restricts injury to the spinothalamic tract, which is the main pain pathway in animals, using tungsten microelectrodes (Nakae et al., 2011). The model provides useful and novel insights into the underlying biological mechanisms of SCI, resembling some features of SCI in humans including hyperalgesia and allodynia in rodent models (Wang and Thompson, 2008). The model is particularly useful in studying pain behaviour, as it works with the central pain pathway, although it has been claimed that the loss of spinothalamic functions in patients with neuropathic pain does not appear to be a predictor for central pain in SCI, but is a contributor (Finnerup et al., 2007).

Zeilig (2011) showed that the hyperexcitabilty of neurones may be due to damage to the spinothalamic tract where the central pain pathway causes a build-up in response (Zeilig et al., 2011). Spinothalamic tract neurones show an increased expression of metabotropic glutamate receptor subtype 1, which parallels the development of hyperalgesia and allodynia, both of which contribute to central pain after injury (Mills and Hulsebosch, 2002).

1.6.6 Canal Stenosis

Canal stenosis is described as the entrapment and narrowing of the cauda equine and/or lumbar nerve roots by hypertrophy of osseous and soft tissue structures surrounding the lumbar spinal cord, causing ischemia at the site of injury (Nakae et al., 2011). The model therefore causes demyelination and subsequent axonal degeneration. Canal stenosis helps to clarify pathophysiology of chronic, light pressure on the spinal cord (Ito et al., 2007, Sekiguchi et al., 2004). Only recently an

animal model has been developed know as, rat lumbar spinal canal stenosis (LCS) model which can be used to study mainly bladder function after injury (Sekido et al., 2012). Trauma contributes to the primary injury sustained but age can play a major factor in narrowing of the spinal canal (Akuthota et al., 2003). Injury to the nerve does not always occur in this model but factors such as degeneration of neurones, ischemia and inflammation around the site of injury play major contributions to the injury of the nerve. It remains to be seen how useful this model will be in understanding some of the pathological changes that occur after SCI.

1.6.7 Limitations of SCI models

As previously discussed, each model presents various limitations with the major holdback being that animal models never truly capitulates the injury seen in humans for a variety of reasons. For example, it may be difficult to assess pain using a contusion model, as sometimes pain behaviour is not always apparent if the weight is released on the specified area from a short distance. The contusion model is also performed mainly in the thoracic region, as cervical contusion can be life-threatening due to respiratory and cardiovascular functions being compromised at the level of injury (Nakae et al., 2011, Yisheng et al., 2007). For example, upper cervical SCI can disrupt the transmission of respiratory signals from the brain stem to the phrenic motor neurones (transmit signals to the diaphragm) therefore causing paralysis (Zimmer et al., 2007). Using computer controlled contusion as a method to obtaining reproducible and reliable SCI is an expensive method due to the sophisticated equipment that is required. The method also produces lesions that are difficult to distinguish between spared and regenerating axons, especially if the focus of the

study is axon regeneration (Talac et al., 2004). Although complete transection models are widely used to asses regeneration with the help of biomaterials and scaffolds, it does produce a large scar at the epicentre and therefore represents a severe model and so animals require intensive post-operative care (Talac et al., 2004, De Winter et al., 2002). However, transection models are difficult to standardise if several segments of the cord are removed (Blight, 2000). In addition this model is rarely seen in humans and therefore has no clinical relevance except to evaluate implantation devices and axon regeneration (Talac et al., 2004). Hemisection models however, do not completely cut the corticospinal tract due to the injury being incomplete. It is also difficult to control the extent of injury if SCI is induced through the photochemical method since large areas may be affected by the ischemic environment created as a result of this model.

The anatomical location of injury between experimental animal models and clinical human SCI differ greatly. As discussed above, experimental SCI is potentially dangerous at the cervical level as it may lead to life threatening complications to the animal. SCI at the thoracic level is more commonly used in experimental models, however humans commonly present with SCI at the cervical region and therefore the site of injury can greatly affect the pathology and the severity of the injury presented in a clinical setting (Akhtar et al., 2008).

Two other factors play a crucial role in experimental SCI not mimicking the clinical injury presented by humans; laminectomy and anaesthesia. If laminectomy is performed on a patient, it not only increases the local trauma but can cause spinal instability. This can also occur in animal models of SCI as surrounding muscle, bone and ligaments are removed during induction of injury. Removal of specific

components at the region of injury can have a major impact and alter the physiological responses to injury. In some ways, laminectomy free methods such as, balloon compression models may mimic the human condition more accurately.

Anaesthesia on the other hand, affects the CNS pathology and recovery following injury, either directly or indirectly (Akhtar et al., 2008). It can affect blood pressure, respiratory rate and metabolism as each individual can react differently under different concentrations of the same anaesthetic. As stated above motor recovery following photochemical SCI being induced before or after intrathecal injection of bupivacaine shows that anaesthesia can affect recovery and functional outcomes after SCI (Lopez et al., 2004).

Functional outcomes and behavioural assessments between clinical models and experimental models of SCI also vary. It is very easy for human's to communicate pain and symptoms that the injury presents but very difficult to do so with animal models. Therefore, specific tests and analysis methods are carried out post-injury to correlate the injury with their behavioural patterns and specific biomarkers. The behavioural patterns often correlate with the severity of the injury produced and is a measurement that is quite reasonable to carry out in a clinical environment but for animal models it is quite limited and indirect (Blight, 2000). The main way that functional outcomes are assessed in animals is by using the BBB score, which is a locomotor activity evaluation, originally developed at the Ohio State University (Basso et al., 1995, Basso et al., 1996). The BBB score evaluates the movements of the hind limb of an animal after injury to express recovery. Although this analysis is reliable and reproducible, researchers have tested it through the severity of the condition, where the BBB score is reproducible in animals with mild

severity but as the condition becomes more serve, reproducibility is reduced (Filho and Molina, 2007). While the BBB score only assess hind limb function, it does not take into account pain, bladder and bowel function which are other symptoms that require coordinated spinal cord activity (Akhtar et al., 2008). Other ways of evaluating locomotor recovery are also commonly used, such as grid-walking, which tests the animal's ability to deal with challenging limb control problems (Blight, 2000). In patients, sensory assessment can be performed by testing whether they can distinguish between a sharp or dull edge of a pin but this cannot accurately be reproduced in animals and researchers solely attempt to assess sensory function based on the loss of motor functions (Akhtar et al., 2008).

However, it is important to note that whilst spinal cord cavitation is extensively documented in the rat, there is evidence that demonstrates that other mammals including rabbits, cats and hamsters do exhibit this detrimental pathology after SCI (Vink et., 1989; Anghelescu et al., 1995; Shimada et al., 1995; Shamir et al., 1997; Inman et al., 2003).

1.7 Hypothesis

Previous research has demonstrated that mice and rats display differential inflammatory, cavity and scarring responses to SCI and it has been further suggested that mice may have a robust wound healing response that demonstrates the cavity free lesioned area after injury. This led to the hypothesis that after SCI there is an increase in angiogenic/wound healing-related factors that aid in the adequate balance of vascularisation, wound healing and scar deposition in mice that ultimately

prevents cavitation, spares axons and results in better functional recovery compared to rats.

1.8 Overall research aims

- Determine cavity lesion responses over time after T8 dorsal column (DC) between mice and rats.
- Analyse the localisation and expression levels of angiogenic/wound healing-related proteins in mice and rat spinal cord sections after SCI using immunohistochemistry and western blot and subsequent densitometry.
- To determine functional recovery in correlation with cavity and angiogenic responses between the two species after SCI using Infar-Red (IR) plantar heat test and Von Frey hair filament test.
- To analyse known genome wide angiogenic/wound healing-related genes between mice and rats after SCI by microarray analysis.
- To assess the inflammatory responses between the two species in correlation to cavity and angiogenic responses observed after SCI.

CHAPTER 2

MATERIALS AND METHODS

2.1 Animal surgery

All surgical procedures were licensed by the UK Home Office and approved by the University of Birmingham Ethical Review Committee. Female Sprague Dawley rats and C57BL6 mice (Charles River, Margate, UK) were the strains used, weighing between 180-250g and 20-25g, respectively, in all experiments. T8 dorsal column (DC) crush was performed according to the established methods described by us previously (Ahmed et al., 2010; Lagord et al., 2002). Animals were anaesthetised using 5% isoflurane with 1.8l/mg of oxygen, and given a subcutaneous injection of the analgesic Temgesic (Buprenorphine); 0.2ml and 0.05ml, respectively, prior to surgery. After a partial laminectomy and identifying the midline of the spinal cord, DC were crushed bilaterally at the level of T8 (Figure 2.1 A and B) using a calibrated watchmaker's forceps inserted through the DC meninges to a depth and width of 0.5mm x 0.5mm in mice and a depth and width of 1mm x 1mm in rats. These dimensions were determined using a spinal cord atlas of T8 in both mice and rats from the Christopher and Dana Reeve Foundation Text and Atlas (Figure 2.2 A and B). Animals were allowed to recover and tissues (defined areas – see relevant section) were harvested at specific time points for various tissue processing and analyses (outlined below).

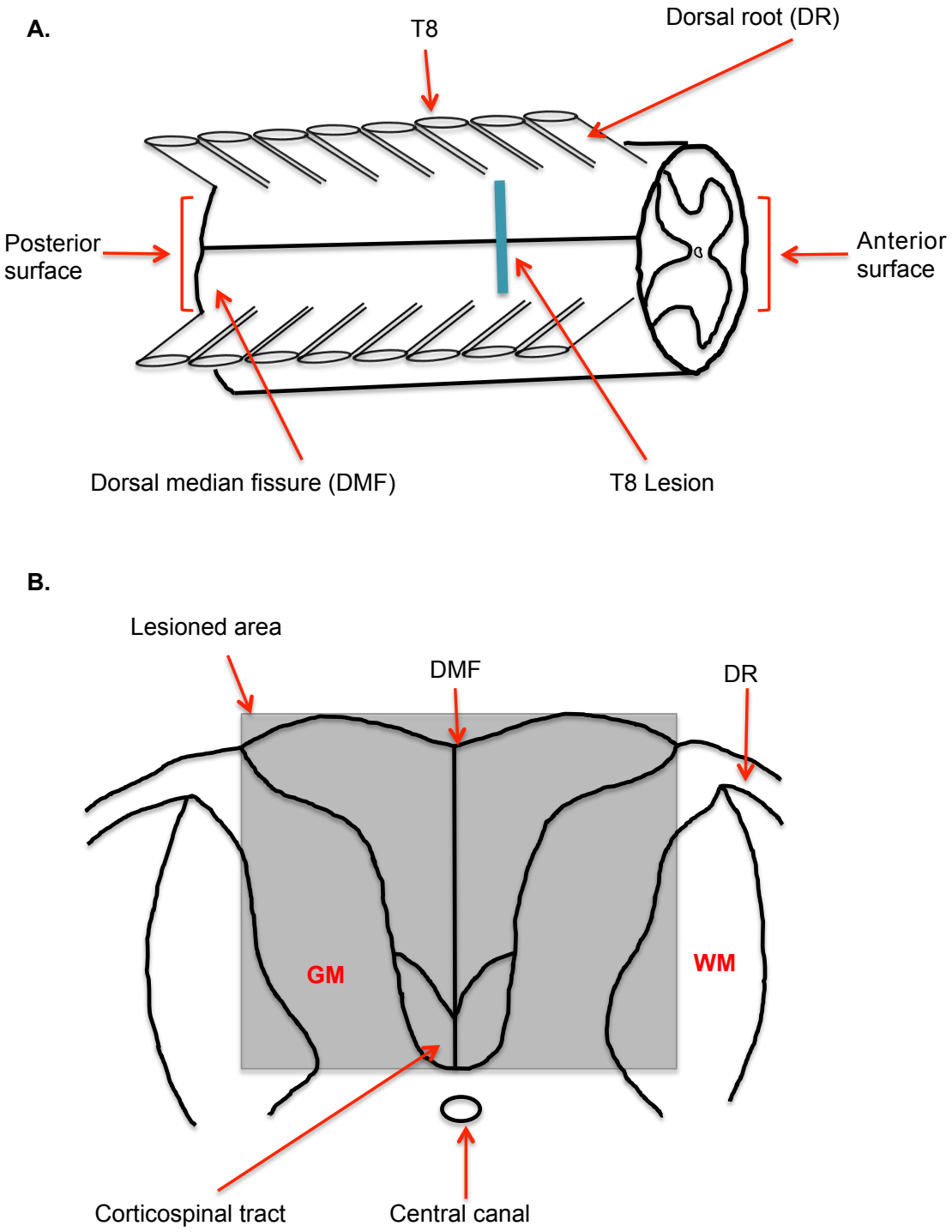

Figure 2.1 Diagrammatic illustration of the spinal cord demonstrating bilateral thoracic 8 (T8) dorsal column (DC) crush lesion (**A**). A cross section of the spinal cord highlighting the area of disruption through the corticospinal tract, the grey matter (GM) and the white matter (WM) (**B**).

A

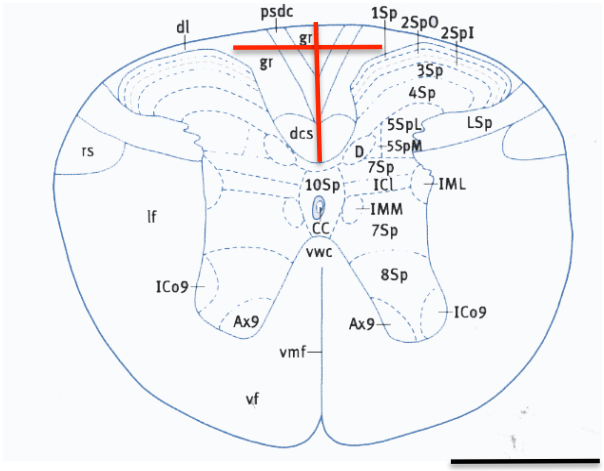

Width and depth measured of the dorsal funiculi = 2.6cm = 0.5mm based on the scale bar.

B

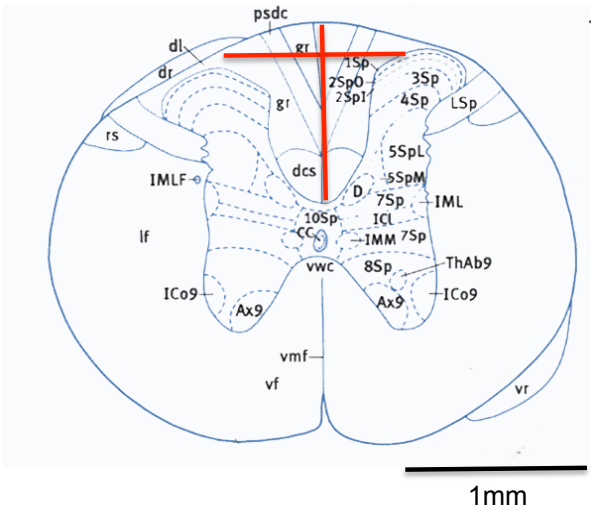

Width and depth measured of the dorsal funiculi = 3.1cm = 1mm based on the scale bar.

Figure 2.2 To achieve disruption of only the dorsal funiculi (DF) for an acute SCI response after a bilateral DC crush in both mouse and rat, the cross-sectional spinal atlas of region T8 from each species was used to measure the exact width and depth of the DF. In this instance watchmakers forceps were calibrated to a width and depth of 0.5 mm x 0.5 mm and 1 mm x 1 mm, respectively, for mouse (**A**) and rat (**B**). (Adapted from "The Spinal Cord: A Christopher and Dana Reeve Foundation Text and Atlas").

2.2 Tissue preparation

2.2.1 Histology and immunohistochemistry

Animals were killed by exposure to rising concentrations of CO_2 and intracardially perfused with 4% paraformaldehyde (PFA; TAAB Laboratories, Berkshire, UK) buffered at pH 7.4 in phosphate buffed saline (PBS, pH 7.3 ± 0.2). The lesion site at T8 was identified and 1 cm portion of the spinal cord (0.5 mm either side of the lesion epicentre in both mice and rats (Figure 2.3)) dissected out, post fixed in PFA for 2 hours at 4ºC followed by cryo-protection by overnight incubations in 10%, 20% and 30% sucrose solutions in PBS. Spinal cord segments were embedded in OCT and stored at -20ºC until required. Sections were cut at 15µm thick using a Bright cryostat (Bright Instrument, Cambridgeshire, UK) through the parasagittal plane of the cord, adhered onto Superfrost Plus Slides (Fisher Scientific, Loughborough, UK) and stored at -20ºC until required.

2.2.2 Western blot and microarray

Animals were killed at 8 dpl by intraperitoneal injection of Euthatal; 0.5ml for rats and 0.2ml for mice to minimise protein and RNA degradation. The T8 lesion sites were isolated (lesion site + 3 mm of cord either side of the lesion epicentre for rats and 2 mm either side of the lesion epicentre for mice (Figure 2.3)) and immediately snap frozen in liquid nitrogen until required.

A. Histology and immunohistochemistry

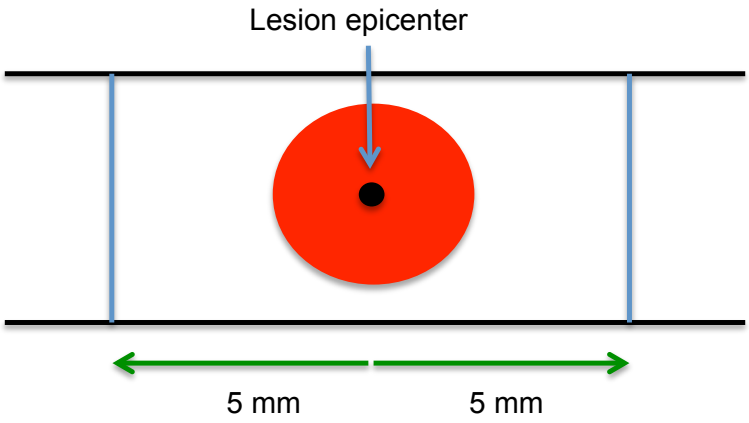

B. Western blot analysis and microarray analysis

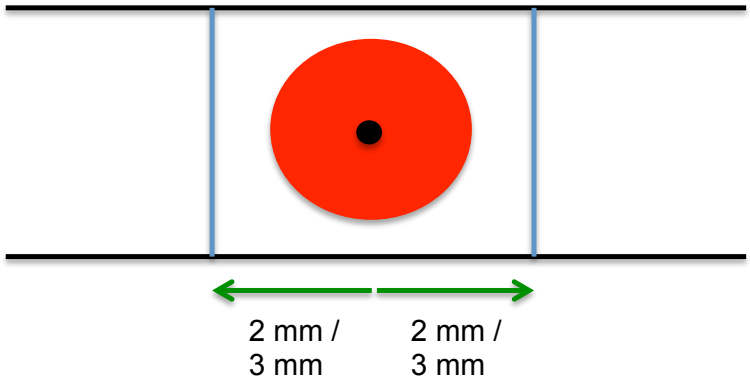

Figure 2.3 After mice and rats underwent an acute T8 bilateral DC crush, tissues were collected at various time points, depending on the type of analysis different amounts of the T8 region was collected. In this instance 5 mm on either side of the lesion epicentre (total 1 cm portion) was collected for histological and immunohistochemical purposes (**A**). Whilst, for western blot analysis and microarray analysis either 2 mm (mice) or 3 mm (rats) on either side of the lesion epicentre was collected to ensure only those genes involved in the injury response were being analysed (**B**).

2.3 Routine histology and immunohistochemistry

2.3.1 Haematoxylin and Eosin staining (H+E)

Sections were thawed for 30 minutes at room temperature (RT), and washed x2 in PBS. Sections were then immersed in Harris's Haematoxylin (BDH, Poole, UK) for 5 mins and washed gently under tap water. Sections were then immersed in Eosin (BDH) for 1 min, washed gently under tap water, dehydrated through graded series of alcohols, and cleared using 2 changes of Histoclear (National Diagnostics, Atlanta, USA) for 1 and 3 mins each. Coverslips were mounted in Vectamount (Vector Laboratories, Peterborough, UK) and viewed under a light microscope (Zeiss, Hertfordshire, UK).

2.3.2 Fluorescent immunohistochemistry

Sections were thawed for 30 mins at RT and washed x2 in PBS, permeabilised in 0.1% Triton X-100 in PBS for 10 mins. After washing sections x3 in PBS, non-specific binding was blocked for 30 minutes at RT using PBS containing 0.5% BSA (Sigma) and 0.5% Tween 20 (Sigma). Sections were incubated in the relevant primary antibody diluted in blocking solution (see relevant sections) and incubated at 4ºC overnight in a humidified chamber (16-18h). Sections were washed x3 in PBS and incubated in appropriate Alexa488/594 (green/red, Molecular Probes)/ labelled secondary antibodies diluted in blocking solution for 1 hour at RT. Finally, sections were washed x3 in PBS and coverslips mounted in the anti-fading agent, Vectashield containing DAPI (Vector Labs) and viewed under a Zeiss epi- fluorescent microscope (Zeiss).

2.3.3 Lesion cavity area

Although sections throughout the lesion cavity were stained to measure the lesion cavity area (Figure 2.4), the middle three sections through each lesion cavity (n = 6 rats/mice/time-point), determined by cutting sections from the start to the end of the DC lesion was used to measure lesion cavity area using ImagePro Analyzer (Media Cybernetics, Inc, USA) and relative fluorescent staining intensity to give the amount of pixels highlighted in a given area (Ahmed et al., 2014). Cavity areas for mice and rats were normalised by recording the ratio of cavity cross-sectional width of the spinal cord in the same sections in Adobe Photoshop CS5. One-way ANOVA with Dunnett's post-hoc test was performed (IBM SPSS statistics 20) to detect statistical differences.

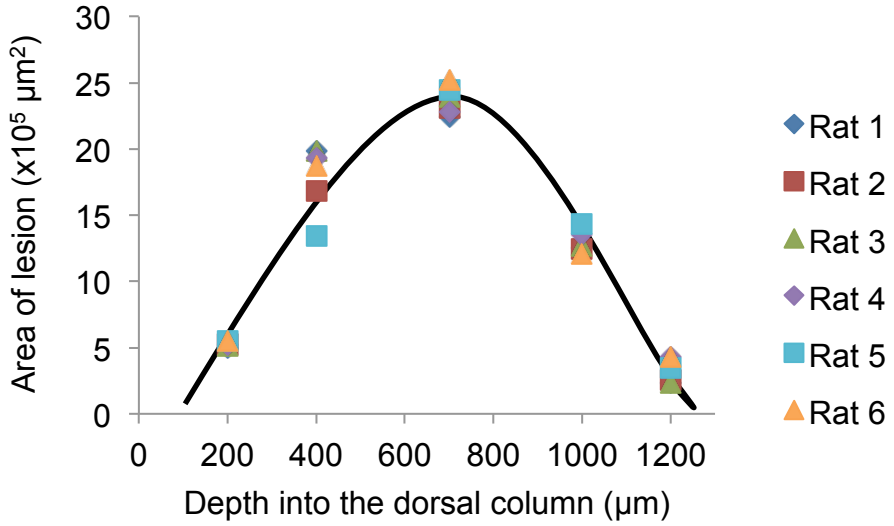

Figure 2.4 Area of acute DC wound cavity at increasing depths from the surface of the spinal cord (n = 6 rats represented by different symbols shown in key). Three sections chosen at different depths through the lesion were immunostained for laminin and GFAP and used to measure the size of the cavity in 6 different rats.

2.3.4 Relative fluorescent staining intensity

All photomicrographs were taken at x 50 magnification with the Zeiss Axioplan 2 fluorescent microscope using the same standardised exposure settings throughout for each antibody. Positive immunostaining was recorded for each antibody in pixel counts from a set area of 1851.8µm x 1389.9µm (Figure 2.5) that included the lesion site at 0 and 8 dpl. Using ImageJ (NIH, USA), images were thresholded and the mean integrated intensity of pixels for each antibody was recorded. Pixel intensities at 0 dpl were subtracted from pixel intensities at 8 dpl to remove any background fluorescence. Averages and standard deviations were determined and a one way ANOVA was performed (IBM SPSS statistics 20) to determine significance. Negative antibody controls (primary antibody omitted) were included in each run and used to set the background threshold intensity for each antibody and each species.

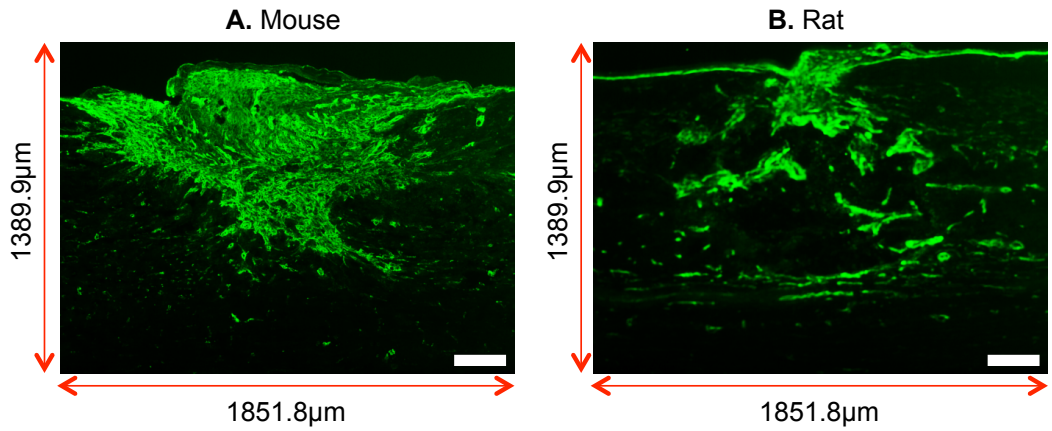

Figure 2.5 A representative picture of the area at x 50 magnification (1851.8µm x 1389.9µm) containing the entire mouse lesion site **(A)** and rat lesion site **(B)** that was fluorescently immunostained and used for quantification of fluorescent pixel intensity of angiogenic/wound healing-related proteins.

2.3.5 Quantification of spared axon density in the dorsal funiculus.

Photomicrographs of the dorsal funiculus were captured using the Zeiss Axioplan 2 fluorescent microscope as described above. Using ImageJ (NIH) the relative intensity of PKC-γ and $NF200^{+}$ was measured in the traced area of the entire dorsal funiculi after normalisation of the background intensity, obtained with omission of primary antibody controls, was subtracted from the intensity value (He et al., 2012). Automatic thresholding for each image in ImageJ was performed to determine the threshold value for specific immunoreactivity. After setting the threshold, pixel intensities above threshold levels were recorded.

2.4 RNA extraction

Total RNA was extracted from intact control and DC injured rat and mouse tissues using TRIzol (Invitrogen, Paisley, UK) RNA extraction reagent according to the manufacturer's protocol. TRIzol was added to 50-100mg of tissue samples and homogenised using a bench top tissue homogeniser (Homogenizer Workcenter T10 basic). Homogenates were centrifuged at 12,000 x g for 10 mins at 4ºC, the fatty layer discarded and the cleared supernatants were transferred to a new tube. Chloroform was used to remove contaminating protein and RNA was precipitated using isopropanol (propan 2-ol; BDH). After centrifugation at 12,000 x g for 10 mins at 4ºC, the RNA pellet was washed several times with 75% ethanol and the pellet was air-dried 5-10 mins at RT. The RNA pellet was resuspended in RNase- free water and stored at -20ºC until required.

2.5 Western blot analysis

2.5.1 Protein extraction and content assay

Total protein was extracted from spinal cords by homogenisation in 400µl of ice-cold lysis buffer (1M Tris HCL (pH 7.4), 5M NaCl, 0.5M EDTA, 0.25M EGTA, 1% NP-40). Homogenates were incubated on ice for 30 mins to allow complete dissociation of proteins and clarified by centrifugation at 13,000 x g for 30 mins at 4ºC. A protein inhibitor cocktail (104mM AEBSF, 80mM Aprotinin, 4mM Bestatin, 1.4mM E-64, 2mM Leupeptin and 1.5mM Pepstatin A in a dimethyl sulfoxide (DMSO) solution) (Sigma) was added to the clarified samples to prevent enzymatic protein degradation. Protein content in each sample was assayed using a colorimetric DC protein assay according to the manufacturer's instructions (Bio-Rad, Hertfordshire, UK). Briefly, a 96 well plate format was used to assay 5µl of sample or a protein standard to which reagent A and B were added. The plate was incubated for 15 mins at RT in the dark for the colour to develop and read on a spectrophotometer at an absorbance of 750nm. Protein concentrations were determined in Microsoft Excel using a standard curve constructed from the protein standards as a reference point.

2.5.2 Polyacrylamide gel electrophoresis and western blot

40µg of total protein from each sample were mixed with 2x Laemmli buffer (Sigma), boiled for 4 mins and loaded onto pre-prepared 12% Tris-glycine SDS-PAGE gels (Invitrogen, UK). Molecular weight standards (5µl of rainbow markers (Invitrogen)) were also loaded and proteins were separated for 1hr 50mins at 125V. Resolved proteins were transferred onto Immobilon-P polyvinylidene fluoride (PVDF) membranes (Millipore, MA, USA) for 2 hours at 25V. Membranes were washed in

TBST (0.12% Tris-base, 0.88% NaCl, pH 7.4, 0.05% Tween20) for 5 mins and incubated in blocking buffer (TBST, 5% dried skimmed milk (Marvel, Lincolnshire, UK)) for 1 hour at RT. Membranes were then incubated with primary antibody (see relevant sections) solution (TBST, 5% dried skimmed milk) in a sealed bag on a tilting platform overnight at 4°C, washed x3 in TBST before being incubated with appropriate secondary antibodies conjugated to HRP (GE Healthcare, Buckinghamshire, UK) for 1 hour at RT.

Protein bands were detected using an enhanced chemiluminescence (ECL) kit according to the manufacturer's instructions (GE Healthcare) and developed by exposure onto Biomax Light film (Kodak, NY, USA). Membranes were stripped in a low pH stripping buffer (25mM glycine-HCl, pH 2, 1% SDS) and re-probed as required.

2.5.3 Densitometry

Bands detected by western blot were quantified using densitometry after scanning into Photoshop (keeping scanning parameters the same for all blots), and analysed using the built-in gel plotting macros in ImageJ (NIH, USA). Each densitometric value was derived from three separate blots from three independent experiments and normalised to α-tubulin loading control densities. The densitometric values were also normalised to the densities of the relevant protein in intact controls for each species and presented as mean ± SEM.

2.6 Functional test procedures

SCI induced in our animal models aimed to transect the DC axons and thus disrupt the sensory and ascending pathways associated with neuropathic pain after SCI (Cruz-Almeida et al., 2012). Infar-Red (IR) plantar heat and Von Frey hair filament tests are behavioural analyses that can test these pathways affected in our injury model (Baliki et al., 2005; Taguchi et al., 2005). Before carrying out any behavioural analyses the plantar surface of both hind limbs on each animal was marked with a permanent marker to ensure consistency when testing each hind limb (Figure 2.6A).

2.6.1 Thermal sensitivity

Using established methods of Plantar heat sensitivity tests described previously (Detloff et al., 2012; Hargreaves et al., 1988; Lindsey et al., 2000), animals were acclimatised 1-wk before surgery and on -1, 0 (2hr after surgery), 7, 14, 21 and 28 dpl and data were collected at the same time of day to ensure consistency (n = 10 rats/mice (5 sham, 5 DC injured)). Animals were acclimatised in clear Perspex compartments (230mm x 170mm) for 5 min before testing commenced. Once the plantar surface of the hind limbs was placed on the glass with weight support and the animal was stationary (Figure 2.6B), the infar-red (IR) heat source (Harvard Apparatus, Massachusetts, USA) was placed directly beneath the centre of the plantar surface. The beam activated was used to produce a thermal stimulus of same heat intensity for both species to start the trial. The reaction time of paw withdrawal was recorded for 5 separate tests for each hind limb with a 30s interval before re-testing on the same paw. The middle three scores for the hind limbs were averaged to produce a single score for each animal and presented as mean ± SEM.

2.6.2 Mechanical allodynia

To quantify mechanical sensitivity, hind limb withdrawal responses were quantified using Von Frey hair filament tests. Animals were acclimatised 1-wk before surgery and on -1, 0 (2hr after surgery), 7, 14, 21 and 28 dpl data were collected at the same time of day to ensure consistency (n = 10 rats/mice (5 sham, 5 DC injured)). Animals were placed in the Perspex compartment and supplied with food for distraction for both species. This was due to animals being placed on a metal grid and therefore can identify movement beneath them when applying the monofilament as opposed to a glass surface used in the plantar heat test. Animals were allowed to acclimatise for 10 min before testing commenced. Monofilaments representing specific gram weight forces (Stoelting Europe, Dublin) were applied to the plantar surface of each hind paw between the foot pads (previously marked with permanent marker) for a 1-2s period in a steady manner. A withdrawal response of the hind limb to the particular monofilament was recorded as a positive response, while a failure to elicit a withdrawal response was recorded as negative. A total of 10 separate trial responses were recorded for each hind limb with a 30s interval between each recording. Monofilament scores from both hind limbs were averaged to the lowest monofilament level used at which 50% or more trials were positive and converted to gram force and presented as mean ± SEM.

A

B

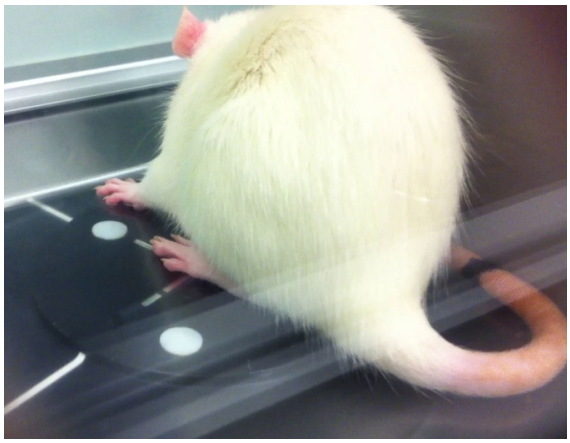

Figure 2.6 Before testing, the plantar surface on each hind limb was marked **(A)** to ensure consistency between each animal. For both behavioural tests (Plantar heat and Von Frey test) to commence the animals plantar surface of their hind limbs should placed on the ground with full weight support, be stationary and relaxed **(B)**.

2.7 Microarray (Performed by Stephen Kissane, MDS Technology Hub)

One-colour microarray based gene expression analysis (low input quick amp labelling) (Agilent Technologies, Berkshire, UK) was used to identify genes that were differentially expressed in mouse and rat after T8 dorsal column (DC) lesion following the manufacturer's instructions (Agilent manual: G4140-90050 version 6.5). One-

colour RNA spike mix was prepared using serial dilution of 1:20, 1:25 and 1:20 (Agilent Technologies, refer to Agilent manual regarding serial dilutions depending on RNA starting material) and 2µl was added to 100ng of RNA starting material to begin the labelling reaction. RNA samples (n = 8 (4 control and 4 injured) per species) were denatured and synthesised using T7 promoter primer and labelled with cyanine 3 dye by amplifying the samples with T7 RNA polymerase master mix containing cyanine 3 (Figure 2.7). Each reaction was incubated for 2 hours in a dark circulating water bath set at 40ºC to avoid light exposure. The labelled cRNA was purified using nuclease-free water, 100% RNA free ethanol, buffer RLT and RPE on RNeasy spin columns (Qiagen, Manchester, UK) at 4ºC, eluting the cleaned cRNA sample in 30µl of RNase-free water. cRNA samples were quantified on a Nanodrop (ND-1000 UV-VIS Spectrophotometer Version 3.2.1) using the microarray measurement software. Measurements including cyanine 3 dye concentration (pmol/µl), RNA absorbance ratio (260nm/280nm) and cRNA concentration (ng/µl) were used to determine the yield and specific activity before continuing. In this instance for 8-pack microarray a yield of 0.825µg and a specific activity of 6pmol Cy3 per µg cRNA was needed before going onto the next step (please refer to Agilent manual for recommended yields and specific activity depending on the microarray format chosen). Samples were then prepared using fragmentation mix (5µl 10X blocking agent, bring total volume to 24µl with nuclease-free water and 1µl 25X fragmentation buffer (Agilent Technologies)) was added to 600ng of cyanine 3 labelled, linearly amplified cRNA samples following the 8-pack microarray formats indicated in the manual. RNA was fragmented for 30 mins at 60ºC before the reaction was stopped by addition of appropriate volumes of hybridisation mix (2x GEx hybridisation buffer HI-RPM and cRNA from fragmentation

mix). 40µl of samples were prepared and loaded onto hybridisation chambers using Agilent's microarray hybridisation chamber user guide (Agilent Technologies, G2534-90001). Chambers were placed in rotisserie in a hybridisation chamber oven set at 65ºC, 10rpm for 17 hours. Time and formation of bubbles was recorded before hybridisation chamber disassembly. Slides were submerged in dish 1 containing Gene Expression Wash Buffer 1 at room temperature (RT), coverslips was removed from the slide and the microarray slide was placed in dish 2 containing Gene Expression Wash Buffer 1 at RT for 1 min. Microarray slides were then placed in dish 3 containing Gene Expression Wash Buffer 2 at 37ºC for 1 min. Slides were then placed in slide holders with Agilent barcode facing up and placed in a nitrogen environment. Slides were scanned immediately using Profile AgilentG3_GX_1Colour for 8 x 60k microarrays using defined Agilent C scanner settings for one-colour scans as indicated in the manual (for 8 x 60k microarrays settings include: dye channel-green, scan region- Scan area (61 x 21.6mm), Scan resolution (µm)- 3 and Tiff- 20 bit). Tiff images are then extracted using Feature Extraction Software and a quality control report is generated for each scan.

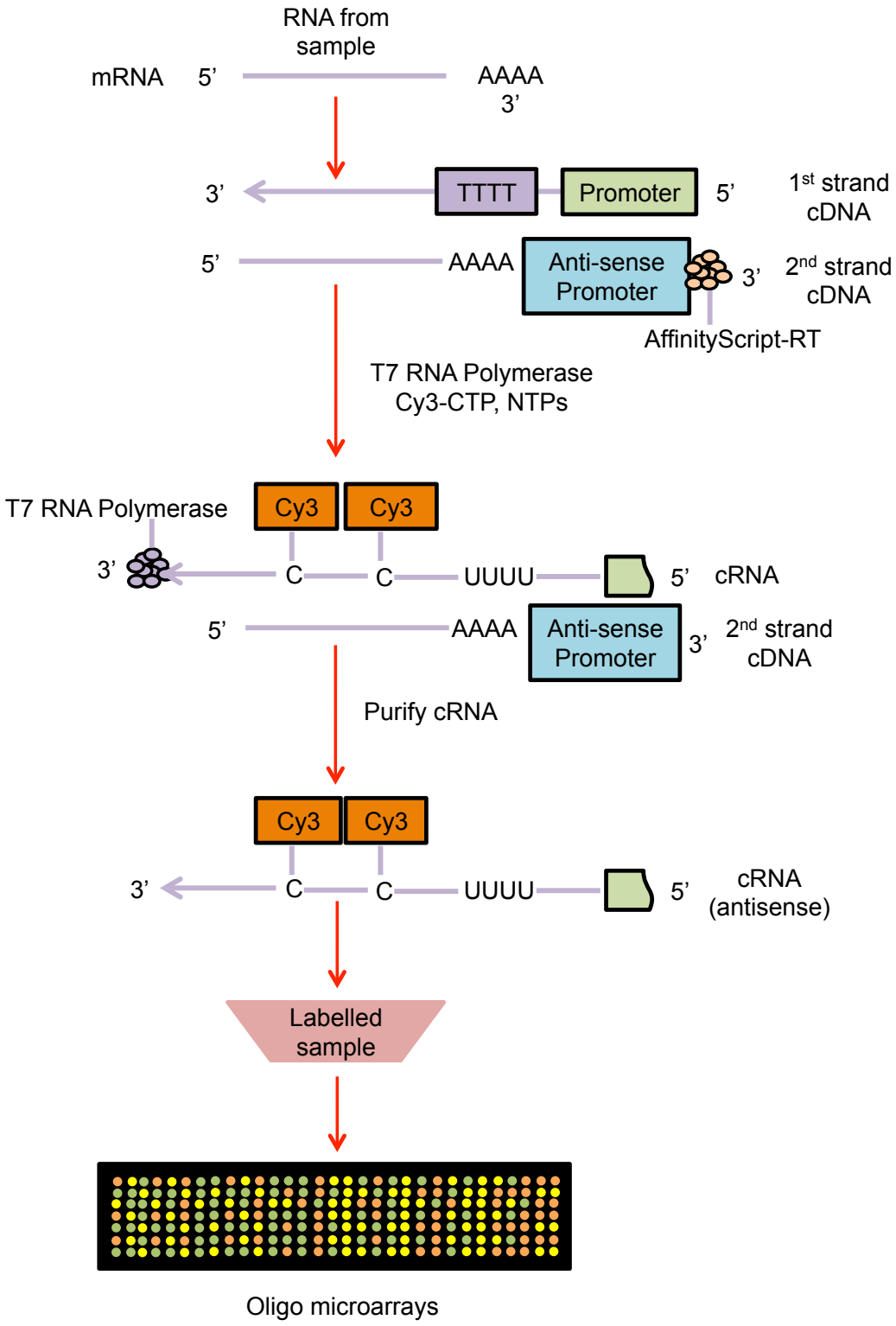

Figure 2.7 A schematic illustration of the amplified cRNA procedure. One-color microarray experiments indicate that the sample tested is only cyanine 3 (Cy3)-labelled.

2.7.1 Microarray data analysis (IPA analysis performed by Dr Zsuzsanna Nagy, University of Birmingham)

'Statistical analysis of microarray' software (SAM (National Institute of Health, USA)) was used to carry out multiclass analysis on raw microarray data between control and treated samples off all genes expressed. Genes with an estimated false discovery rate (FDR) <10% and p-value = <0.025 were considered to be differentially expressed. SAM was carried out with 1000 permutations and the output processed to remove duplicates. IPA Ingenuity software was used to interrogate functional analysis of those genes that were differentially regulated. IPA Ingenuity software is a web-based application that accurately enables the analysis and integration and understanding of the biological data from gene expression, providing interactive pathway analysis on how genes are related or go on to affect other pathways after injury. Cluster and TreeView programs were used to generate heat maps for the microarray data (Yates et al., 2013). Genome wide normalisation of raw data files was assessed in LIMMA (statistical package) so each treated sample was compared to a control sample to show variation between animals of the same species and thus biological variation based on average.

2.8 Microarray validation

2.8.1 cDNA preparation

High-capacity cDNA reverse transcription Kit (Life Technologies Ltd, Paisley, UK) was used to convert RNA to total complementary cDNA following the manufacturer's instructions. 10µl of master mix (10X RT buffer, 25X dNTP mix, 10X random primers, RNA-free water, multiscribe RT) was added to each RNA sample that was diluted to

500ng in 10µl of RNA-free water. Samples were incubated at 25ºC for 10 mins and further incubated for 2 hours at 37ºC. Samples were stored at -20ºC until needed.

2.8.2 Real-time quantitative polymerase chain reaction (qPCR)

Exiqon universal probe system was used to perform real-time qPCR with forward and reverse primers (Table 6.2) designed using a web-based tool produced by Roche Applied Science (Roche Diagnostics Ltd, UK). A reaction mix totalling 25µl (12.5µl 2 x express qPCR supermix (Life Technologies, Paisley, UK), 1µl forward primer (10µM), 1µl reverse primer (10µM), 0.25µl of probe (Table 6.2), 0.25µl deionised water and 10µl cDNA) was loaded onto a 36-well rotor, qPCR was conducted using a Rotor-Gene RG-3000 qPCR machine (Corbett Research Ltd, Australia) and set on the following programme (1) 92ºC for 10 mins, (2) 92ºC for 15 secs and (3) 60ºC for 45 secs, steps 2 and 3 were repeated for a total of 40 cycles for all genes. Expression levels were determined using known dilutions of cDNA (1:10, 1:100, 1:1000) to generate standard curves using Rotor-Gene 6 software (Corbett Research Ltd, Australia). All genes were normalised to the expression of housekeeping gene β-actin to accurately quantify gene expression and compare between samples and species. Mean and standard deviations were determined and all statistical comparisons were made in SPSS (IBM) using non-parametric Kruskal-Wallis method.

CHAPTER 3

CHARACTERISATION OF THE INJURY RESPONSE IN MICE AND RATS AFTER SUB-ACUTE SPINAL CORD INJURY

Sections of the introduction are published in the following review:

Kundi S., Bicknell R., Ahmed Z. (2013). Spinal cord injury: Current mammalian models. American Journal of Neuroscience. 4 (1), 1-12.

Surey S., Berry M., Logan A., Bicknell R., Ahmed Z (2014). Differential cavitation, angiogenesis and wound healing responses in injured mouse and rat spinal cords. Neuroscience. 275, 62-80.

3.1 Introduction

It has been known and accepted that mice and rats display differential responses after SCI but research between the two species is limited. However, the research available highlights, in particular, the cavity, inflammatory and blood-spinal cord barrier (BSCB) responses between mice and rats after SCI.

3.1.1 Differential cavitation and inflammatory responses after SCI

After SCI, the differential responses of mice and rats have previously been documented at a later time-point (28dpl) using MRI analysis after a moderate contusion to the thoracic level of the cord (Byrnes et al., 2010). Results demonstrated a restricted injury site in mouse tissue with a small area of cavitation surrounded by disordered scar tissues, whereas, rat lesion sites displayed multiple cavities, a large degree of disordered tissue and significant scar formation around the lesion site. Quantification of lesion volume using the Cavalieri method (an accurate volumetric calculation that allows organ volumes to be estimated without bias by means of consecutive serial sections) showed an increase in lesion volume in rats compared to mice (Sonmez et al., 2002, Sahin et al., 2003).

Inflammation is part of the body's natural response to harmful stimuli such as pathogens, where vascular tissues aim to remove the harmful stimuli and initiate the healing response to bring damaged tissue back to normal. It is a process that needs to be closely monitored as chronic inflammation can be detrimental causing rheumatoid arthritis, and chronic wound healing for example. Research on the inflammatory response comparing the two species has shown that microglia and macrophage infiltration is similar after injury, with a marked difference in T-cell numbers; in rats T-cell infiltration reached its highest between 3-7 days after injury but then declined by 50% at three weeks, whereas in mice T-cell infiltration was not evident until 14 days after injury and increased by 50% between 2-6 weeks (Sroga et al., 2003). Furthermore, Sroga et al, observed a unique fibroblast-like cell population in the newly formed connective tissue matrix in injured mouse spinal cord only. It was first under assumption that these cells resembled lymphocytes, however, they did not express lymphocyte-specific markers. Immunohistochemical analysis was done to see if the nonlymphocytic subpopulation shared the same phenotype as fibrocytes (a unique population of blood-derived fibroblast-like cells). Results showed that these cells expressed fibronectin, collagen-1, CD43, CD13 and CD45 that extended from blood vessels within the tissue matrix. This is characteristic of blood-borne cells (fibrocytes) involved in wound healing and immunity.

It has been shown that there is an increase in the number of white blood cells in the cerebrospinal fluid within 7 days after injury with recent studies showing an increase in plasma levels of inflammatory mediators in patients with long-standing SCI (Segal et al., 1997). It is also thought that the accumulation of activated microglia

and macrophages contribute to the progression of secondary injury (Blight, 1992, Blight et al., 1995, Bethea et al., 1998).

3.1.2 Differential BSCB responses to SCI

BSCB (more commonly known as the blood-brain barrier- BBB) is composed of specialised endothelial cells that regulate the transport of molecules in and out of the CNS, providing a stable environment that is essential for normal neuronal function (Mautes et al., 2000). The BSCB is composed of tight junctions between adjacent endothelial cells that block intracellular movement of large molecules, including plasma proteins (Reese and Karnovsky, 1967). Disruption of BSCB leads to vascular permeability due to tight junctions allowing leakage of proteins and exposure to toxic effects of inflammatory cells to the spinal cord which could contribute to progression of the secondary injury after SCI (Mautes et al., 2000, Whetstone et al., 2003a). The BSCB has been investigated in the two species 28 days post-injury using sodium fluorescein, showing that after a weight drop injury BSCB permeability was apparent at the lesion site of the small cavity in mice with little extension to surrounding tissue, whilst in rats the tracer was more diffuse and spread rostral and caudal to the injury site (Byrnes et al., 2010). Some reports suggest that BSCB permeability at this time-point after SCI may be related to inflammation or angiogenesis (Popovich et al., 1996).

3.1.3 Angiogenic and structural extracellular matrix molecule Laminin

Laminin is a structural, cross-linked, heterotrimeric glycoprotein that is a major component of the basement membrane, in particular the basal lamina containing

alpha, beta and gamma chains (Cheng et al., 1997) (Figure 3.1). There are currently 5 alpha, 3 beta and 3 gamma chains that assemble to form the 19 laminin isoforms (LN-1 to LN-19) with LN-1 being the most studied isoform consisting of α1, β1 and γ1 chains (Ekblom et al., 1998, Siler et al., 2000, Koch et al., 1999, Ramadhani et al., 2012). These chains are binding regions for integrins, collagen and proteoglycans whilst also binding to itself to form sheets in the basal lamina of the basement membrane. Laminin isoforms are expressed in a tissue-specific manner located in various tissues, nerves and neuromuscular junction (Hallmann et al., 2005).

In the CNS the presence of laminin has shown regenerative potential *ex vivo* in adult rat and goldfish retinal explants (Ford-Holevinski et al., 1986, Liesi et al., 1984). Furthermore, it has been demonstrated that laminin γ1 chain in particular is important in not only axon regeneration but also axon myelination after injury to both the CNS and PNS (Chen and Strickland, 2003, Grimpe et al., 2002, Wallquist et al., 2002). Laminin expression in chick retina, spinal roots, dorsal root ganglion (DRG), and developing rat cerebellum is present in areas where outgrowing axons and migrating neurons are present (Cohen et al., 1987, Kalil and Reh, 1979, Rogers et al., 1986). An acute injection of polylaminin, a polymeric form of laminin, after thoracic compression, partial or complete transection demonstrated improved locomotor function (Menezes et al., 2010). Furthermore, polylaminin also demonstrated axon regeneration of long and short fibers across the complete transection with an unsuspected anti-inflammatory role. This suggested that laminin may play a role in SCI and axon regeneration. After ischemic stroke in the CNS components of the ECM, in particular laminin was highly upregulated on endothelial cells suggesting that ECM remodeling takes places early after ischemic stroke and

that the presence of ECM protein expression is an effort to revascularise and oxygenate the damaged tissues and thus play a role not only in neuroregeneration but also inflammation (Ji and Tsirka, 2012).

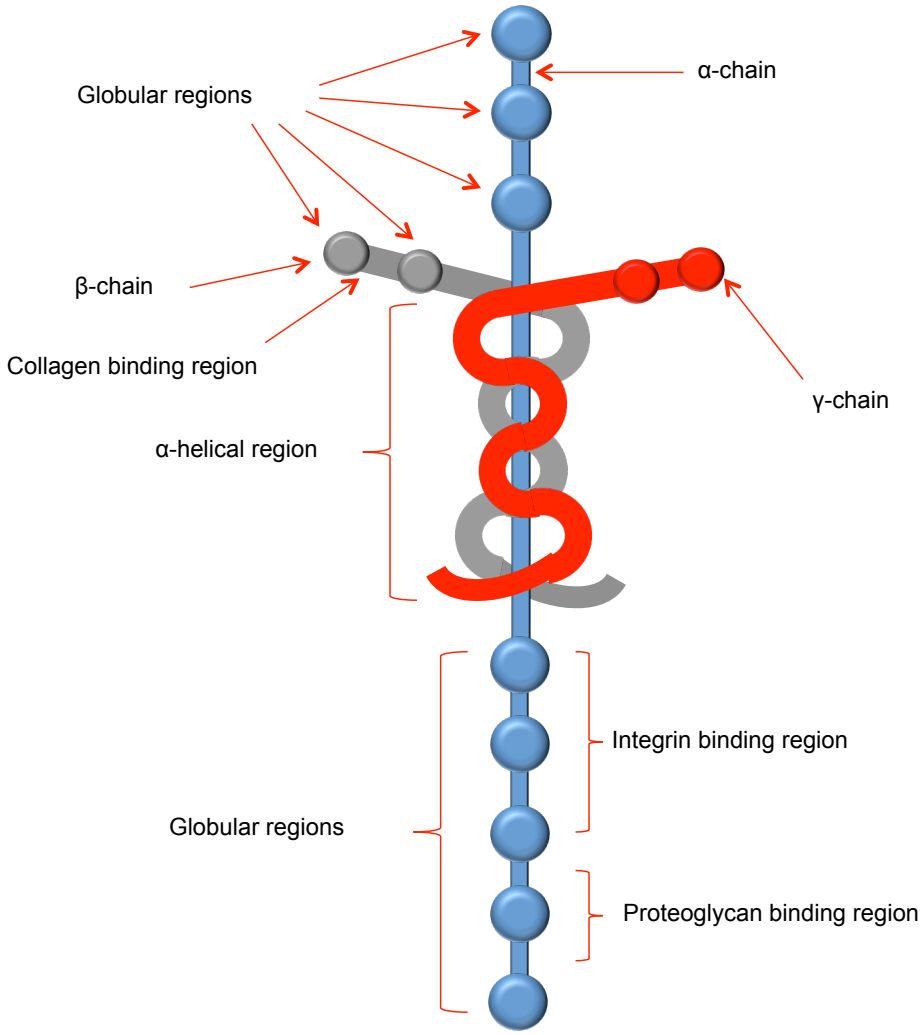

Figure 3.1 Laminins; a heterotrimeric glycoprotein, is a major component of the basal lamina of the ECM Laminins contain binding regions for collagen, integrins and proteoglycans, it can also bind to itself to form sheets in the basal lamina (Adapted from Sigma-Aldrich).

3.1.4 Laminin after SCI

Although reports suggest that laminin expression may be associated with outgrowing axons and migrating neurons and thus axon regeneration within the nervous system, other reports have contradictory views on this matter. In the PNS, Schwann cells express laminin as a major component of the PNS basal lamina (Cornbrooks et al., 1983). Laminin immunoreactivity is seen around blood vessels and meninges from embryonic to adult rats, the distribution of laminin within the GM and WM was very much age-dependent (Sosale et al., 1988). Immunoreactivity of laminin in normal spinal cord was present in small amounts in early embryos but absent from postnatal animals. However, after injury intense immunoreactivity was present at the lesion area in both newborn and adults and was especially prominent in the matrix of the lesion, and therefore concluded that the distribution of laminin before and after injury did not correlate with axonal growth. The temporal progression of angiogenesis and basal lamina deposition after SCI shows an angiogenic response with RECA-1 (rat endothelial cell antigen) and SM171 (endothelial barrier antigen) with the robust deposition of basal lamina 7 days post lesion within the ventral GM epicenter (Loy et al., 2002).

Motor function after thoracic compression, partial or complete in rats using an acute local injection of polylaminin improved 8 weeks post injury, also showing neurons of short and long origin to be detected in the spinal cord and brain stem after being retrogradely labeled. This indicated regrowth across the complete transection site, suggesting its role in promoting axon regeneration after SCI (Menezes et al., 2010). With laminin demonstrating a contradictory role in axon regeneration in the nervous system it also plays a part in endothelial cells and inflammation after injury,

this led to the investigation of comparing laminin after sub-acute SCI in mice and rats.

3.1.5 Scar related ECM molecules

The scar related responses after SCI can be tested using known markers such as ED1, fibronectin, GFAP and NG2. Although CD68 (ED-1) was originally identified as a marker of macrophages, recent studies demonstrate that CD68 (cluster of differentiation 68) is also expressed in human fibroblasts and active endothelial cells (Beranek, 2005, Kunz-Schughart et al., 2003, Holness and Simmons, 1993). CD68 can be used as a marker of active phagocytosis after injury (Perego et al., 2011). Fibronectin is a 220 kDa ECM glycoprotein composed of nearly two identical disulfide-bound polypeptides. Fibronectin molecule has several distinct domains that may bind to collagen, fibrinogen, cell surfaces, heparin, proteoglycans and glycoaminoglycans and therefore is a component of the ECM (Meland et al., 2010). Fibronectin is a marker of increased fibroblast expression in overgrown lesions (Sume et al., 2010).

Glial fibrillary acidic protein (GFAP) is an intermediate filament protein expressed in many cell types in the CNS including ependymal cells during development, neural stem cells in the postnatal subventicular zone and astrocytes (Liu et al., 2006, Roessmann et al., 1980, Jacque et al., 1978). The increased expression of GFAP generally represents activation of astrocytes and glial cells during neurodegeneration (Brahmachari et al., 2006). Neural/Glial antigen 2 (NG2) is a member of the transmembrane chondroitin sulfate proteoglycan class of inhibitory ECM molecules that is highly upregulated after SCI (Jones et al., 2002). NG2

expression was not only found in reactive macrophages but also oligodendrocyte progenitor cells.

3.2 Rationale

Unlike humans, mice do not exhibit progressive necrosis, apoptosis and cavitation after SCI (Bilgen et al., 2007). Instead, the lesion sites become completely filled with ECM molecules, reduced BBB permeability and an adequate balance between glial scar and inflammatory markers (Byrnes et al., 2010). Thus, the failure of spinal cord cavity formation in mice after injury may be conducive to wound healing, leading to ECM deposition and the contraction of the scar with time. This differential response between mice and rats was used to investigate cavity lesion area, laminin deposition and the local inflammatory response after injury between the two species.

3.3 Hypothesis

Cavitation leads to secondary axonal damage and the presence of cavities in the rat SCI model is linked to inadequate wound healing, neo-vascularisation and reduced inflammatory responses after SCI, whilst the cavity-free SCI response of mice is linked to an adequate balance between scar deposition, wound healing, vascularisation and inflammation.

3.4 Aims

- To compare and establish a timeline of cavitation through staining of the lesion site after T8 DC crush between the two species.
- Determine differences in the relative lesion area of the injury site that develops after SCI in mice and rats.
- To compare the localisation of laminin (a surrogate marker of angiogenesis and an ECM molecule) over time after SCI, establishing a time-point that shows the greatest differences between mice and rats.
- To establish the local sub-acute inflammatory response between the two species after T8 DC crush 8 days post lesion (dpl).

3.5 Materials and Methods

3.5.1 Experimental design

Please refer to Materials and Methods section 2.1 Animal surgery and 2.2.1 Tissue preparation for histology and immunohistochemistry for standard protocols used.

Type of analysis	**N -numbers**	**End-points (days)**
Cavitation timeline	6 (per time point/species)	0, 2, 8, 15
Laminin timeline	6 (per time point/species)	0, 2, 8, 15
DC scarring response	6 (per time point/species)	0, 8

Table 3.1 Experimental design of n numbers and end-points used to assess cavitation and laminin over time and DC scarring responses to sub-acute SCI in mice and rats.

3.5.2 Antibodies used for fluorescent immunohistochemistry

Please refer to Material and Methods section 2.3.2 Fluorescent immunohistochemistry for standard protocol used. Fluorescent immunohistochemistry was used to assess laminin deposition and the scarring responses after SCI in mice and rats (Laminin (1/200, rabbit polyclonal, L9393, Sigma, USA); GFAP (1:400, rabbit polyclonal, G9269, Sigma, USA), fibronectin (1:200, rabbit polyclonal, F3648, Sigma, USA), EDI (CD68) (1:400, rabbit polyclonal, sc-9139, Santa Cruz Biotechnology, Dallas, Texas, USA), NG2 (1:400, rabbit polyclonal, Abcam, ab101807, Cambridge, MA, USA)).

3.6 Results

3.6.1 Relative proportions of mouse size vs. rat

Relative proportions between mice and rats were determined using n = 12 animals/species and calculated by dividing the average width of a mouse cord with that of the rat (1036μm / 1443μm = 0.7). This resulted in mouse spinal cords being 0.7 x smaller than rat and therefore this proportion was taken into consideration when determining values in rats.

3.6.2 Acute cavity development

The histological timeline showed clear pathological differences in the post-injury response in mice and rats (Figure 3.2 A-H). Little or no differences in gross histology were observed at T8 in intact mouse and rat spinal cords (Figure 3.2 A, B). At 2 dpl, there was disruption to the normal structure of the cord in the two species (Figure 3.2 C, D), but, in rats a large lesion cavity had already begun to develop

(Figure 3.2 D). Differences between mice and rat DC lesion sites were more obvious at 8 dpl, with tissue disruption in the cord in mice (Figure 3.2 E) but the development of a wound cavity in rats filled with haematogenous cells, debris, fibrous material and occasional small empty cavities (Figure 3.2 F). Both type I and II cavities were present in rat cords at 8 dpl. By 15 dpl, scar tissue had formed at the SCI site but no lesion cavities had developed in mouse cords (Figure 3.2 G) while, in rats the wound contained Type I cavities consisting haematogenous cells (Figure 3.2 H).

Differences in wound cavity area were quantified at the various time points in defined sections by image analysis using Image ProAnalyzer (Figure 3.3 A) (Please refer to Materials and Methods section 2.3.3 Lesion cavity area for detailed methodology). The mean pixel intensity count in the defined area showed a marked difference between rats and mice (Figure 3.3 B) such that mean wound cavity area in the rat was $19 \times 10^4 \pm 7.5 \times 10^4$ μm² and $26 \times 10^4 \pm 4 \times 10^4$ μm² at 8 and 15 dpl, respectively (Figure 3.3 B). These results confirm that wound cavitation is extensive in the rat cord after DC lesion while in the mouse cavities do not develop.

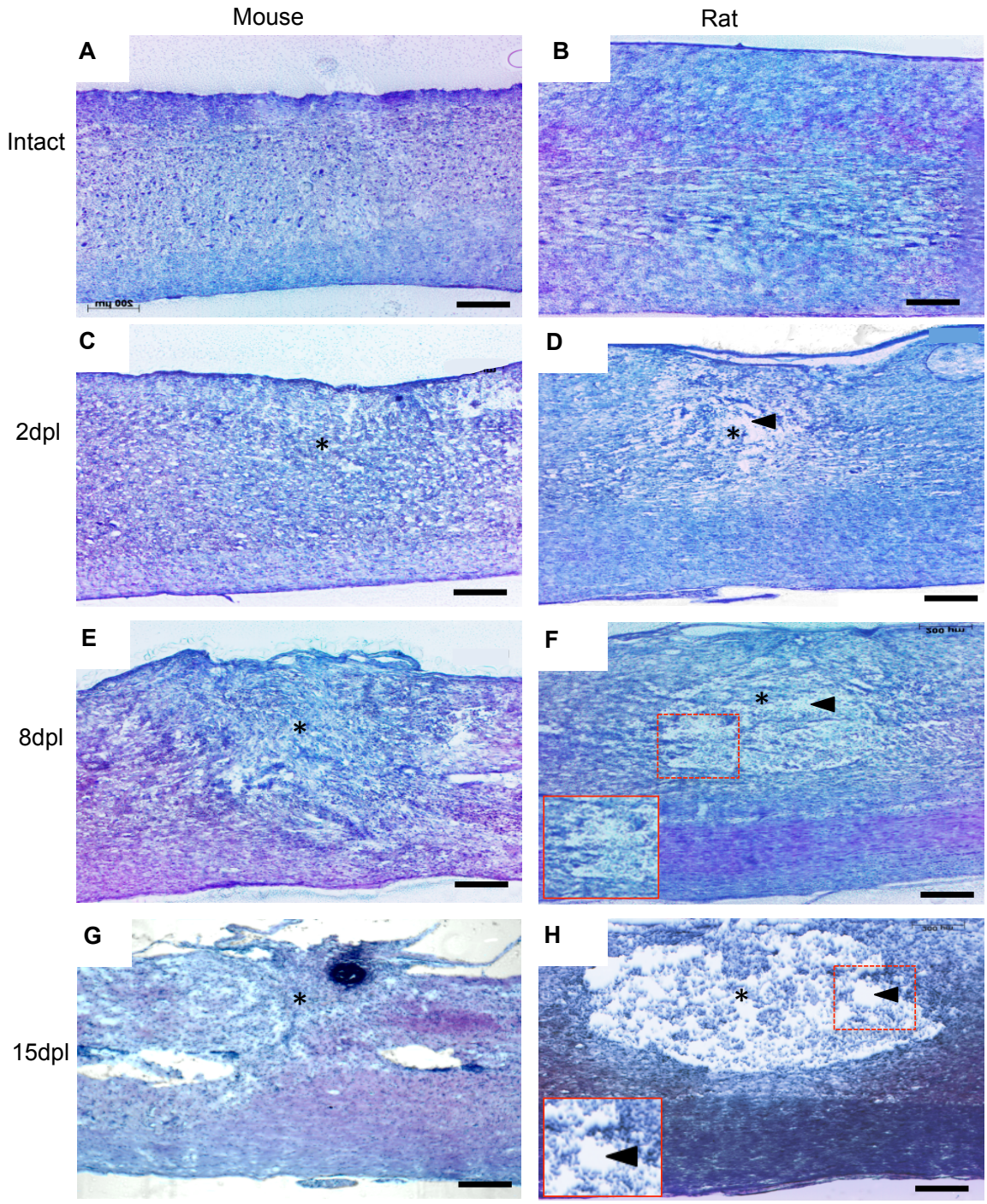

Figure 3.2 Histological timeline using a haematoxylin and eosin stain to show the development of cavitation at the lesion site at day 0 **(A and B)** 2 **(C and D)**, 8 **(E and F)** and 15 dpl **(G and H)**, which presented clear post-injury differences between mice and rats. Inset picture demonstrates type I cavity at 8 dpl in rats **(J)** whilst at 15 dpl

rats demonstrated type II cavities **(H)** (n=6/group/time-point; * = lesion epicentre; scale bars in A-H = 200µm; arrowheads in D, F and H = cell free areas in rat SCI cavities).

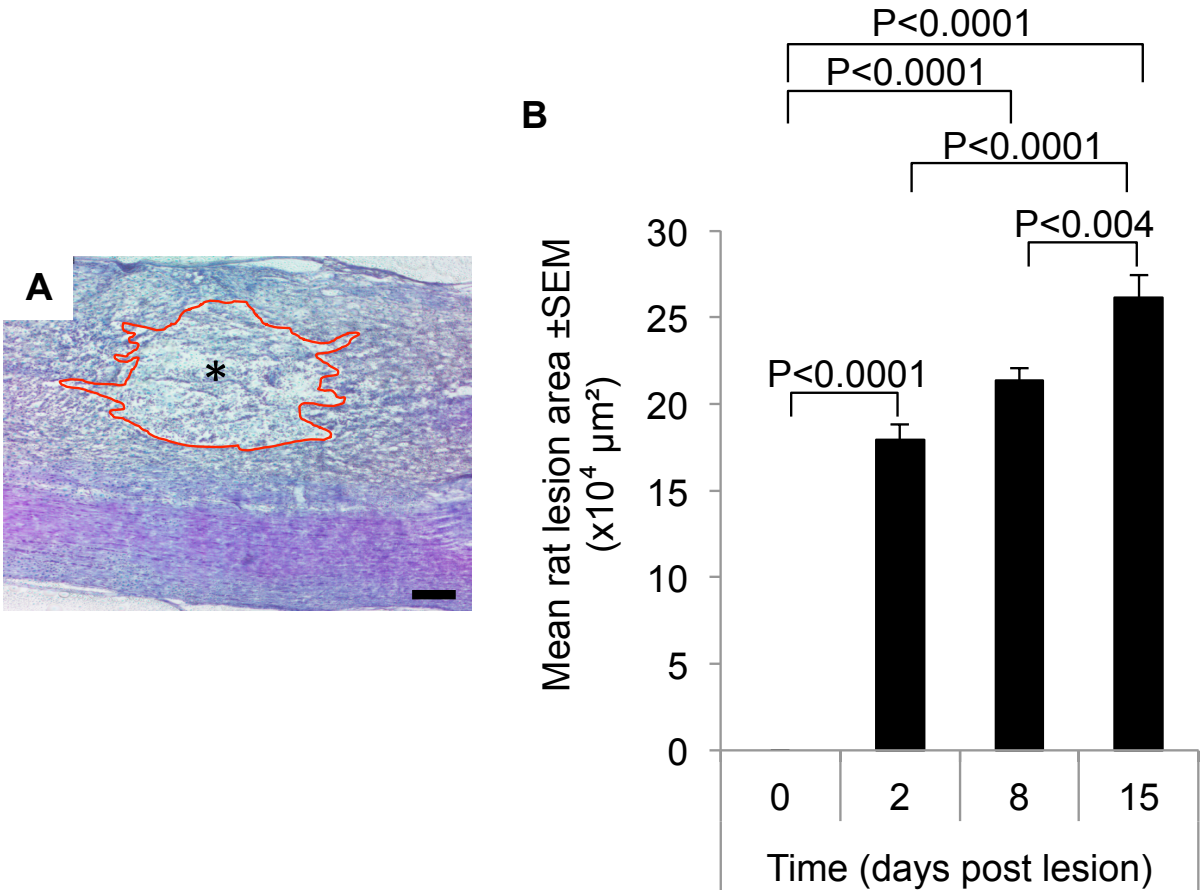

Figure 3.3 Quantification of the cavity area in rats at each time-point was achieved by drawing around the cavity in Image ProAnalyzer **(A)** and measuring the mean pixel area within the isolated area showed there was a significant increase after performing One way ANOVA in lesion area at 0 and 8 dpl, 0 and 15 dpl and 2 and 15 dpl **(B)**. (n=6/group/time-point; scale bar in A = 200µm).

3.6.3 Laminin timeline

The timeline of laminin deposition after injury was determined using fluorescent immunohistochemistry to show the localisation and assess the levels of laminin in mice and rats (Figure 3.4 A-H). In the intact cord, the meninges and the basal laminae of blood vessels were laminin^{+} in both mice and rats (Figure 3.4 A and B). At 2 dpl, the levels of laminin deposition did not change significantly, compared to that observed at 0 dpl in both species (Figure 3.4 C and D), but was enhanced in mice compared to rats in the vascular basal lamina and the lining of Type I cavities at 8 dpl (Figure 3.4 E and F). Enhanced levels of laminin^{+} immunoreactive vascular and glia limitans accessoria remained in 15 dpl mouse lesions (Figure 3.4 G). In rats at 15 dpl, laminin^{+} immunoreactivity was primarily associated with the glia limitans accessoria (Figure 3.4 H), while the laminin^{+} immunoreactivity did not change in the glia limitans externa of both mouse and rat.

Quantification of laminin immunoreactivity in ImageJ by thresholding the original image (Figure 3.5 A and B) reflected these changes, and following a One way ANOVA there was significantly enhanced levels of laminin in mice compared to rats at 8dpl (27 x10^{6} ± 2.6 x 10^{6} in mice compared to 7 x 10^{6} ± 1.4 x 10^{6} pixels in rats, $P<0.002$) and 15 dpl (18 x 10^{6} ± 1.1 x 10^{6} in mice compared to 13 x 10^{6} ± 0.5 x 10^{6} pixels in rats, $P<0.003$) (Figure 3.5 C). These results demonstrate that fundamental differences in injury related parameters are present in mice compared to rats, i.e. compared to rats mice SCI sites have greater neovascularisation, do not develop a glia limitans accessoria, do not cavitate and deposit higher levels of ECM molecules. This time point analysis confirmed that 8 dpl would be the best time-point to investigate angiogenic/wound healing-related proteins and gene changes (by

microarray analysis) rather than using 15 dpl, since we are interested in the early angiogenic response rather during the maturation of scarring that occurs in the spinal cord between 12-15 dpl. As opposed to humans maturation of the scar tissue normally occurs weeks to months after the initial injury to the CNS, where the progressively dense glial scar isolates but does not undergo repair to the injured area (Stroncek and Reichert, 2008).

3.6.4 Characterisation of the DC scarring response to injury

Abundant GFAP$^+$ astrocytes were present in the neuropil and about the lesion site in mice (Figure 3.6 A) and in the fibronectin$^+$ lesion core (Figure 3.6 C: inset). In rats, fewer GFAP$^+$ astrocytes were localised within the lesion and the lesion core was astrocyte-free (Figure 3.6 B and inset). Abundant immunostaining for fibronectin was present within the lesion core in mice (Figure 3.6 C and inset) whereas little or no immunoreactivity was present in rat SCI sites (Figure 3.6 D and inset). Low numbers of ED1$^+$ cells were present in both mice (Figure 3.6 E and inset) and rats (Figure 3.6 F and inset), and low levels of NG2 were also present in the SCI wounds of both species.

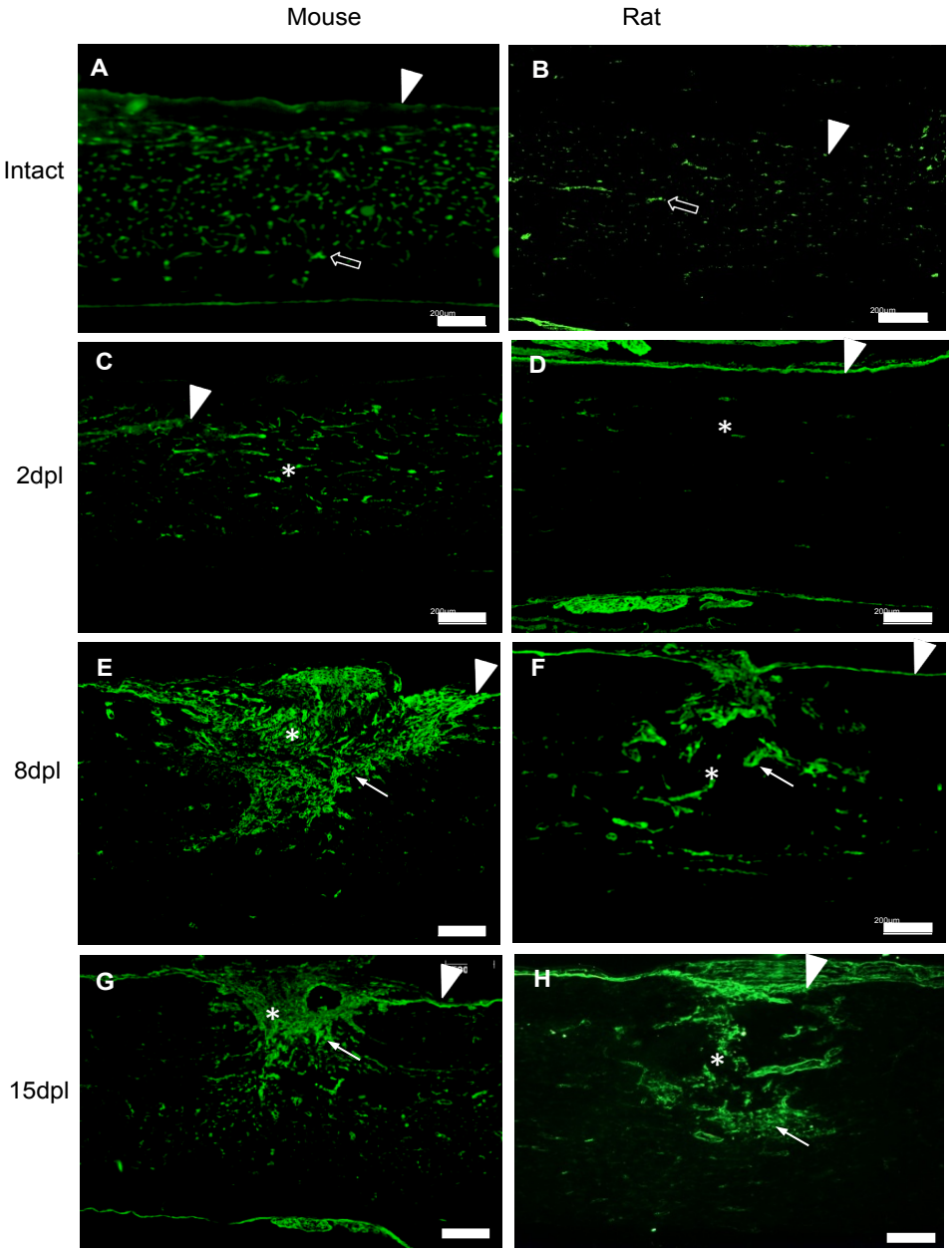

Figure 3.4 Localisation of laminin in the lesion site over time in DC lesions in mice and rats. Expression of laminin in intact controls **(A and B)** and at 2 **(C and D)**, 8 **(E and F)** and 15 dpl **(G and H)**. The localisation of laminin deposition after DC injury displayed clear differences between the two species at 8 and 15 dpl. (n = 6/group/time-point; * = lesion epicentre; scale bars in A-H = 200 µm; arrowheads = glia limitans externa (GLE); arrows = glia limitans accessoria (GLA); open arrows = blood vessels).

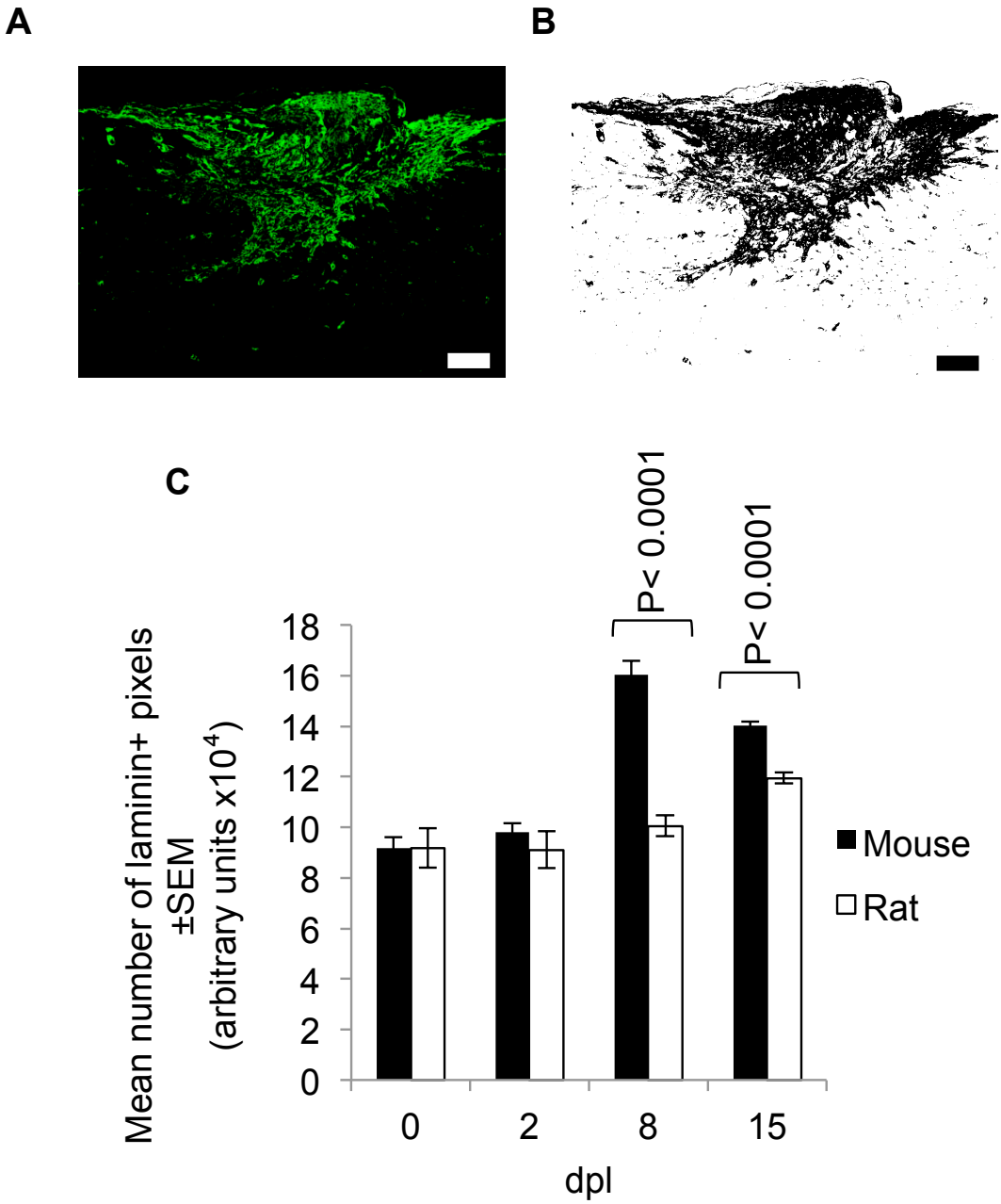

Figure 3.5 Pixel intensities from the original image **(A)** were calculated in ImageJ by thresholding the image **(B)** and average pixel counts were plotted showing significant differences following a One way ANOVA in laminin expression between mice and rats at 8 and 15 dpl; with 8 dpl showing the greatest differences in laminin expression between the two species **(C)**. (n = 6/group/time-point; scale bars in A and B = 200µm)

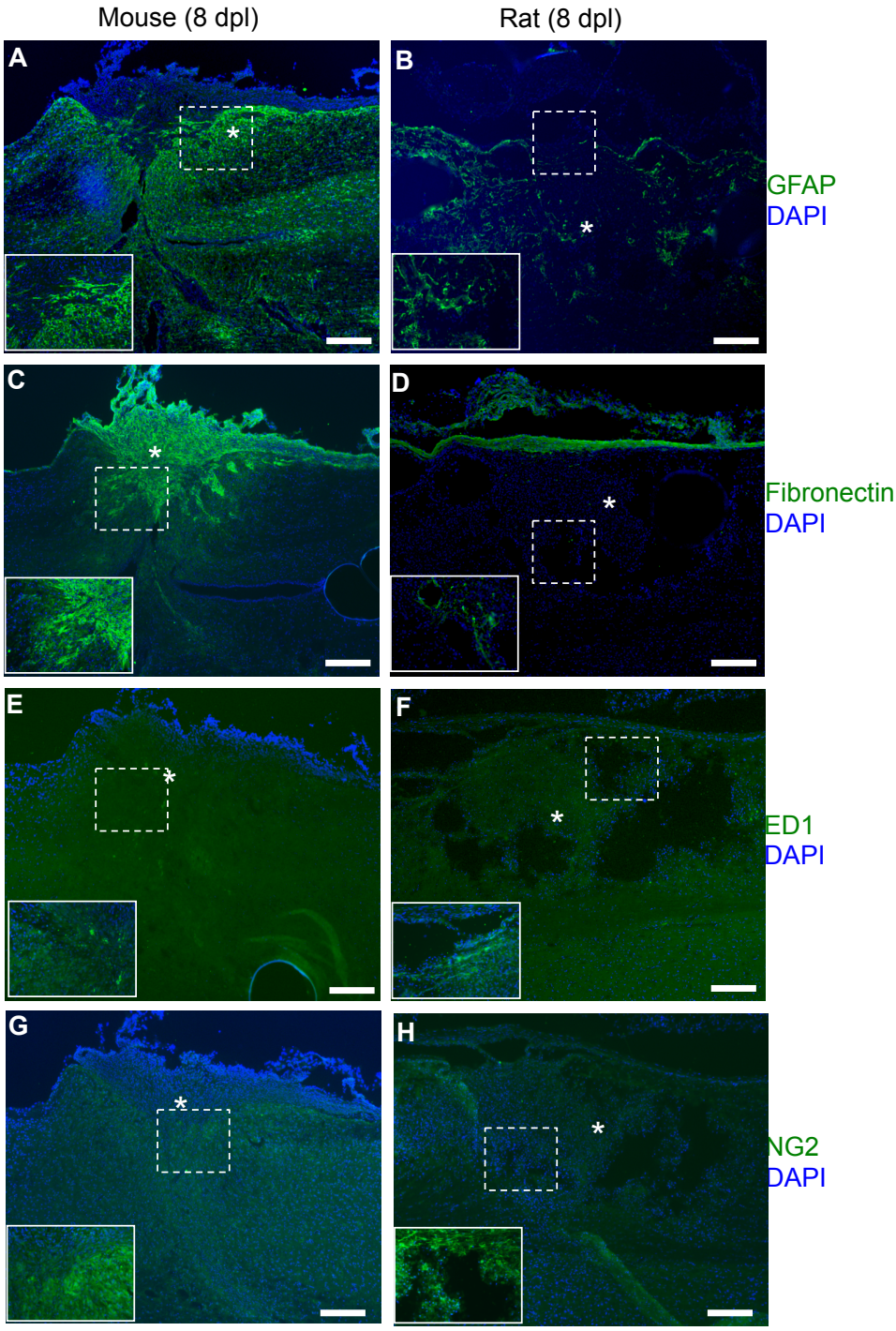

Figure 3.6 Acute SCI responses in mice and rats. Immunohistochemistry to show changes in GFAP (A and B), fibronectin (C and D), ED1 (E and F) and NG2 (G and H) at 8 dpl within and about DC lesions (* = lesion epicentre; scale bars in A-H = 200 μm).

3.7 Discussion

Our model of T8 sub-acute SCI in mice and rats demonstrates fundamental differences seen between the two species early after injury. Cavity development in rats begins as early as 2 dpl and continues to expand up until 15 dpl. However, in mice only disruption of the cord was evident. Cavity development further coincided with a lack of laminin deposition after injury in the lesion epicenter in rats and thus a decrease in angiogenesis. However, in mice the lack of cavity development resulted in increased laminin deposition in the lesion epicenter after injury and thus an increase in angiogenesis.

3.7.1 Differential cavitation expression between mice and rats

Although our results only extend to 15 dpl, cavity area is thought to continue to increase beyond 15 dpl (James et al., 2011, Byrnes et al., 2010). However, by 15 dpl the scar tissue around the lesion site is fully mature and the wound-healing response is absent beyond this time-point after injury. However, in humans maturation of the scar tissue occurs weeks to months after the initial injury to the CNS, where the progressively dense glial scar isolates but does not repair the injured area (Stroncek and Reichert, 2008). Immunohistochemical studies on human spinal cord after traumatic SCI have shown that NG2 and phophacan; members of the CSPGs, are present up to a month after injury and thus present in the evolving astroglial scar after injury (Buss et al., 2009). Furthermore, GFAP staining in the earlier repair stages of wound healing can be observed not only in the lesion epicenter but up to 400μm outside the lesion (Stroncek and Reichert, 2008). However, when the scar is in the remodeling stages, i.e. maturation of scar tissue the GFAP immunoreactivity is

more centered to the lesion epicenter. Our intention was to investigate the early angiogenic/wound-healing responses that may be responsible for the formation of the cavities. Indeed, the mechanisms for the expansion of the cavity area in rats beyond 15dpl is currently unknown but is thought to occur as a result of maturation of the cavity area and secondary mechanisms due to the failure to lay down appropriate ECM molecules (James et al., 2011, Byrnes et al., 2010). Although small severity-dependent injury cavities have been reported in mouse SCI sites, our results confirm those of others that ECM deposition without cavitation is a more characteristic response (Inman and Steward, 2003, Bilgen et al., 2007). In contrast, rat SCI wounds cavitated by 8 dpl and by 15 dpl a large Type II cavity had formed which extended rostrally and caudally from the injury epicenter, filled with haematogenous macrophages and cellular debris. Cavities may develop after vascular regression and endothelial cell loss and their expansion may be exacerbated by hypoxia, necrosis, apoptosis and increased vascular permeability (disruption of the blood spinal cord barrier (BSCB)) (Loy et al., 2002, Casella et al., 2006). Demyelination and neuronal degeneration occur in the surrounding neuropil as the cavity expands (Blight, 2000, Mautes et al., 2000, Hunt et al., 2002, Whetstone et al., 2003b, Sandvig et al., 2004, Berry et al., 2008, Casella et al., 2006, Fassbender et al., 2011).

3.7.2 Characterisation of lesion laminin expression between mice and rats

The expression of laminin as a surrogate marker of angiogenesis/wound healing through the early time course mirrored that of cavity area; after injury in mice the cavity area was filled with ECM components where laminin levels and protein expression was greatly increased correlating angiogenesis and ECM deposition,

whereas, in rats after injury cavitation could be seen which increased with time but laminin expression was significantly reduced and thus correlated with little angiogenesis and reduced ECM deposition.

3.7.3 Inflammatory responses after spinal cord injury

Cavities may expand as damaged tissues are removed by inflammatory macrophages and microglia, explaining the beneficial effects of immunosuppressive therapies which probably maintain structural and functional integrity of the spinal cord (Giulian and Robertson, 1990, Blight, 1994, Guth et al., 1994, Popovich et al., 1999).

Although Sroga et al (2003) reported similar responses of macrophages and microglia in mouse and rat SCI sites, accumulation of T-cells at the wound is highest in rats between 3 and 7 dpl and declines by 50% over the next three weeks, while T-cell entry is not evident in the mouse until after 14 dpl (Sroga et al., 2003). Dendritic cell (normally absent in control rat or mouse spinal cord) infiltrate SCI wounds with T-cells in rats but not in mice, suggesting another difference in inflammatory reactions to SCI between mice and rats (Sroga et al., 2003). Dendritic cells are potent antigen-presenting cells and have ranging from T-cell activation to T-cell killing (Bernstein, 1986). Thus, accumulation of dendritic cells in a SCI wound could potentially be detrimental by stimulating infiltration of T-cells into the cord or protective by removing cytotoxic T-cells. Furthermore, a unique fibroblast-like cell population was observed in the newly formed ECM that resembled lymphocytes but did not express lymphocyte markers. This phenotype was characteristic of specialised blood-borne cells (fibrocytes) that are involved in wound healing and immunity, which are also present only in mice (Sroga et al., 2003, Chesney and Bucala, 1997). Although these

differential responses may explain why mice do not cavitate, it remains to be determined whether they contribute to different injury responsive molecular profiles observed in the two species. The differences in the inflammatory response between the two species may thus be a contributing factor to the development of cavities within the lesion site in rats.

CHAPTER 4

DIFFERENTIAL EXPRESSION OF ANGIOGENIC AND WOUND HEALING RESPONSES IN MICE AND RATS AFTER SUB-ACUTE SPINAL CORD INJURY

Sections of the introduction are published in the following review:

Kundi S., Bicknell R., Ahmed Z. (2013). The role of angiogenic and wound-healing factors after spinal cord injury in mammals. Neuroscience Research. 76, 1-9.

Surey S., Berry M., Logan A., Bicknell R., Ahmed Z (2014). Differential cavitation, angiogenesis and wound healing responses in injured mouse and rat spinal cords. Neuroscience. 275, 62-80.

4.1 Introduction

4.1.1 Angiogenesis

As previously mentioned angiogenesis is a multistep process requiring the interaction of the ECM and its component cells that is primarily triggered by tissue hypoxia (Chung et al., 2010). Each stage of angiogenesis requires different angiogenic molecules to aid in the degradation of the basement membrane, pericyte recruitment, outgrowth of endothelial tip-cells, and proliferation of stalk cells and migration, proliferation and maturation of the endothelial cells. Dysfunctional angiogenesis not only induces cavitation in human cancer, but further results in ischemia, haemorrhage and disruption of the blood spinal cord barrier (BSCB) that contribute to the detrimental secondary pathogenesis after SCI in rat lesion sites (Johnson et al., 2004, Marom et al., 2008, Crabb et al., 2009, Loy et al., 2002, Casella et al., 2006).

4.1.2 Vascular changes after SCI

Traumatic SCI causes an immediate loss of vascular supply initiating a multifaceted response to the injury. This alters the microvascular permeability for

days to weeks after injury resulting in neuronal loss and long-lasting damage to neuronal elements in the cord. Ischemia is one of the detrimental effects that play a part in the vascular changes after SCI that is exacerbated by haemorrhage, edema, excitotoxcity and poor perfusion resulting from vasospasm/vasoconstriction (Bullock and Fujisawa, 1992, Ducker and Assenmacher, 1969, Yang et al., 1994). Prolonged ischemia stimulates neovascularisation and the newly formed vasculature decreases glucose transport and increases BSCB permeability and 'leaky' tight junctions (Benton et al., 2009, Noble et al., 1996, Benton et al., 2008).

4.1.3 Hypoxia and hypoxia inducible factor (HIF) in SCI

Hypoxia regulates transcription of hypoxia inducible factor (HIF). HIF has three isoforms: HIF-1α, HIF-2α and HIF-3α. HIF-1 is a heterodimer of two DNA-binding proteins; HIF-1α and the aryl hydrocarbon nuclear translocator (ARNT or HIF-1β) (Ahmed and Bicknell, 2009). HIF-1α is rapidly degraded in normal oxygen levels and binds to ubiquitin ligase; Von Hippel-Lindau protein (pVHL) targeting HIF-1α for proteasomal degradation. When oxygen levels drop lower than 2%, HIF-1α is no longer degraded, translocates to the nucleus, dimerises with HIF-1β and causes the initiation of a complex transcriptional response in genes having specific hypoxia response elements (HRE).

In the CNS, activation of HIF-1α in the hypoxia-induced ischemia tolerance model of brain injury protects the brain from ischemic tissue by preconditioning with known activators of HIF-1α, such as cobalt chloride and desferrioxamine, before hypoxia induces ischemia (Nordal et al., 2004, Bergeron et al., 1999, Bergeron et al., 2000, Marti et al., 2000). Ischemia and hypoxia are prominent in the acute phase of

SCI and HIF-1α mRNA is expressed 12 hours after injury, peaking at 3 days and reducing gradually thereafter to near basal levels (Xiaowei et al., 2006, Yu et al., 2001). Most HIF-1α mRNA is localised in neurons but is also present in ependymal and endothelial cells (Xiaowei et al., 2006). Upregulation of glycolytic enzymes after SCI correlates with the expression of HIF-1α mRNA suggesting that active glycolysis takes place during these early time-points after SCI (Xiaowei et al., 2006). These data suggest that HIF-1α and its target genes such as VEGF limit damage after SCI by inducing hypoxia tolerance and neovascularisation in SCI lesions and are therefore potential for the treatment of SCI (Kundi et al., 2013).

4.1.4 Angiogenic Factors

4.1.4.1 Von Willebrand Factor (vWF)

vWF is a multimeric glycoprotein that was first identified in 1971 playing a vital role in haemostasis by functioning as both an anti-haemophilic factor carrier and a platelet-vessel wall mediator in the blood coagulation system (Zimmerman et al., 1971). The synthesis and storage of vWF is found in endothelial cells and megakarocytes (platelet precursor haematopoietic cells in the bone marrow) (Reininger, 2008). Glycoprotein 1bα (GP1bα); receptor for vWF, is expressed on the surface of platelets requiring no activation prior to binding with vWF (Reininger, 2008, Monteiro et al., 1999). Upon a vessel becoming injured three processes are activated as the first line of defense against bleeding, termed primary haemostasis (Reininger, 2008). Platelets react with an initial arrest from the flowing blood, followed by permanent adhesion and aggregation at the site of injury (Reininger, 2008).

Deficiencies or mutations in the protein or gene can result in the Von Willebrand's disease; the most common hereditary bleeding disorder, and atherosclerosis (van Galen et al., 2012). It is important to understand that elevated levels of vWF are equally as detrimental and have been associated with increased risk of ischemic cardiovascular events (van Galen et al., 2012).

vWF has been highlighted as a possible biomarker in the CNS when detecting childhood primary CNS vasculitis due to elevated levels of vWF at diagnosis in 65% of the children assessed with this condition (Cellucci et al., 2012). Increased blood-brain barrier (BBB) permeability is a hallmark of many CNS diseases and deficiencies in vWF have shown to promote BBB preservation in mouse models that are presented with increased BBB permeability, hypoxia/re-oxygenation and seizures (Suidan et al., 2013). The partial protection in BBB permeability did not provide protection but more surprisingly displayed a more severe pathology compared to wild-type mice. Given its role in the CNS as a biomarker and potentially reducing BBB permeability, research has been instigated to examine the levels of vWF after SCI and whether it could be a target for therapeutic options after injury.

4.1.4.2 vWF after SCI

For many years, vWF has been shown to play a part in the SCI response, but few researchers have used this molecule as a therapeutic target in treating patients, but more so in recognising the effect of SCI on vWF levels. After acute SCI in patients, levels of vWF were high at 6 and 10 days compared to patients who were immobilized without paralysis due to a fracture of the cervical spine (Petaja et al., 1989). Furthermore components of vWF increase after injury causing an increase in

platelet aggregability that contributes to hypercoagulation (Mammen, 1992). A major cause of morbidity and mortality in patients that suffer from SCI is thromboembolism. Following injury there is increase in activity of vWF and its antigen (Green, 1991). Contradictory to the earlier reports, levels of vWF and fibronectin remained normal in patients with uncomplicated chronic SCI compared to normal patients (Pahl et al., 1994). SCI has also been associated with coagulation abnormalities and using coagulation assays on patients with SCI that either had no deep vein thrombosis (DVT) or had DVT, showed no significant differences in the levels of vWF between the two groups (Fujii et al., 1992). It may be that due to the contradictory reports on vWF researchers have not considered as a target for therapeutic interventions after SCI.

4.1.5 Angiogenic Growth Factors

4.1.5.1 Vascular Endothelial Growth Factor (VEGF)

VEGF was first described as a tumor-derived factor, approximately 40kDa in size and a member of a family of 6 isoforms; VEGF-A, VEGF-B, VEGF-C, VEGF-D, VEGF-E and placental growth factor (PGF) (Senger et al., 1983). VEGF-A is considered as the most important isoform that stimulates mature angiogenesis, cell migration and proliferation whereas VEGF-B, VEGF-C and VEGF-D stimulate embryonic angiogenesis and lymphangiogenesis, respectively (Chung et al., 2010, Gerhardt et al., 2003, Ruhrberg et al., 2002). VEGF-A has several splice variants; VEGF-A 121, 145, 165, 189 and 206, with VEGF-A 165 being the predominant form, while VEGF isoforms are expressed in every tissue in adults (Acker et al., 2001, Bernini et al., 2002, Maharaj et al., 2006, Robinson and Stringer, 2001). VEGF is

upregulated during hypoxia by the action of HIF-1α and stimulates blood vessel morphogenesis by binding to VEGF receptor (VEGF-R) located on the cell surface of endothelial cells. VEGF is also neuroprotective, axogenic and supports the survival and proliferation of various types of glial cells (Rosenstein and Krum, 2004, Jin et al., 2000, Matsuzaki et al., 2001, Khaibullina et al., 2004, Mani et al., 2005, Sondell et al., 1999).

VEGF is a major angiogenic factor signaling through VEGF-R and many other pathways including the RAS/RAF and HIF-1α pathways, thereby restoring oxygen supply to tissues with inadequate blood circulation (Ahmed and Bicknell, 2009). Upon interaction with VEGF-R, several pathways are activated leading to: (1), gene expression and cell proliferation through induction of the MAPK cascade *via* Raf stimulation; (2), cell survival through PI_3K and PKB activation; and (3), cell proliferation and vasopermeability through activation of PLC-gamma (Figure 4.1). All these pathways are angiogenic and regulate endothelial cell function. However, over-expression of VEGF may contribute to disease, e.g. the formation of metastatic CNS tumours, particularly, primary brain tumours that correlate with disease progression (Stockhammer et al., 2000; Tassone et al., 2011, Olsson et al., 2006).

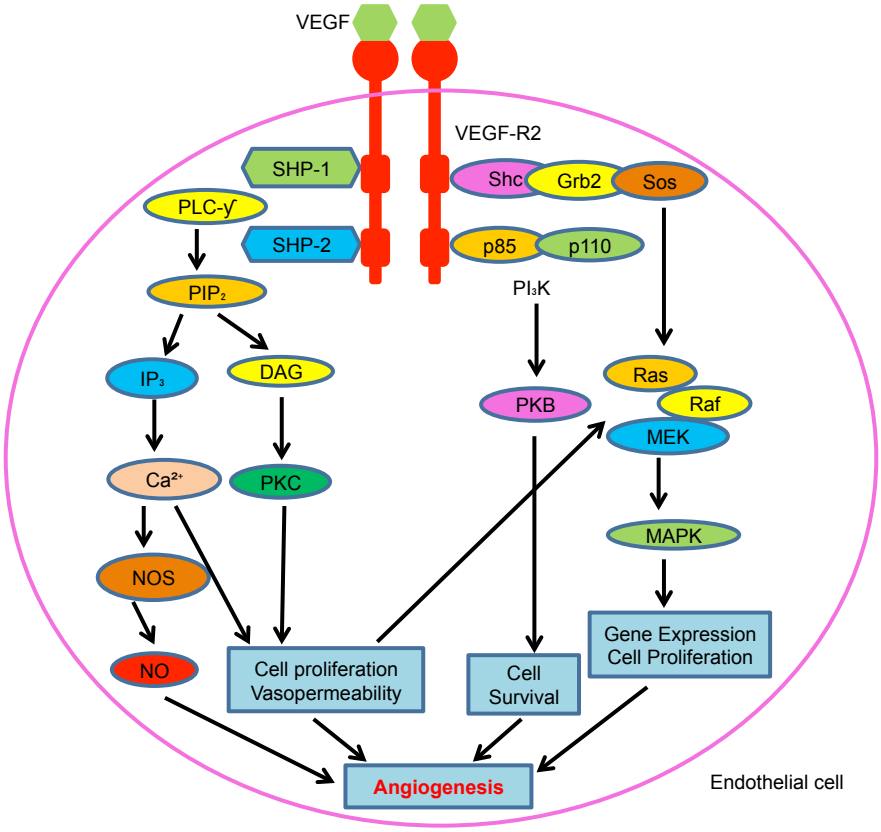

Figure 4.1 Vascular endothelial growth factor (VEGF) signalling pathway in angiogenesis. The building of VEGF to its receptor tyrosine kinase; VEGF-R2 causes the activation of various signalling molecules leading to a range of cellular responses. VEGF binding causes the activation of SHP-1 and SHP-2 resulting in other downstream molecules to become activated such as PLC-γ that goes on to activate PIP_2. Once PIP_2 is activated it goes down one of two pathways: DAG, PKC or IP_3, Ca^{2+}, NOS and NO, eventually leading to cell proliferation and vasopermeability. The activation of Shc, Grb2 and Sos causes activation of the MAPK cascade via Ras, Raf, and MEK stimulation resulting in gene expression and cell proliferation. The activation of p85 and p110 causes activation of PKB through PI_3K playing a part in cell survival. All these different processes lead to angiogenesis through the activation of VEGF (Adapted from Sigma-Aldrich).

4.1.5.2 VEGF after SCI

Studies on the role of VEGF in SCI are often contradictory and therefore it is difficult to judge the therapeutic utility of VEGF in promoting tissue sparing and functional recovery. Contradictory reports exist in the literature about changes in the expression of VEGF after SCI. For example, immediately after SCI tissue levels of VEGF mRNA and protein rise and eventually normalize by 14 days correlating with vascular permeability, rises in HIF-1α and the permeability of the BSCB that can have detrimental effects on recovery after SCI (Vaquero et al., 1999, Bartholdi et al., 1997, Skold et al., 2000, Akiyama et al., 2004, Casella et al., 2002, Loy et al., 2002, Benton et al., 2009). Later studies reported a reduction in VEGF isoforms 165, 121 and 189, in the SCI lesion epicenter where levels remained low for 1 month (Herrera et al., 2009). These findings cast doubt on the role of VEGF in regulating vascular events after SCI. Moreover, neutralizing VEGF after SCI neither altered the vascular density in the lesion epicenter nor exacerbates the histopathology and functional recovery after SCI (Benton et al., 2009).

Furthermore, studies on the use of the predominant form of VEGF; VEGF 165, further complicates whether the use of VEGF after SCI is beneficial or detrimental to the pathology of the injury. Administration of human recombinant VEGF-A_{165} via intraparenchymal injection into SCI lesions does not affect the microvascular architecture but does increase SCI lesion volume, suggesting that intraparenchymal injection of VEGF-A_{165} exacerbates the SCI injury by maintaining vascular permeability (Benton and Whittemore, 2003). However, repetitive intrathecal administration of VEGF-A_{165} after SCI neither changes tissue sparing, measures of behavioural recovery nor pain hypersensitivity through plasticity of pain afferents

(van Neerven et al., 2010, Deumens et al., 2008, Deumens et al., 2005). Aberrant sprouting of primary afferent pathways and rewiring of termination patterns result in abnormal processing of sensory stimuli, amplification of nociceptive signals causing debilitating chronic pain in >69% of SCI patients (Ondarza et al., 2003, Christensen and Hulsebosch, 1997, Finnerup et al., 2001, Siddall et al., 2003). SCI treatments are designed to reduce the development of chronic pain and promote maximal functional recovery (Deumens et al., 2008, Berger et al., 2011). $VEGF_{165}$ injection into a SCI lesion improves tissue sparing during the acute (early) phase but had no effect on the chronic (late) phase after SCI (Sundberg et al., 2011). Furthermore, $VEGF_{165}$ treatment enhances sensory recovery and possible remyelination, suggesting that it promotes plasticity of the sensory CNS pathways. However, VEGF treated animals showed increased incidence of persistent allodynia (a pain stimuli that does not normally elicit pain responses) and thus may be an inappropriate treatment for human SCI.

VEGF-A_{165} increases blood vessel density and tissue sparing in SCI wounds significantly enhancing behavioural recovery by 6 weeks (Widenfalk et al., 2003). Transplantation of immortalized human neural stem cells into SCI sites, stably expressing VEGF, increases blood vessel density, enhances tissue sparing and improves Basso, Beattie and Bresnahan (BBB) locomotor scores (Kim et al., 2009). While treatment with VEGF-A_{165} gives conflicting outcomes, it is important to recognise that other isoforms of VEGF such as VEGF-$A_{121/189}$ promote neuroprotection (Herrera et al., 2009).

Administration of engineered zinc finger protein (ZFP) transcription factor, which activates all isoforms of VEGF-A, improves outcomes in SCI, stroke, optic

nerve injury and traumatic brain injury probably by induction of angiogenesis (Liu et al., 2010, D'Onofrio et al., 2011, Siddiq et al., 2012). Raised VEGF-A mRNA and protein levels, increase vascularity, decrease neuronal apoptosis, attenuate axon degeneration, and improve both tissue preservation and neurobehavioural outcomes after treatment. These results are confirmed using optic nerve injury and cortical pial strip ischemia models, through the delivery of adeno-associated vector (AAV) encoded VEGF-ZFP's (D'Onofrio et al., 2011). VEGF-ZFP is neuroprotective, inducing angiogenesis and improving functional recovery (Siddiq et al., 2012). Sustained release of VEGF in combination with FGF-2 from microfabricated spinal cord bridges promotes angiogenesis and axon regeneration within CNS injury sites (De Laporte et al., 2011).

Administration of a VEGF/PDGF combination provides synergistic modulation of inflammatory reactions after SCI and creates a microenvironment that contributes to axon preservation and sprouting (Lutton et al., 2012). Co-administration of $VEGF_{165}$ and ANG-1 using viral vectors injected directly into the SCI lesion site immediately after injury reduces lesion volume and enhances vascular stabilization, improving locomotor recovery, suggesting that combining angiogenesis with vascular stabilization might have potential therapeutic applications for SCI lesions (Herrera et al., 2010).

The inconsistent results using VEGF in SCI, may be explained by the short half-life of VEGF peptide (3 min in circulation (George et al., 2000)). Hypoxia stabilises VEGF and increases its half-life while better outcomes are observed when VEGF is injected either exogenously, intraparenchymal or intrathecally and therefore route of administration should be taken into consideration for VEGF as a therapeutic

option for SCI (van Neerven et al., 2010, Benton et al., 2009, Levy, 1998, Benton and Whittemore, 2003, Yoo et al., 2006).

4.1.5.3 Fibroblast Growth Factors (FGF)

FGF belong to a family of heparin-binding growth factors with a high affinity for heparin sulphate proteoglycans (HSPG) (Cross and Claesson-Welsh, 2001). FGF were first purified from bovine pituitary glands, are approximately 18kDa in size and have 22 isoforms (Jonker et al., 2012, Ornitz and Itoh, 2001). FGF-1 – FGF-10 are the most well studied and bind to one of four tyrosine kinase receptors; FGFR1, FGFR2, FGFR3 and FGFR4 (Cross and Claesson-Welsh, 2001). FGF-1 is acidic whereas FGF-2 is basic and both are more potent pro-angiogenic factors than VEGF. FGF-1 and FGF-2 are normally sequestered in ECM and regulate endothelial cell proliferation (i.e. angiogenesis), cell differentiation and growth, tissue homeostasis and wound repair through the MAPK pathway (Jonker et al., 2012, Chung et al., 2010, Brooks et al., 2012, Cross and Claesson-Welsh, 2001, Abraham et al., 1986b, Abraham et al., 1986a). FGF-2 is present in both neuronal and non-neuronal cells whereas FGF-1 is confined to neurons (Dono, 2003, Reuss and von Bohlen und Halbach, 2003). In addition, FGF-1 and FGF-2 are neuroprotective and improve functional recovery in experimental models of head trauma and stroke (Moyer et al., 1998, Hossain et al., 1998, Madiai and Hackshaw, 2002, Hsu et al., 2009, Hattori et al., 1997b, Hattori et al., 1997a, Dono, 2003).

4.1.5.4 FGF after SCI

The levels of FGF-2 mRNA and protein increase adjacent to a SCI epicenter over the first 24 hours and peak 4 days later (Eckenstein et al., 1991, Frautschy et al., 1991, Follesa et al., 1994, Mocchetti et al., 1996). In models of SCI, FGF-2 rescues ventral horn neurons from death and by preserving axons it enhances functional recovery (Teng et al., 1998). Promising recovery of locomotor function occurs after injection of FGF-2 in a completely transected rat SCI model after 6 weeks, when animals begin to move their hind-limbs (Furukawa and Furukawa, 2007).

As mentioned previously, combined FGF-2 and VEGF therapy increases endothelial cell infiltration and blood vessel formation and protects grey matter from necrosis, improving both motor function and sensory re-innervation (De Laporte et al., 2011, Nordblom et al., 2012, Lee et al., 2011). Co-delivery of stem cells derived from bone marrow stromal cells (BMSC), amniotic epithelial cells or neural stem cells with FGF-1 and FGF-2 improves motor and sensory scores in patients 24 months after treatment (Wu et al., 2011, Liu et al., 2011). The delivery of FGF-1 and FGF-2 to the SCI sites using mononuclear cells, viral vectors and in combination with drugs such as Methylprednisolone (MP) promotes myelination and functional recovery (Shaimardanova et al., 2011, Huang et al., 2011, Baffour et al., 1995). Although the combined treatment of MP with FGF-1/-2 is beneficial in animal models, efficacy in human SCI is unproven (Akhtar et al., 2008, Blight, 2000, Hall, 1992, Hugenholtz, 2003, Hurlbert, 2000).

4.1.5.5 Angiopoietins (ANG)

ANG are a four-member secreted glycoprotein family comprising; ANG-1, ANG-2, ANG-3 and ANG-4 of which ANG-1 and -2 are most well characterised (Durham-Lee et al., 2012). ANG-1, -2 and -4 are expressed in humans, whereas ANG-3 is expressed in mice (Hansen et al., 2008, Valenzuela et al., 1999). ANG mediates angiogenesis, maturation and endothelial cell survival in all parts of the body including the brain and spinal cord (Valable et al., 2005, Zacharek et al., 2007, Kim et al., 2008, Han et al., 2010, Herrera et al., 2010, Ritz et al., 2010, Hansen et al., 2008, Thomas and Augustin, 2009). ANG mediate their responses through two receptor tyrosine kinases, Tie-1 and -2 (Thomas and Augustin, 2009). ANG-1 activates Tie-2 by phosphorylation through either the PI_3K or RAS pathways to promote cell survival, vessel growth and stabilisation, whereas ANG-2 does not induce Tie-2 autophosphorylation, but causes destabilisation of mature vessels by blocking the stabilising effects of ANG-1 (Procopio et al., 1999, Maisonpierre et al., 1997). ANG-2 also blocks the effects of ANG-1, promoting neovascularisation in the presence of VEGF (Pufe et al., 2005).

ANG-1 is expressed at low levels in normal brain and adult vasculature and is present on pericytes and smooth muscle cells, whereas ANG-2 is expressed more actively in endothelial cells to counteract ANG-1 signaling (Davis et al., 1996, Nag et al., 2005, Kim et al., 2000, Mandriota and Pepper, 1998, Sundberg et al., 2002, Ng et al., 2011, Adams and Alitalo, 2007). ANG-2 expression increases in blood vessels in hypoxic environments e.g. after stroke and brain injury and is angiogenic and also neurogenic for neural stem cells (Maisonpierre et al., 1997, Zhang et al., 2002, Nag et al., 2005, Ward and Lamanna, 2004, Marteau et al., 2011).

4.1.5.6 ANG-1 and ANG-2 after SCI

In normal tissues, ANG-1 maintains BSCB integrity by limiting vascular permeability through induction of PECAM1, occludin and ZO-2 tight junction proteins, thus strengthening paracellular interactions and reducing the number and size of endothelial gap junctions (Lee et al., 2009, Baffert et al., 2006, Hori et al., 2004, Gamble et al., 2000, Wong et al., 1997). After SCI, mRNA and protein levels of ANG-1 are downregulated and therefore the BSCB integrity is compromised (Ritz et al., 2010, Herrera et al., 2010, Durham-Lee et al., 2012). ANG-1 arrests the progression of the CNS injury-induced inflammation by activation of PI_3K and Akt, inhibiting inflammatory cytokines and adhesion molecules required for inflammatory cell migration, thus limiting the infiltration of inflammatory cells from the bloodstream (Fuxe et al., 2011, Gamble et al., 2000, Kim et al., 2001, Hughes et al., 2003). Although ANG-1 does not contribute to early angiogenic responses, it does play a role in the latter stages of migration, stabilisation and maturation of blood vessels (Wong et al., 1997). Intravenous injections of ANG-1 after SCI, improves locomotor function by rescuing blood vessels in and around the lesion epicenter and reducing inflammation (Han et al., 2010). Treatment with ANG-1 and C16 (αvβ3 binding peptide) restores almost full functional recovery by acting through αvβ3 integrin to promote angiogenesis.

Whilst ANG-1 is downregulated after SCI, the mRNA and protein levels of ANG-2 are upregulated up to 10 weeks after SCI but a role for ANG-2 in endothelial barrier breakdown was not supported in this study (Durham-Lee et al., 2012, Ritz et al., 2010). ANG-2 is not localised in endothelial cells after SCI but in astrocytes and $NG2^+$ oligodendrocyte precursor cells and high levels of ANG-2 correlate with

enhanced locomotor recovery, suggesting a beneficial role of ANG-2 in SCI (Durham-Lee et al., 2012, Ritz et al., 2010).

4.1.5.7 Transforming growth factor-βetas (TGFβ)

TGFβs are a superfamily of secreted cytokines of which there are three isoforms in mammals: TGFβ-1, TGFβ-2 and TGFβ-3 (Cui and Ackhurst, 1996, Khalil, 1999). Although Type I and II TGFβ receptor activation leads to phosphorylation of signal regulated mothers against decapentaplegic homolog-2 (Smad-2), TGFβ complexes with Smad4 allowing translocation to the nucleus and transcription of target genes that either stimulate or suppress tumorigenesis. TGFβ regulates cell growth, proliferation, tissue homeostasis, wound healing, apoptosis and scarring (Lagord et al., 2002, Huang and Huang, 2005, Kohta et al., 2009) (Figure 4.2). TGFβ, like many other angiogenic proteins may be tumorigenic when components of the signal transduction pathway become mutated (de Caestecker et al., 2000, Massague et al., 2000, Culhaci et al., 2005). In the adult mammalian brain, TGFβ-1 is restricted to the choroid plexus, meningeal cells and absent in neurons, whereas TGFβ-2 and TGFβ-3 is present in neurons in the developing adult brain and in astrocytes of adult CNS ((Maharaj et al., 2008, Bottner et al., 2000, Unsicker et al., 1991, Wilcox and Derynck, 1988). In the adult mammalian CNS TGFβ-R1 and TGFβ-R2 mRNA and protein are present in neurons and astrocytes, with TGF-βR2 being confined to several regions that include the choroid plexus particularly the epithelial and ependymal cells, cortex, midbrain, brain stem and the hippocampus (Maharaj et al, 2008, Vivien et al., 1998, Bottner et al, 1996).

4.1.5.8 TGFβ after SCI

In normal human spinal cord tissue TGFβ-1 is confined to the occasional blood vessels, motor neurons and intravascular monocytes, whilst TGFβ-2 is only found in intravascular monocytes (Buss et al, 2008). However, after traumatic SCI TGFβ-1 is localised to neurons, astrocytes and invading macrophages, whilst TGFβ-2 is localised to macrophages and astrocytes in the injured spinal cord. Immunoreactivity of TGFβ-1 was significantly upregulated 2 days post injury continuing for the first few weeks with a gradual decline up to 1 year in the human samples. Whilst TGFβ-2 was first detected 24 hours after injury and remained elevated for up to 1 year (Buss et al., 2008). TGFβ-1 and β-2 mRNA and protein levels increase after SCI and have possible roles in angiogenesis, inflammatory responses and wound healing (Lagord et al., 2002, Benton et al., 2009, Wang et al., 2009, Kritis et al., 2010, Aigner and Bogdahn, 2008). The levels of TGFβ-1 mRNA are highest 7 days post injury, whereas TGFβ-2 mRNA levels become elevated later at 8-14 days post injury (Semple-Rowland et al., 1995, McTigue et al., 2000, Lagord et al., 2002, Buss et al., 2008, Ritz et al., 2010).

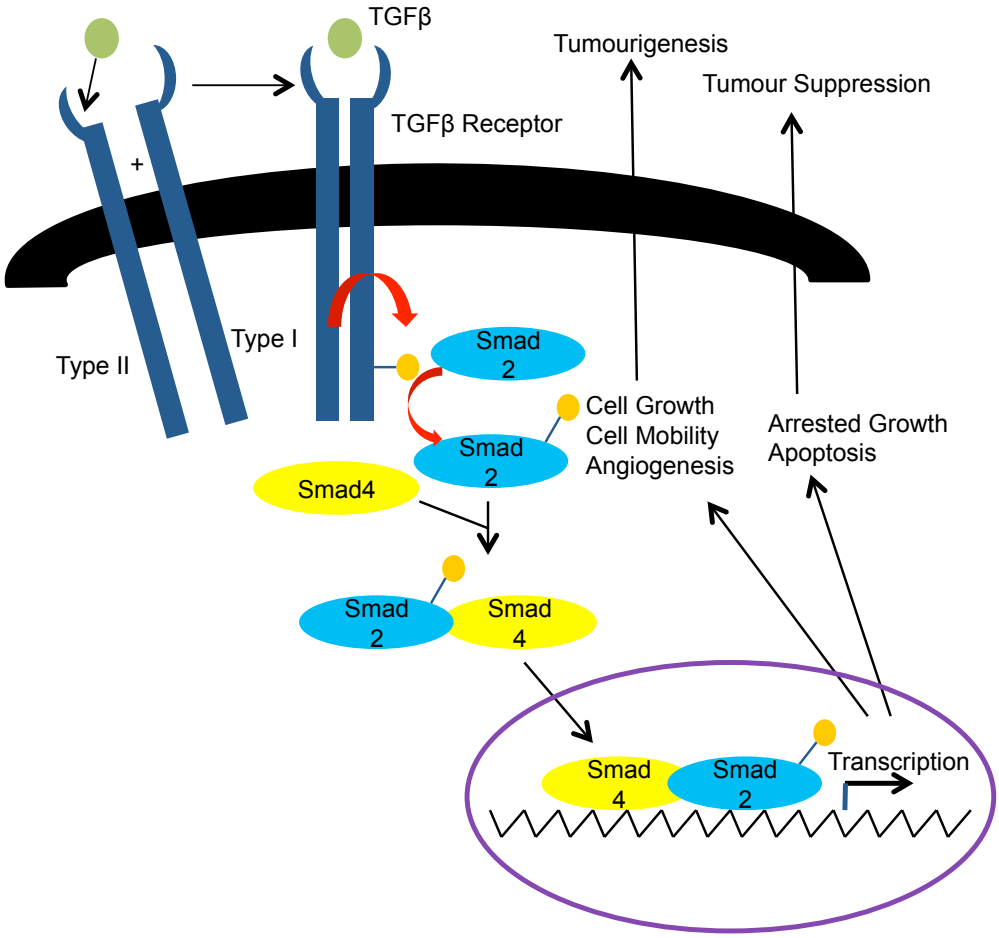

Figure 4.2 Transforming growth factor-beta (TGFβ) pathway and how it signals angiogenesis through signal regulated mothers against decapentaplegic homolog-(Smad)-2. The binding of TGFβ to its cell surface receptor TGFB-RII causes the phosphorylation of TGFB-RI. This allows TGFB-RI to phosphorylate and activate Smad2 protein. The activation of Smad2 causes it to bind with Smad4, once bound the Smad2/Smad4 complex translocates to the nucleus where it recruits various transcription factors. The activated Smad complex and transcription factors together activate the expression of target genes that regulate the biological effects of TGFβ. Some of the target genes act as tumour suppressors through arrested growth and apoptosis, whilst some stimulate tumourigenesis through angiogenesis cell mobility and cell growth (Adapted from Sigma- Aldrich).

However, titres of TGFβ-1 have been reported to decrease after SCI (Konya et al., 2008). Nonetheless, delivery of TGFβ-1 to SCI sites affect vascular recovery favourably since inhibition with a neutralizing antibody suppresses glial scar formation and enhances axon growth and preservation of axons caudal to the site of SCI (Kohta et al., 2009). Similarly, intravenous treatment with TGFβ after SCI reduces lesion volume by 50% at 48 hours post injury, probably due to the reduced accumulation of mononuclear phagocytes in and around the wound (Tyor et al., 2002). Therefore the decrease of mononuclear phagocyte numbers around the site of injury reduced their contribution to the detrimental secondary injury suggesting a beneficial role of TGFβ after SCI.

4.1.5.9 Platelet-derived growth factor (PDGF-BB)

PDGF's are a family of glycoprotein mitogens for mesenchymal cells that include smooth muscle cells, fibroblast and some populations of neuroectodermal origin such as oligodendrocytes (Fredriksson et al., 2004). PDGF's are made up of five dimeric isoforms; PDGF-AA, PDGF-BB, PDGF-AB, PDGF-CC and PDGF-DD with the expression patterns differing between isoforms. PDGF-AA and PDGF-CC are mainly expressed in epithelial cells, muscle and neuronal progenitors cells (NPC), whilst PDGF-BB are expressed in vascular endothelial cells, megakaryocytes and neurons. The expression patterns for PDGF-DD is the less characterized isoform but has been known to be found in fibroblasts and smooth muscle cells (Andrae et al., 2008).

PDGF bind to their tyrosine kinase receptors; PDGF receptor α (PDGFRα) and PDGF receptor β (PDGFRβ). Upon receptor binding the ligand-receptor complex

undergoes autophosphorylation causing downstream activation of the $P1_3K$/Akt and PLC-γ pathway, similar to that of VEGF, resulting in the regulation of cell growth, migration, proliferation, and therefore angiogenesis (Wu et al., 2008, Andrae et al., 2008). But continuous upregulation of PDGF can result in deleterious effects as demonstrated in many CNS diseases including stroke, Huntington's and Parkinson's disease (Funa and Sasahara, 2014, Ohno et al., 1999, Iihara et al, 1997, Ballagi et al., 1994).

Early research on PDGF-BB demonstrates endothelial proliferation and angiogenesis in an *in vitro* model of bovine aortic endothelial cells (Battegay et al., 1994). Neutralisation of PDGF-BB reduced cord/tube formation 37 +/- 10%, whilst neutralising PDGF-AA had no effect. PDGF-BB DNA synthesis also increased as cords and tubes were developed with its receptor; PDGFRβ and thus PDGF-BB being specific for cord/tube-forming endothelial cells only. It has been reported that PDGF-BB in conditioned medium is important for cell migration and invasion in radiation-induced senescence in securing-deficient human breast cancer cells, but also conditioned medium promoted angiogenesis in chicken chorioallantoic membrane through PDGF-BB (Yu et al., 2013).

The stimulating research of PDGF-BB led to instigate studies in the CNS. Early reports suggested a role of PDGF-BB in the developing cortex of the CNS by enhancing protein phosphorylation in neurons and type 1 astrocytes as well as inducing migration *in vitro* in neuroepithelial cells cultured from embryonic rat cortex (Forsberg-Nilsson et al., 1998, Zhang and Hutchins, 1997). Furthermore, PDGF-BB exerts neurotrophic and neuromodulatory effects in the CNS, whilst restoring proliferation and impaired neurogenesis in a rat model of HIV-associated neurological

disorder (HAND) after drug use (Yao et al., 2012, Pela et al., 2000, Kastin et al., 2003). PDGF-BB and its receptor have been suggested to induce angiogenesis and neuroprotection in humans after ischemic stroke (Krupinski et al., 1997). Contradictory to reports that PDGF-BB has beneficial effects to the CNS, in a recent study human serum samples were analysed using microarray analysis and validated by immunoassays from patients suffering from neurodegenerative syndromes; Parkinson's disease (PD), multiple system atrophy (MSA), progressive supranuclear palsy (PSP) and corticobasal syndrome (CBS). The levels of PDGF-BB increased in patients that suffered from these neurodegenerative syndromes, suggesting it as a possible biomarker (Mahlknecht et al., 2012).

4.1.5.10 PDGF-BB after SCI

Although research on PDGF-BB has shown positive yet contradictory results in the CNS, the available research on PDGF-BB as a therapeutic strategy after SCI is limited. Research has utilized re-vascularisation methods after SCI in an attempt to reduce secondary damage and increase the blood supply at the injury site. But regulation of the imbalance of pro- and anti-angiogenic factors after injury has shown to participate in the failure of blood vessel stabilisation and re-vascularisation (Graumann et al., 2011). Reduced expression of not only PDGF-BB but also VEGF-A, Ang-1 and PGF at the lesioned area results in vessel reduction at the injury site 2 days post injury before disappearing into the developing cavity in rats (Graumann et al., 2011, Ritz et al., 2010). It is proposed that reduction in pro-angiogenic factors also contributes to vessel regression and that applying angiogenic factors to the injury site may be a promising therapeutic application in resorting blood flow after SCI

(Ritz et al., 2010). As previously mentioned administration of a VEGF/PDGF combination provides synergistic modulation of inflammatory reactions after SCI and creates a microenvironment that contributes to axon preservation and sprouting (Lutton et al., 2012). This suggests that therapeutic application of PDGF-BB after SCI may be beneficial to the microenvironment displayed after injury by targeting endothelial cells.

4.1.5.11 Angiogenin

Angiogenin was first characterized in 1985 as a tumour-derived angiogenic protein that promotes angiogenesis and neovascularisation (Fett et al., 1985, Kishimoto et al., 2005, Tsuji et al., 2005). Human angiogenin is a secreted 123 amino acid, 14kDa protein located on chromosome 14q11 that belongs to the ribonuclease superfamily sharing 33% sequence homology with pancreatic ribonuclease A (Kurachi et al., 1985, Strydom et al., 1985, Weremowicz et al., 1990, Gao and Xu, 2008). In order for angiogenin-induced angiogenesis to occur four processes are necessary. These include ribonuclease activity, basement membrane degradation, signaling transduction and nuclear translocation (Gao and Xu, 2008). Whilst the ribonucleolytic activity of angiogenin is weak the ribonucleolytic site on angiogenin has shown to be essential for its role in angiogenesis (Hu et al., 1994, Moroianu and Riordan, 1994, Curran et al., 1993).

The binding of angiogenin to the endothelial cell surface is crucial for its biological function. In endothelial cells the angiogenin receptor is a 42kDa cell surface protein that was later discovered to be a smooth muscle type α-actin (Hu et al, 1991, Hu et al., 1993). Upon binding the angiogenin-actin complexes induces

degradation of the blood vessel basement membrane and the extracellular matrix thus promoting migration of vascular components (Hu et al., 1991, Hu et al., 1993, Hu et al., 1994). However in order for signal transduction to occur through angiogenin a different receptor is required. It was later identified that a potential angiogenin receptor for signal transduction was a 170kDa cell surface receptor located on the endothelial cell surface which has shown angiogenin-responsive abilities (Hu et al., 1997, Liu et al., 2001, Kim et al., 2007, Xu et al., 2001b).

Upon angiogenin binding it undergoes nuclear translocation where it regulates genes responsible for proliferation of endothelial cells by activating various pathways that include ERK, Akt, and SAPK/JNK pathways (Hu et al., 1997, Liu et al., 2001, Kim et al., 2007, Xu et al., 2001b). Nuclear angiogenin is particularly essential for angiogenesis induced by other angiogenic factors such as VEGF (Kishimoto et al., 2005). Though the expression of angiogenin is predominantly through endothelial cells, it is also expressed by a variety of anchorage-dependent proliferating cells that include fibroblasts, aortic smooth muscle cells, and tumor cells (Moenner et al., 1994). Furthermore, the expression of angiogenin is induced by HIF-1α under hypoxic conditions and cellular stress (Nakamura et al., 2006, Sebastia et al., 2009).

In mice angiogenin is expressed strongly in the CNS during development (Subramanian and Feng, 2007), whilst, in humans angiogenin is expressed strongly in motor neurons but also endothelial cells of normal fetal and adult spinal cords (Wu et al., 2007). It has been shown that wild type angiogenin stimulates neurite outgrowth and path-finding of motor neurons in culture, whilst mutant angiogenin not only lacks these properties but also induces motor neuron degeneration (Subramanian et al., 2008). Genetic mutations in angiogenin have been linked with

incurable amyotrophic lateral sclerosis (ALS); a progressive neurodegenerative disease with specific loss of motor neurons in the brain, brain stem and spinal cord (Crabtree et al., 2007, Greenway et al., 2006, Kishikawa et al., 2008, Pasinelli and Brown, 2006). It has further been proven that angiogenin plays a key factor to motor neuron survival *in vitro* and *in vivo* and that knock-down of angiogenin induced excitotoxic motor neuron death in mouse models of ALS (Kieran et al., 2008). It has been suggested that using angiogenin as therapeutic modulation in the spinal cord may be beneficial for patients suffering from ALS (Pasinelli and Brown, 2006, Kishikawa et al., 2008).

4.1.5.12 Angiogenin after SCI

Given the role angiogenin plays in CNS, the studies that report angiogenin as a therapeutic option after SCI is limited. However, the levels of angiogenin have been investigated using CSF from patients with and without SCI (Ng et al., 2011). After SCI patients showed significantly lower angiogenin CSF levels between 72 and 84 hours compared to controls with maximal differences seen at 72 hours, whilst in serum there was no change until 60 hours post-injury which continued to increase up until 120 hours (Ng et al., 2011). The serum values were not significantly different compared to controls. It is thought that using angiogenin as a therapy option after injury to the spinal cord may aid in motor neuron survival (Ng et al., 2011).

4.1.6 Anti-angiogenic factors

4.1.6.1 Tissue inhibitor of metalloproteinase-2 (TIMP-2)

TIMPs are natural, regulatory, inhibitors of matrix metalloproteinases apart of a four member family (TIMP-1, TIMP-2, TIMP-3 and TIMP-4) of peptidases involved in degradation of the ECM and processes required for metastasis and angiogenesis (Murphy, 2011, Valente et al., 1998). TIMPs have the ability to suppress proliferation of endothelial cells thus playing an essential role in tissue homeostasis. TIMP-1 was first cloned in 1985 where it was first recognised that TIMPs are inhibitors of metalloproteinases, followed shortly by TIMP-2; 1990/1989, TIMP-3; 1992, and TIMP-4; 1996 (Gasson et al., 1985, Docherty et al., 1985, Stetler-Stevenson et al., 1990, Stetler-Stevenson et al., 1989, Pavloff et al., 1992, Greene et al., 1996). The amino-terminal inhibitory domain of TIMPs bind to the active site of MMPs, in particular TIMP-2 binds to the active site found on proMMP-2 (Murphy, 2011). TIMP-2 is unique in that it not only inhibits MMP activity but also selectively interacts with membrane type 1 matrix metalloproteinase (MT_1-MMP) to induce cell-surface activation of proMMP-2. TIMPs show tissue-specific expression which is regulated at the transcriptional level by various growth factors and cytokines (Murphy, 2011). The molecular mechanism of TIMP-2 expression is controlled through ERK1/2 and p38 MAPKs and inhibition of ERK1/2 phosphorylation decreases TIMP-2 production, whilst downregulation of p38 MAPK activity enhances TIMP-2 synthesis (Munshi et al., 2004).

Early research on neurological diseases report the presence of TIMPs in the CNS particularly TIMP-1 and TIMP-2, for example, in patients with relapsing multiple sclerosis significantly higher levels of TIMP-1 and TIMP-2 were found than patients

with other neurological diseases compared to healthy controls (Lee et al., 1999). During viral and bacterial meningitis in the CNS immunohistochemical analysis from autopsy tissue revealed that mononuclear cells are highly immunoreactive for TIMP-2 in viral meningitis but even higher in bacterial meningitis (Sulik and Chyczewski, 2008). Whilst *in vitro* TIMP-2 is constitutively expressed in primary cultures from rat brain microvascular endothelial cells and in human neuroepithelial stem cells that once differentiated into neurons and glia the expression of TIMP-2 does not change (Harkness et al., 2000, Frolichsthal-Schoeller et al., 1999). Human astrocytes stimulated by conditioned medium from *myobacterium tuberculosis* monocytes (CoMTB) significantly increase the secretion of TIMP-2 by 3-fold at 120hrs in response to CoMTB treatment (Harris et al., 2007).

In vivo experiments supports the expression of TIMP-2 in the CNS, for example, in normal mice TIMP-2 is expressed in spinal motor neurons and skeletal muscle, and TIMP-2 deficient mice displayed motor deficits due to peripheral and central defects (Jaworski et al., 2006). In a stab injury model to adult rat brain the mRNA expression of TIMP-2 is significantly upregulated after injury in the neurons and microglia, also significant levels of TIMP-2 were seen 5 days after injury suggesting that it may play a part in biphasic opening in the BBB permeability after injury (Jaworski, 2000, Rosenberg et al., 1998).

4.1.6.2 TIMP-2 after SCI

TIMP-2, especially in the CNS have shown to play a part in BBB permeability, inflammation and tissue remodeling in response to injury so the question remains as to whether they play a crucial role after SCI. After traumatic SCI in patients with

complete injuries, the distribution of TIMP-2 was limited, with the occasional TIMP immuno-positive macrophages seen at short survival times. The strong induction of MMPs was not accompanied by expression of their inhibitors allowing the MMPs to exert their effects on the lesioned spinal cord (Buss et al., 2007).

In experimental spinal-cord ischemia-reperfusion injury in rats, TIMP-2 immunoreactivity at 3 hrs was similar to sham treated controls, that significantly increased by 24 hrs, suggesting that the levels may relate to biphasic breakdown of BBB permeability and glial scar formation with respect to collagen staining and that 3 hr perfusion may provide a critical reversible period to the injury response (Anik et al., 2011b). TIMPs have been investigated to understand whether they contribute the failure of regenerating sensory axons after dorsal root injury in rats (Zhang et al., 2006). TIMP-2 was significantly upregulated in the dorsal root entry zones, degenerating dorsal column and also upregulated by microglia/macrophages, especially at later postoperative survival times. This suggests that TIMPs may be involved in controlling tissue remodeling after dorsal root injury and that manipulation of the expression on TIMPs may provide a potential therapeutic option in promoting axonal regeneration into the lesioned area.

4.1.6.3 Semaphorin 3A (Sema 3A)

Semaphorins; originally named collapsin, were identified originally as axon guidance molecules but more recently they have been thought to be involved in other biological functions such as, angiogenesis and cancer (Luo et al., 1993, Kolodkin et al., 1993, Neufeld et al., 2005, Capparuccia and Tamagnone, 2009).

Semaphorins are grouped into classes; 1-8, depending on the species that they are located in (Table 4.1) (Yazdani and Terman, 2006).

Class	Species	Members of Semaphorin
1	*Caenorhabditis elegans* *Drosophila melanogaster*	Sema-1a Sema-1b
2	*Caenorhabditis elegans* *Drosophila melanogaster*	Sema-2a Sema-2b
3	*Danio rerio* *Mus musculus* *Homo sapiens*	Sema 3A, Sema 3B, Sema 3C, Sema 3D, Sema 3E, Sema 3F, Sema 3G
4	*Danio rerio* *Mus musculus* *Homo sapiens*	Sema 4A, Sema 4B, Sema 4C, Sema 4D, Sema 4E, Sema 4F, Sema 4G
5	*Drosophila melanogaster* *Danio rerio* *Mus musculus* *Homo sapiens*	Sema 5A Sema 5B Sema 5C
6	*Danio rerio* *Mus musculus* *Homo sapiens*	Sema 6A, Sema 6B, Sema 6C, Sema 6D
7	*Danio rerio* *Mus musculus* *Homo sapiens*	Sema 7A
V	Virus	Sema VA Sema VB

Table 4.1 The members of semaphorins, the species that they are generally located in and the class that they belong to and are ultimately named after (Yazdani and Terman, 2006).

Semaphorin 3A (Sema 3A) binds to plexins indirectly through the help of co-receptors; neuropilin-1 and neuropilin-2 (NP1 and NP2), and dimerisation of Sema 3A is important for its activity in growth-cone collapse and repulsive axon guidance through the RhoA pathway (Figure 4.3) (Neufeld et al., 2005, Tamagnone et al., 1999, Klostermann et al., 1998, Koppel and Raper, 1998). NP's bind to VEGF family members and their receptors therefore playing a vital role in angiogenesis rather than axon guidance (Rosenstein and Krum, 2004, Soker et al., 2002). Casaza et *al*, showed that Sema 3A does inhibit tumor cell migration in an NP1 dependent manner

by inhibiting vessel function without promoting metastasis whilst increasing hypoxia and necrosis in multiple mouse tumor models (Casazza et al., 2011). More recently it has been shown that Sema 3A suppresses VEGF-mediated angiogenesis in mice (Acevedo et al., 2008).

Sema 3A plays a role in the CNS as repulsive axon guidance molecules in demyelinating diseases such as multiple sclerosis (MS). *In vitro* studies demonstrate that in rat models of MS Sema 3A applied to demyelinating lesions resulted in failure of remyelination by inhibiting oligodendrocyte precursor cells (OPC), and in an adult murine model of MS, Sema 3A impairs OPCs recruitment in the active demyelinated area (Piaton et al., 2011, Syed et al., 2011). In a model of optic nerve injury in goldfish there was a decrease in Sema 3A in the retina in the early stages after injury (Rosenzweig et al., 2010). Intravitreal injections of Sema 3A after optic nerve injury led to irreparable damage to several pathways of the regenerative processes that include axon growth, survival of retinal ganglion cells and the clearance of myelin in the lesioned area. Demyelinating models of the CNS demonstrate that Sema 3A plays a detrimental role to the injury response.

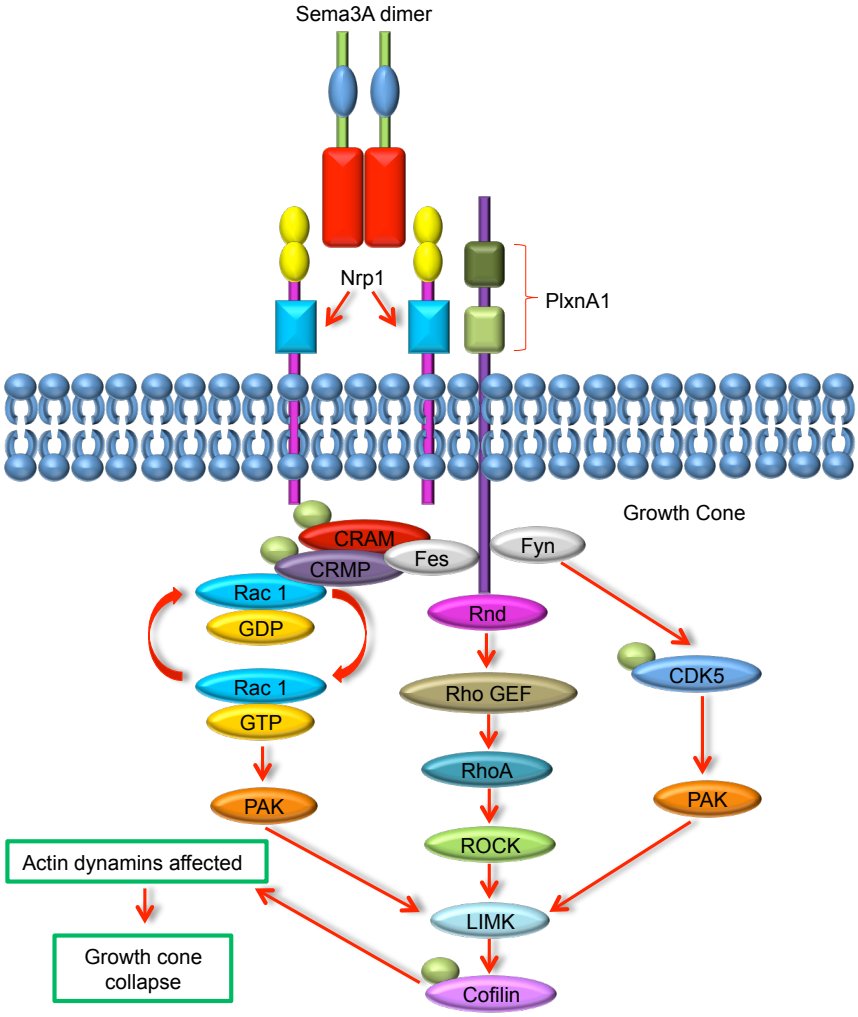

Figure 4.3 Semaphorin 3A is part of a family of growth cone guidance molecules that requires Nrp1 and PlxnA1 complex as the functional receptor. Sema 3A elicits a response from two signalling pathways upon binding to Nrp1; (1) Rac1; a small GTPase, that results in the depolymerisation of actin filaments and (2) PlxnA1 that binds the Rho-family GTPases; Rnd1 and RhoD pathway that results in the loss of integrin-mediated substrate adhesion and ultimately the initiation and modulation of cytoskeleton collapse. The activation of Nrp1/PlxnA1 complex also stimulates phosphorylation of Cofilin that down regulates its ability to promote actin filament turnover when phosphorylated by serine/threonine kinase; LIMK (Adapted from Qiagen genes and pathways).

4.1.6.4 Sema 3A after SCI

Providing the negative role Sema 3A plays in the CNS after injury it's no surprise that it provides a detrimental effect after neurodegenerative SCI. The expression of Sema 3A is seen in normal rat spinal cord and after T8 hemisection the expression decreases rapidly reaching its lowest level 1 day after injury and thereafter Sema 3A expression recovered when reaching 28 days. Immunoreactivity results revealed that neurons not glia were positive for Sema 3A in the spinal cord (Hashimoto et al., 2004). In situ hybridization and qPCR results demonstrated that mRNA and active protein of Sema 3A is produced in meningeal cell- conditioned medium from neonatal rat DRGs, further inducing the collapse of DRG growth cones, as well as inhibit neurite outgrowth of embryonic DRGs (Niclou et al., 2003).

Earlier reports in rats revealed that after complete transection and contusion lesions the expression of class 3 semaphorins is induced by fibroblasts in the neural scar and distribution through the scar differs between the two different lesions, suggesting that class 3 semaphorins contribute to the inhibitory environment of the neuronal scar tissue after SCI (De Winter et al., 2002). Inhibition of class 3 semaphorins, in particular Sema 3A, resulted in better functional recovery that was supported by enhanced regeneration and preservation of injured axons in rats after SCI (Kaneko et al., 2006). Sciatic nerve pre-conditioning before inducing SCI saw no change in Sema 3A levels and results remained the same (Pasterkamp et al., 2001). Sema 3A mRNA and protein are upregulated in the scar and motor neurons from 3 days up to 3 weeks after injury to the lumbar region of rats after intraspinal axotomy (Lindholm et al., 2004). The reports all demonstrate that Sema 3A plays a detrimental

role to axon regeneration, fibrotic scar tissue and neurite outgrowth and inhibition of Sema 3A should be considered as a therapeutic strategy for clinical SCI.

4.1.7 Matrix proteases

4.1.7.1 Matrix metalloproteinase 1, 2 & 9 (MMP-1, MMP-2 & MMP-9)

Matrix metalloproteinases (MMPs) are a family of zinc- and calcium-dependent endopeptidases that play an essential role in wound healing, repair and normal development throughout life via matrix remodeling (Page-McCaw et al., 2007, Yong, 2005, Birkedal-Hansen et al., 1993). There are 23 human and 24 murine MMP members that are classified into five specific groups dependent on protein structure and substrate specificity; (1) collagenases, (2) gelatinases, (3) stromelysins, (4) membrane-type and (5) others (Page-McCaw et al., 2007, Yong, 2005). Most MMPs are produced and secreted as inactive zymogens containing three structural domains; (1) the N-terminal propeptide domain, (2) an internal catalytic domain, and (3) a C-terminal hemopexin domain, whilst the membrane-type MMPs also contain a transmembrane domain that is linked to a plasma membrane (Zhang et al., 2011a). MMPs become activated once the propeptide domain is removed revealing the active catalytic site containing the zinc ion. There are a subset of MMPs that are activated intracellularly by serine proteases of pro-protein convertase such as MMP-11 and MMP-27 (Sternlicht and Werb, 2001). The activity and modulation of MMPs is regulated by their inhibitors; TIMPs, binding to their catalytic regions, but it is important to remember that their interaction with MMPs does not always lead to inhibition (Sternlicht and Werb, 2001, Crocker et al., 2004).

Over expression of MMPs can have detrimental effects, for example, the expression of MMP-2 correlates with increased angiogenesis by enhancing vascular proliferation in brain tumors, therefore enhancing the growth and invasive properties within the CNS in lung carcinomas (Rojiani et al., 2010). MMP-1 has shown to be upregulated in many cancers including colorectal and breast cancer, and that elevated expression of MMP-1 can promote local growth and formation of brain metastases by breast cancer cells (Liu et al., 2012, Sunami et al., 2000)

The expression and localization of MMPs in the adult CNS varies in humans, mice and rats and it is important to take this into consideration when modeling clinical SCI especially when comparing the responses of clinical to experimental SCI. The localization of MMP-1 in humans is confined to motor neurons of the spinal cord, whilst in rats MMP-1 is distributed in the spinal cord (Buss et al., 2007, Zhou et al., 2014). The localization of MMP-2 is confined to neurons, astrocytes and endothelium in the brain and DRGN's of the spinal cord in rats (Planas et al., 2001, Kawasaki et al., 2008). But in humans MMP-2 is confined mainly to astrocytes and microglia in the brain (Cuzner et al., 1996, Rosenberg et al., 2001). The localization of MMP-9 is confined to the meninges and ventral horn motor neurons in the spinal cord in mice, whilst in rats MMP-9 is confined to the DRGN's in the spinal cord and confined to neurons and myelinated fiber tracts in the brain (Planas et al., 2001, Noble et al., 2002, Kawasaki et al., 2008). But in humans MMP-9 is confined only to astrocytes and microglia in the brain (Cuzner et al., 1996).

The expression and localization of MMPs suggested that they may play a part in the CNS after injury and an early *in vitro* study comparing rat CNS microvascular endothelial cells to endothelial cells derived from rat aorta revealed differences in

expression in MMP-2 and MMP-9 between CNS and non-CNS endothelial cells (Harkness et al., 1999). Both MMP-2 and MMP-9 were constitutively expressed in CNS endothelium, but once CNS endothelium was activated with pro-inflammatory cytokines, no significant changes were seen in MMP-2 expression but expression was selective to upregulation of MMP-9 levels only. MMP-9 is a potent regulator of acute neuroinflammation and in a rat model of intracerebral hemorrhage MMP-9 levels increased (Hansen et al., 2013). Furthermore, edema and inflammation was reduced once MMP-9 was inhibited using Dexamethasone; a drug that is used to reduce edema clinically in brain and SCI patients (Yang et al., 2011).

4.1.7.2 MMP-1, MMP-2 and MMP-9 after SCI

The localization of MMPs after SCI has been investigated and found that the localization of MMP-1 was increased predominantly in astrocytes and neurons after injury, whilst, MMP-2 and MMP-9 was increased in reactive astrocytes that bordered the lesion epicenter (Hsu et al., 2006, Hsu et al., 2008, Zhou et al., 2014). This localization of MMPs after SCI differs in humans with MMP1 showing an early upregulation in macrophages in the lesion epicenter with a later induction in peri-lesional activated astrocytes (Buss et al, 2007). Furthermore, MMP-2 and MMP-9 was predominantly expressed in macrophages at the lesion epicenter only.

Given the role MMPs have on the microvasculature of the CNS, this lead to the effect of MMPs, in particular MMP-1, 2 and 9, have after SCI. After inducing a weight drop SCI in rats the expression of not only MMP-1 but also MMP-9 was increased in the injured cord and using Methylprednisolone inhibited the expression of both MMPs by inhibiting activator protein-1 and nuclear factor $_{\kappa}$B cascades (Xu et

al., 2001a). Human traumatic SCI displayed a lesion-induced bi-phasic expression of raised MMP-1 levels that was associated with an early up-regulation of macrophages within the lesion epicenter and later the induction of activated astrocytes (Buss et al., 2007). In response to tissue hypoxia following SCI angiogenesis occurs, and MMP-1; found on endothelial cells, is required for endothelial cell migration during angiogenesis (Mautes et al., 2000, Hiraoka et al., 1998).

Neuropathic pain is also a major consequence after SCI, and in a chronic constriction injury model in rats increases in MMP-2 were found in the sciatic nerve and spinal cord after injury, and using Atorvastatin; an inhibitor of MMP-2, levels reduced (Pathak et al., 2013). After partial sciatic nerve injury in mice MMP-9; confined to neurons and microglia, was expressed immediately after injury but returned to baseline levels 3 day post-injury, whilst MMP-2; confined to glial-like cells, was increasingly expressed gradually after nerve injury (Liou et al., 2013). The results indicated that MMP-2 should be considered as a therapeutic option when managing neuropathic pain after sciatic nerve or SCI. Inhibition of MMP-9 and MMP-2 activation after SCI in rats improves functional recovery using an ethanol extract; Bupleurum falcatum, further more reducing lesion volume (Lee et al., 2010, Lee et al., 2012). After photochemically inducing SCI in rats using rose Bengal significant upregulation of MMP-9 protein levels in the cord were observed at 6 hours and minimal levels were reached by 24 hours after the ischemic insult, whilst MMP-2 was not detected at any time point in both injured or control groups (Jang et al., 2011). MMPs in particular MMP-2 and MMP-9 are involved in the migration of olfactory ensheathing cells (OECs) *in vitro* on various CNS ECM substrates (Gueye et al., 2011).

The levels of MMP-9 are highly associated with the inflammatory responses after SCI due to infiltration of monocytes, and after C57BL/6 and MMP-9 knockout mice received lumbar enlargement to the cord, there was an increase in resident microglia within 24 hours in wild-type mice and by 7 dpl increases in MMP-9 expression were evident along with pro-inflammatory TNF-α (Zhang et al., 2011b). Deletion of MMP-9 attenuated remote microglia activation and restored TNF-α expression to homeostatic levels (Hansen et al., 2013). After spinal cord ischemic preconditioning injury in white Japanese rabbits, MMP-9 protein expression was reduced after injury which further attenuates increases in BSCB permeability due better preservation of tight junctions (Fang et al., 2013a, Lee et al., 2012). It has further been shown that traumatic SCI induced with arachnoiditis produced greater inflammation, measured by significant increases in MMP-9 activity and BSCB permeability, compared to both SCI and arachnoiditis on their own (Austin et al., 2012). Acute inhibition of MMP-9 using an MMP-9 inhibitor (SB-3CT), for two days after T9-T10 spinal cord hemisection produced significant increase in mitosis of NG2+ glia cells but not astrocytes, macrophages or microglia and thus causing an increase in oligodendrocytes during remyelination (Liu and Shubayev, 2011).

Nuclear factor erythroid 2-related factor 2 (Nrf2) is a key transcription factor against inflammation in the spinal cord, and after SCI in wild type Nrf2 and Nrf2 deficient mice MMP-9 expression was increased compared to sham controls, however in Nrf2 deficient mice there was an increase in edema, and more production and activation of MMP-9 compared the Nrf2 wild type mice after SCI (Mao et al., 2010a, Mao et al., 2010b). Sulforaphane; an anti-inflammatory extract reduced the levels and expression of MMP-9 and edema in mice that were treated after SCI than

those that simply had SCI with no treatment (Mao et al., 2010c). In rodents and humans, injury to the spinal cord triggered the expression of CD95 ligand (CD95L) on peripheral blood myeloid cells. Stimulation of CD95 on these cells activated phosphoinositide 3-kinase ($P1_3K$) and MMP-9 through the recruitment and activation of Syk kinase, resulted in increased migration. But deletion of CD95L on myeloid cells decreased the infiltration of neutrophils and macrophages into the injury site after SCI, ultimately leading to better functional recovery when only the ligand is deleted, and thus indicates that CD95L induces tissue damage by increasing the inflammatory response after injury (Letellier et al., 2010).

The effect stem cells have on the levels of MMPs have been investigated following spinal cord ischemia-reperfusion injury on white Japanese rabbits using bone marrow stromal cells that were injected 2 days before injury (Fang et al., 2013b). There was reduced expression of MMP-9 and this inhibition of MMP-9 provided a beneficial effect by stabilising the BSCB. In an *in vitro* model of axonal dieback and adult rat dorsal column crush, using multipotent adult progenitor cells (MAPCs) significantly decreased levels of MMP-9 release from macrophages and simultaneously prevented the induction of axonal dieback (Busch et al., 2011). Although the research may look contradictory, it is clear to see that the expression of MMPs after SCI is dependent on the type of injury model produced. MMPs do play a fundamental role in matrix remodeling and inflammation after SCI and therefore MMP-1 and MMP-2, but not MMP-9 at best should be considered as potential therapeutic options.

4.1.8 ECM/scar-related factors

4.1.8.1 Platelet endothelial cell adhesion molecule-1 (PECAM-1)

PECAM-1 is a 130kDa type 1 transmembrane glycoprotein originally cloned by Newman and colleagues, is also known as cluster of differentiation 31 (CD31) (Newman and Newman, 2003, Newman et al., 1990, Newman et al., 1987). PECAM-1 is a member of the immunoglobulin supergene family adhesion molecule found on the surface of circulating platelets, monocytes, neutrophils, a subset of T-cells and endothelial cells, is involved in various processes that include leukocyte migration, angiogenesis and integrin activation (Williams et al., 1996). PECAM-1, located on chromosome 17, is encoded by a 75-kb gene of which the extracellular domain consists of 574 amino acids organised into 6 immunoglobulin-like homology domains, a 19-residue transmembrane domain, and a 118- amino acid cytoplasmic tail (Newman and Newman, 2003). It makes up a large portion of endothelial cell intercellular junctions and in response to cellular stimulation the serine and tyrosine residues in the cytoplasmic domain of PECAM-1 requires regulated phosphorylation of signaling complexes and interactions with components of the cytoskeleton (Newman and Newman, 2003).

Early research has demonstrated that PECAM-1 plays an important role in inflammation in the CNS (Williams et al., 1996). In a rat model of experimental allergic encephalomyelitis (EAE) the expression of PECAM-1 by CNS endothelial cells is not necessary for the initiation of inflammation following the adoptive transfer of myelin reactive CD4+ T cells, but that PECAM-1 may play a role in regulating antigen-specific T cell trafficking in CNS inflammatory diseases (Williams et al., 1996, Qing et al., 2001). Whilst, in a PECAM-1 deficient KO mouse model of EAE

infiltration and mononuclear cell extravasation of the CNS occurred at earlier time-points in PECAM-1-KO mice compared to wild-type and T cell transendothelial migration across PECAM-1-KO endothelial cells is enhanced regardless of PECAM-1 expression (Graesser et al., 2002).

Early studies show that PECAM-1 also plays a part in the BBB permeability in the developing CNS in mice (Lossinsky et al., 1997). PECAM-1 is expressed on the endothelial cell surface in newborn animals which increases at 7-10 days post-partum and then decreases to weak labeling on endothelial cell surface by 2 weeks after birth. The results display active angiogenesis during early brain development in the mouse and that upregulation of PECAM-1 may help in the development of an 'immune' BBB prior to anatomical closure of the BBB (Lossinsky et al., 1997). Brain tissue from individuals with HIV encephalitis displayed an accumulation of cleaved, soluble form of the extracellular region of PECAM-1 (sPECAM-1) including elevated levels in their serum, thus correlating with enhanced transmigration of leukocytes into the CNS and the changes in BBB permeability (Eugenin et al., 2006).

4.1.8.2 PECAM-1 after SCI

Considering the role PECAM-1 plays in the CNS not only a part of the inflammatory response but also the integrity of the BBB in early development, it's surprising the amount of research instigated on the effect and response it has on SCI is limited. The vascular response during wound healing in adult mice has been assessed using PECAM-1 in a weight drop model (Whetstone et al., 2003). There was a significant loss of PECAM-1^+ blood vessels 1-3 days post injury, but by 3-7 days there was a significant increase in the number of PECAM-1^+ vessels that had

returned to control values by 7 days. Within the healing cord at 7 days after injury majority of vessels were PECAM-1^{+}, contributing to the wound healing response in mice (Whetstone et al., 2003, Goussev et al., 2003).

In a spinal cord reperfusion model in rabbits using an intravenous injection of ATL-146e; a selective adenosine A(2A) agonist, demonstrated a reduction in spinal cord endothelial PECAM-1 expression compared to animals that did not receive ATL-146e (Cassada et al., 2002). The adenosine agonist reduced spinal cord reperfusion injury in animals due to the reduction in spinal cord PECAM-1^{+} endothelium upregulation.

The effect of stem cell transplantation using PECAM-1 cells in SCI model has been investigated to see whether functional recovery by angiogenesis and neurogenesis stimulation is improved. In particular, using three-dimensional cell mass of human adipose-derived stem cells (3DCM-ASCs) *in vitro* confirmed that the stem cells differentiated into PECAM-1^{+} endothelial cells (Oh et al., 2012). Furthermore, *in vivo* experiments where 3DCM-ASCs were transplanted into an injured cord model differentiated into PECAM-1^{+} endothelial cells and remained differentiated compared to PBS and adipose-derived stem cell (ASCs) controls. The transplantation of 3DCM-ASCs significantly elevated the density of vascular formations due to angiogenic factors released by 3DCM-ASCs at the lesion site, enhancing axonal growth and functional recovery compared to PBS and ASCs controls. Research using PECAM-1 as a therapeutic strategy after SCI shows promising results in the wound healing, angiogenic and axonal growth responses that ultimately result in better functional recovery. These factors make PECAM-1 favorable especially when considered for clinical environment.

4.1.8.3 Collagen-1 (Col-1)

In the body collagen is the most abundant protein, and with 16 members 80-90% consists of collagen types I, II and III (Lodish et al., 2000). Being the main component of connective tissue and the ECM it's expression, particularly collagen type 1, is confined to skin, tendon, bone, dentin, ligaments and interstitial tissues. Collagen type 1 was first characterised due to its ease of isolation and high abundance in rat tail. Collagen type I is a long, thin protein of which the structural unit consists of three coiled subunits: two α1 and one α2 chains. Each chain consists of 1050 amino acids that wind around each other to form a characteristic right-handed triple helix (Shoulders and Raines, 2009). The interruptions in the triple helix and other three dimensional structures give each collagen its unique properties.

Given that collagen is the main component of the ECM and connective tissue, studies in the CNS demonstrate the advantage of using collagen type 1 in tissue engineering using scaffolds or gels to assess the repair, regeneration and proliferation of cells after injury (Ding et al., 2010, Ma et al., 2004). In a rabbit model of sciatic nerve injury nano-silver and collagen type 1 scaffolds were immersed into laminin solution and implanted into the lesioned area to repair 10mm of injury. The nano-silver containing collagen scaffolds showed higher rate of laminin absorption, regenerated nerve with a thick myelin sheath and improved nerve conduction compared to control scaffold without nano-silver demonstrating that nano-silver-collagen scaffolds are essential to the functionality in repair of peripheral nerves (Ding et al., 2010). Neural stem and progenitor cells isolated from embryonic rat cortical or subcortical neuroepithelium were cultured in 3D collagen gels (Ma et al., 2004). These 3D gels were first to demonstrate functional synapse and neuronal

network formation in a 3D matrix gel in the CNS, suggesting it as a possible therapeutic in promoting neuronal regeneration *in vivo*.

4.1.8.4 Col-1 after SCI

Collagen type 1 has shown to play a role in CNS especially after injury which instigated the effect collagen type 1 may have after SCI. Early research has demonstrated that application of rat tail collagen type 1 to the lesioned area after SCI in rats supports functional recovery despite the absence of corticospinal axons (Houweling et al., 1998a, Houweling et al., 1998b). And using rat tail collagen type 1 as a matrix on cervical spinal injury shows that four weeks after injury provided directional re-growth of injured axon tracts into the collagen implant (Joosten et al., 1995).

The expression of collagen type 1 after contusive SCI in adult rats was detected in mRNA. Collagen type 1 was observed around blood vessels in the white matter at 4 weeks after injury along with an increase in fibroblast immunoreactivity, suggesting that collagen type 1 may play a role in angiogenesis after SCI and that fibroblast may produce collagen type 1 in rat spinal cord (Okada et al., 2007). Confirming that fibroblasts produce collagen type 1, after contusive SCI perivascular collagen 1α1 cells were found to be the main source of cellular components of the fibrotic scar in transgenic mice. These type 1 collagen cells were identified as perivascular fibroblasts that were located around larger blood vessels and were distinct from pericytes that are typically located around microvessels (Soderblom et al., 2013). Pericytes are important in regulating endothelial cell function including vascular formation, stabilization and remodeling (Hirsch and D'Amore, 1996).

However, in the brain they contribute largely to BBB permeability and the integrity of structural vessels and thus play an important role in the wound healing process and therefore scarring after injury (Karén, 2010).

Collagen-filament scaffolds have demonstrated to support axonal regeneration and functional recovery in transected spinal cord in rabbits at 12 and 24 weeks after injury (Yoshii et al., 2009). BBB scores remained high in animals treated with the scaffold compared to controls suggesting the possibility of therapeutic application in humans. Various studies report that transplantation of neural stem/precursor cells (NSPCs) into adult rat injured spinal cord promotes functional recovery and using collagen type 1 as a scaffold for NSPC transplantation, or NSPCs in 3D collagen type 1 gels support cell survival and cell migration under optimal conditions that potentially allows NSPCs to differentiate into neurons, astrocytes and oligodendrocytes into the injured spinal cord (Watanabe et al., 2004, Watanabe et al., 2007). Using collagen type I in SCI especially as a matrix aiding molecule to the lesioned area shows promising results as a therapeutic strategy that should be considered clinically. All these various factors provide evidence to the effect that they have on the microvasculature of the injured cord whether it is beneficial or detrimental when using it as a therapeutic application.

4.2 Rationale

Our model so far has demonstrated differential responses in cavitation, laminin deposition and inflammatory responses after sub-acute SCI between mice and rats. Mice revealed no cavity formation, increased laminin deposition confined only to the lesion area and increased localisation of inflammatory markers 8 dpl after sub-acute

SCI. Whilst, rats developed large cavities which were almost devoid of laminin deposition within the lesion area and decreased inflammatory response after injury. This led to propose that mice may have a more robust wound-healing response and are able to overcome the adverse conditions compared to rats after injury. Therefore, using 8 dpl as a time point that showed the greatest differences between these factors, to investigate early angiogenic responses between the two species using other known angiogenic/wound healing-related proteins.

4.3 Hypothesis

The increased expression and localisation of angiogenic/wound-healing related proteins after sub-acute SCI in mice correlates with no cavity development and an adequate balance between wound healing, vascularisation and scar tissue. Thus, large cavity development in rats is due to an inadequate balance in scar tissue, neovascularistion and wound healing and therefore a decrease in the expression and localisation of angiogenic/wound healing-related factors. Therefore preventing cavitation will spare axons from damage, resulting in better functional recovery.

4.4 Aims

- To analyse rat and mouse lesion areas using known angiogenic/wound healing-related proteins at 8 dpl using immunohistochemistry.
- To confirm immunohistochemical results by western blot and densitometric analysis.
- To determine the levels of hypoxia using CNS specific carbonic anhydrase 10 (CA10) between mice and rats after injury.

- To examine the levels of axonal sparing in the corticospinal tract using protein kinase C and neurofilament 200 between mice and rats at 8 dpl.
- To determine differences in functional recovery after sub-acute SCI between mice and rats using planter heat and Von Frey hair test.

4.5 Materials and Methods

4.5.1 Experimental design

Please refer to Material and Methods section 2.1 Animal surgery, 2.2.1 and 2.2.2 Tissue preparation for immunohistochemistry and western blotting and 2.6 Functional test procedures for standard protocols used.

Type of analysis	N -numbers	End-points (days)
Angiogenic/wound healing immunohistochemistry	6 (per time point/species	0, 8
Angiogenic/wound healing western blot analysis	6 (per time point/species	0, 8
Functional tests	5 (per species/group)	-1 (day before), 0 (2hrs after surgery), 7, 14, 21
Axonal sparring	6 (per time point/species	0, 8

Table 4.2 Experimental design indicating n numbers and end-points used to assess angiogenic/wound healing localisation and protein expression after sub-acute SCI in mice and rats and the effect this has on functionality and axonal sparring.

4.5.2 Antibodies used for fluorescent immunohistochemistry

Please refer to Materials and Methods section 2.3.2 Fluorescent immunohistochemistry for standard protocol used. Fluorescent immunohistochemistry was used to assess the localisation of various angiogenic/wound-healing related proteins at 8 dpl (Table 4.3).

Angiogenic/Wound-healing related proteins	Dilution Factor	Species	Supplier (catalogue no.)
Primary Antibodies			
Von Willebrand Factor (VWF)	1:200	Rabbit	Dako (A0082)
FGF2 (Fibroblast Growth Factor)	1:200	Rabbit	Selective Genetics (7115193)
Angiopoietin-1	1:200	Rabbit	Abcam (ab8451)
Semaphorin	1:200	Rabbit	Abcam (ab23393)
VEGF-A	1:400	Rabbit	Abcam (ab46154)
Angiogenin	1:100	Rabbit	Santa Cruz Biotechnology (sc-9044)
TIMP-2 (Tissue Inhibitor of Matrix Metalloproteinases)	1:200	Rabbit	Neomarkers (Rb-1789-P1)
MMP-1 (Matrix Metalloproteinases)	1:200	Sheep	Biogenesis (5980-0111)
MMP-2 (Matrix Metalloproteinases)	1:100	Rabbit	Chemicon International (ab37150)
MMP-9 (Matrix Metalloproteinases)	1:100	Rabbit	Santa Cruz Biotechnology (sc-10737)
PECAM-1 (Platelet Endothelial Cell Adhesion Molecule)- CD31	1:100	Rabbit	Santa Cruz Biotechnology (sc-28188)
TGFβ-2 (Transforming Growth Factor)	1:200	Rabbit	Santa Cruz Biotechnology (sc-90)
PDGF-BB (Platelet-Derived Growth Factor)	1:200	Rabbit	Genzyme (AB1487)
Collagen-1	1:200	Rabbit	Abcam (ab292)
Carbonic Anhydrase X	1:100	Rabbit	Abcam (ab91247)
Protein kinase C	1:250	Rabbit	Abcam (ab71558)
Neurofilament 200	1:200	Rabbit	Sigma-Aldrich (N4142)
Secondary Antibodies			
Alexa 488	1:400	Rabbit	Molecular Probes (A11034)
Alexa 594	1:400	Sheep	Molecular Probes (A1105)

Table 4.3 Primary and secondary antibodies used to label wound healing/angiogenic- related proteins by immunohistochemistry.

4.5.3 Antibodies used for western blotting

Please refer to Materials and Methods section 2.5 Western blot analysis for standard protocol used. Western blot analysis was used to assess the protein expression of various angiogenic/wound-healing related proteins at 8 dpl (Table 4.4).

Angiogenic/Wound-healing related proteins	Dilution Factor	Species	Supplier (catalogue no.)
Primary Antibodies			
Laminin	1:100	Rabbit	Sigma (L9393)
Von Willebrand Factor (VWF)	1:200	Rabbit	Dako (A0082)
FGF2 (Fibroblast Growth Factor)	1:200	Rabbit	Selective Genetics (7115193)
Angiopoietin-1	1:100	Rabbit	Abcam (ab8451)

Semaphorin	1:200	Rabbit	Abcam (ab23393)
VEGF-A	1:1000	Rabbit	Abcam (ab46154)
Angiogenin	1:100	Rabbit	Santa Cruz Biotechnology (sc-9044)
TIMP-2 (Tissue Inhibitor of Matrix Metalloproteinases)	1:200	Rabbit	Neomarkers (Rb-1789-P1)
MMP-1 (Matrix Metalloproteinases)	1:100	Sheep	Biogenesis (5980-0111)
MMP-2 (Matrix Metalloproteinases)	1:100	Rabbit	Chemicon International (ab37150)
MMP-9 (Matrix Metalloproteinases)	1:100	Rabbit	Santa Cruz Biotechnology (sc-10737)
PECAM-1 (Platelet Endothelial Cell Adhesion Molecule)- CD31	1:1000	Rabbit	Santa Cruz Biotechnology (sc-28188)
TGFβ-2 (Transforming Growth Factor)	1:200	Rabbit	Santa Cruz Biotechnology (sc-90)
PDGF-BB (Platelet-Derived Growth Factor)	1:200	Rabbit	Genzyme (AB1487)
Carbonic Anhydrase X	1:200	Rabbit	Abcam (ab91247)
Alpha Tubulin	1:2000	Rabbit	Abcam (ab125267)
Secondary Antibodies			
Horseradish Peroxidase (HRP)	1:1000	Sheep	GE Healthcare (RPN4201)
Horseradish Peroxidase (HRP)	1:1000	Rabbit	GE Healthcare (NA934)

Table 4.4 Primary and secondary antibodies used to label wound healing/angiogenic- related proteins by western blot.

4.6 Results

4.6.1 Comparison of factors in rat and mouse DC wounds at 8 dpl

Since our results have demonstrated the greatest differences in cavitation, laminin and inflammatory (GFAP, fibronectin, ED1 and NG2) immunoreactivity at 8 dpl, we selected this time point for further analysis using 15 different known angiogenic/wound healing-related proteins in mice and rats.

4.6.1.1. Angiogenic factors

vWF immunoreactivity was present within the lesion area and surrounding white (WM) and grey matter (GM) in mice (Figure 4.4A). Although similar observations were seen in WM and GM in rats, vWF was confined to the boundaries of the

lesioned area (Figure 4.4B). Immunoreactivity quantification was done in ImageJ by measuring integrated density in an area containing the lesion site in mice and rats, levels were normalised to intact controls revealing no significant difference between mouse and rat vWF immunoreactivity levels in the lesion sites 8 dpl (Figure 4.4C).

To confirm differences observed by immunohistochemistry in mice and rats, western blot analysis (Figure 4.4D) followed by densitometry (Figure 4.4F) was used to quantify relative levels of proteins in spinal cords after injury. Results confirmed that there was no significant difference in the comparison of vWF in mouse and rat lesion areas after sub-acute DC injury.

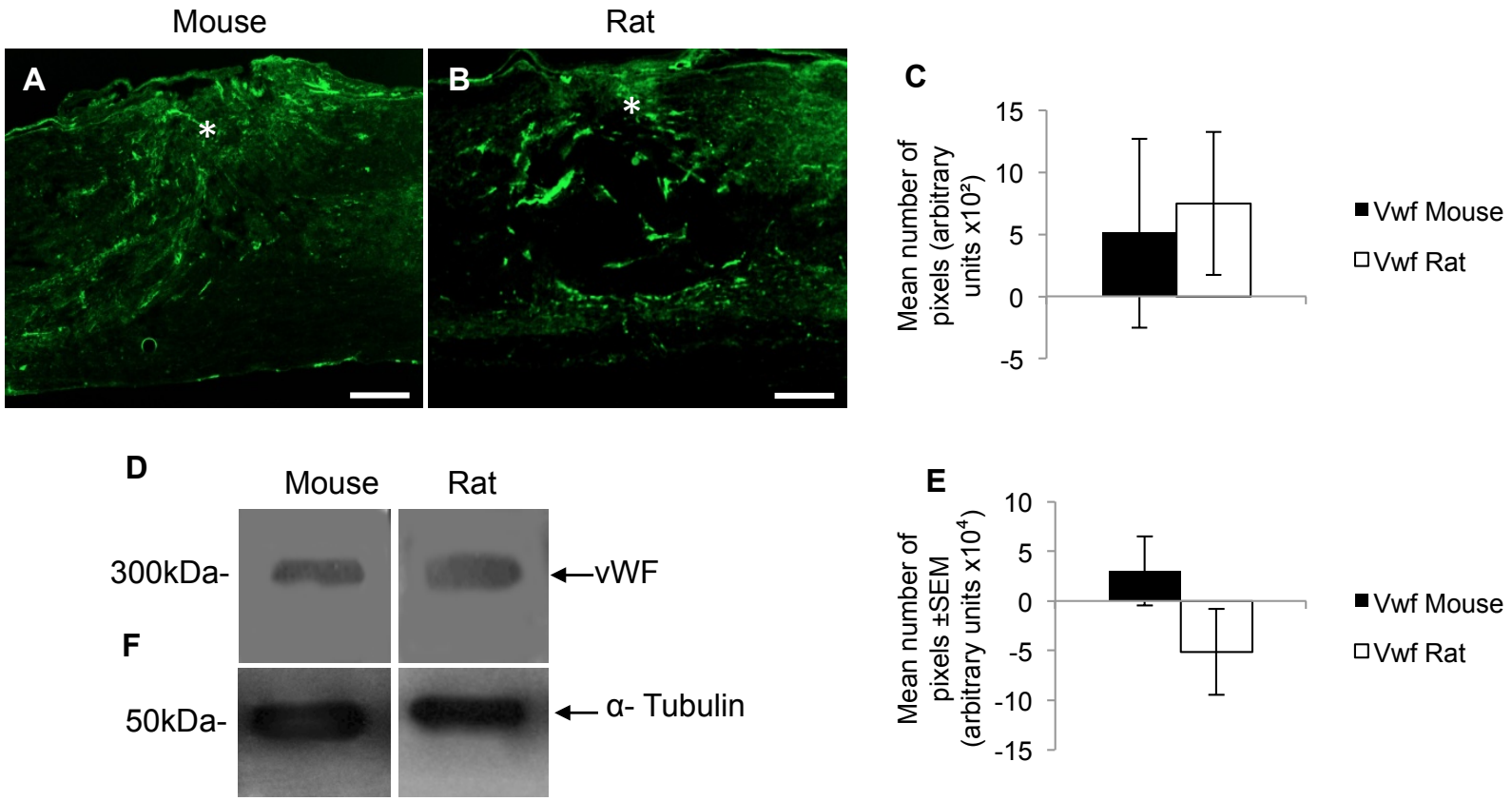

Figure 4.4 The localisation of vWF at 8 dpl in DC lesions. Immunohistochemistry for vWF in mice **(A)** and rats **(B)** and pixel intensities of vWF^{+} fluorescence **(C)** revealed no significant differences. Western blot **(D)** and densitometry **(E)** corroborated the immunohistochemistry results (α-tubulin was used as a protein loading control, image demonstrates a representative picture **(F)**; scale bars in A and B = 200 μm, * = lesion epicentre).

4.6.1.2. Angiogenic growth factors

The immunoreactivity of VEGF-A, TGFβ-2, PDGF-BB, FGF2, angiogenin and angiopoeitin-1 was observed in mouse and rat lesion areas 8 dpl (respectively, Figure 4.5-4.10 A-C). In the mouse these growth factors were localised within the lesion site, surrounding neuropil and parenchyma and up to 5 mm either side of the lesion epicenter (respectively, Figure 4.5-4.10A), whilst in rats these angiogenic growth factors were absent from the lesion site with low levels of immunoreactivity in the surrounding neuropil (respectively, Figure 4.5-4.10B). Quantification at 8 dpl revealed significantly increased immunoreactivity of VEGF-A, TGFβ-2, PDGF-BB, FGF2, angiogenin and angiopoeitin-1 by 0.6-, 3.5-, 3.1-, 0.7-, 1.9-, 0.3-fold, respectively, in mice compared to rats (respectively, Figure 4.5-4.10C and Table 4.5).

Factor	**Mean Intensity (pixels) (± SEM)**	
	Mouse	**Rat**
VEGF-A	$15 \times 10^2 \pm 5 \times 10^2$	$-25 \times 10^2 \pm 7 \times 10^2$
TGFβ2	$28 \times 10^2 \pm 6 \times 10^2$	$-8 \times 10^2 \pm 4 \times 10^2$
PDGF-BB	$31 \times 10^2 \pm 3 \times 10^2$	$10 \times 10^2 \pm 4 \times 10^2$
FGF2	$6 \times 10^2 \pm 2 \times 10^2$	$-8 \times 10^2 \pm 2.5 \times 10^2$
Angiogenin	$19.9 \times 10^2 \pm 3 \times 10^2$	$10 \times 10^2 \pm 5.4 \times 10^2$
Angiopoeitin-1	$8 \times 10^2 \pm 3 \times 10^2$	$-24 \times 10^2 \pm 9 \times 10^2$

Table 4.5 Mean fluorescence intensities of angiogenic growth factors in sections of spinal cord at 8 dpl after DC injury.

Western blotting (respectively, Figure 4.5-4.10D) and subsequent densitometry (respectively, Figure 4.5-4.10E) demonstrated that the levels of angiogenic growth factors; VEGF-A, TGF-β2, PDGF-BB, FGF2, angiogenin and angiopoeitin-1, were significantly higher in mice compared to rats (Table 4.6).

Factor	Mean integrated density (arbitrary units) (± SEM)	
	Mouse	Rat
VEGF-A	$5 \times 10^4 \pm 0.8 \times 10^4$	$-1 \times 10^4 \pm 0.6 \times 10^4$
TGFβ2	$2 \times 10^4 \pm 0.1 \times 10^4$	$0.5 \times 10^4 \times 0.1 \times 10^4$
PDGF-BB	$-9 \times 10^4 \pm 1.2 \times 10^4$	$-13 \times 10^4 \pm 0.2 \times 10^4$
FGF2	$17 \times 10^4 \pm 5 \times 10^4$	$1 \times 10^4 \pm 0.15 \times 10^4$
Angiogenin	$10 \times 10^4 \pm 0.2 \times 10^4$	$-2 \times 10^4 \pm 0.12 \times 10^4$
Angiopoeitin-1	$4 \times 10^4 \pm 0.8 \times 10^4$	$-3 \times 10^4 \pm 0.2 \times 10^4$

Table 4.6 Mean integrated density of angiogenic growth factors in mouse and rat SCI sites at 8 dpl, determined by western blotting.

These results confirm that after sub-acute SCI, there is activation of angiogenic growth factors that aid in the wound healing, vascularisation responses seen in mice 8 dpl compared to rats.

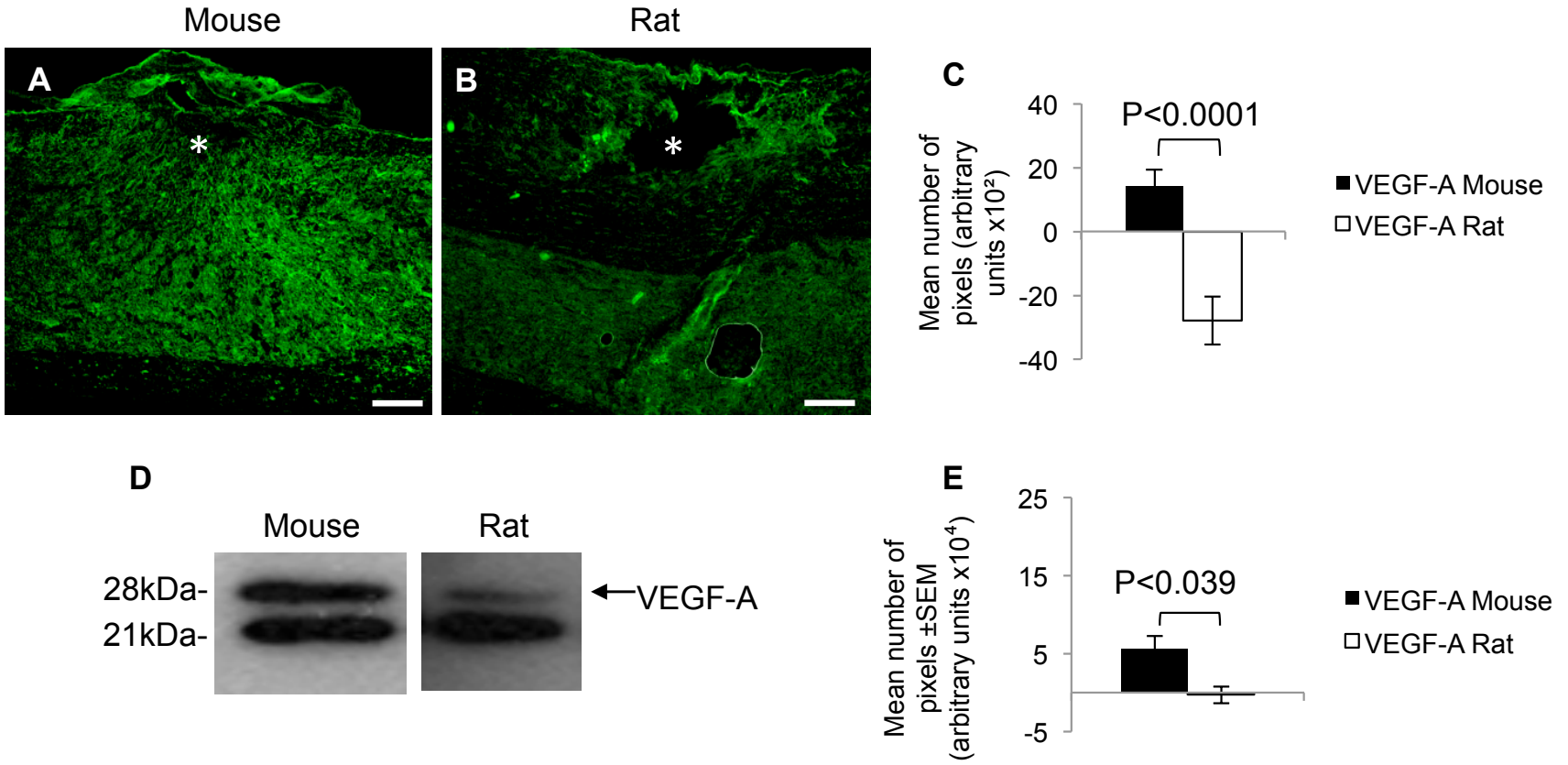

Figure 4.5 The localisation of VEGF-A at 8 dpl in DC lesions. Immunohistochemistry for VEGF-A in mice **(A)** and rats **(B)** and pixel intensities of VEGF-A^{+} fluorescence **(C)**. Western blot **(D)** and densitometry **(E)** corroborated the immunohistochemistry results (the same α-tubulin was used as a protein loading control as in Figure 4.4F; scale bars in A and B = 200 μm; * = lesion epicentre).

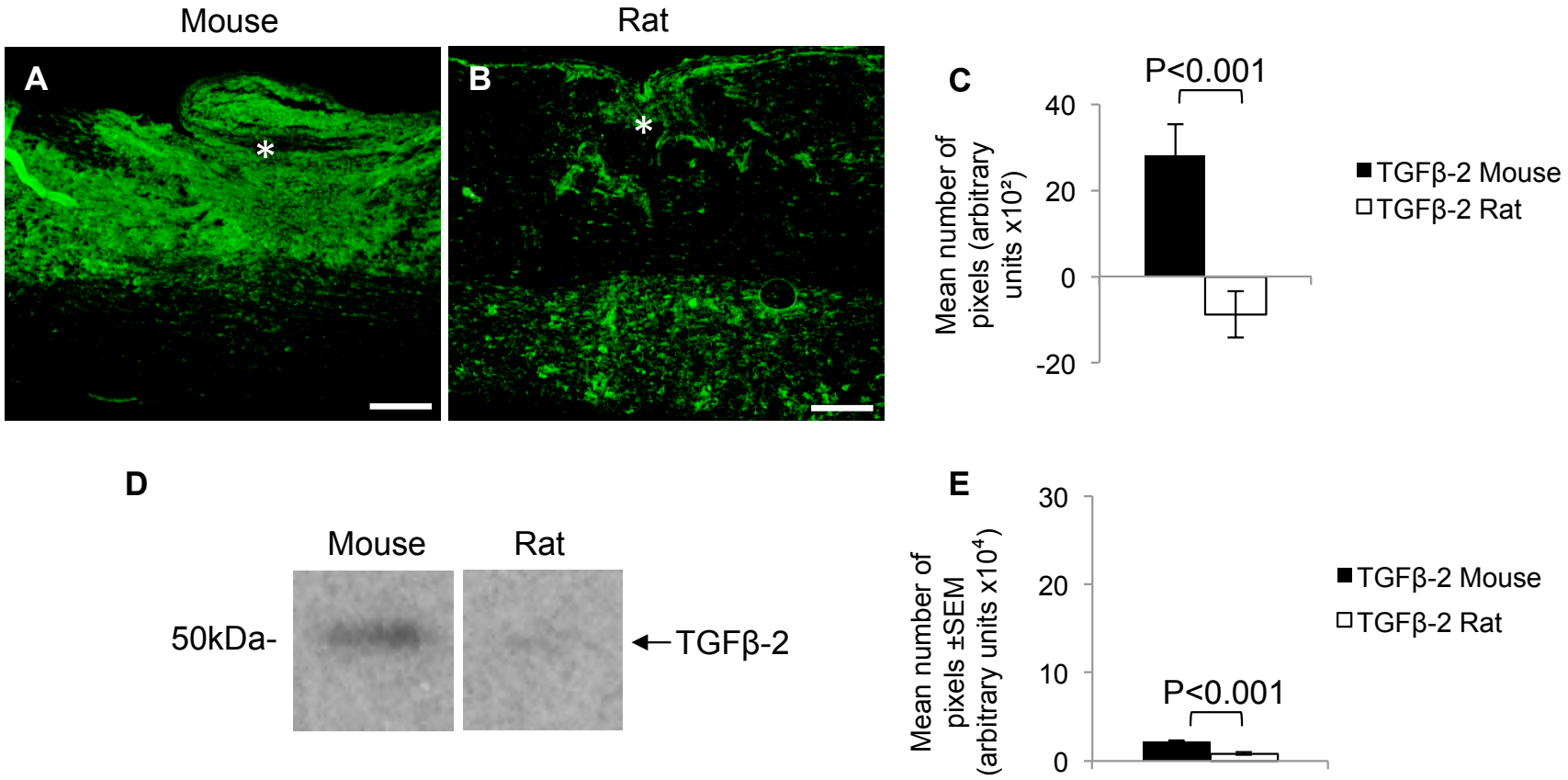

Figure 4.6 The localisation of TGFβ-2 at 8 dpl in DC lesions. Immunohistochemistry for TGFβ-2 in mice **(A)** and rats **(B)** and pixel intensities of TGFβ-2^{+} fluorescence **(C)**. Western blot **(D)** and densitometry **(E)** corroborated the immunohistochemistry results (the same α-tubulin was used as a protein loading control as in Figure 4.4F; scale bars in A and B = 200 μm; * = lesion epicentre).

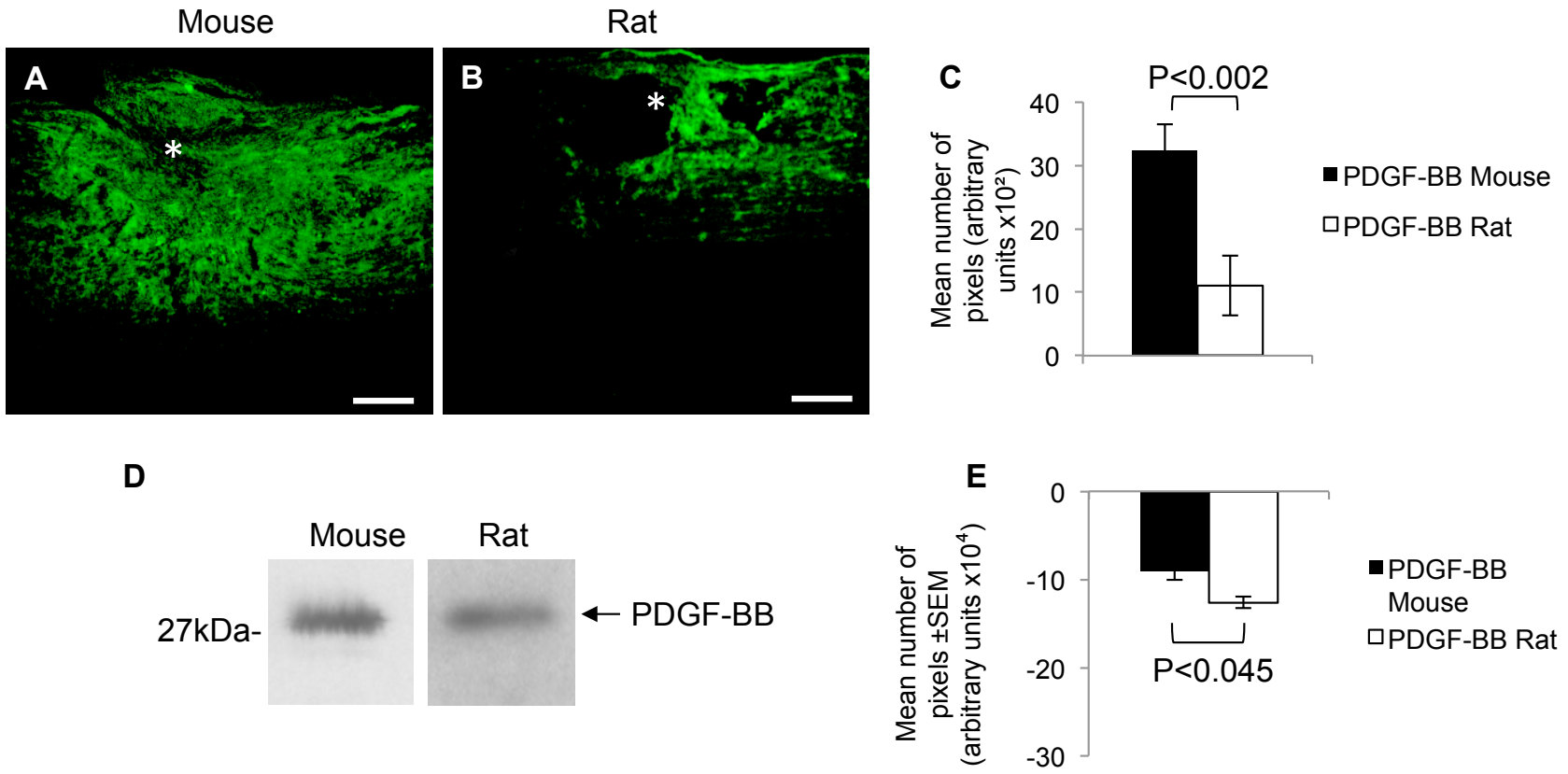

Figure 4.7 The localisation of PDGF-BB at 8 dpl in DC lesions. Immunohistochemistry for PDGF-BB in mice **(A)** and rats **(B)** and pixel intensities of PDGF-BB$^+$ fluorescence **(C)**. Western blot **(D)** and densitometry **(E)** corroborated the immunohistochemistry results (the same α-tubulin was used as a protein loading control as in Figure 4.4F; scale bars in A and B = 200 μm; * = lesion epicentre).

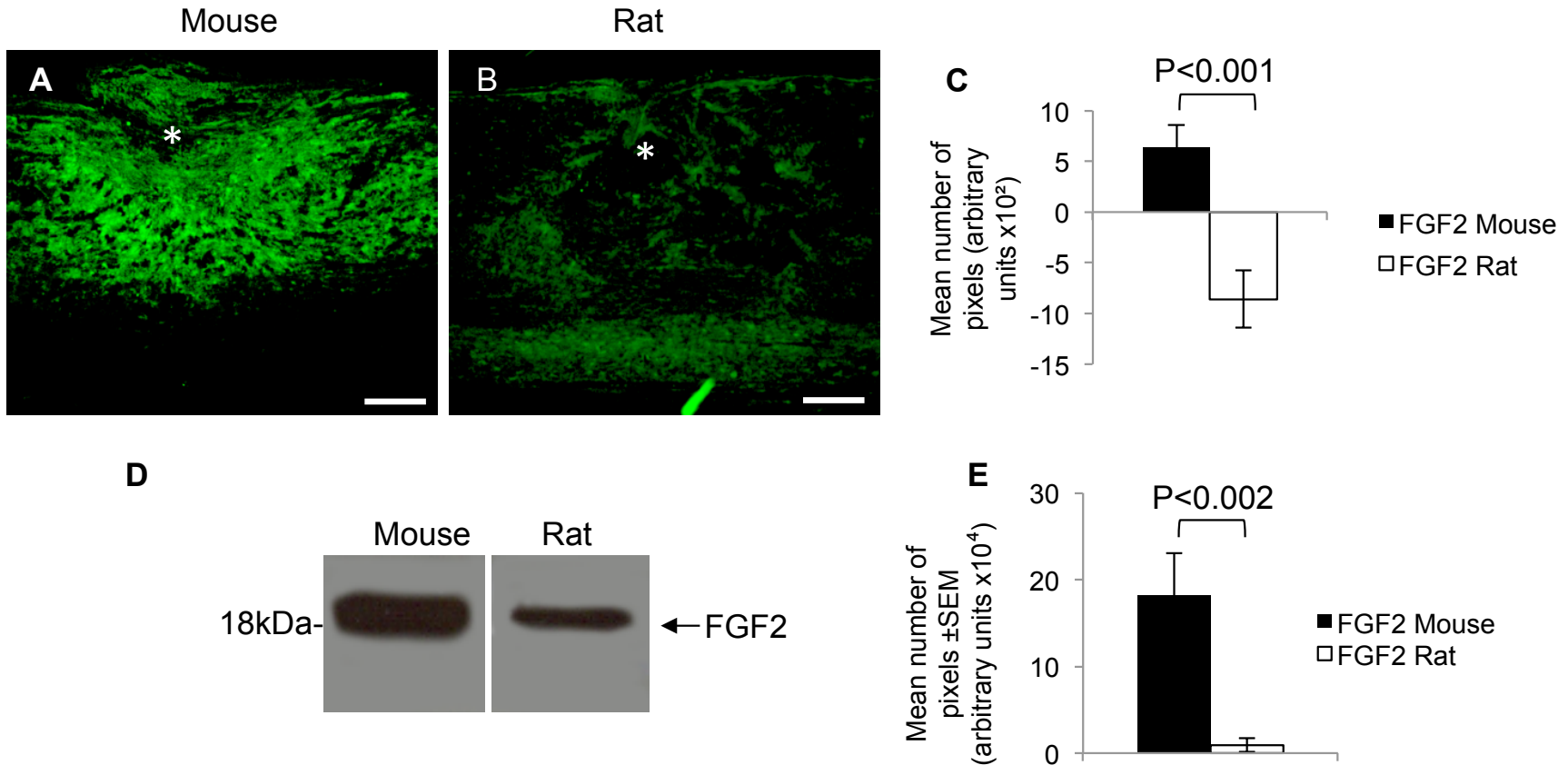

Figure 4.8 The localisation of FGF2 at 8 dpl in DC lesions. Immunohistochemistry for FGF2 in mice **(A)** and rats **(B)** and pixel intensities of $FGF2^{+}$ fluorescence **(C)**. Western blot **(D)** and densitometry **(E)** corroborated the immunohistochemistry results (the same α-tubulin was used as a protein loading control as in Figure 4.4F; scale bars in A and B = 200 μm; * = lesion epicentre).

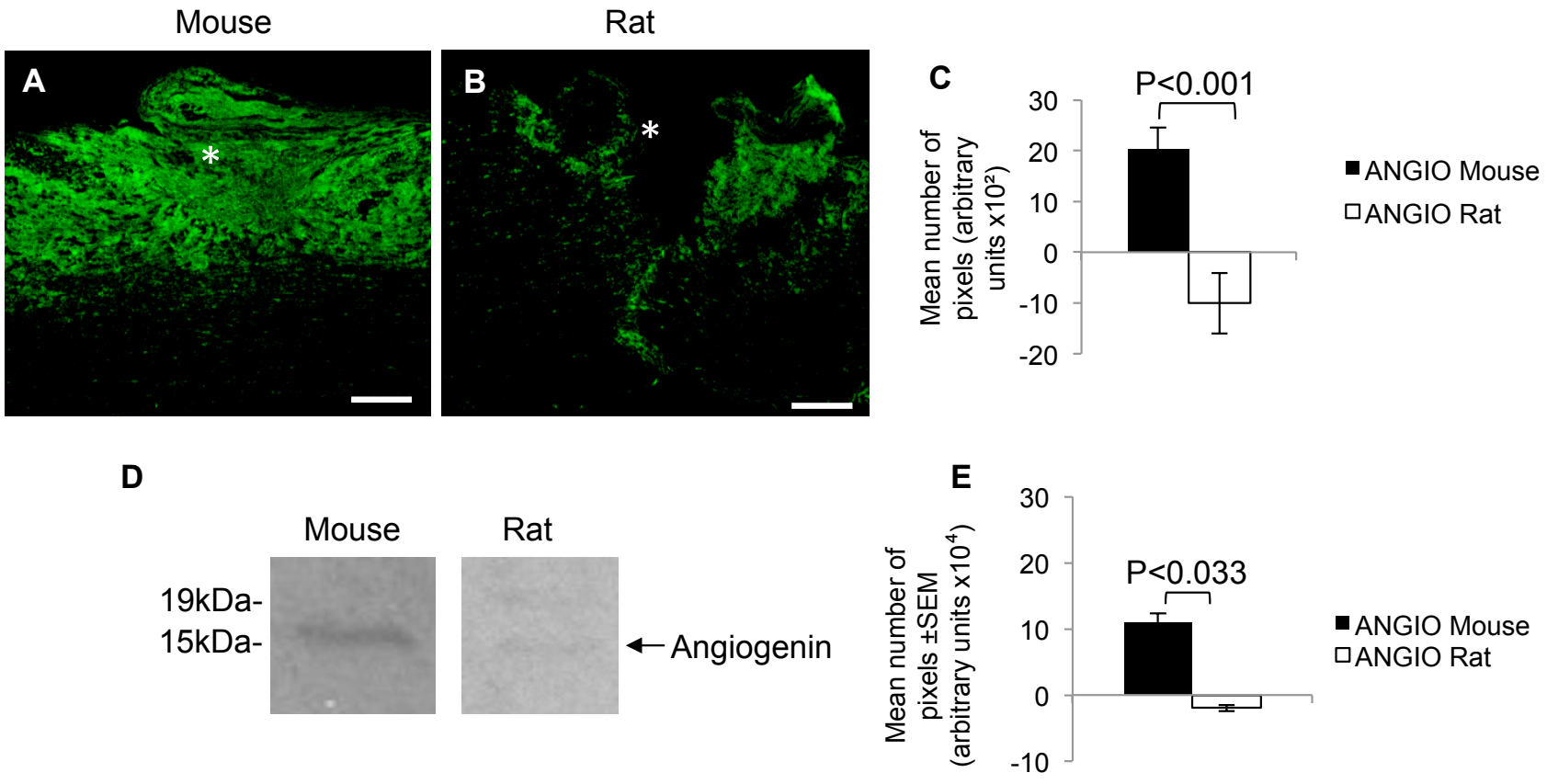

Figure 4.9 The localisation of Angiogenin at 8 dpl in DC lesions. Immunohistochemistry for Angiogenin in mice **(A)** and rats **(B)** and pixel intensities of Angiogenin^{+} fluorescence **(C)**. Western blot **(D)** and densitometry **(E)** corroborated the immunohistochemistry results (the same α-tubulin was used as a protein loading control as in Figure 4.4F; scale bars in A and B = 200 μm; * = lesion epicentre).

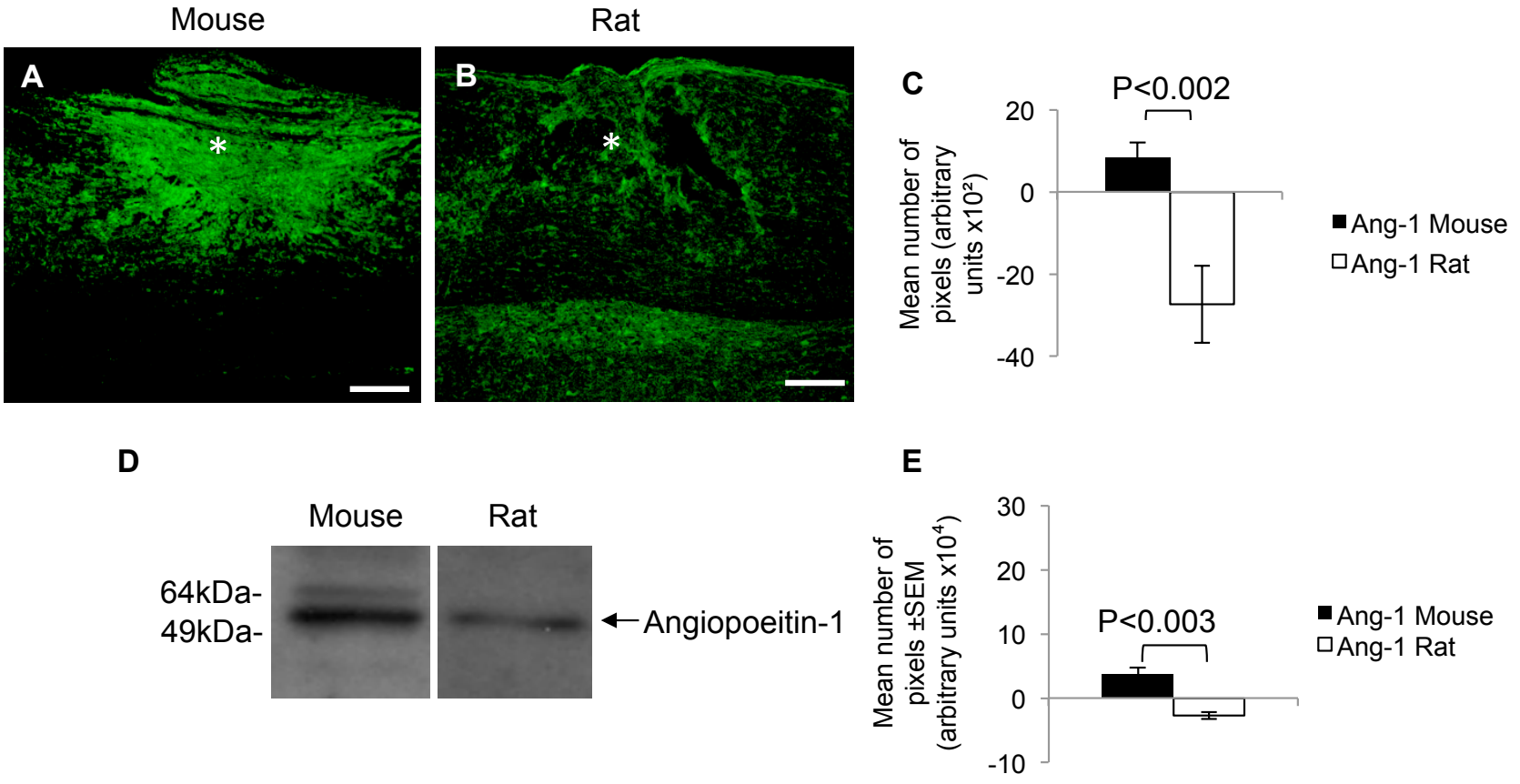

Figure 4.10 The localisation of Angiopoeitin-1 at 8 dpl in DC lesions. Immunohistochemistry for Angiopoeitin-1 in mice **(A)** and in rats **(B)** and the pixel intensities of Angiopoeitin-1 $^{+}$ fluorescence **(C)**. Western blot **(D)** and densitometry **(E)** corroborated the immunohistochemistry results (the same α-tubulin was used as a protein loading control as in Figure 4.4F; scale bars in A and B = 200 μm; * = lesion epicentre).

4.6.1.3. Anti-angiogenic factors

The immunoreactivity of anti-angiogenic factors; TIMP-2 and Sema 3A was observed in mouse and rat lesion areas 8 dpl (respectively, Figure 4.11-4.12A-C). In the mouse, there were low levels of immunoreactivity of TIMP-2 in the parenchyma and the lesion epicenter, whilst in the rat cord TIMP-2 was distributed in the surrounding neuropil but absent in the wound cavity (respectively, Figure 4.11A and B). In contrast, Sema 3A immunoreactivity was absent in mice lesion areas but high levels were seen in rat lesion cavities and the peri-lesion neuropil (respectively, Figure 4.12A and B). Quantification at 8 dpl revealed significantly increased immunoreactivity of TIMP-2 and Sema 3A by 0.48- and 0.7-fold, respectively, in rats compared to mice (respectively, Figure 4.11-4.12C and Table 4.7).

Factor	**Mean Intensity (pixels) (± SEM)**	
	Mouse	**Rat**
TIMP-2	$-37 \times 10^2 \pm 9 \times 10^2$	$18 \times 10^2 \pm 5.9 \times 10^2$
Sema 3A	$-23 \times 10^2 \pm 7.5 \times 10^2$	$16 \times 10^2 \pm 7.6 \times 10^2$

Table 4.7 Mean fluorescence intensities of anti- angiogenic growth factors in sections of spinal cord at 8 dpl after DC injury.

Western blotting (respectively, Figure 4.11-4.12D) and subsequent densitometry (respectively, Figure 4.11-4.12E) coincided with immunohistochemical results demonstrating that TIMP-2 and Sema 3A levels were significantly higher in rats compared to mice (Table 4.8). These results confirm that mice have a robust wound healing response after sub-acute SCI due to the decreased expression of anti-angiogenic factors compared to rats. The increased expression of anti-angiogenic factors in rat spinal cord after injury aids in the detrimental cavitation seen.

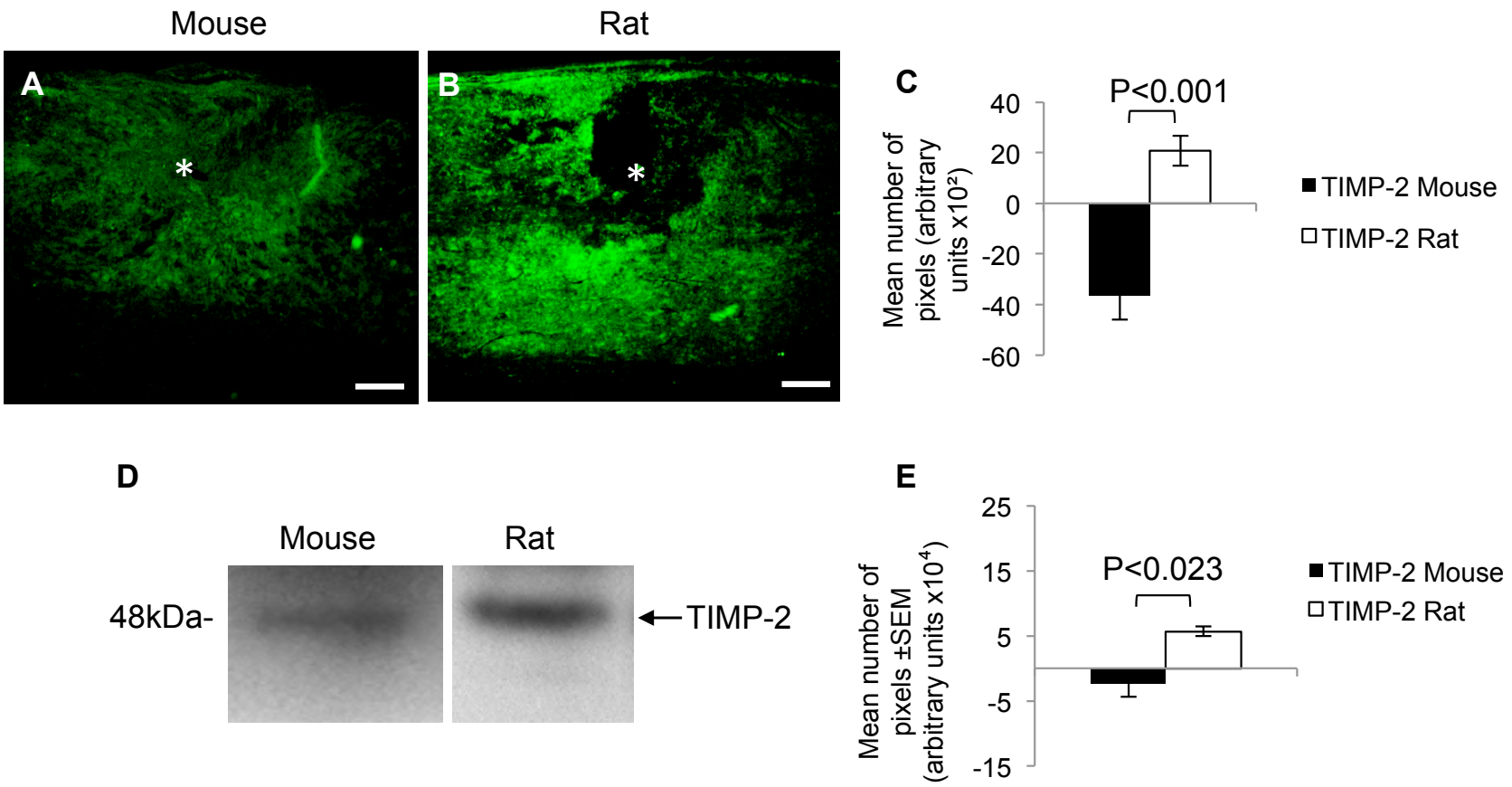

Figure 4.11 The localisation of TIMP-2 at 8 dpl in DC lesions. Immunohistochemistry for TIMP-2 in mice **(A)** and rats **(B)** and the pixel intensities of TIMP-2^{+} fluorescence **(C)**. Western blot **(D)** and densitometry **(E)** corroborated the immunohistochemistry results (the same α-tubulin was used as a protein loading control as in Figure 4.4F; scale bars in A and B = 200 μm; * = lesion epicentre).

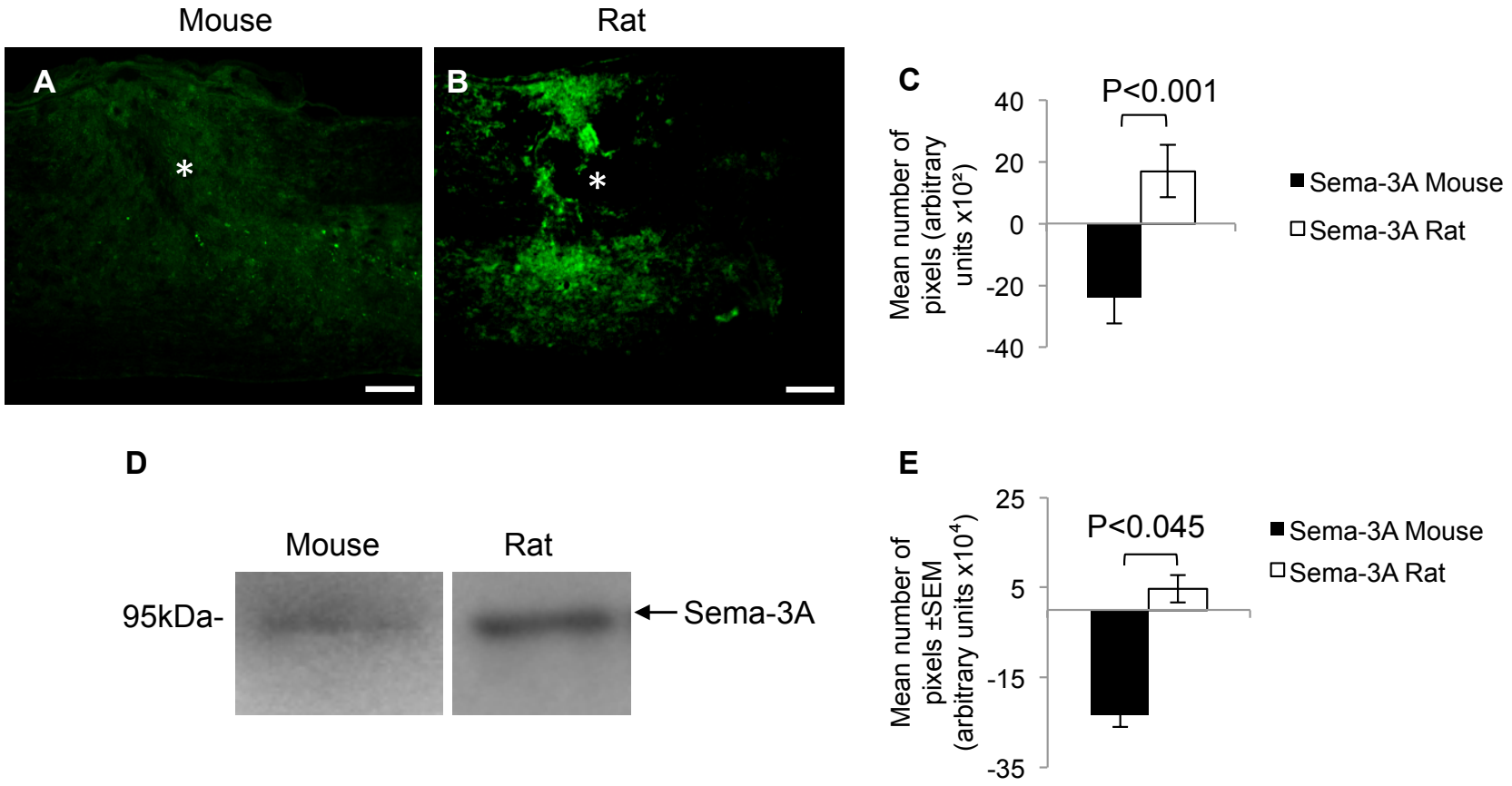

Figure 4.12 The localisation of Semaphorin 3A at 8 dpl in DC lesions. Immunohistochemistry for Semaphorin 3A in mice **(A)** and in rats **(B)** and the pixel intensities of Semaphorin $3A^{+}$ fluorescence **(C)**. Western blot **(D)** and densitometry **(E)** corroborated the immunohistochemistry results (the same α-tubulin was used as a protein loading control as in Figure 4.4F; scale bars in A and B = 200 μm; * = lesion epicentre).

Factor	Mean integrated density (arbitrary units) (± SEM)	
	Mouse	Rat
TIMP-2	$-2 \times 10^4 \pm 1.1 \times 10^6$	$5 \times 10^4 \pm 0.5 \times 10^4$
Sema 3A	$-4 \times 10^6 \pm 1.8 \times 10^6$	$27 \times 10^6 \pm 0.87 \times 10^6$

Table 4.8 Mean integrated density of anti- angiogenic growth factors in mouse and rat SCI sites at 8 dpl, determined by western blotting.

4.6.1.4. Matrix proteases

MMP-1 MMP-2 and MMP-9 immunoreactivity was observed after sub-acute SCI in mice and rats at 8 dpl (respectively, Figure 4.13-4.15A-C). The levels of these matrix proteases were higher in mouse lesion sites and surrounding parenchyma compared to the rats. The localization of MMPs was found to be in the lesioned area and surrounding WM and GM (respectively, Figure 4.13-4.15A and B). Quantification of MMP levels revealed significantly higher immunoreactivity levels in mice by 0.36-, 1.46- and 4.0-fold, respectively, compared to rats (respectively, Figure 4.13-4.15C and Table 4.9).

Factor	Mean Intensity (pixels) (± SEM)	
	Mouse	Rat
MMP-1	$16 \times 10^2 \pm 7 \times 10^2$	$-44 \times 10^2 \pm 12 \times 10^2$
MMP-2	$-19 \times 10^2 \pm 8 \times 10^2$	$-13 \times 10^2 \pm 6 \times 10^2$
MMP-9	$12 \times 10^2 \pm 1.7 \times 10^2$	$3 \times 10^2 \pm 2.9 \times 10^2$

Table 4.9 Mean fluorescence intensities of matrix proteases in sections of spinal cord at 8 dpl after DC injury.

Western blotting (respectively, Figure 4.13-4.15D) and subsequent densitometry (respectively, Figure 4.13-4.15E) of MMP coincided with immunohistochemical results demonstrating that MMP-1, MMP-2 and MMP-9 levels were greater in mouse lesion sites compared to rats (Table 4.10).

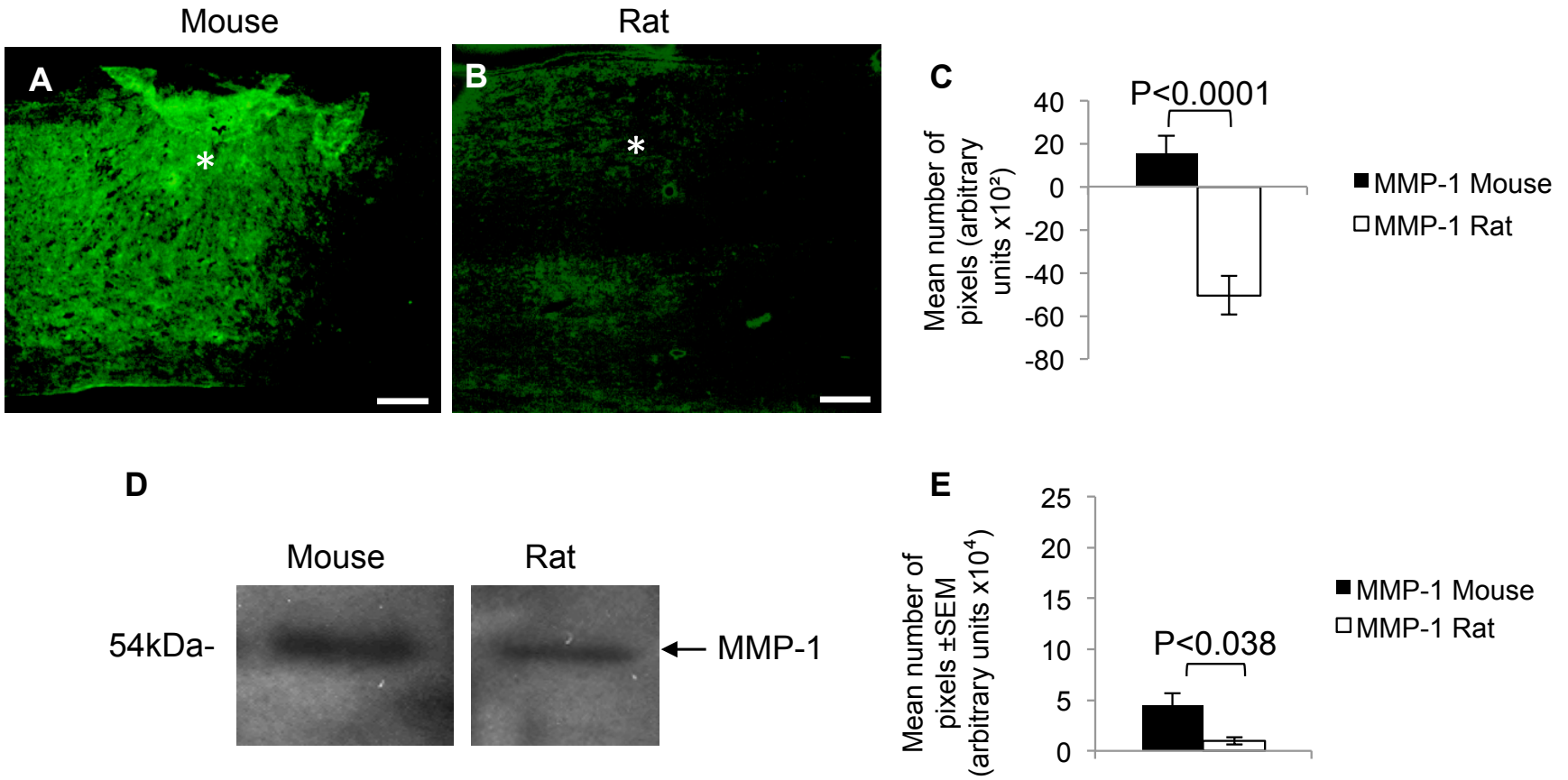

Figure 4.13 The localisation of MMP-1 at 8 dpl in DC lesions. Immunohistochemistry for MMP-1 in mice **(A)** and rats **(B)** and the pixel intensities of MMP-1^{+} fluorescence **(C)**. Western blot **(D)** and densitometry **(E)** corroborated the immunohistochemistry results (the same α-tubulin was used as a protein loading control as in Figure 2.4F; scale bars in A and B = 200 μm; * = lesion epicentre).

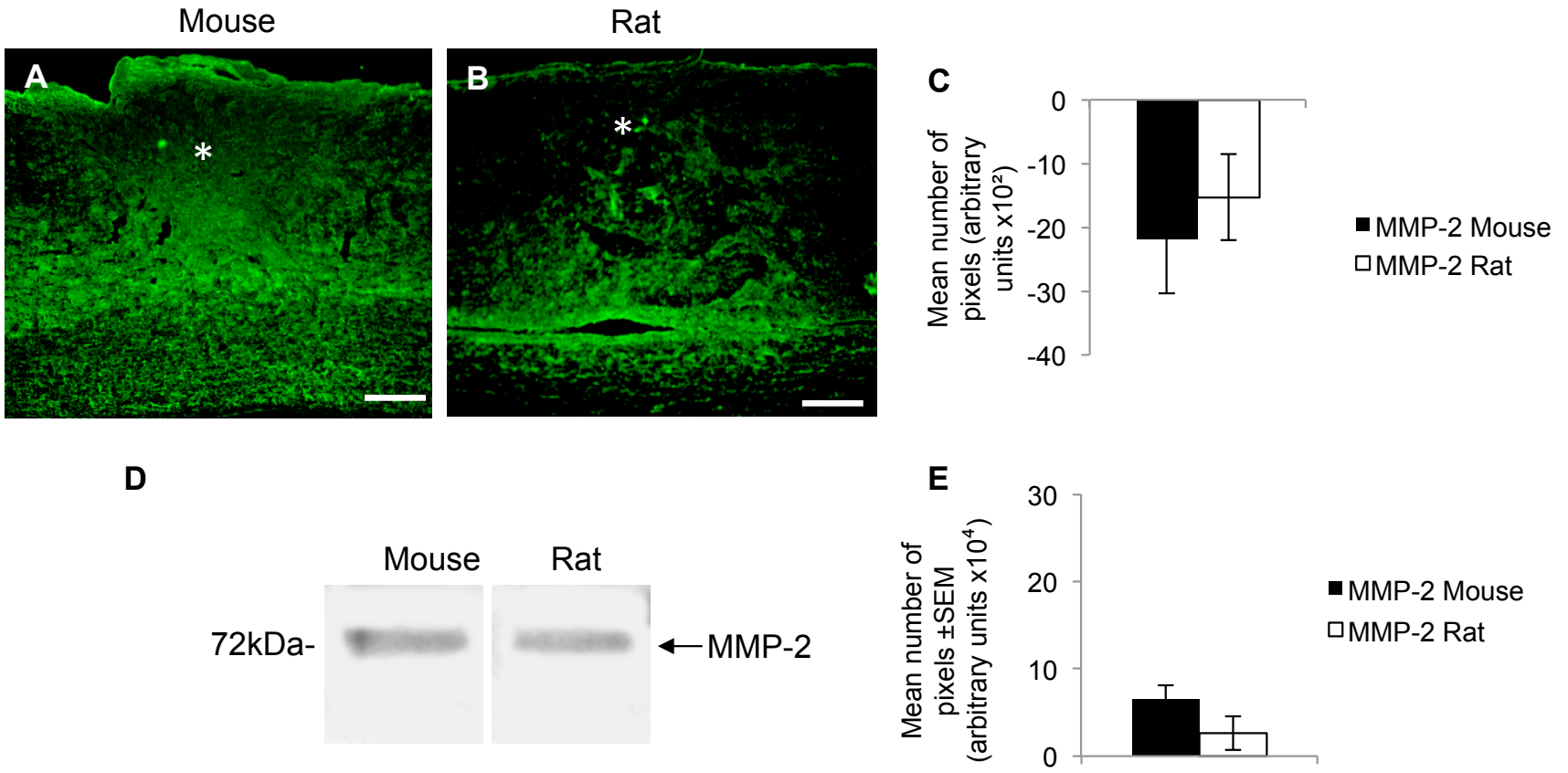

Figure 4.14 The localisation of MMP-2 at 8 dpl in DC lesions. Immunohistochemistry for MMP-2 in mice **(A)** and rats **(B)** and the pixel intensities of MMP-2^{+} fluorescence **(C)**. Western blot **(D)** and densitometry **(E)** corroborated the immunohistochemistry results (the same α-tubulin was used as a protein loading control as in Figure 2.4F; scale bars in A and B = 200 μm; * = lesion epicentre).

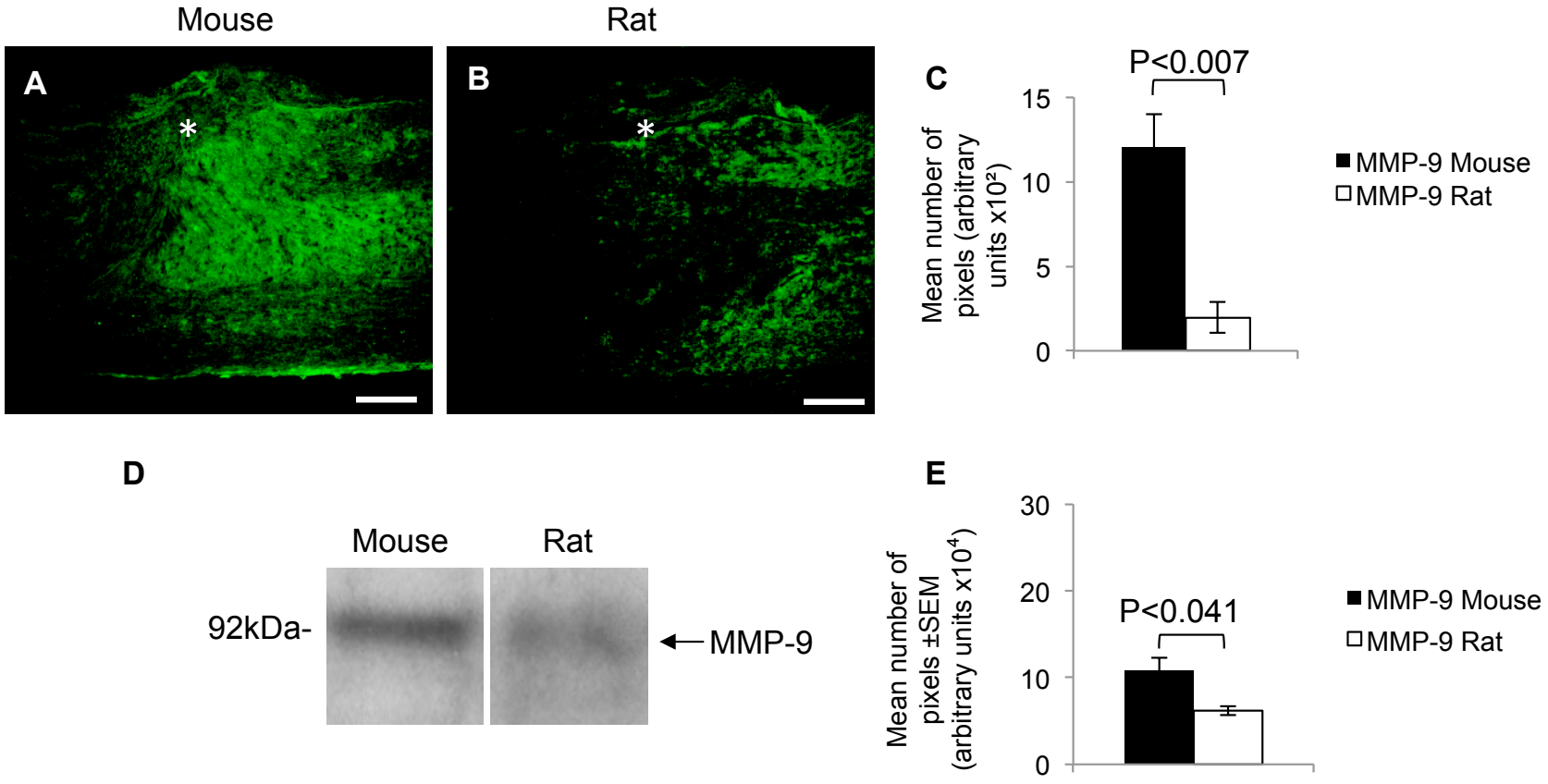

Figure 4.15 The localisation of MMP-9 at 8 dpl in DC lesions. Immunohistochemistry for MMP-9 in mice **(A)** and rats **(B)** and the pixel intensities of MMP-9^{+} fluorescence **(C)**. Western blot **(D)** and densitometry **(E)** corroborated the immunohistochemistry results (the same α-tubulin was used as a protein loading control as in Figure 2.4F; scale bars in A and B = 200 μm; * = lesion epicentre).

Factor	Mean integrated density (arbitrary units) (± SEM)	
	Mouse	**Rat**
MMP-1	$4.7 \times 10^4 \pm 0.05 \times 10^4$	$1 \times 10^4 \pm 0.8 \times 10^4$
MMP-2	$7 \times 10^4 \pm 0.5 \times 10^6$	$2.5 \times 10^4 \pm 0.05 \times 10^6$
MMP-9	$10 \times 10^4 \pm 0.25 \times 10^6$	$6 \times 10^6 \pm 0.07 \times 10^6$

Table 4.10 Mean integrated density of matrix proteases in mouse and rat SCI sites at 8 dpl, determined by western blotting.

4.6.1.5. ECM/scar-related molecules

The Immunoreactivity of ECM molecules; Collagen-1 and PECAM-1, have been observed between mice and rats after sub-acute SCI at 8 dpl (respectively, Figure 4.16-4.17A-C). Collagen-1 localisation and its distribution mirrored that of laminin, i.e. within the lesion in mice and localised to the GLA in the rat (not shown) (Figure 4.16A and B). Whilst, the cell adhesion molecule, PECAM-1, was localised to the lesion site and peri-lesion neuropil (not shown) (Figure 4.17A and B). Quantification of immunoreactivity levels revealed that levels were significantly upregulated by 10- and 3.4-fold, respectively, in mice compared to rats (respectively, Figure 4.16-4.17C and Table 4.11).

Western blotting (respectively, Figure 4.16-4.17D) and densitometry (respectively, Figure 4.16-4.17E) confirmed that laminin (for immunoreactivity results please refer to chapter 3) and PECAM-1 levels were significantly higher in rats compared to mice at 8 dpl (respectively, Figure 4.16-4.17E and Table 4.12).

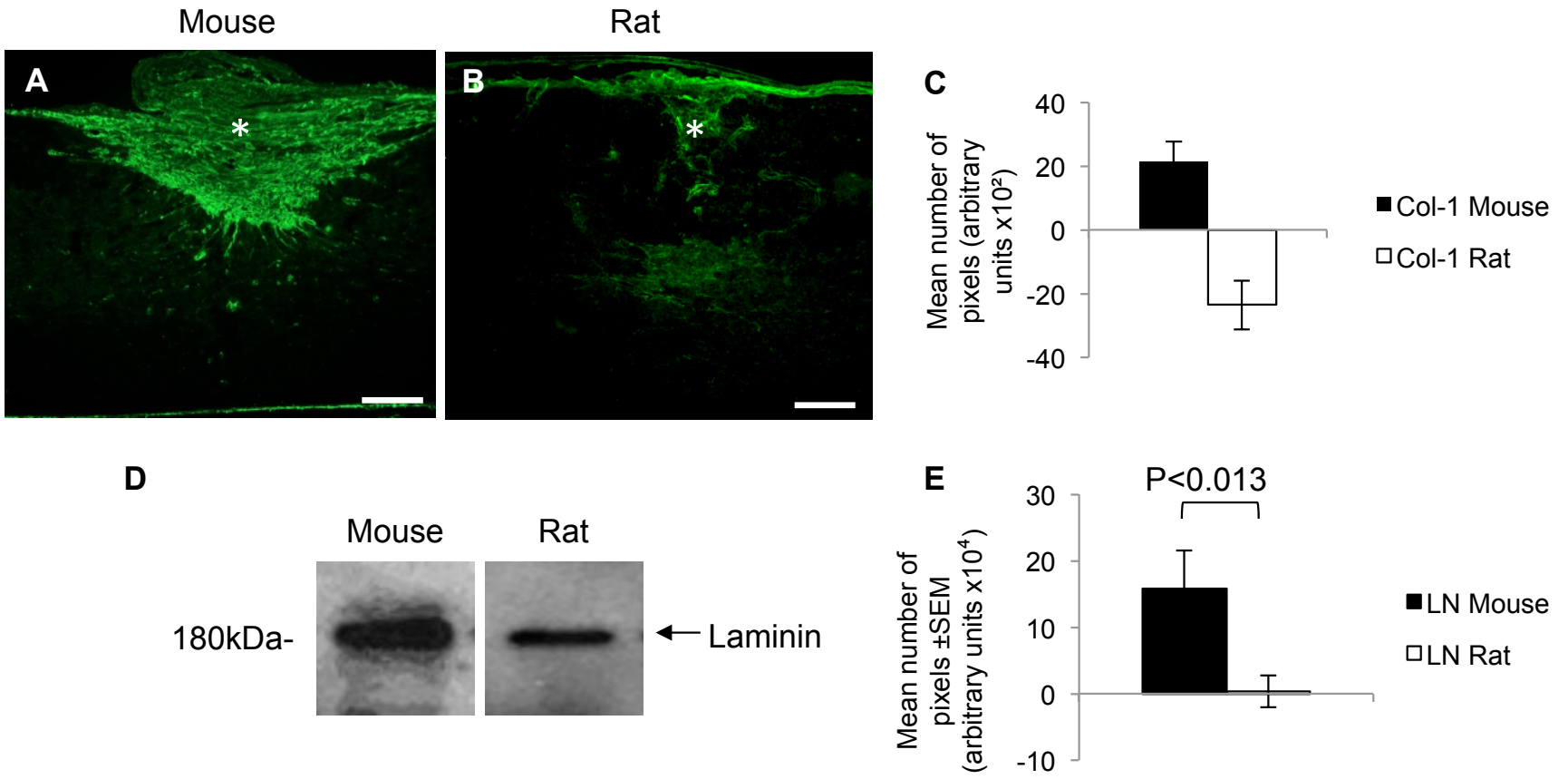

Figure 4.16 The localisation of Collagen-1 at 8 dpl in DC lesions. Immunohistochemistry for Collagen-1 in mice **(A)** and in rats **(B)** and the pixel intensities of Collagen-1 $^{+}$ fluorescence **(C)**. Western blot **(D)** and densitometry **(E)** for laminin corroborated the immunohistochemistry results seen in chapter 1 (the same α-tubulin was used as a protein loading control as in Figure 2.4F (Scale bars in A and B = 200 μm; * = lesion epicentre).

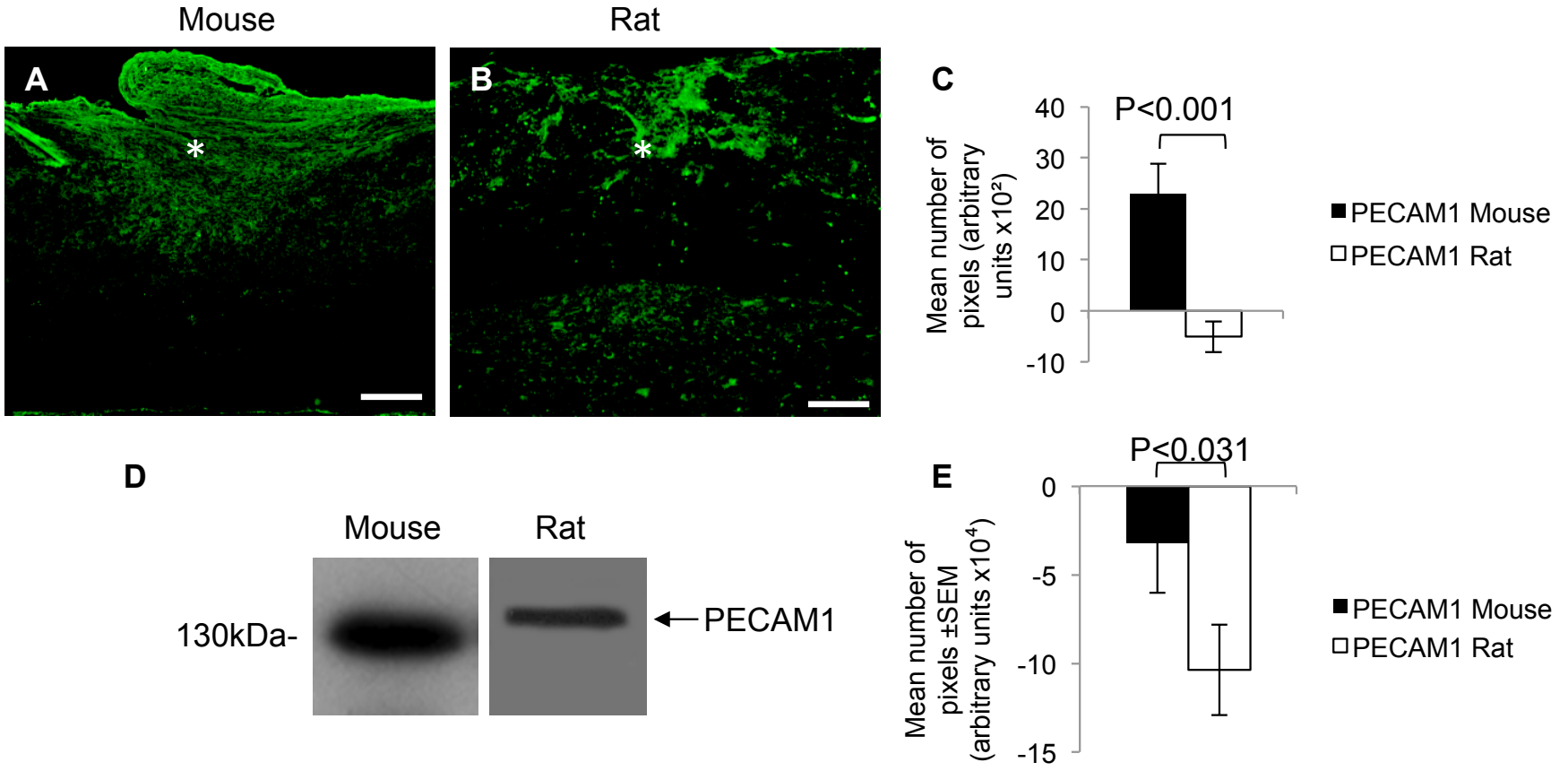

Figure 4.17 The localisation of PECAM1 at 8 dpl in DC lesions. Immunohistochemistry for PECAM1 in mice **(A)** and in rats **(B)** and the pixel intensities of PECAM1^{+} fluorescence **(C)**. Western blot **(D)** and densitometry **(E)** corroborated the immunohistochemistry results (the same α-tubulin was used as a protein loading control as in Figure 2.4F; scale bars in A and B = 200 μm; * = lesion epicentre).

Factor	Mean Intensity (pixels) (± SEM)	
	Mouse	Rat
Collagen-1	$20 \times 10^2 \pm 5 \times 10^2$	$-2 \times 10^2 \pm 8.5 \times 10^2$
PECAM-1	$23 \times 10^2 \pm 5.2 \times 10^2$	$-6.7 \times 10^2 \pm 3.5 \times 10^2$

Table 4.11 Mean fluorescence intensities of ECM/scarring-related molecules in sections of spinal cord at 8 dpl after DC injury.

Factor	Mean integrated density (arbitrary units) (± SEM)	
	Mouse	Rat
laminin	$1.5 \times 10^4 \pm 0.05 \times 10^4$	$3.2 \times 10^2 \pm 0.8 \times 10^2$
PECAM-1	$6 \times 10^6 \pm 0.28 \times 10^6$	$0.5 \times 10^6 \pm 0.01 \times 10^6$

Table 4.12 Mean integrated density of ECM/scarring-related molecules in mouse and rat SCI sites at 8 dpl, determined by western blotting.

These results demonstrate fundamental differences in healing of SCI wounds in mice compared to rats, i.e. aggressive wound healing in mice marked by increased deposition of matrix proteins, pro-angiogenic growth factors correlated with raised levels of MMP and reduced TIMP titres.

4.6.2 Induced hypoxia after SCI

Histological and protein differences in carbonic anhydrase-X (CA10) indicate that hypoxia may play a role in mediating the differential responses after SCI (Figure 4.18A-E). CA10 immunoreactivity was seen in the lesion site and peri-lesion neuropil in mice and rats (Figure 4.18A and B). At 8 dpl, there was significantly higher levels of CA10 in rats compared to mice ($5.6 \times 10^2 \pm 2.5 \times 10^2$ pixels in rats compared to $-7.6 \times 10^2 \pm 1.6 \times 10^2$ pixels in mice, $P<0.001$, Figure 4.18C). These results were confirmed by western blotting, demonstrating that the protein levels of CA10 were

significantly higher in rat compared to mouse DC lesions (5.2 x10^3 ± 1.2 x 10^3 pixels in rat compared to -5.4 x 10^3 ± 2.6 x 10^3 in mice, P<0.021, Figure 4.18D and E). These results demonstrate that increased levels of CA10 are induced by hypoxia after DC injury in rats.

4.6.3 Behavioural analysis

The response to thermal stimuli in both rats and mice was significantly impaired 2 hr after DC injury compared to sham-treated control animals (Figure 4.19A and B). For example, the reaction time (paw withdrawal latency) was delayed by 3.38s in mice (P<0.041) and by 5.63s in rats (P<0.002). However, by 7dpl the response to thermal stimuli had returned to sham-treated control levels and showed no further differences in withdrawal latency over the course of the experimental time-period of 28dpl (Figure 4.19A and B). Unlike thermal responses, mechanical allodynia responses were not significantly different in mice or rats, with or without DC injury and did not vary over the experimental time-period (Figure 4.20A and B). These results indicate that despite the presence of a large wound cavity in rats, DC injury did not affect responses to mechanical stimuli but temporarily affected responses to thermal stimuli in the early stages after DC injury. However, within 7 dpl, animals regained normal function response times and were no different to those observed in sham-treated control animals.

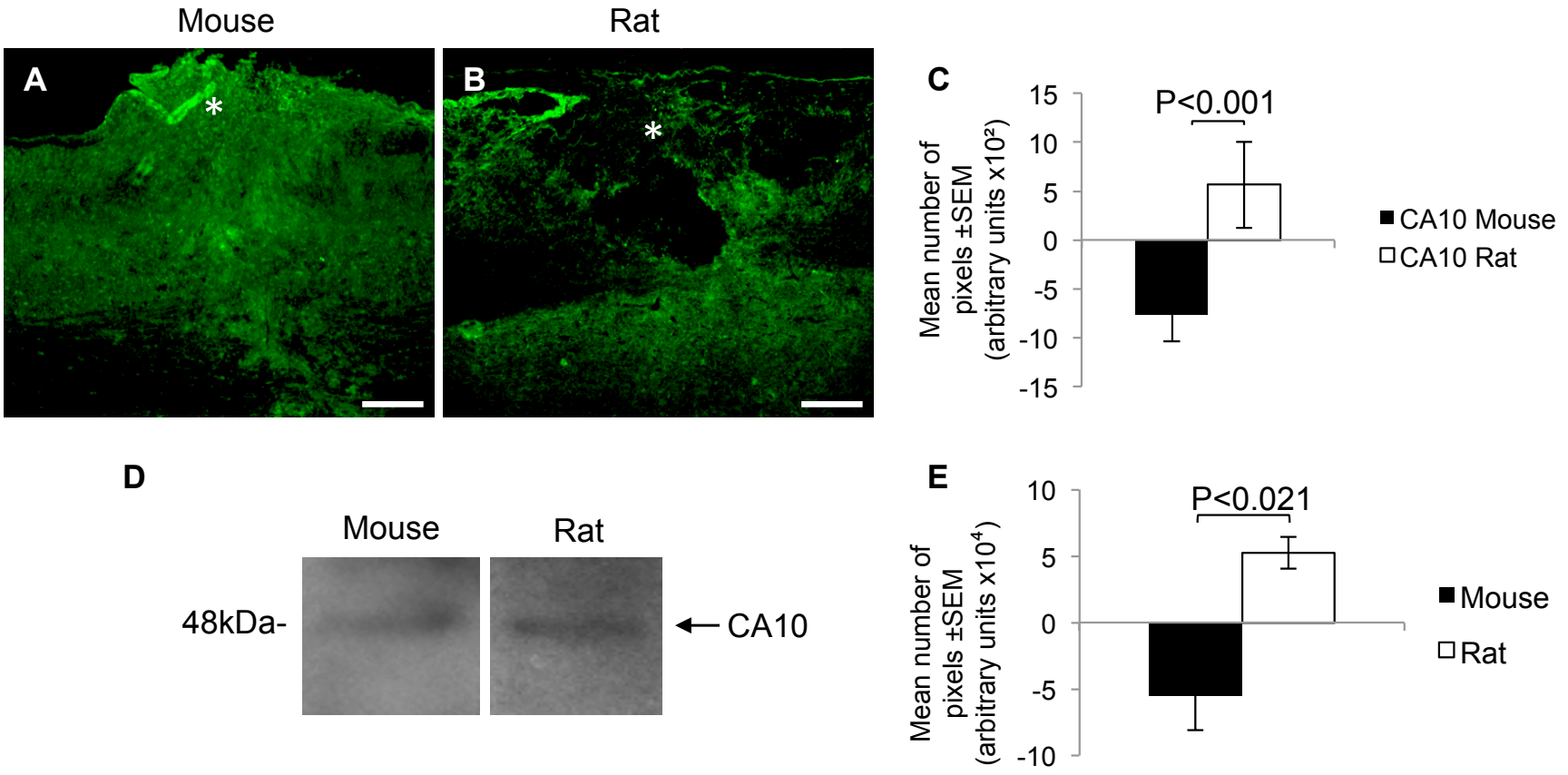

Figure 4.18 The localisation of Carbonic Anhydrase 10 at 8 dpl in DC lesions. Immunohistochemistry for Carbonic Anhydrase 10 in mice **(A)** and in rats **(B)** and the pixel intensities of Carbonic Anhydrase 10^{+} fluorescence **(C)**. Western blot **(D)** and densitometry **(E)** corroborated the immunohistochemistry results (the same α-tubulin was used as a protein loading control as in Figure 2.4F; scale bars in A and B = 200 μm; * = lesion epicentre).

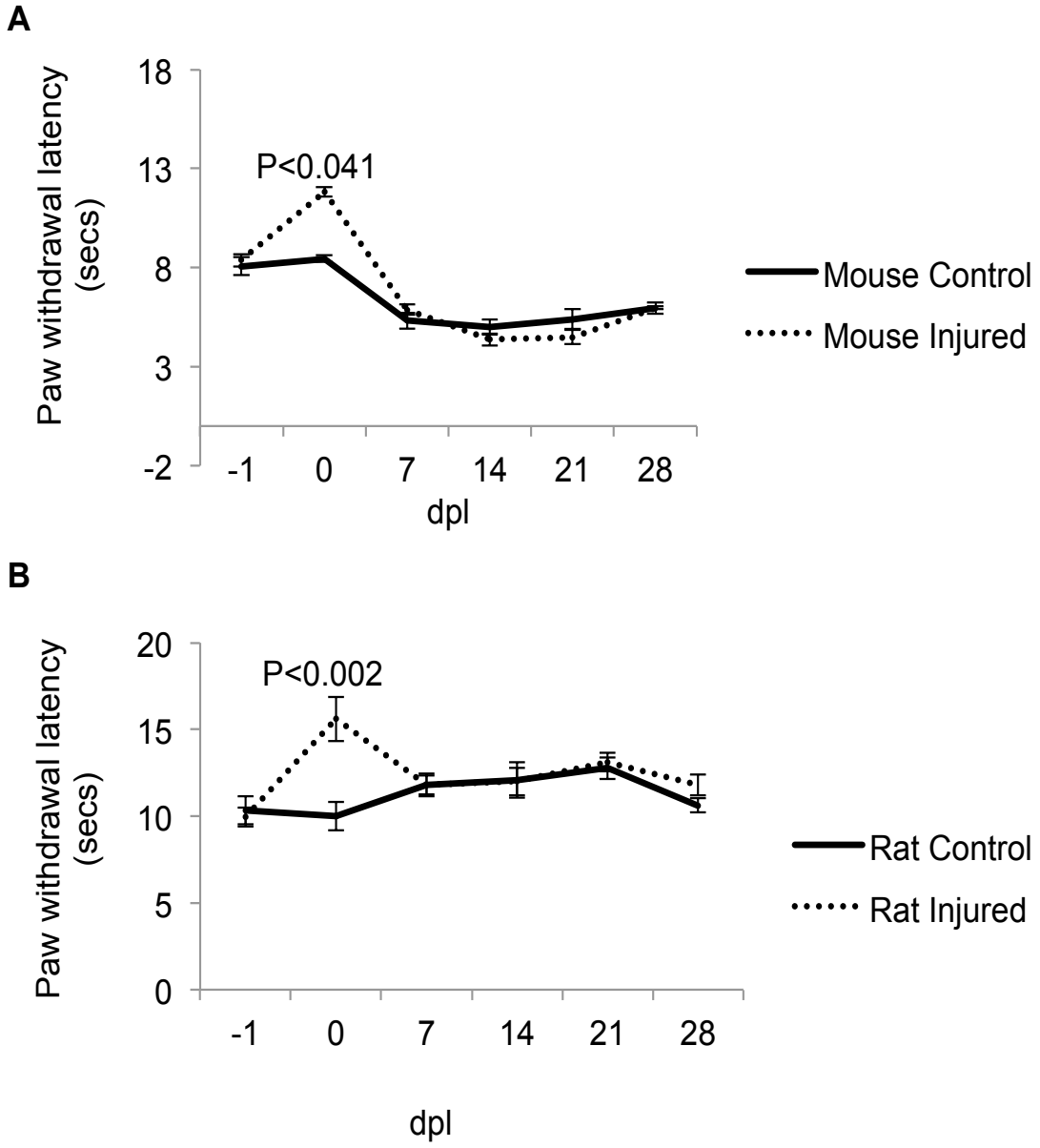

Figure 4.19 Comparison of the behavioural deficits observed after T8 DC injury in mice and rats over time using IR plantar heat test. Quantification on the average reaction time before surgery (-1), 2 hours after surgery (0), 7, 14, 21 and 28 dpl showed significant differences in mice **(A)** and rats **(B)** at 0dpl only compared to sham operated control.

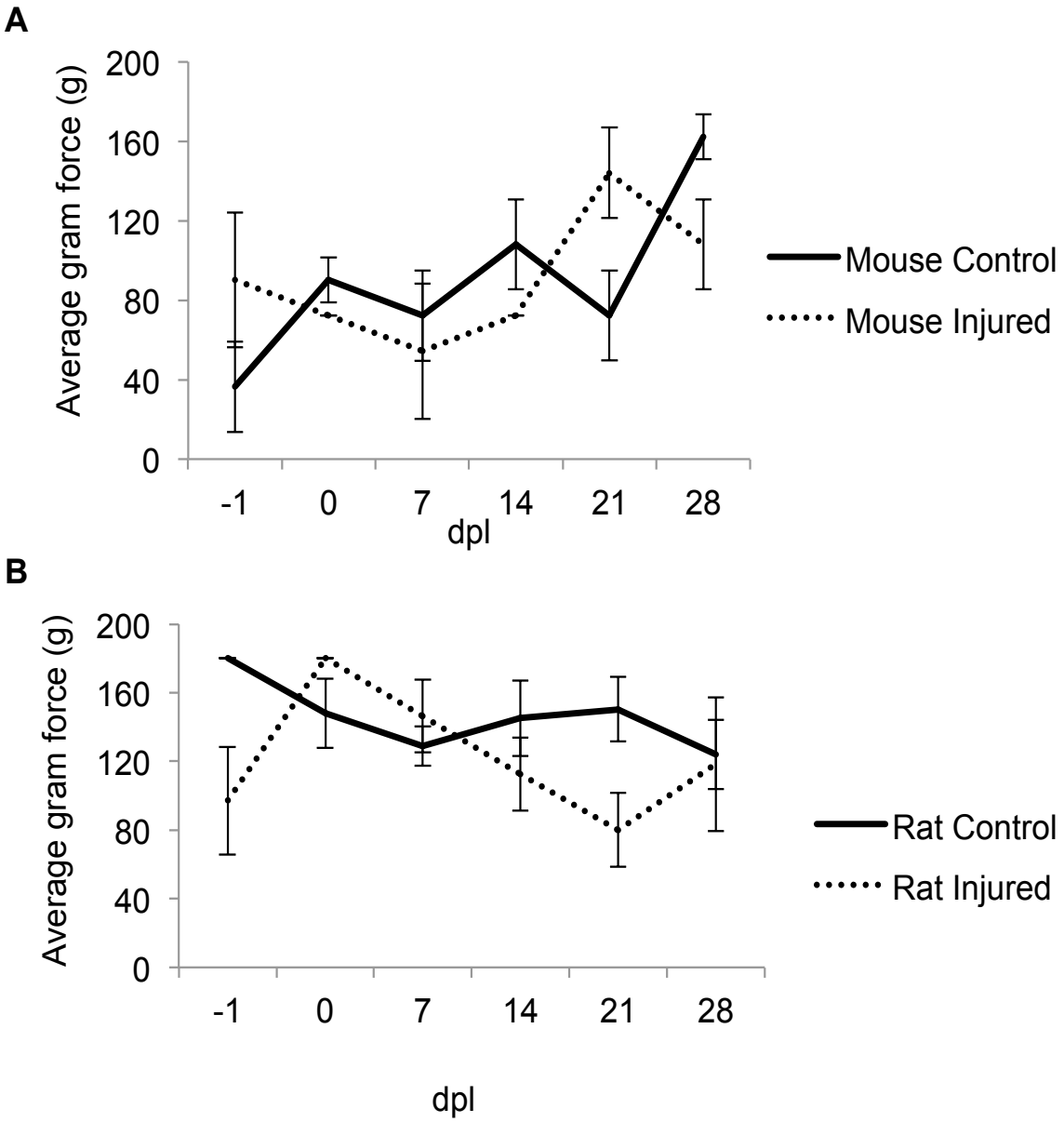

Figure 4.20 Comparison of the behavioural deficits observed after T8 DC injury in mice and rats over time using Vonfrey hair test. Quantification on the average gram force required to elicit paw withdrawal before surgery (-1), 2 hours after surgery (0), 7, 14, 21 and 28 dpl showed no significant differences in DC lesioned mice **(A)** and rats **(B)** compared to sham operated control.

4.6.4 Greater sparing of PKC-γ$^+$ and NF200$^+$ DC axons in mice compared to rats

Spared and established axons in the DC of mice and rats after injury were assessed by calculating the area occupied by NF200 labeling in the whole dorsal funiculi to identify the level of spared axons (smaller axon fibers) left after injury and thus plasticity (Bouhy et al., 2011, Butt et al., 1997). In spinal segments T7 (above lesion) and T9 (below lesion), normal basal levels of NF200$^+$ immunostaining was observed in control mice (Figure 4.21A and B, respectively) and rats (Figure 4.21E and F, respectively), in the CST and in interneurons and their axons in the superficial dorsal horn. After DC in mice NF200 immunoreactivity was significantly reduced in the CST at T7 and T9 compared to intact controls, indicative of retrograde axonal dyeback of axons that originate from the motor cortex, respectively (Figure 4.21C and D). In rat lesioned DC, reduced NF200 immunohistochemistry was observed in spinal segment in the CST from T7 and T9 (Figure 4.21G and H), compared to control rats. Pixel intensities were measured in a given area i.e. the dorsal funiculi to reveal the reduction in NF200 immunoreactivity in the DC was greater in rat T7 (65 ± 4% in rat *versus* 42 ± 3% in mice, $P<0.01$) and T9 (45 ± 3% in mice *versus* 20 ± 4% in rat $P<0.01$) segments (Figure 4.22A and B and 4.22I) compared to mice.

Similar changes were observed with PKC-γ immunostaining (Figure 4.23A and B), in the CST and in interneurons and their axons in the superficial dorsal horn (Barritt et al., 2006). PKC-γ is an isotope of the classical PKC subfamily, solely expressed in the brain and spinal cord and localization is restricted to neurons (Saito and Shirai, 2002). After DC injury in mice, PKC-γ immunohistochemistry was significantly reduced at T7 and T9, indicative of Wallerian degeneration and

retrograde axonal dyeback, respectively (Figure 4.23C and D). In rat lesioned DC, reduced PKC-γ immunohistochemistry was observed in spinal segments T7 and T9 of control rats (Figure 4.22E and F), while after DC injury, reduced PKC-γ immunoreactivity was also observed at T7 and T9 segments (Figure 4.23G and H). The reduction in PKC-γ immunoreactivity in the DC (Figure 4.24A) was greater in rat T7 (14 ± 2% in mice *versus* 25 ± 3% in rat, $P<0.01$) and T9 (18 ± 3% in mice *versus* 31 ± 1.5% in rat, $P<0.01$) segments (Figure 4.24B).

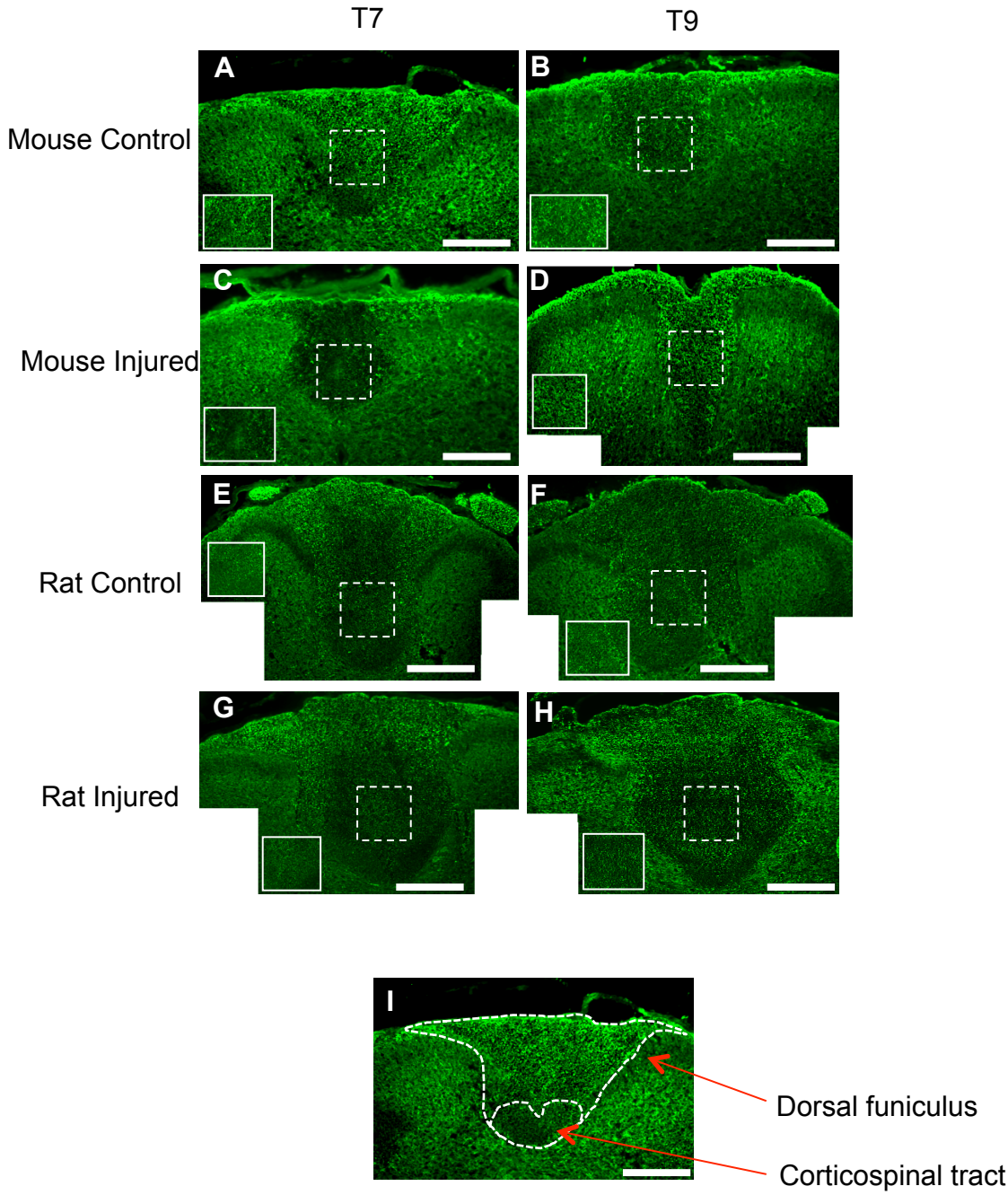

Figure 4.21 NF200 immunoreactivity as an indicator of axonal sparing at 8 dpl after DC injury in spinal segments above and below the lesion. Representative NF200 staining at T7 (above lesion) in mouse control **(A)** and injured **(C)** and at T9 control **(B)** and injured **(D)** cords. Representative NF200 staining at T7 in rat control **(E)** and

injured **(G)** and at T9 control **(F)** and injured **(H)** cords (Scale bars = 200 μm). A representative image outlining the dorsal funiculi that was used for quantification and the corticospinal tract **(I)**.

A

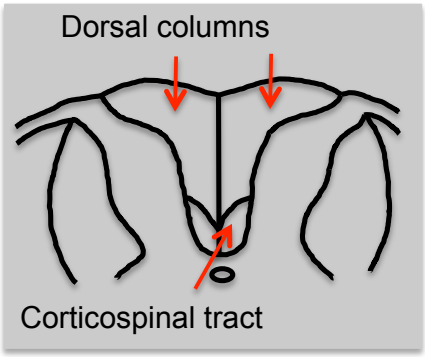

B

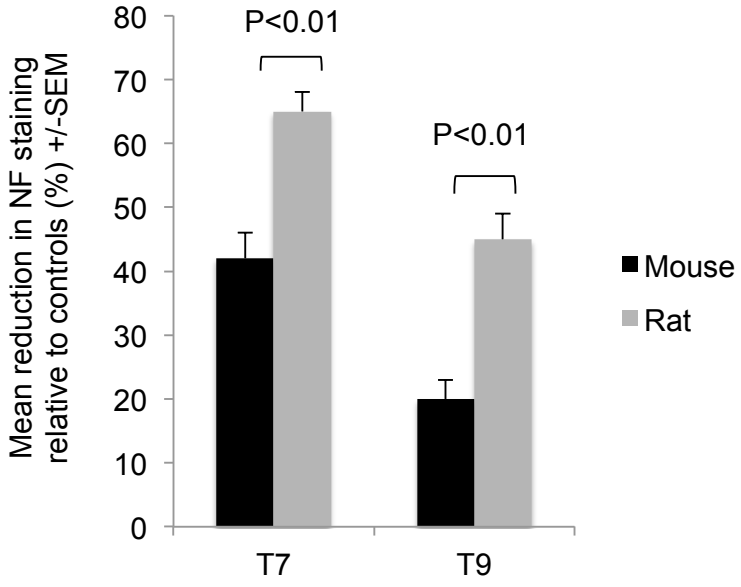

Figure 4.22 Diagram shows dorsal column and corticospinal tract axons quantified before and after injury **(A)**. Quantification of the immunoreactivity of NF200 **(B)** demonstrated that NF200 immunoreactivity was reduced in rats compared to mice at both T7 and T9 spinal segments.

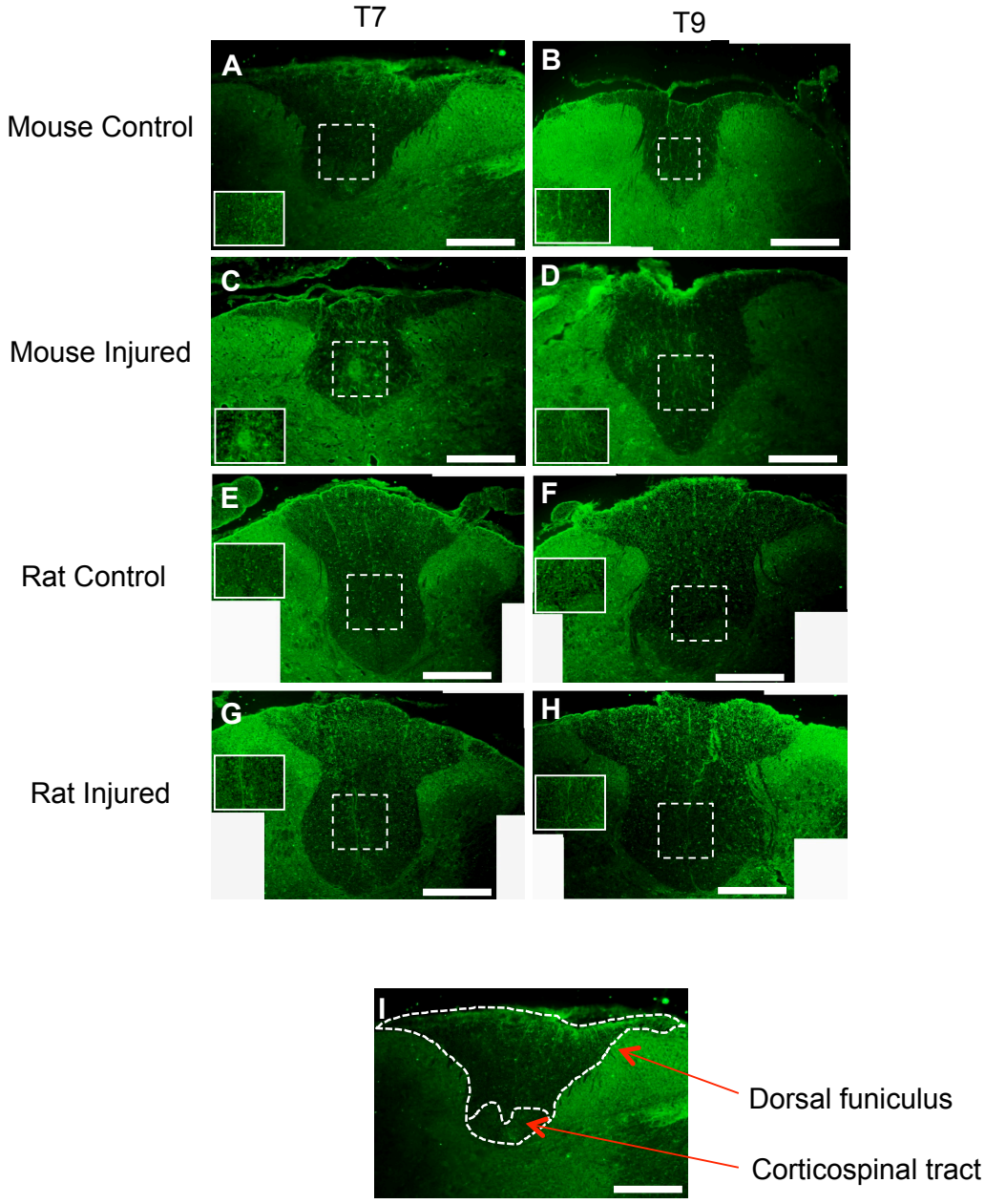

Figure 4.23 PKC-γ immunoreactivity as an indicator of axonal sparing at 8dpl after DC injury in spinal segments above and below the lesion. Representative PKC-γ staining at T7 (above lesion) in mouse control **(A)** and injured **(C)** and at T9 control **(B)** and injured **(D)** cords. Representative PKC-γ staining at T7 in rat control **(E)** and injured **(G)** and at T9 control **(F)** and injured **(H)** cords. (Scale bars = 200 μm). A

representative image outlining the dorsal funiculi that was used for quantification and the corticospinal tract **(I)**.

A

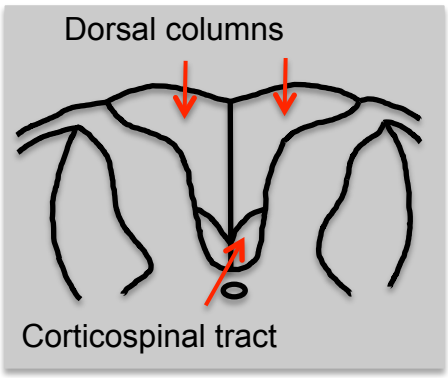

B

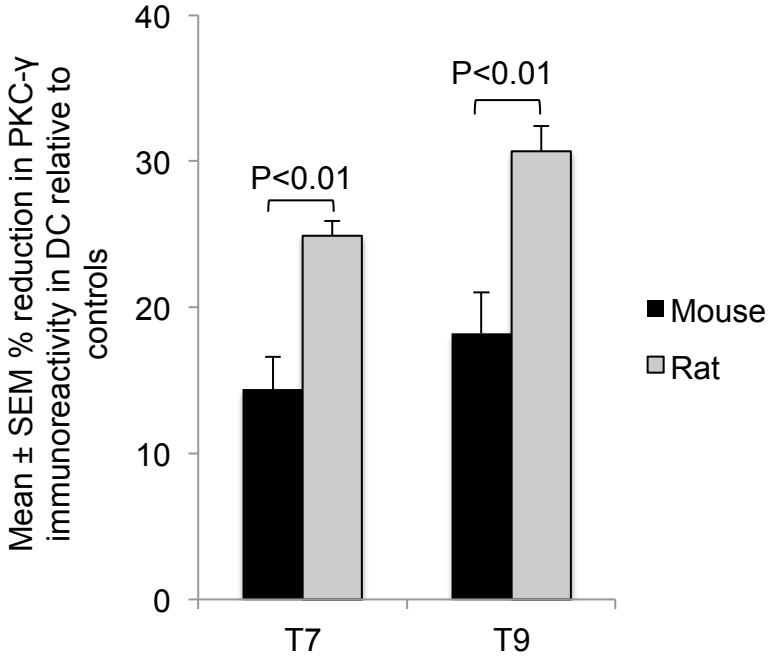

Figure 4.24 Diagram shows dorsal column and corticospinal tract axons quantified before and after injury **(A)**. Quantification of the immunoreactivity of PKC-γ **(B)** demonstrated that PKC-γ immunoreactivity was reduced in rats compared to mice at both T7 and T9 spinal segments.

4.7 Discussion

In our animal model of sub-acute T8 DC injury at 8 dpl demonstrates that there are fundamental differences in angiogenic/wound healing-related proteins between mice and rats, confirming that mice have a robust wound healing response that correlates with the no cavity development compared to rats. But the cavity free response seen in mice did not aid in better functional recovery as originally hypothesised, but did have increased axonal sparing.

However, using other endpoints such as MRI/gadolinium (a contrast medium that improves the clarity of internal structures) would allow for a more accurate determination of cavity development and lesion volume between mice and rats after SCI. Furthermore, blood vessels and scarring could also be assessed in the animals. If time permitted, earlier time points would also be useful in determining the early angiogenic/wound healing responses between the two species after sub-acute SCI.

4.7.1 Angiogenic factors

Although there were no significant differences in expression of vWF after T8 sub-acute SCI in mice and rats at 8dpl, there is evidence to demonstrate that vWF is upregulated after injury to the CNS and more importantly after SCI in humans (Petaja et al., 1989, Mammen, 1992, Cellucci et al., 2012, Suidan et al., 2013). But conflicting results indicate that no changes are seen in vWF levels after injury to the cord in patients (Fujii et al., 1992, Pahl et al., 1994). Due to inconsistent results in the literature vWF is not considered as an appropriate therapeutic option after SCI.

4.7.2 Angiogenic growth factors

VEGF-A; a potent stimulator of angiogenesis and formation of new vessel sprouts, is up-regulated in many cancers and is important in the angiogenic processes in particular cell migration and proliferation (Gerhardt et al., 2003, Ruhrberg et al., 2002, Ito et al., 2007, Chung and Ferrara, 2010). In our model there was a significant upregulation of VEGF-A in mice compared to rats at the lesion epicenter. Although VEGF is neuroprotective, the levels reported after SCI are inconsistent along with the use of VEGF-A_{165} isoform (Bartholdi et al., 1997, Skold et al., 2000, Jin et al., 2000, Matsuzaki et al., 2001, Benton and Whittemore, 2003, Akiyama et al., 2004, Rosenstein and Krum, 2004, Deumens et al., 2005, Herrera et al., 2009, van Neerven et al., 2010, Berger et al., 2011). However, the use of VEGF-$A_{121/189}$ isoforms has demonstrated to be neuroprotective and in combination with spinal cord bridges and viral vectors induces angiogenesis and thus axon regeneration (Herrera et al., 2009, D'Onofrio et al., 2011, Siddiq et al., 2012, De Laporte et al., 2011).

In our model the levels of FGF-2 was increased in mice compared to rats after sub-acute SCI. In experimental models of CNS injury, FGF-2 has demonstrated a role in neuroprotection and functional recovery (Dono, 2003, Hattori et al., 1997b, Hattori et al., 1997a, Hossain et al., 1998, Hsu et al., 2009, Madiai and Hackshaw, 2002). This phenomenon has also been observed in animal models of SCI and in clinical situations where patients treated with stem cells co-delivered with FGF-2 to the injured site, improved motor and sensory scores were observed 24 months after treatment (Teng et al., 1998, Furukawa and Furukawa, 2007, Liu et al., 2011, Wu et al., 2011). Furthermore, FGF-1 induced the stimulation of blood vessels via

proliferation of endothelial cells and smooth muscle cells that resulted in enhanced mitotic activity of the neural stem cells and thus promote cell differentiation and survival. The decrease in deficit seen after plantar heat test in mice compared to rats may be supported by the increase in FGF-2 and thus improve functional outcome in our model.

ANG-1 not only promotes endothelial cell survival, vessel stabilisation and maturation, but also inhibits and reduces inflammation that results in tissue loss after SCI and therefore promotes angiogenesis (Thurston et al., 2005, Thurston et al., 2000, Fleming et al., 2006, Chung and Ferrara, 2010, Han et al., 2010). Our immunohistochemical results showed that there was an increase in expression of ANG-1 after SCI in mice compared to the rats. This may imply that the upregulation of reactive astrocytes as a result of inflammatory response causes secondary damage and decreases the chances of angiogenesis occurring in and around the lesion site but also the BSCB integrity is compromised in rats due to down regulation of ANG-1 after SCI (Durham-Lee et al., 2012, Herrera et al., 2009, Ritz et al., 2010). The localization and levels of ANG-2 was not investigated in this study despite the beneficial role it has shown after SCI due to previous studies showing an upregulation 10 weeks after injury (Durham-Lee et al., 2012, Ritz et al., 2010). Our study investigated the early angiogenic/wound healing effects at 8 dpl after sub-acute SCI, therefore if time permitted and later time points were to be investigated then ANG-1 vs. ANG-2 would be considered.

TGFβ-2 regulates many processes including angiogenesis, inflammation and wound-healing (Khalil et al., 1989). It also induces generalised scar tissue formation but has also been demonstrated to correlate with the deposition of the scar in the

CNS (Lagord et al., 2002, Shah et al., 1995). Our results show that there is significantly higher localisation of TGFβ-2 around the lesion site in mice whilst in rats it was present in lower levels. The higher levels of TGFβ-2 in mice supports our hypothesis that mice have a better wound healing response due to an adequate balance of angiogenesis and scar deposition.

PDGF is responsible for recruitment of pericytes in promoting tumour angiogenesis and vessel maturation during angiogenesis along with MMPs and TGFβ (Abramsson et al., 2003, Chung and Ferrara, 2010). In our studies there was a significant upregulation of PDGF-BB in and around the lesion site after injury in the mouse where low levels were observed in rats. It has been reported that human dermal wounds and patients with chronic neuropathic diabetic ulcers treated with recombinant PDGF-BB (rPDGF-BB) increases wound healing with fibroblast activation and granulation tissue formation by increasing the expression of PDGF-AA isoform which is present in endothelial cells, capillaries and smooth muscle. Therefore, treating chronic wounds with exogenous rPDGF-BB maybe a promising therapeutic application of wound healing (Pierce et al., 1995, Wieman et al, 1998). More recently it has been demonstrated that using a peri-ulcer injection of a replication-incompetent adenoviral construct expressing PDGF-BB in patients with venous leg ulcers (a disease responsible for chronic lower extremity wounds), was able to increase wound healing and have a systemic effect on parts of the wound that were not injected (Margolis et al., 2009). The multifaceted role that PDGF-BB plays in the CNS instigated studies that utilise PDGF-BB as a therapeutic strategy after SCI.

Angiogenin is well characterized in the pathogenesis of amyotrophic lateral sclerosis (ALS), a motor neurodegenerative disease of the CNS that was first

characterised by Fett *et* al. as a tumour-derived angiogenic protein (Fett et al., 1985, Boillée et al., 2006, Kishikawa et al., 2008). In our hands, angiogenin was significantly increased in and around the lesion site in mice. Although there is angiogenin expression around the lesion after following injury in rats there was no positive immunoreactivity in the lesion site. It is thought that using angiogenin as a therapy option after SCI may aid in motor neuron survival and that the increase seen in the mouse correlates with increased angiogenesis and thus wound healing (Ng et al., 2011). Angiogenesis and wound healing are two closely liked dynamic processes that demonstrate a strong correlation particularly after injury where impaired angiogenesis can delay or accelerate wound healing (Guo and Dipietro, 2010, Gosain and DiPietro, 2004, Zhou et al., 2004, Echtermeyer et al., 2001, Nanney et al., 2001, Swift et al., 1999, Lee et al., 1999).

4.7.3 Anti-angiogenic factors

In order for successful angiogenesis to occur after injury, a balance in pro- and anti-angiogenic protein expression is required. TIMP's regulates MMPs but high levels of TIMP-2 have shown to inhibit MMP-2 in which TIMP-2 strongly binds to and controls degradation of collagen-1 (Anik et al., 2011a). High levels of TIMP-2 have been observed in the degenerating dorsal column suggesting that TIMP-2 may be used as a therapeutic strategy after SCI (Zhang et al., 2006). This supports our data in which higher levels of TIMP-2 were localised to rat lesion areas compared to lower levels in mice, suggesting mice have an equal balance in the levels of pro- and anti-angiogenic factors.

Due to NP's binding to VEGF family members and its receptors, semaphorins play a vital role in angiogenesis rather than axon guidance (Soker et al., 2002). Sema 3A does inhibit tumor cell migration in an NP1 dependent manner by inhibiting vessel function and increasing hypoxia and necrosis in multiple mouse tumor models (Casazza et al., 2011). Our fluorescent immunohistochemistry results confirm the role of Sema3A as an inhibitory molecule in and around the lesion site after SCI in rats by displaying a significant increase in localisation of Sema 3A compared to mice. Sema 3A was almost absent in mice lesions and further supports the idea that cavity free response seen in the mouse after SCI is conducive to angiogenesis, wound-healing and a better balance of scar deposition which we originally hypothesised from preliminary results that showed an increase in laminin deposition in the mouse compared to that of the rat lesion site. It is important to note that whilst the mice in our model seemed to recover fully after mild sub-acute SCI this may not be that case if a more severe model was to be inflicted, such as the weight drop model, which would result in increased functional deficits.

4.7.4 Matrix proteases

MMP-1 is required for cell migration during angiogenesis and is upregulated in many cancers and in humans MMP-1 levels are associated with an early up-regulation of macrophages (Hiraoka et al., 1998, buss et al, 2007). Our results show that MMP-1 was significantly higher in mouse lesion sites compared to rat lesion sites after sub-acute SCI. This suggests that there is induction of angiogenesis after SCI in mice supporting our hypothesis but also an early induction of inflammation to remove debris after injury.

Whilst, MMP-2 and MMP-9 are associated with angiogenesis and inflammation reaction after injury and is thought they play a part in BBB disruption, edema, migration and infiltration of inflammatory cells (Mautes et al., 2000, Biddison et al., 1997, Di Girolamo et al., 1998, Romanic et al., 1998). It is reported that expression of VEGF up-regulates MMP-9 expression, which correlates with our immunohistochemical observations that show significant expression of VEGF and MMP-9 in mouse lesions compared to rats (Wang and Keiser, 1998). Whilst there was no significant difference in the levels of MMP-2 after injury between mice and rats and it has been demonstrated that in the CNS MMP-2 is constitutively expressed in the endothelium. But once activated with pro-inflammatory cytokines no changes were seen in MMP-2 expression coinciding with our results (Harkness et al., 1999).

4.7.5 ECM/scar-related molecules

PECAM-1 plays a key role in removing aged neutrophils, aids leukocyte migration, activates integrins and promotes angiogenesis (Newman, 1997). Our results showed that there was a significant increase in PECAM-1 localisation around the lesion site in rats and mice. PECAM-1 has been demonstrated to play a role in the integrity of the BBB in the CNS (Lossinsky et al., 1997). However in a weight drop model in mice there was a significant increase in PECAM-1^{+} vessels at 3-7 days suggesting that it contributes to wound healing (Goussev et al., 2003, Whetstone et al., 2003). This supports our data seen and thus our hypothesis that mice have a robust wound healing response correlating with angiogenesis compared to rats.

Laminin and collagen-1 localisation in both species mirror each other's response. In the sub-acute stage, one would expect there to be an adequate balance

between angiogenesis (i.e. laminin expression) and scar deposition (i.e. collagen-1 deposition) in order for damaged tissue and neurons to effectively repair the lesion site. However in the chronic stages one would expect there to be more collagen-1 deposition than laminin due to the scar maturing. It has been demonstrated that using collagen type 1 scaffolds in the CNS promotes neuronal regeneration but more importantly after SCI provides directional axonal growth and functional recovery (Ma et al., 2004, Ding et al., 2010, Watanabe et al., 2007, Joosten et al., 1995). However, our results showed that only mice are able to fill the lesion site with laminin and collagen-1 while the response by rats was poor, failing to fill the lesion site with these molecules. This may reflect the difference in cavitation observed between mice and rats.

4.7.6 Behavioural testing

We originally hypothesised that mice have a robust wound healing response resulting in increased angiogenesis and better functional recovery than rats, correlating with little or no cavity formation while a large cavity in rats correlate with little angiogenesis and poorer functional outcomes. After observing significant differences in pro-angiogenic and anti-angiogenic protein localisation and levels after DC injury between mice and rats, part of our hypothesis was vindicated. However, our hypothesis that behavioural deficits would be present correlating with little angiogenesis and large cavities in rats was not borne out by our behavioural assessments. Our behavioural tests showed that despite post-injury deficits, animals regained normal responses within 7 days even though the cavity is still forming and expanding in rats beyond 1 month when cavities are fully established (Byrnes et al.,

2010, Sroga et al., 2003, James et al., 2011). A similar unaffected behavioural response was shown by Hill et al (2009) where they used a LISA-Vibraknife to generate precise dorsal lacerations at varying depths from 0.5, 0.8, 1.1 to 1.4mm in mice (Hill et al., 2009). Using similar behavioural assessments to that used by us, the authors showed that a comparable 0.8mm laceration of the dorsal spinal cord at the same T8 lesion site, produced no significant differences in behavioural assessment parameters, in injured mice compared to control mice. However as the lesion depth increased to 1.1 and 1.4mm, behavioural deficits were observed. Previous studies have shown that lesion severity correlates with the extent of behavioural deficits in mouse SCI models (Farooque, 2000, Seki et al., 2002, Ma et al., 2001). Similar results were shown in rats using small lesions at T8 within the corticospinal tract, similar to our model, rats reached recovery within a week (Majczynski and Slawinska, 2007, Muir and Whishaw, 2000). In our SCI model, lesion depth of 0.8mm is therefore considered a mild injury and therefore slight behavioural deficits were seen only 2 hours after injury in both mice and rats returning back to baseline control levels. Our results demonstrate that despite the presence of a large cavity in rats, behavioural deficits are not observed suggesting remarkable spinal plasticity in the rat. After injury the spinal cord is capable a degree of injury-induced spinal plasticity and therefore the ability of the animal to regain an apparent degree of functional recovery increases (Dietz, 2006). Activity dependent training to enhance limb movement and reinforce appropriate connections have shown to result in better functional recovery through spinal plasticity in both humans and animal models after SCI (Edgerton and Roy, 2002, Dietz, 2002, Dietz, 2006, Krajacic et al., 2010).

Another explanation as to why an acute deficit was observed only 2 hours after injury in both species could be a result of the model itself. Our aim was to transect only the DC axons to produce a SCI in both mice and rats and to use mechanical and thermal stimuli to assess neuropathic pain. However, the spinothalamic tract, located in the lateral section of the spinal cord is the central pain pathway that would show true pain deficits once injured (Purves et al, 2001). Therefore the deficits seen could be due to the Buprenorphine; an analgesic opioid used to relieve pain, wearing off after surgery as opposed the model itself.

Although we have used an inbred mouse (C57Bl6) and outbred rat (Sprague-Dawley) strain to investigate cavitation, equivalent responses to DC injury have been observed in other outbred rat strains such as Long Evans and Wistar rats as well as inbred strains such as Lewis rats (Jimenez Hamann et al., 2005, Byrnes et al., 2010, Schwartz et al., 1999, Poon et al., 2007, Lagord et al., 2002, Figley et al., 2014, Sroga et al., 2003). The extent of cavitation however, is dependent in the severity of the initial injury (Poon et al., 2007). Furthermore, there is no consistency across inbred and outbred strain to indicate that cavitation would be different in one group of animals versus the other group. For example, SCI in inbred and outbred strains of mice that are either resistant or susceptible to excitotoxcity all showed increases in lesion size over the first 7 days followed by decreases in cavity and wound healing from 7 to 56 days, although animals susceptible to excitotoxcity showed larger lesion sizes across all strains (Inman and Steward, 2003). Therefore, our results are valid across a range of rat and mouse strains and highlights the differences in cavity formation, matrix deposition and wound healing responses.

In summary, this data for known pro-angiogenic/wound healing-related proteins supports the notion that the cavity free response seen after SCI in mice is due to an adequate balance of scar deposition, wound-healing and vascularisation but do not correlate with acute functional deficits but a reduced amount of axonal sparing. The injury response observed in rats correlates with the presences of cavity formation after injury very much the same as what has previously been documented in humans after SCI (Fleming et al., 2006). However, in our animal model of mild T8 sub-acute SCI, the observation of functional deficits was minimal and therefore did not correlate with our injury response and histological data observed in rats.

CHAPTER 5

DISTINCT INFLAMMATORY-INDUCED ANGIOGENIC RESPONSES DISPLAYED AFTER SUB-ACUTE SPINAL INJURY IN MAMMALS

5.1 Introduction

5.1.1 Inflammation

Inflammation is part of the body's natural response to harmful stimuli such as pathogens, where vascular tissues aim to remove harmful stimuli and initiate the healing response bringing damaged tissue back to normal. The acute phase of inflammation requires a rapid influx of blood granulocytes, typically neutrophils, followed shortly by monocytes that mature into inflammatory macrophages. The process of acute inflammation results in redness, swelling and pain, symptoms typically associated with inflammation, around the sight of infection/injury (Ricciotti and FitzGerald, 2011). Once the harmful stimulus is removed via phagocytosis, the inflammatory reaction begins to resolve allowing macrophages and lymphocytes to return back to pre-inflammatory levels. Successful inflammation results in repair and resolution of tissue damage but it is a process that needs to be closely monitored as persistent inflammation can typically result in scarring and loss of organ function thus leading to excessive tissue damage and chronic inflammation (Nathan, 2002). Chronic inflammation can be detrimental resulting in the cause of autoimmune demyelinating diseases of the central and peripheral nervous system such as multiple sclerosis (MS) and chronic demyelinating polyradiculoneuropathy (CIDP) (Melzer and Meuth, 2014).

5.1.2 Inflammation and cavitation

Many studies report that inflammation contributes to cavitation which also aids in the deleterious pathology seen in many pathological conditions and diseases. Clinical intra-operative pathology of the salivary/parotid gland swelling revealed

granulomatous inflammation accompanied by central cavitation (Ho et al., 2013). Whilst in cases of congenital cystic adenomatoid malformation massive amounts of cavitation containing multiloculated cysts of vary size was observed with noticeable inflammation (Kim et al., 2013). Uncontrolled inflammation in tuberculosis can lead to excessive tissue remodelling, causing fibrosis and/or cavitation (Perez et al., 2003). Inflammation-induced cavitation not only plays a dual role in organs but also other areas of the body. An infection in soft tissue and joints demonstrates that inflammation proceeds through necrosis to cavitation (Wilson, 2004).

Previous studies have demonstrated that inflammation may contribute to secondary injury and therefore cavitation after injuries to the CNS. Inducing inflammation using zymosan; a macrophage activator, into the corpus callosum of rats initiates a cascade of secondary tissue damage, progressive cavitation and glial scarring in the CNS (Fitch et al., 1999). In models of traumatic brain injury vascular fluid cavitation and cell death, are both exacerbated by the progression of neuroinflammation (Abdul-Muneer et al., 2013, Atkins et al., 2013). Patients developing spinal arachnoiditis after peridural anaesthesia developed meningeal inflammation that later induced ischemia and cavitation (Torres et al., 1993).

Inflammatory cells and in particular macrophages, participate not only in tissue destruction but also cavity enlargement and thus contribute to the secondary pathology response after SCI (Glaser et al., 2006). In models of SCI, rats receiving dural repair after cervical laceration to the spinal cord resulted in reduced infiltration of macrophage/microglial into the lesioned area that further reduced lesion volume and cystic cavitation (Iannotti et al., 2006). The use of self-assembling peptides combined with neural/progenitor cells in rats after cervical SCI reduces cystic

cavitation volume whilst attenuating peri-lesional inflammation (Iwasaki et al., 2014). Interestingly endogenous expression of interleukin-4 regulates macrophage activation but also confines cavity formation after traumatic SCI in rats (Lee et al., 2010). The presence of a large cavity in the rat is proposed to be the result of the presence of macrophages and microglia removing debris, whilst mice fail to demonstrate cavitation (Inman and Steward, 2003, Gonzalez-Lara et al., 2009). The lesioned area in mice is normally filled with ECM and inflammatory cells (Inman and Steward, 2003).

5.1.3 Inflammation after SCI

After human SCI neutrophils entered the injured spinal cord between 1-3 days and were detectable for up to 10 days after SCI. There were significant numbers of CD68 microglia but few monocytes/macrophages in the injured tissue 1-3 days after injury and remained in the cord up to weeks and months after SCI. Through the time periods tested only a few $CD8^+$ lymphocytes were observed (Fleming et al., 2006). It has been shown that there is an increase in the number of white blood cells in the cerebrospinal fluid within the 7 days after injury showing an increase in plasma levels of inflammatory mediators in patients with long-standing SCI (Segal et al., 1997). The accumulation of activated microglia and macrophages may contribute to the progression of secondary injury (Blight, 1992, Blight et al., 1995, Bethea et al., 1998).

As previously mentioned the inflammatory response between mice and rats has previously been investigated showing marked differences in T-cell numbers between the two species (Sroga et al., 2003, Byrnes et al., 2010). However, the difference in the pathological progression after SCI in rats and mice appears to be

the formation of a cavity near and around the lesioned area and the extent of inflammation (Byrnes et al., 2010). The differences in the inflammatory response between the two species may thus be a contributing factor to the development of cavities within the lesion site.

5.1.4 Inflammatory markers

The localisation and protein expression of inflammatory mediators can be tested using known inflammatory markers, in particular, OX-42, CD68, CD4, CD8, fibronectin and GFAP after SCI. OX-42 (CD11b) is a β-integrin marker of activated microglia and macrophages that can be used to mark the activation and recruitment after injury especially after neurodegenerative inflammation (Roy et al., 2006, Perego et al., 2011). As previously mentioned (Chapter 3 introduction) CD68 (ED-1) was originally identified as a marker of macrophages and active phagocytosis and is also expressed in human fibroblasts and active endothelial cells (Holness and Simmons, 1993, Kunz-Schughart et al., 2003, Beranek, 2005, Perego et al., 2011).

CD4 and CD8 (cluster of differentiation 4 and 8) are transmembrane glycoprotein's used as a marker of T-cells after injury (Luckheeram et al., 2012). CD4 are known as the 'helper' T-cells that activate B cells, whilst CD8 are known as the 'cytotoxic' T-cells that kill other 'target' cells, and are used to identify T-cells involved in the injury response (Alberts et al., 2002).

As previously mentioned (Chapter 3 introduction) Fibronectin is an ECM glycoprotein and is a marker of increased fibroblast expression in overgrown lesions (Sume et al., 2010). However, glial fibrillary acidic protein (GFAP) is an intermediate

filament protein where increased expression of GFAP represents activation of astrocytes and glial cells during neurodegeneration (Brahmachari et al., 2006).

5.2 Rationale

After sub-acute SCI, mice and rats displayed distinct differences in cavitation, laminin deposition and inflammatory/angiogenic responses. The increased angiogenic responses at 8 dpl supported no cavity formation in mice after sub-acute SCI, whilst rats developed large cavities that coincided with decreased angiogenic responses. Many studies have shown that inflammation along with other mechanisms can contribute to the secondary damage after injury and that inducing inflammation in rats can potentiate cavitation. This led us to propose that inducing inflammation immediately after injury in mice may cause cavity formation similar to that seen in rats after SCI at 8 dpl; a time point that has demonstrated the greatest difference between the two species.

5.3 Hypothesis

In vivo induction of inflammation using an acute injection of zymosan; a macrophage activator, directly to the lesioned area immediately after injury would increase inflammatory cell infiltration, resulting in wound cavities in the microenvironment of the mouse SCI site similar to those seen in rat SCI at 8 dpl compared to control PBS treated animals.

5.4 Aims

- To compare histological analyses after PBS and zymosan injection into the mouse lesion site with PBS and zymosan injected rat lesion sites after T8 DC crush.
- To determine cavity development in PBS and zymosan injected mouse and rat lesion sites using Image ProAnalyzer.
- To analyse mouse and rat lesion sites using known inflammatory markers at 8 dpl using immunohistochemistry.
- To determine the effect that induced inflammation has on angiogenesis in mouse and rat lesion sites using known angiogenic markers.
- To confirm immunohistochemical results by western blot and densitometric analysis.

5.5 Material and Methods

5.5.1 Experimental design

Please refer to Material and Methods section 2.1 Animal surgery, 2.2.1 and 2.2.2 Tissue preparation for immunohistochemistry and western blotting for standard protocols used. To induce inflammation after sub-acute SCI, DC were crushed and immediately after injury mice and rats received either injection of PBS or zymosan directly to the lesioned area (stock concentration 12.5µg/ml (Fitch et al., 1999), 3µL or 5µl, respectively (maximum volume injected into mouse and rat previously used in the lab) (Table 5.1).

Type of analysis	N -numbers	End-points (days)
Inflammatory/angiogenic immunohistochemistry	3 (species/treatment group)	0, 8
Inflammatory/angiogenic western blot analysis	3 (species/treatment group)	0, 8

Table 5.1 Experimental design of n numbers and end-points used to assess inflammatory/angiogenic localisation and protein expression after sub-acute SCI in mice and rats.

5.5.2 Antibodies used for fluorescent immunohistochemistry

Please refer to Materials and Methods section 2.3.2 Fluorescent immunohistochemistry for standard protocol used. Fluorescent immunohistochemistry was used to assess the localisation of inflammatory and angiogenic related proteins (Table 5.2).

Inflammatory and wound healing/angiogenic-related proteins	Dilution factor	Species	Supplier (catalogue no.)
Primary antibodies			
Glial fibrillary acidic protein (GFAP)	1:400	Rabbit	Sigma (G9269)
Fibronectin	1:200	Rabbit	Sigma (F3648)
ED1 (CD68)	1:400	Rabbit	Santa Cruz Biotechnology (sc-9139)
OX-42 (CD11b)	1:100	Rabbit	Abcam (ab28664)
CD8	1:400	Rabbit	Novus Biologicals (NBP1-42051)
CD4	1:400	Rabbit	Novus Biologicals (NBP1-19371)
Laminin	1:200	Rabbit	Sigma (L9393)
VEGF-A (Vascular Endothelial Growth Factor-A)	1:400	Rabbit	Abcam (ab46154)
MMP-1 (Matrix Metalloproteinases)	1:200	Sheep	Biogenesis (5980-0111)
TIMP-2 (Tissue Inhibitor of Matrix Metalloproteinases)	1:200	Rabbit	Neomarkers (Rb-1789-P1)
Semaphorin 3A	1:200	Rabbit	Abcam (ab23393)
Secondary Antibodies			
Alexa 488	1:400	Rabbit	Molecular Probes (A11034)

Alexa 488	1:400	Sheep	Molecular Probes (A1105)

Table 5.2 Primary and secondary antibodies used to label inflammatory and wound healing/angiogenic-related proteins by immunohistochemistry.

5.5.3 Antibodies used for western blotting

Please refer to Materials and Methods section 2.5 western blot analysis for standard protocol used. Western blot analysis was used the protein expression of various inflammatory/angiogenic-related proteins at 8 dpl (Table 5.3)

Inflammatory and wound healing/angiogenic-related proteins	Dilution factor	Species	Supplier (catalogue no.)
Primary antibodies			
Glial fibrillary acidic protein (GFAP)	1:500	Rabbit	Sigma (G9269)
Fibronectin	1:200	Rabbit	Sigma (F3648)
OX-42 (CD11b)	1:400	Rabbit	Abcam (ab28664)
CD8	1:400	Rabbit	Novus Biologicals (NBP1-42051)
CD4	1:400	Rabbit	Novus Biologicals (NBP1-19371)
Laminin	1:100	Rabbit	Sigma (L9393)
VEGF-A (Vascular Endothelial Growth Factor-A)	1:1000	Rabbit	Abcam (ab46154)
MMP-1 (Matrix Metalloproteinases)	1:100	Sheep	Biogenesis (5980-0111)
TIMP-2 (Tissue Inhibitor of Matrix Metalloproteinases)	1:200	Rabbit	Neomarkers (Rb-1789-P1)
Semaphorin 3A	1:200	Rabbit	Abcam (ab23393)
Secondary Antibodies			
Horseradish Peroxidase (HRP)	1:1000	Rabbit	GE Healthcare (NA934)
Horseradish Peroxidase (HRP)	1:1000	Sheep	GE Healthcare (RPN4201)

Table 5.3 Primary and secondary antibodies used to label inflammatory and wound healing/angiogenic-related proteins by western blot.

5.5.4 Lesion cavity area

Please refer to Material and Methods section 2.3.3 Lesion cavity area for standard protocol used. Due to micro-cavities being present in the zymosan injected mouse

spinal cord after injury, cavities were determined using GFAP immunostaining in mouse and rat lesion sites. Cavities were considered to be free of $GFAP^+$ astrocytes whilst the border was surrounded by $GFAP^+$ astrocytes (Figure 5.1).

5.5.5 Relative fluorescent staining intensity

Please refer to Material and Methods section 2.3.4 Relative fluorescent staining intensity for standard protocol used for quantification of antibody immunoreactivity. Mice and rats injected with PBS were considered as controls whilst those injected with zymosan were the treatment groups. Quantification of pixel intensities were measured within a set area in ImageJ by thresholding the original image as described in previous chapters (Please refer to Chapter 2 Figure 2.5, Chapter 3 Figure 3.6 and Chapter 4).

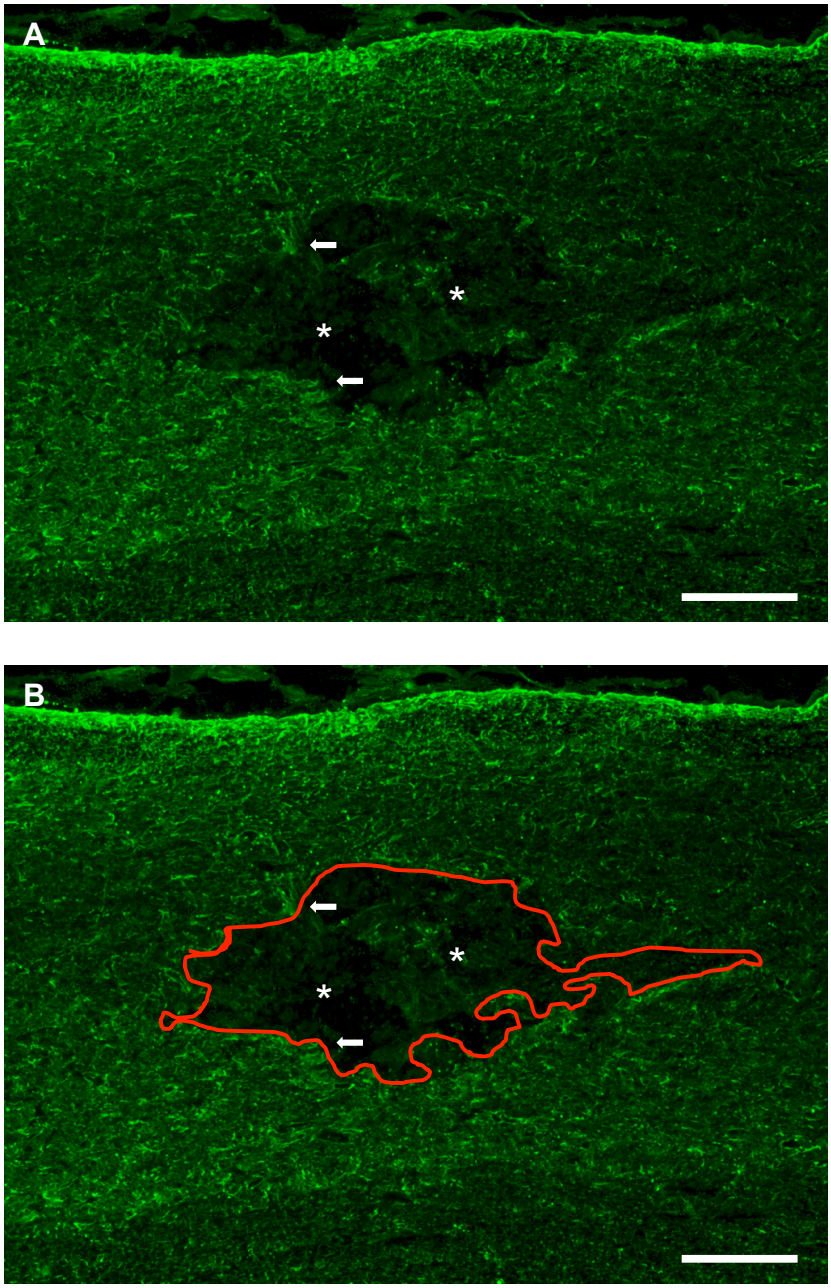

Figure 5.1 Lesion cavity area of mice and rats injected with PBS or zymosan was determined using GFAP stained sections **(A)**. The lesion area was measured in Image ProAnalyzer by drawing around the edge of the astrocyte free cavity **(B)** using the middle section of each cavity in mice and rats. (n = 3/species/treatment group; scale bars in A - B = 200µm; arrowheads in A-B = GFAP positive astrocytes; * = astrocyte-free areas).

5.6 Results

5.6.1 Microenvironment responses after induced inflammation

After receiving an acute injection of control PBS, the microenvironment of the spinal cord in both mice and rats at 8 dpl displayed what is typically seen after SCI i.e. no cavitation seen in the mouse lesion area compared to wound cavities present in the rat (Figure 5.2A and B, arrows). Zymosan injection caused a greater degree of tissue disruption around the lesion epicentre (Figure 5.2C and D) when compared to their representative PBS controls, such that a larger cavity was apparent. In the rat cord this disruption continued rostrally and caudally after zymosan injection compared to PBS controls (Figure 5.2B and D). It is also apparent that small wound cavities, not normally present in PBS treated lesions, had developed around the lesion epicentre in mice treated with zymosan (Figure 5.2A and C, arrow).

Quantification of the lesion/micro-cavity area in mice (Figure 5.3A) and the lesion/micro-cavity area in rats (Figure 5.3B) at 8 dpl demonstrated significant difference in animals that were injected with PBS compared to those injected with zymosan. The cavity area in zymosan injected mice and rats were significantly higher ($P<0.040$ and $P<0.005$, respectively) compared to their controls. These results confirm that there is a greater degree of tissue damage and cavitation after zymosan injection compared to PBS controls in both mice and rats at 8 dpl.

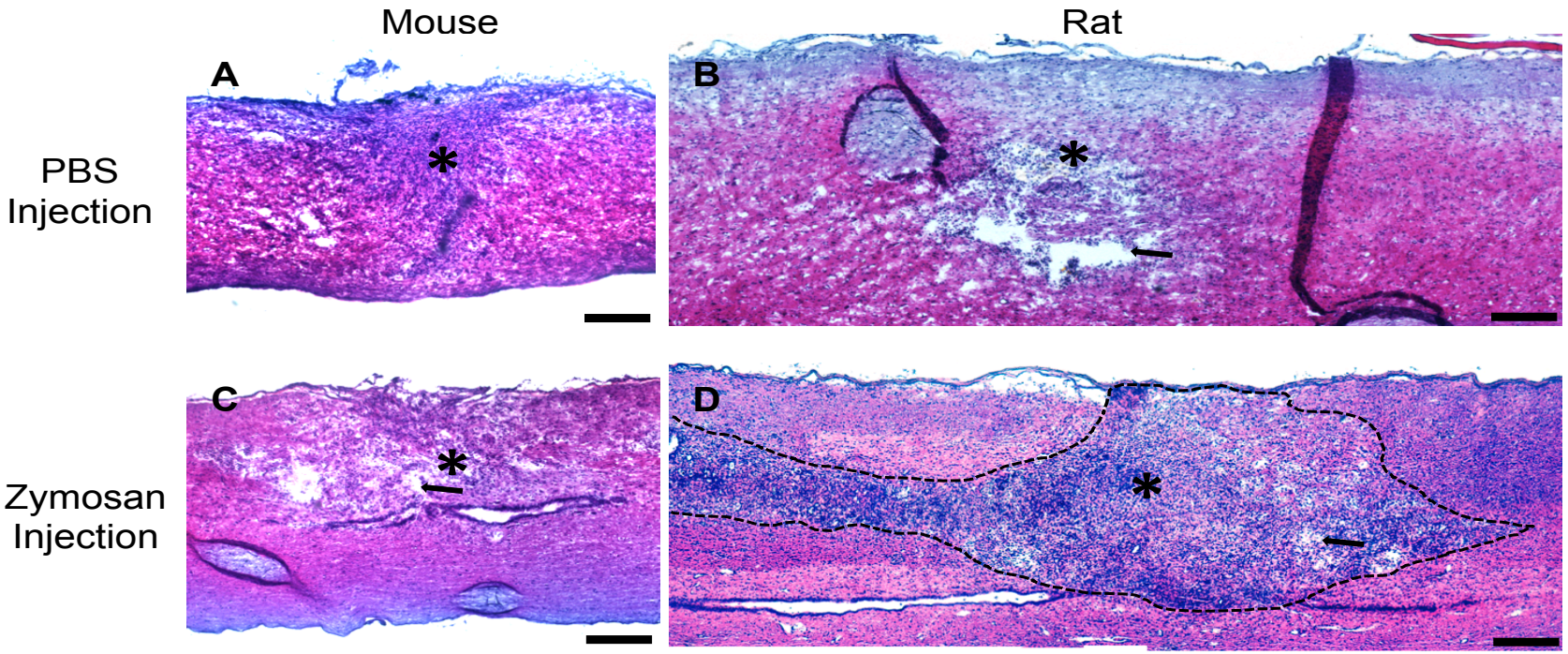

Figure 5.2 Histological differences in wound cavitation after SCI in mice treated with PBS **(A)** or zymosan **(C)** and rats treated with PBS **(B)** or zymosan **(D)** at 8dpl. Tissue disruption was examined by haematoxylin and eosin staining of the middle section of each cavity to understand the greatest difference between PBS or zymosan treated cords in mice and rats. (n = 3/species/treatment group; * = lesion epicentre; scale bars in A-D = 200 μm; arrows in B, C and D = cell free areas in mouse and rat SCI cavities; dotted black line in D = extent of tissue damage after zymosan injection).

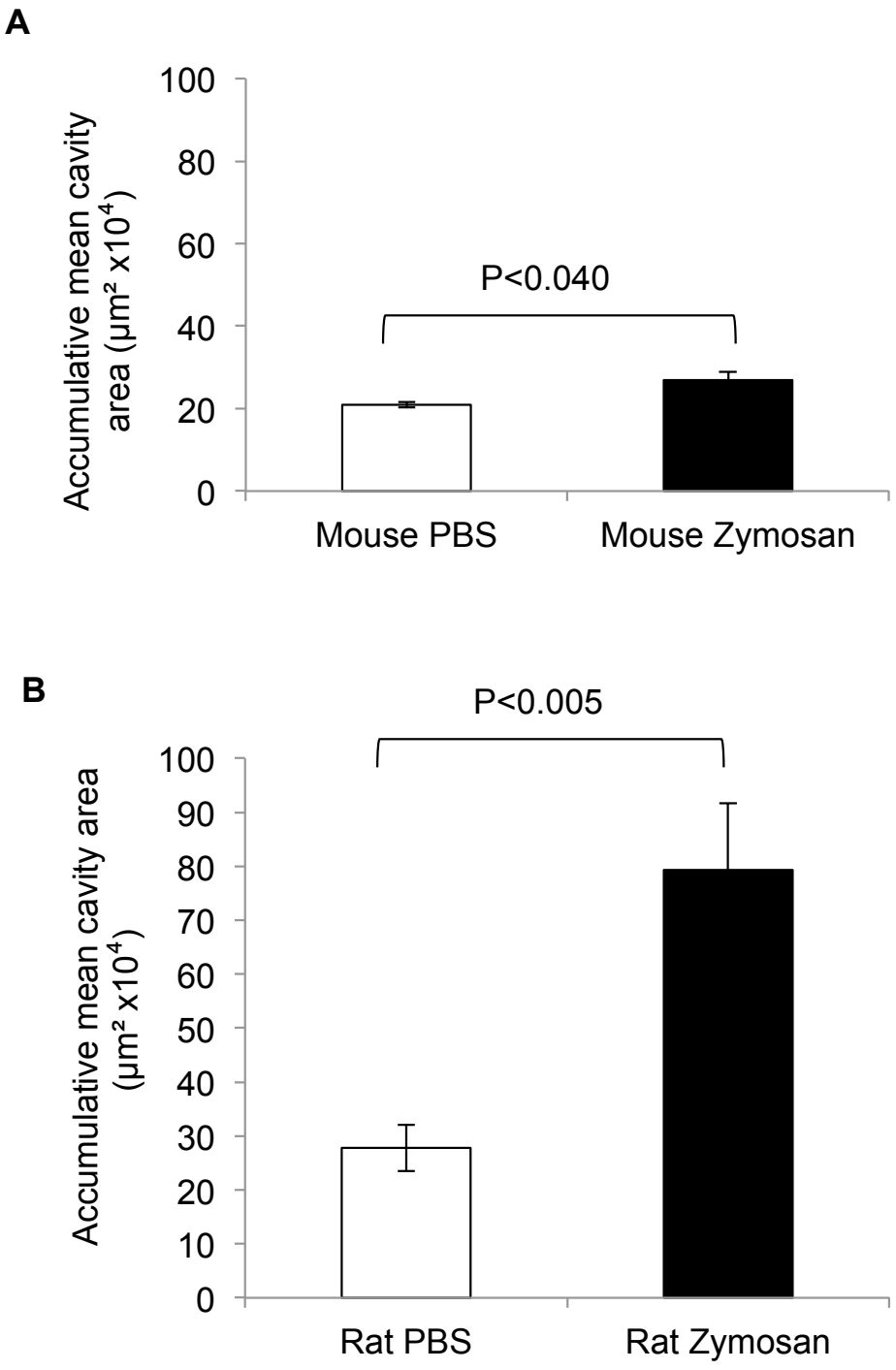

Figure 5.3 Accumulative mean micro-cavity area in mice **(A)** and accumulative mean micro-cavity area in rats **(B)** was compared in animals injected with PBS and Zymosan using $GFAP^+$ staining in the middle section of each cavity at 8 dpl. (n = 3/species/treatment group).

5.6.2 Characterisation of the inflammatory response to sub-acute SCI

1. Microglia. OX-42$^+$ quiescent and activated microglia were localised mainly to the lesion site and surrounding tissue after PBS injection with no apparent change after zymosan injection in mice (Figure 5.4A and B: inset), whilst in rats after zymosan injection there was slight decrease compared to PBS controls (Figure 5.4C and D: inset). OX-42$^+$ microglia immunoreactivity showed significant increase in rats compared to mice in PBS controls only (Figure 5.4E). Western blotting (Figure 5.4F) and subsequent densitometry (Figure 5.4G) demonstrated that OX-42 protein expression was significantly higher in rats compared to mice in PBS controls only at 8 dpl, coinciding with immunohistochemistry results.

2. Macrophages. The immunoreactivity of CD68$^+$ (ED1) activated macrophages was confined not only to the lesion site but surrounding tissue with a slight increase in CD68$^+$ macrophages after zymosan injection compared to PBS control in mice at 8 dpl (Figure 5.5A and B: inset). In PBS injected rats CD68$^+$ macrophages were present and once treated with zymosan there was an increase in CD68$^+$ macrophages that were confined mainly to the lesioned area (Figure 5.5C and D, arrow: inset). Immunoreactivity of CD68$^+$ macrophages revealed significant increase in zymosan injected rats compared to zymosan injected mice and their representative PBS controls (Figure 5.5E).

3. Resident T-cells. CD4$^+$ resident T-cells followed a similar pattern to CD68$^+$; no significant differences were observed in PBS/zymosan injected mice (Figure 5.6A and B; inset), whilst there was an increase in zymosan injected rats compared to their PBS controls (Figure 5.6C and D, arrow: inset) with the localisation confined only to the lesioned area. Immunoreactivity of CD4$^+$ cells were significantly increased

after zymosan injected rats compared to mice (Figure 5.6E). Western blotting (Figure 5.6F) and subsequent densitometry (Figure 5.6G) confirmed immunoreactivity levels; an increase in protein expression of $CD4^+$ cells after zymosan injected rats compared to zymosan injected mice.

Whilst $CD8^+$ resident T-cells revealed a decrease after zymosan injection in mice compared to PBS controls (Figure 5.7A and B: inset). However, in rats there was an increase in $CD8^+$ T-cells after zymosan injection compared to PBS controls where $CD8^+$ staining was confined mainly to the lesioned area (Figure 5.7C and D: inset). Quantification of immunoreactivity levels confirmed that there was an increase in $CD8^+$ cells in rats compared to mice after zymosan injection (Figure 5.7E). Western blot and subsequent densitometry confirmed that there was not only a significant increase in CD8 protein expression in rats compared to mice after zymosan injection, but that there was also a significant increase in CD8 protein in mice compared to rats after PBS injection (Figure 5.7F - G).

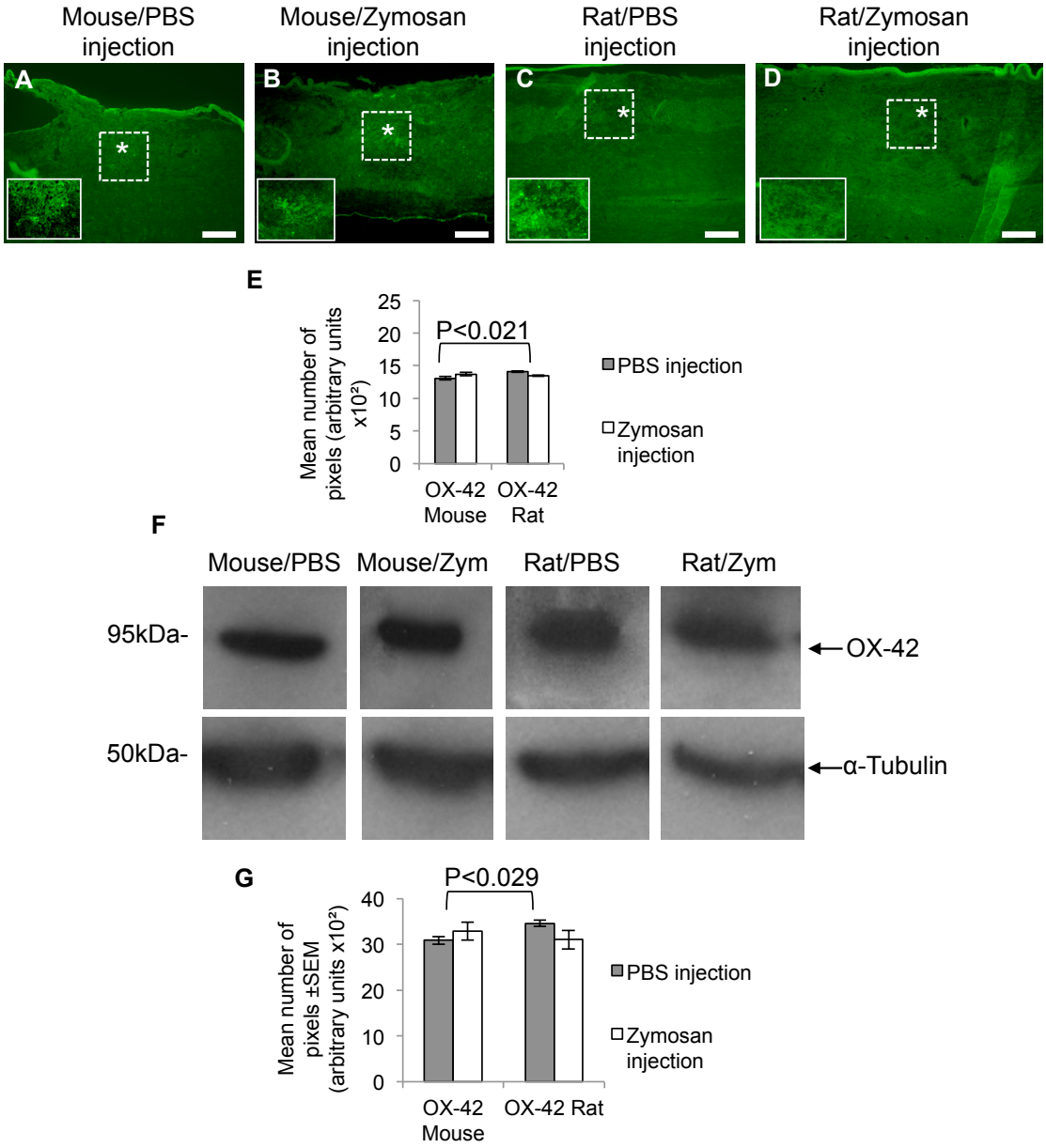

Figure 5.4 The localisation of OX-42 at 8dpl in DC lesions after induced inflammation. Immunohistochemistry for OX-42 in mice either treated with PBS **(A)** or zymosan **(B)** and rats either treated with PBS **(C)** or zymosan **(D)** and the pixel intensities of OX-42^{+} fluorescence **(E)**. Western blot **(F)** and densitometry **(G)** corroborated the immunohistochemistry results (α-tubulin was used as a protein loading control, image demonstrates a representative picture **(F)**; n = 3/species/treatment group; * = lesion epicentre; scale bars in A - D = 200μm).

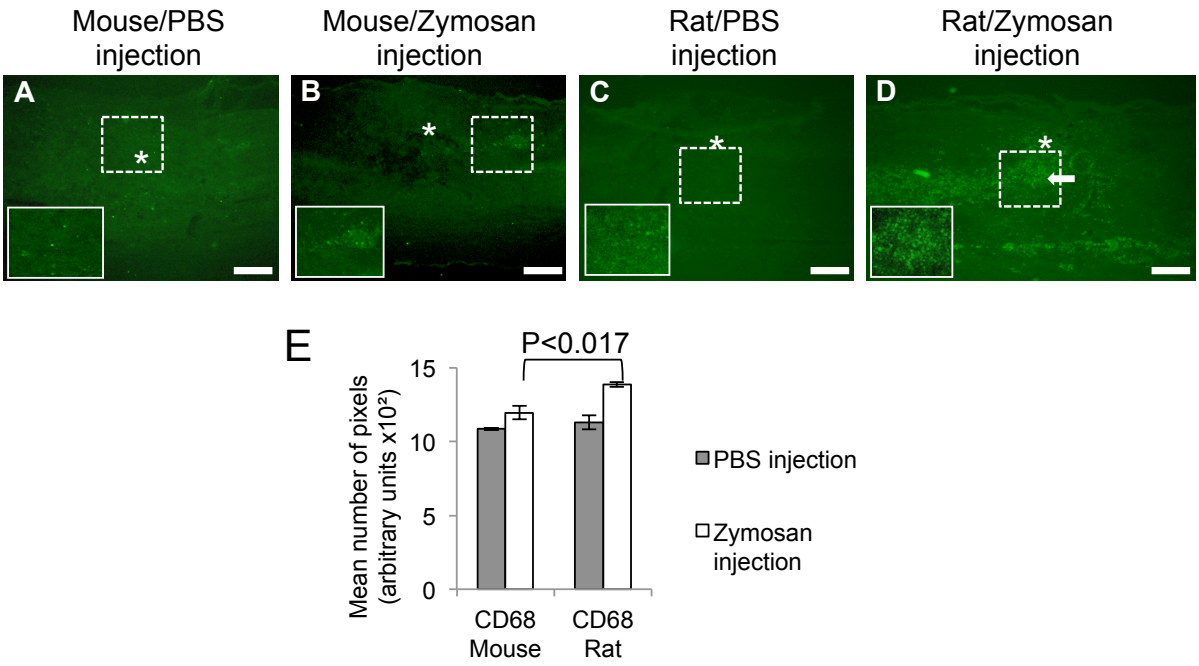

Figure 5.5 The localisation of CD68 (ED1) at 8dpl in DC lesions after induced inflammation. Immunohistochemistry for CD-68 in mice either treated with PBS **(A)** or zymosan **(B)** and rats either treated with PBS **(C)** or zymosan **(D)** and the pixel intensities of $CD68^{+}$ fluorescence **(E)**. (n = 3/species/treatment group; * = lesion epicentre; scale bars in A - D = 200µm; arrow in D = $CD68^{+}$ macrophages).

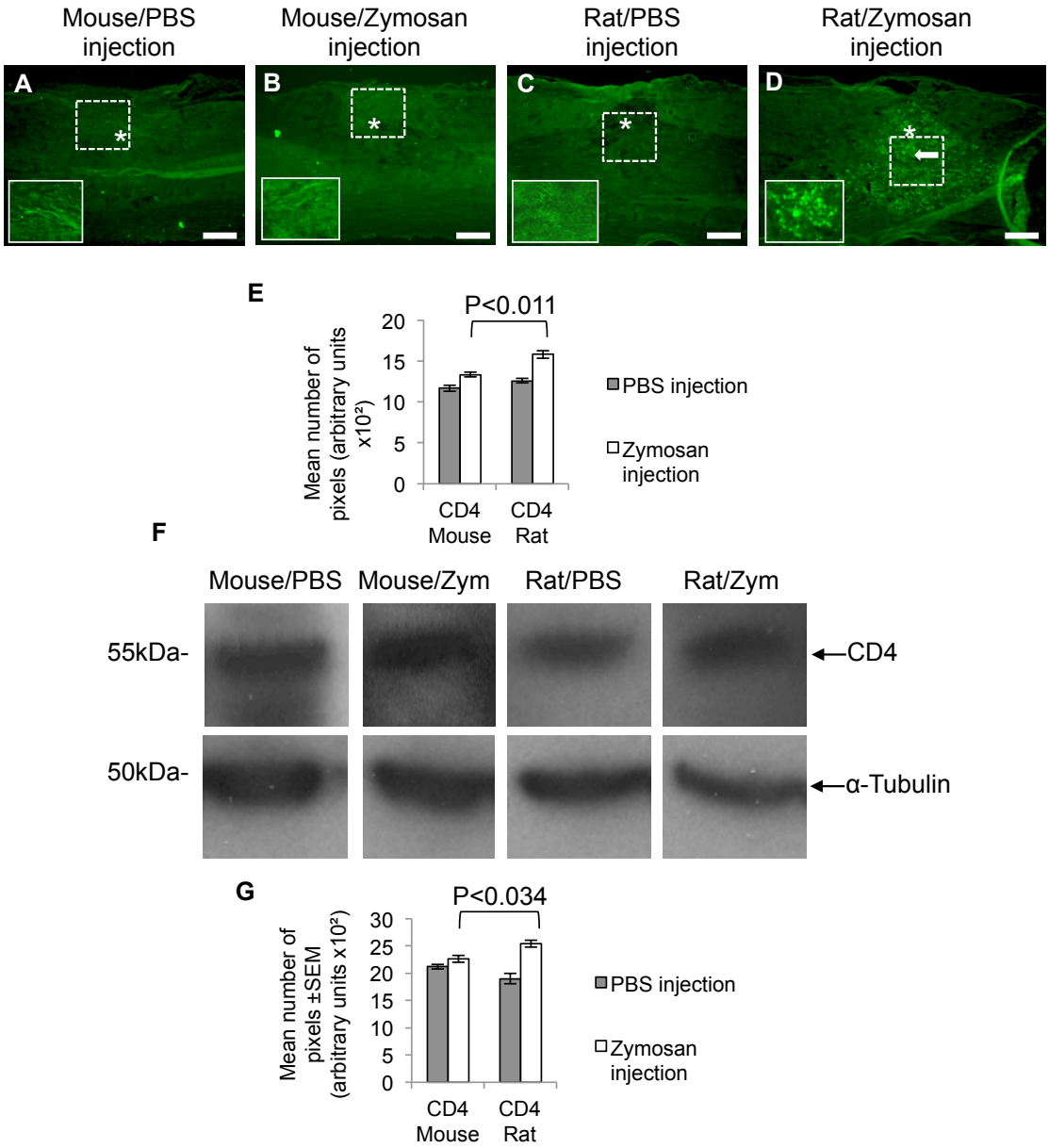

Figure 5.6 The localisation of CD4 at 8dpl in DC lesions after induced inflammation. Immunohistochemistry for CD4 in mice either treated with PBS **(A)** or zymosan **(B)** and rats either treated with PBS **(C)** or zymosan **(D)** and the pixel intensities of $CD4^{+}$ fluorescence **(E)**. Western blot **(F)** and densitometry **(G)** corroborated the immunohistochemistry results (α-tubulin was used as a protein loading control, image demonstrates a representative picture **(F)**; n = 3/species/treatment group; * = lesion epicentre; scale bars in A - D = 200μm; arrow in D = CD4+ T-cells).

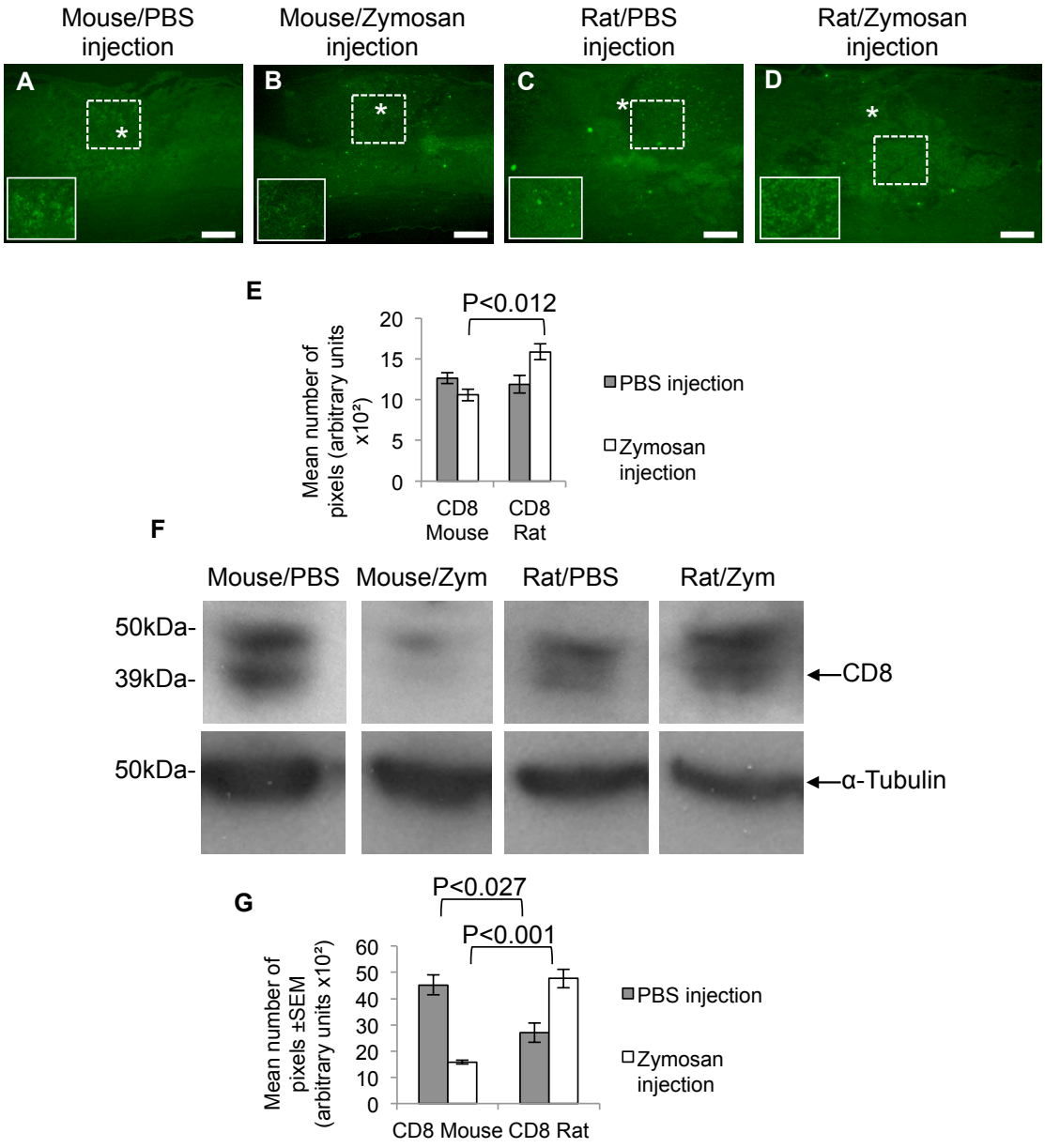

Figure 5.7 The localisation of CD8 at 8dpl in DC lesions after induced inflammation. Immunohistochemistry for CD8 in mice either treated with PBS **(A)** or zymosan **(B)** and rats either treated with PBS **(C)** or zymosan **(D)** and the pixel intensities of $CD8^{+}$ fluorescence **(E)**. Western blot **(F)** and densitometry **(G)** corroborated the immunohistochemistry results (α-tubulin was used as a protein loading control, image demonstrates a representative picture **(F)**; n = 3/species/treatment group; * = lesion epicentre; scale bars in A - D = 200μm).

5.6.3 Characterisation of the DC scarring response to injury

After injury, fibronectin$^+$ ECM filled the lesion core in mice when injected with PBS or zymosan showing similar responses (Figure 5.8A and B, arrows: inset), whereas in rats injected with PBS, very little or no fibronectin was present in the SCI wounds but after zymosan injection fibronectin$^+$ ECM material filled the lesion core in rats (Figure 5.8C and D, arrow: inset). Quantification of immunoreactivity revealed a significant increase in fibronectin$^+$ immunohistochemistry in rats after zymosan injection compared to mice (Figure 5.8E). Western blot and subsequent densitometry not only confirmed that there is a significant increase in fibronectin$^+$ protein expression after zymosan injection in rats compared to mice but that there was also a significant increase in fibronectin$^+$ protein expression in mice compared to rats after PBS injection (Figure 5.8F - G).

GFAP$^+$ astrocytes were abundant in the neuropil around the lesion site and invading the lesion core in mice injected with either PBS or zymosan (Figure 5.9A and B, arrows: inset). In rats injected with PBS, fewer GFAP$^+$ astrocytes were localised within the lesion and virtually absent in the lesion core, but there was an increase around the lesion site of GFAP$^+$ astrocytes in rats that were injected with zymosan (Figure 5.9C and D: inset). Pixel intensities demonstrated there was no significant difference in GFAP$^+$ astrocytes in mice injected with PBS or zymosan compared to rats treated with PBS or zymosan (Figure 5.9E). However, western blot and subsequent densitometry confirmed that no difference was seen between the two treatment groups for both mice and rats for GFAP$^+$ protein expression (Figure 5.9F and G).

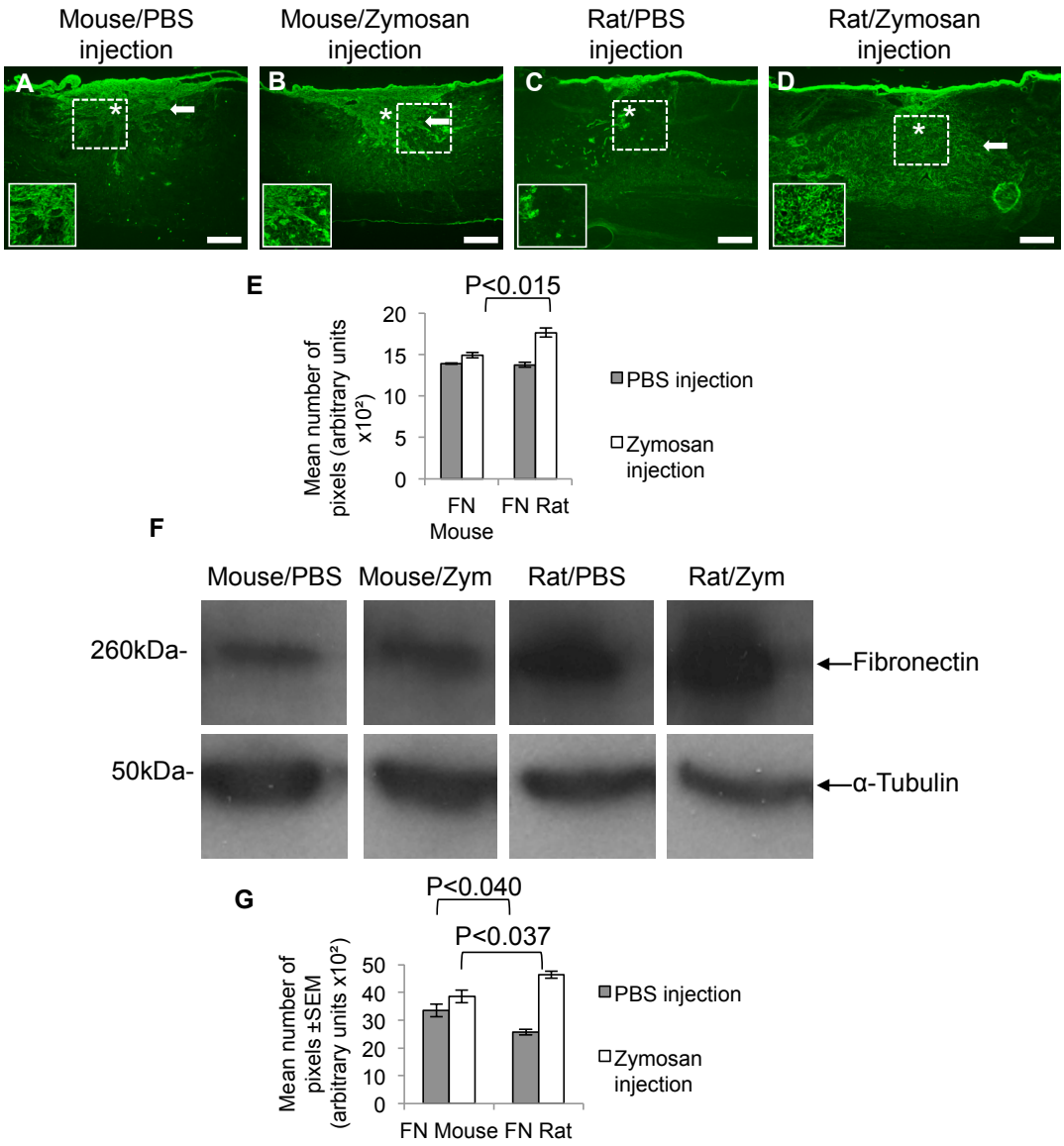

Figure 5.8 The localisation of FN 8dpl in DC lesions after induced inflammation. Immunohistochemistry for FN in mice either treated with PBS **(A)** or zymosan **(B)** and rats either treated with PBS **(C)** or zymosan **(D)** and the pixel intensities of FN^{+} fluorescence **(E)**. Western blot **(F)** and densitometry **(G)** corroborated the immunohistochemistry results (α-tubulin was used as a protein loading control, image demonstrates a representative picture **(F)**; n = 3/species/treatment group; * = lesion epicentre; scale bars in A - D = 200μm; fibronectin = FN; arrows in A, B and D = FN^{+} cells confined to lesioned area).

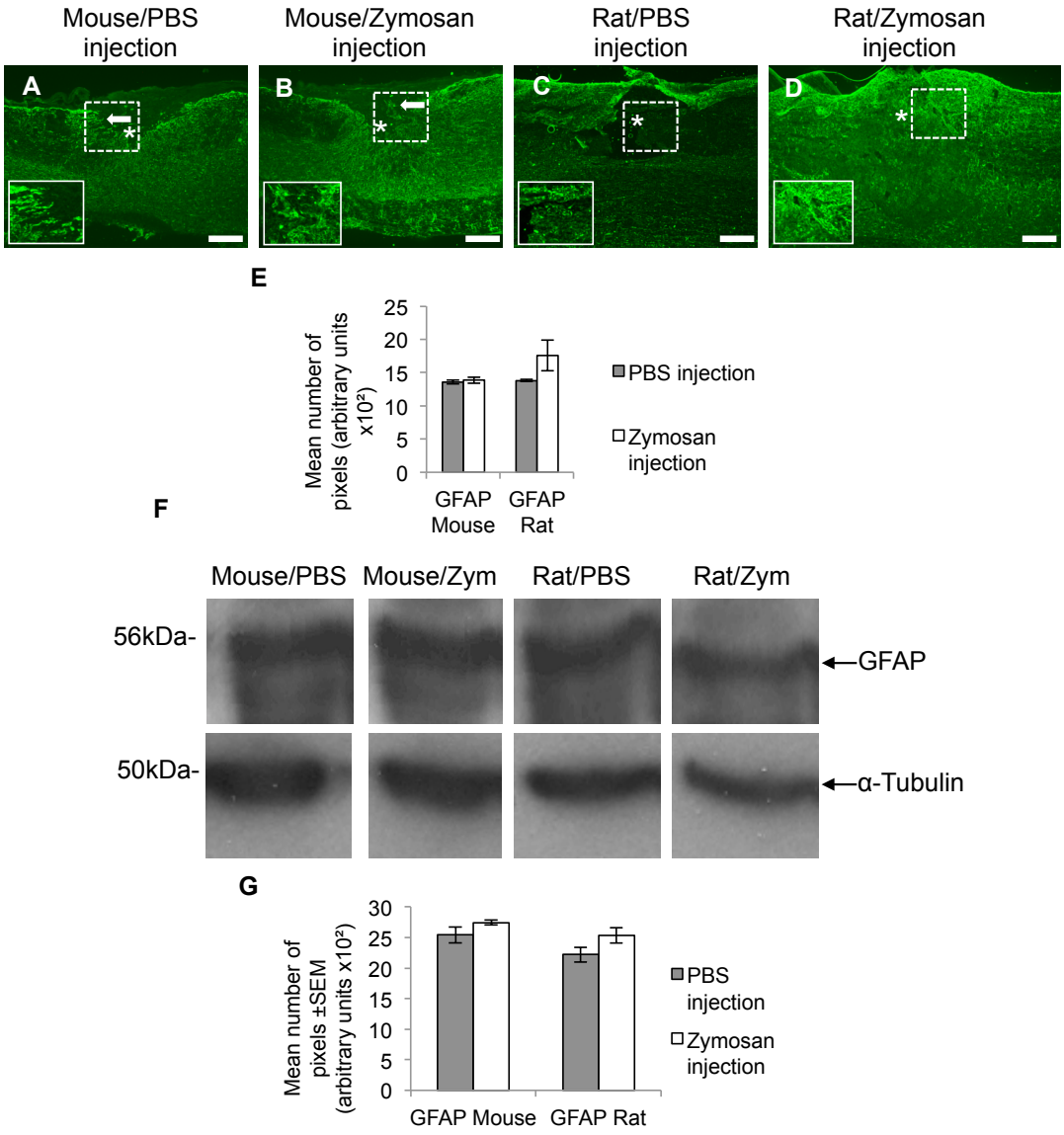

Figure 5.9 The localisation of GFAP 8dpl in DC lesions after induced inflammation. Immunohistochemistry for GFAP in mice either treated with PBS **(A)** or zymosan **(B)** and rats either treated with PBS **(C)** or zymosan **(D)** and the pixel intensities of GFAP$^+$ fluorescence **(E)**. Western blot **(F)** and densitometry **(G)** corroborated the immunohistochemistry results (α-tubulin was used as a protein loading control, image demonstrates a representative picture **(F)**; n = 3/species/treatment group; * = lesion epicentre; scale bars in A - D = 200μm; glial fibrillary acidic protein = GFAP; arrows in A and B = GFAP$^+$ astrocytes invading the lesion core).

4.6.4 Characterisation of angiogenic response to induced inflammation

1. Pro-angiogenic molecules. The immunoreactivity of VEGF-A did not differ after sub-acute injury in mice whether treated with PBS or zymosan (Figure 5.10A and B: inset), whilst in rats there was a slight reduction in VEGF-A once treated with zymosan compared to the PBS control (Figure 5.10C and D: inset). Quantification of immunoreactivity revealed a significant increase in VEGF-A^+ staining in mice once injected with zymosan compared to rats injected with zymosan (Figure 5.10E). Western blot and subsequent densitometry correlated with the immunohistochemical results (Figure 5.10F and G), demonstrating a significant increase in VEGF-A protein expression in mice compared to rats injected with zymosan after injury.

The immunoreactivity of MMP-1, like VEGF-A levels did not alter in the mouse regardless of injection received after injury (Figure 5.11A and B: inset), whilst in rats there was an increase in MMP-1 after being injected with zymosan compared to PBS controls, particularly localised to the lesion area (Figure 5.11C and D, arrow: inset). Quantification of immunoreactivity levels revealed a significant decrease in MMP-1^+ cells in rats injected with PBS compared to mice, whilst, after zymosan injection there was a significant increase in MMP-1^+ staining in rats compared to mice (Figure 5.11E). Western blot and subsequent densitometry correlated with immunohistochemical results showing a significant increase in MMP-1 protein expression in rats injected with zymosan compared to mice injected with zymosan only (Figure 5.11F and G).

After injury to the DC the lesioned area in mice becomes highly enriched with LN^+ staining and regardless of the mouse being injected with PBS or zymosan the outcome remains the same (Figure 5.12A and B: inset), whereas with rats after being

injected with PBS the lesioned area is mostly devoid of LN^+ ECM but once injected with zymosan there is an increase in LN^+ ECM mainly confined to the lesioned area (Figure 5.12C and D: inset). Quantification of immunoreactivity revealed there was a significant increase in laminin in rats after zymosan injection compared to mice injected with zymosan (Figure 5.12E). Western blot and subsequent densitometry not only confirmed that there was a significant increase in LN^+ protein expression in rats in injured cords injected with zymosan compared to mice but also revealed a significant increase in LN^+ protein expression in PBS control mice compared to PBS control rats (Figure 5.12F and G).

2. Anti-angiogenic molecules. The immunoreactivity of TIMP-2 was localised to the lesioned site and surrounding tissue in mice injected with PBS or zymosan (Figure 5.13A and B: inset), whereas in rats injected with PBS the lesion site was mostly devoid of TIMP-2 immunoreactivity but is localised to the boundaries of the SCI wound and surrounding tissue (Figure 5.13C and arrow: inset). Rats injected with zymosan displayed an upregulation of TIMP-2 confined mainly to the lesion epicentre compared to PBS controls with surrounding tissue devoid of immunoreactivity for TIMP-2 (Figure 5.13D and arrow: inset). Quantification of pixel intensities revealed no significant differences between the treatment groups (Figure 5.13E). However, western blot and subsequent densitometry demonstrated a significant increase in TIMP-2 levels in PBS injected mice compared to PBS injected rats after SCI (Figure 5.13F and G).

Semaphorin 3A immunoreactivity was mainly confined to the lesion site in mice treated with PBS or zymosan (Figure 5.14A and B: inset), whereas rats receiving a PBS or zymosan injection at the lesion site were devoid of Semaphorin

3A immunoreactivity and was localised to the boundaries of the wound cavity (Figure 5.14C and D, arrows: inset). Following quantification of pixel intensities, a significant increase in Semaphorin 3A protein expression was observed in mice injected with zymosan compared to rats injected with zymosan (Figure 5.14E). Western blot and subsequent densitometry confirmed what was observed immunohistochemically; significant increase in semaphorin 3A protein levels in mice compared to rats injected with zymosan (Figure 5.14F and G).

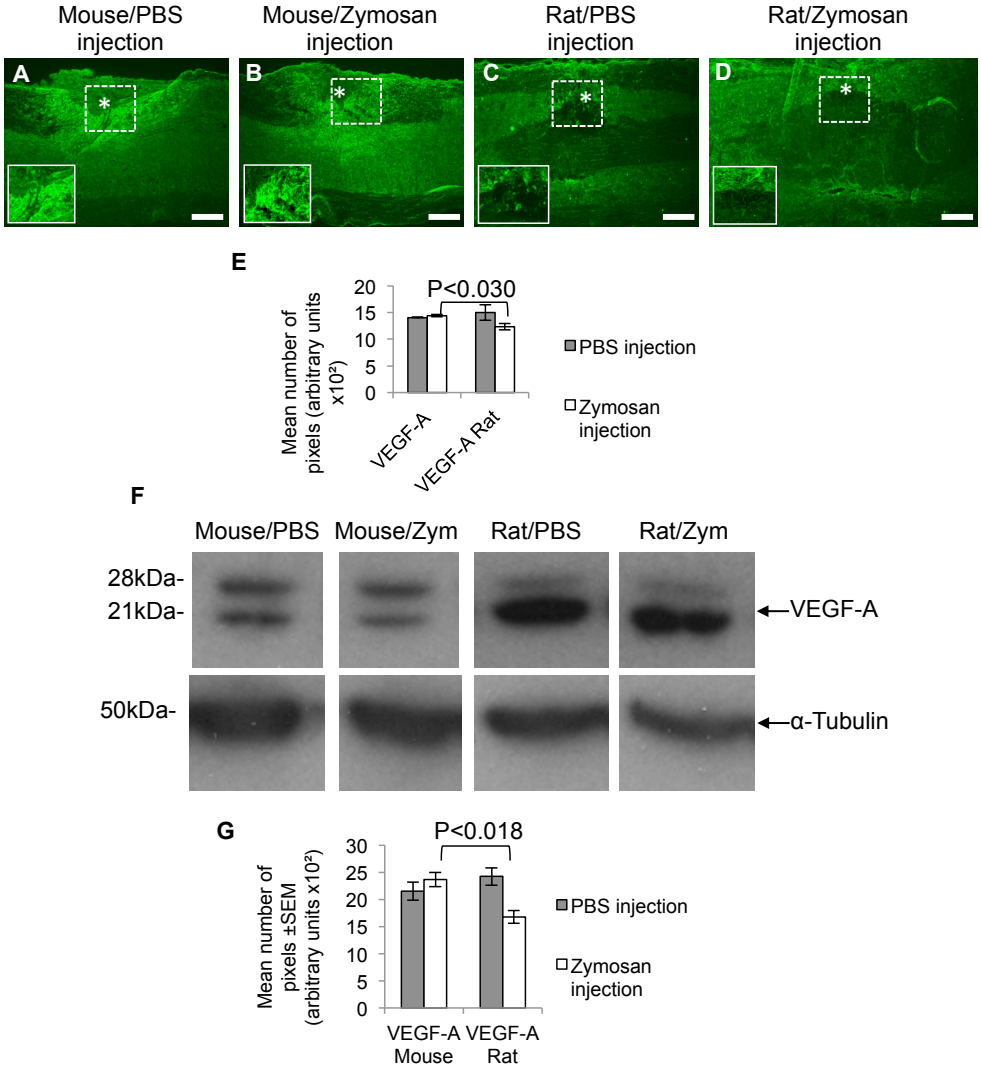

Figure 5.10 The localisation of VEGF-A (21 and 28 kDa proteins detected in the gel correspond to VEGF isoforms 165 and 189, respectively (Jauhianinen et al., 2011)) 8dpl in DC lesions after induced inflammation. Immunohistochemistry for VEGF-A in mice either treated with PBS **(A)** or zymosan **(B)** and rats either treated with PBS **(C)** or zymosan **(D)** and the pixel intensities of VEGF-A^{+} fluorescence **(E)**. Western blot **(F)** and densitometry **(G)** corroborated the immunohistochemistry results (α-tubulin was used as a protein loading control, image demonstrates a representative picture **(F)**; n = 3/species/treatment group; * = lesion epicentre; scale bars in A - D = 200μm; vascular endothelial growth factor- A = VEGF-A).

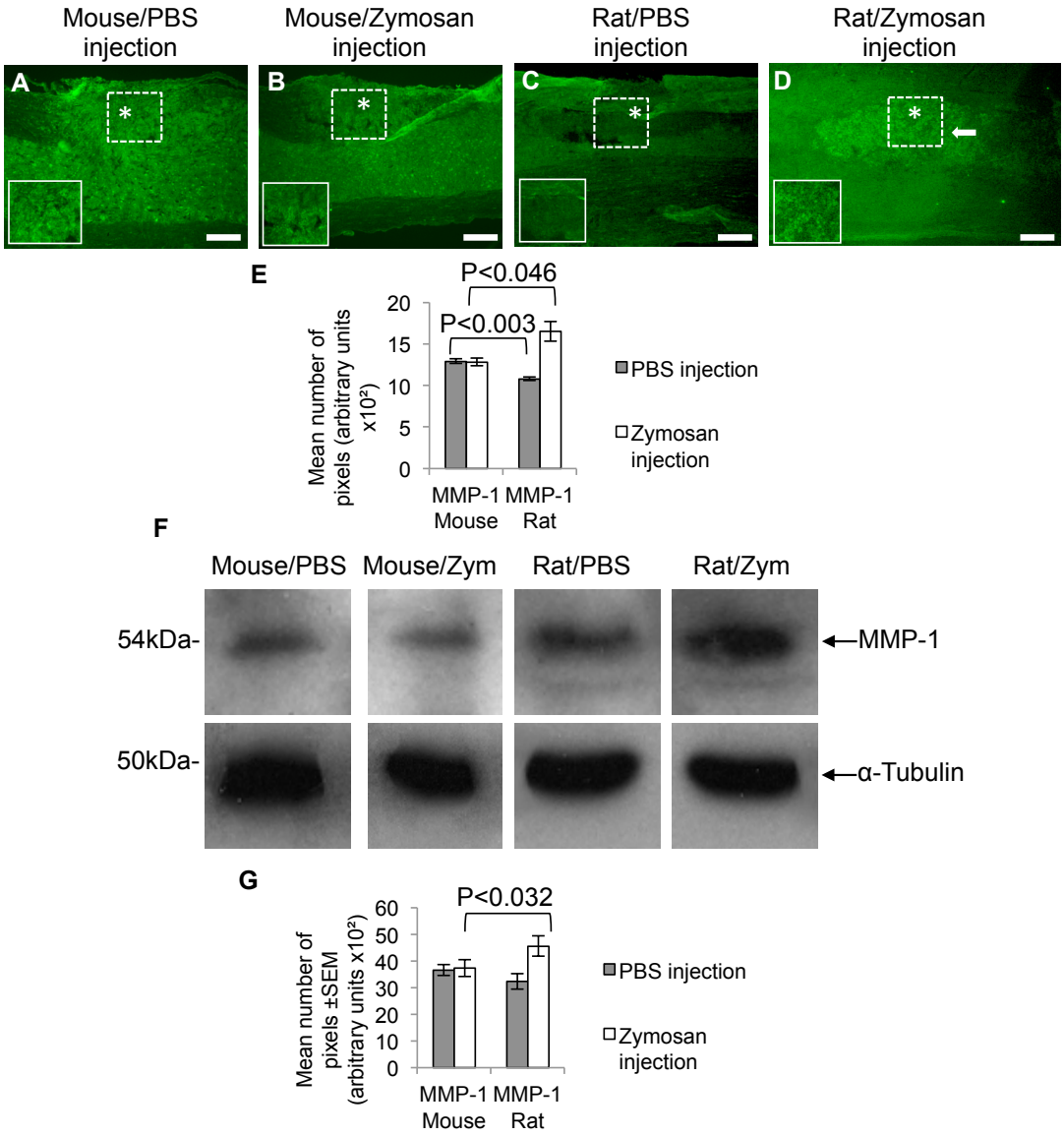

Figure 5.11 The localisation of MMP-1 8dpl in DC lesions after induced inflammation. Immunohistochemistry for MMP-1 in mice either treated with PBS **(A)** or zymosan **(B)** and rats either treated with PBS **(C)** or zymosan **(D)** and the pixel intensities of MMP-1^{+} fluorescence **(E)**. Western blot **(F)** and densitometry **(G)** corroborated the immunohistochemistry results (α-tubulin was used as a protein loading control, image demonstrates a representative picture **(F)**; n = 3/species/treatment group; * = lesion epicentre; scale bars in A - D = 200μm; matrix metalloproteinase 1 = MMP-1; arrow in D = MMP-1^{+} cells confined to the lesioned area).

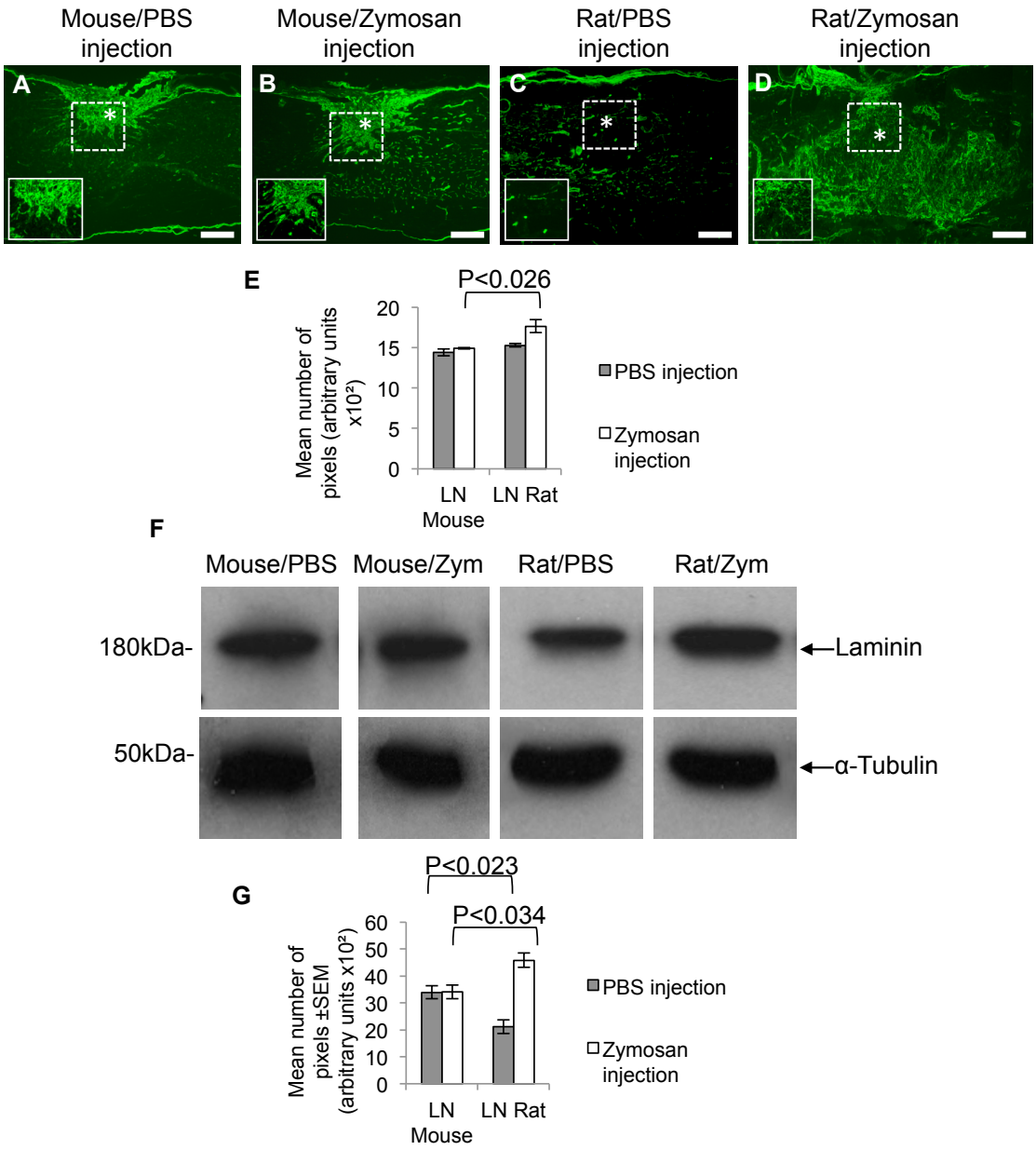

Figure 5.12 The localisation of LN 8dpl in DC lesions after induced inflammation. Immunohistochemistry for LN in mice either treated with PBS **(A)** or zymosan **(B**) and rats either treated with PBS **(C)** or zymosan **(D)** and the pixel intensities of LN^{+} fluorescence **(E)**. Western blot **(F)** and densitometry **(G)** corroborated the immunohistochemistry results (α-tubulin was used as a protein loading control, image demonstrates a representative picture **(F)**; n = 3/species/treatment group; * = lesion epicentre; scale bars in A - D = 200μm; laminin = LN).

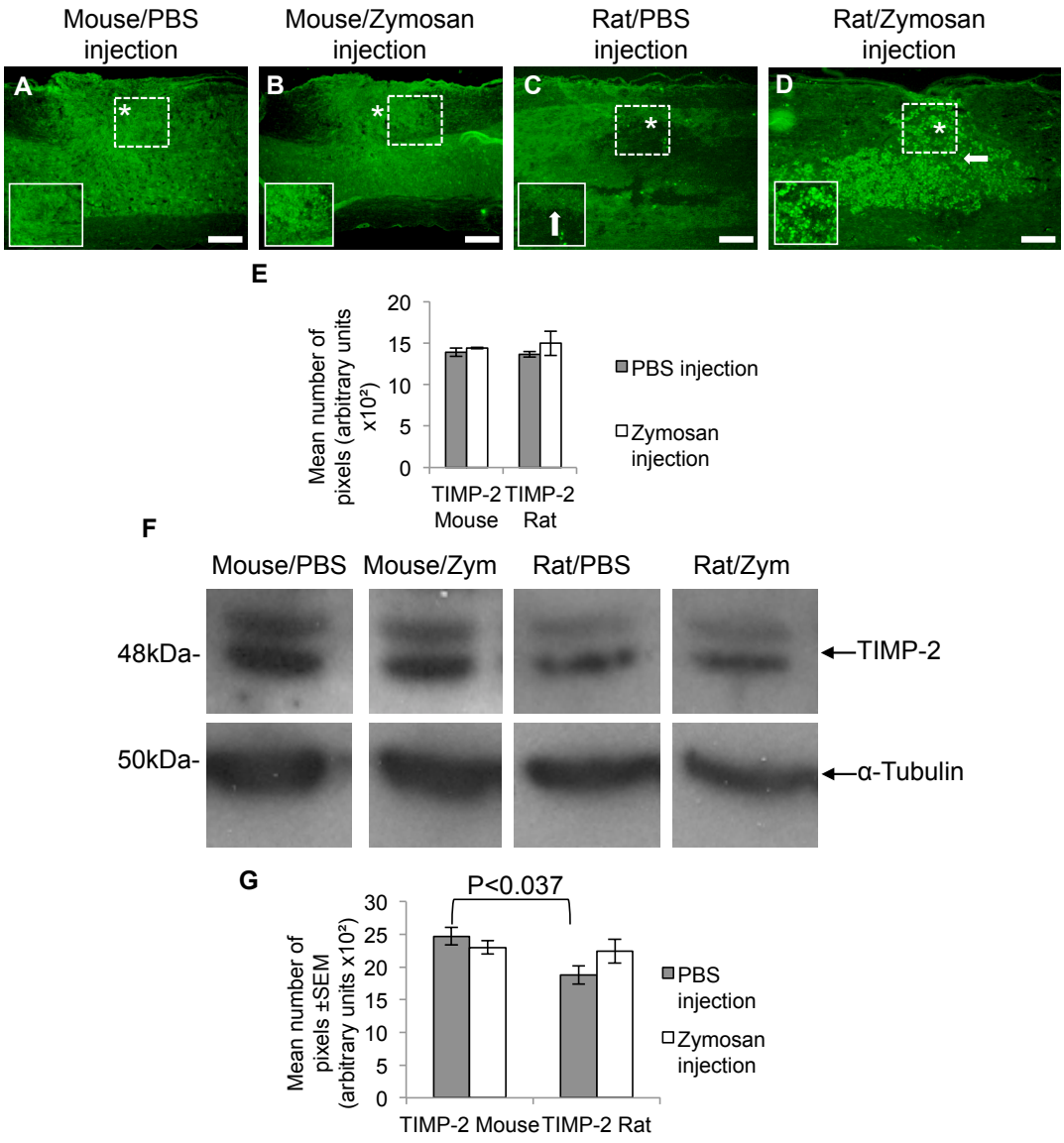

Figure 5.13 The localisation of TIMP-2 8dpl in DC lesions after induced inflammation. Immunohistochemistry for TIMP-2 in mice either treated with PBS **(A)** or zymosan **(B)** and rats either treated with PBS **(C)** or zymosan **(D)** and the pixel intensities of TIMP-2^{+} fluorescence **(E)**. Western blot **(F)** and densitometry **(G)** corroborated the immunohistochemistry results (α-tubulin was used as a protein loading control, image demonstrates a representative picture **(F)**; n = 3/species/treatment group; * = lesion epicentre; scale bars in A - D = 200μm; Tissue inhibitor of matrix metalloproteinase 2 = TIMP-2; arrow = TIMP-2^{+} cells confined to the lesioned area).

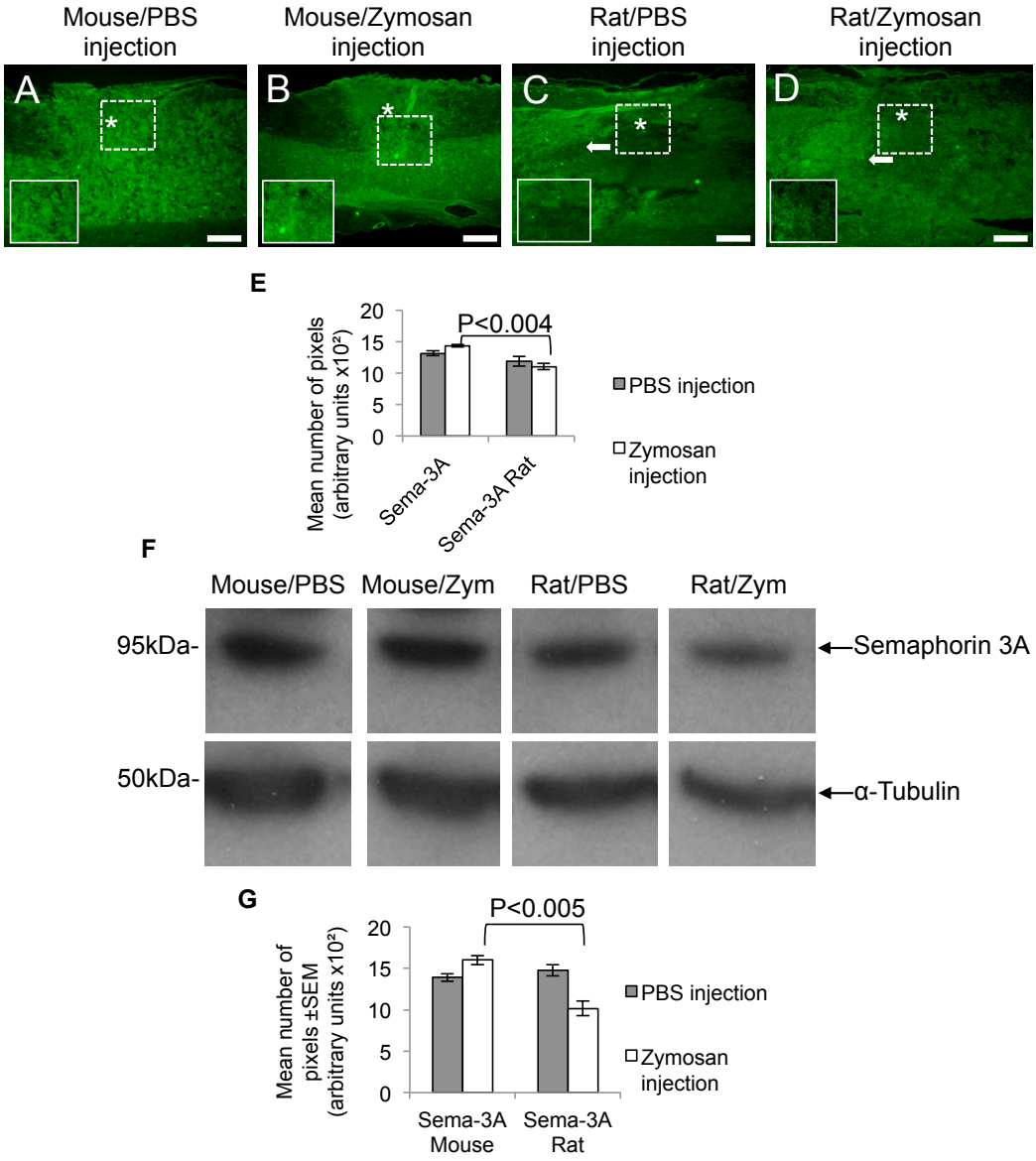

Figure 5.14 The localisation of Sema-3A 8dpl in DC lesions after induced inflammation. Immunohistochemistry for Sema-3A in mice either treated with PBS **(A)** or zymosan **(B)** and rats either treated with PBS **(C)** or zymosan **(D)** and the pixel intensities of Sema-3A^{+} fluorescence **(E)**. Western blot **(F)** and densitometry **(G)** corroborated the immunohistochemistry results (α-tubulin was used as a protein loading control, image demonstrates a representative picture **(F)**; n = 3/species/treatment group; * = lesion epicentre; scale bars in A - D = 200μm; Semaphorin 3A = Sema-3A).

5.7 Discussion

We report here that significant differences in the inflammatory response exist in mice and rats after T8 sub-acute SCI following exacerbation of inflammation using zymosan. In both mice and rats, the degree of tissue damage and cavitation seen at 8 dpl after zymosan injection was greater compared to PBS controls. Of note, the cavity free response normally seen in mice was challenged by the injection of zymosan into the lesion site such that micro-cavities were now present in and around the lesion site. An influx of macrophages and resident T-cells, but not microglia was observed in zymosan injected rats compared to mice that correlated with a deleterious, rich fibronectin^{+} scar tissue but not GFAP^{+} astrocytes. In addition, the expression of pro-angiogenic MMP-1 and laminin were significantly up-regulated within the lesioned area in response to induced inflammation in rats compared to mice.

5.7.1 Inflammatory responses

Zymosan injected into the corpus callosum in the brain, was first used as a model of cavitation in 1999 (Fitch et al., 1999). This model removed the presence of the inflammatory response that may result from primary direct tissue damage and thus allowed assessment of progressive cavitation commonly found after CNS injuries. Their results demonstrated that injection of zymosan resulted in persistent inflammation causing a significant increase in astrocyte-free cavities that was maintained up to 2 weeks after initial injection. Whilst our inflammation induced injury was direct it still demonstrated that the lesioned areas in both mice and rats displayed larger cavities that were devoid of GFAP^{+} astrocytes.

The inflammatory response between mice and rats has previously been documented to show marked differences in T-cell numbers (Sroga et al., 2003). In rats T-cell infiltration was highest between 3-7days after injury but then decline by 50% after three weeks, whereas in mice T-cell infiltration was not evident until 14 days after injury and increased by 50% between 2-6 weeks. However, at an earlier time point, our results demonstrated similar outcomes after zymosan injection i.e. T-cell infiltration was significantly increased in rats compared to mice.

Activated microglia after thoracic SCI has been shown to play a role in chronic pain by contributing to the maintenance of pain-related behaviours and hyper-responsiveness (Hains and Waxman, 2006). Furthermore using an anti-inflammatory treatment, Minocycline, in an adult rat model of SCI demonstrated reduced microglia activation along with reduced lesion size and increased functional recovery (Stirling et al., 2004). In our mouse model of SCI, the presence of activated microglia immunoreactivity observed after zymosan injection may contribute to the microcavities present. Therefore, if the injury produced was severe enough to damage the sensory pain pathways, hypersensitivity and chronic pain may be observed. Furthermore, after injury microglia adopt an activated state in response to neurodegeneration and multiply (Perry and Holmes, 2014). This is a process known as priming that result in the microglia becoming more susceptible to the inflammatory stimulus and thus further result in an exaggerated inflammatory response. This may explain the detrimental inflammatory response documented after SCI.

5.7.2 Macrophages and their responses to SCI

Macrophages are heterogeneous cells that have the ability to switch phenotypes and alter their functions by local factors present in the inflammatory microenvironment after SCI (Ren and Young, 2013). There are a range of macrophage subtypes that are distinguished from one another based on their distinct functions. These include classically activated macrophages (M1 macrophages), alternatively activated macrophages (M2 macrophages), 'regulatory' macrophages, tumour-associated macrophages (TAMs), and myeloid-derived suppressor cells (MDSCs) (Murray and Wynn, 2011). M1 macrophages function to mediate defence of the host from a variety of viruses, bacteria, and protozoa whilst M2 macrophages regulate wound healing and have anti-inflammatory functions (Murray and Wynn, 2011). 'Regulatory' macrophages are able to secrete large amounts of interleukin-10 (a monocyte / macrophage-derived cytokine involved in the immune response) in response to macrophage receptor ligation (Sutterwala et al, 1997, Sutterwala et al., 1998). TAMs play a role in suppressing anti-tumour immunity with MDSCs being linked to TAMs. Furthermore, MDSCs have been suggested as precursors for TAMs (Murray and Wynn, 2001, Mosser and Edwards, 2008).

As mentioned and documented previously by various studies inflammation plays a detrimental role to the secondary pathogenesis after SCI (Kim et al., 2013, Perez et al., 2003). After SCI M1 macrophages, activated by Th1 cytokines, produce proinflammatory cytokines, NO and reactive oxygen species (ROS) that contribute to tissue inflammation and therefore contribute the deleterious effects seen after SCI (Shechter et al., 2013, Kigerl et al., 2009). However, M2 macrophages, activated by Th2 cytokines, produce anti-inflammatory factors and demonstrate a reduced

capacity to produce proinflammatory molecules and therefore contribute more to wound healing and tissue remodelling (Ren and Young, 2013). M2 macrophages can be further subdivided into three classes; M2a, M2b and M2c subtypes, that are dependent on the type of stimulation and expression of surface molecules and cytokines (Mantovani et al., 2004).

Many studies into the inflammatory responses after SCI in animal models has been aimed at blocking the detrimental M1 activation pathway to demonstrate a reduction in tissue damage, an induction of myelin regeneration and improved locomotor recovery (Wang et al., 2013, Chen et al, 2011). However, it has been suggested that the potential therapeutic application of reprogramming macrophages to the M2 phenotype may control and resolve the inflammation after SCI (Ren and Young, 2013). Currently there are many ongoing clinical trials that are investigating the potential therapeutic utility of treatments that alter macrophages from M1 to M2 phenotype, cell transplantation of macrophages into the injured area or inhibition of M1 pathway to aid in the beneficial effects that M2 macrophages possess after SCI (Gensel et al., 2011). But it is important to note that whilst it has been documented that the immune systems between mice and humans are quite similar and as animal models of human diseases they do demonstrate limitations due to a few differences in their immunology (Mestas and Hughes, 2004, Haley, 2003). Many studies in the literature demonstrate potential clinical therapies in mice but fail to provide beneficial results in the clinic (Shepherd and Sridhar, 2003, Oehler and Bicknell, 2000, Panitch et al., 1987).

Distinguishing between the levels of M1 and M2 macrophages in this model of sub-acute SCI at 8 dpl using zymosan would help establish the inflammatory

response to induced inflammation further. A proposed hypothesis would be that inducing inflammation directly after SCI using zymosan in mice and rats would result in a higher proportion of M1 macrophages in the rat microenvironment compared to mice and thus contribute to cavitation. Whilst a higher proportion of M2 macrophages would be observed in mice compared to rats and thus aid in the beneficial wound healing responses that mice have previously demonstrated after SCI. Due to mice and rats demonstrating differences in inflammatory responses after SCI, the difference in M1 and M2 macrophages between the two species would add knowledge to the inflammatory research in SCI and the already ongoing clinical trials.

5.7.3 Inflammatory-induced angiogenic response

In response to tissue damage, it is important to accept that angiogenesis and inflammation are two separate, but closely linked multi-complex pathways (Ono, 2008, Granger and Senchenkova, 2010, Naldini and Carraro, 2005). They interact in 3 main ways: (1) playing a dual role in particular diseases such as cancer; (2) in the inflamed areas inflammatory cells interact with endothelial cells, ECM and fibroblasts; and (3) the same molecular events and particular cytokines, growth factors, proteases and adhesion molecules promote and trigger both processes (Costa et al., 2007, Ono, 2008). But mediators of the inflammatory response such as monocytes and macrophages are sufficient to induce angiogenesis alone (Koch et al., 1986, Sunderkotter et al., 1994). Chronic inflammation results in large areas of hypoxia that can cause inflammatory mediators to either directly or indirectly promote angiogenesis and thus further contribute to the prolonged inflammatory pathology therefore intensifying the response in disease states (Jackson et al., 1997,

Koutroubakis et al., 2006, Nagy et al., 2008). Inflammation-induced angiogenesis can have 2 distinct fates: persistence of vasculature and chronic inflammation or vascular regression and tissue repair (Arroyo and Iruela-Arispe, 2010). However, in a model of EAE, angiogenesis induced by CNS inflammation promoted neuronal remodelling (Muramatsu et al., 2012, Arroyo and Iruela-Arispe, 2010). This may explain the increase in angiogenic protein expression in rats compared to mice in response to induced inflammation in our results.

5.7.4 Vascular permeability and inflammation

Vascular permeability is one of the hallmarks of inflammation that is induced by an upregulation of VEGF, allowing plasma components and inflammatory cells to exit the bloodstream (Arroyo and Iruela-Arispe, 2010). The resulting acute inflammation can induce angiogenic responses, producing a highly vascularised granulated tissue, that would normally occur during wound healing (Singer and Clark, 1999). During tissue repair, vascular regression helps to restore homeostatic control after inflammation, but the absence of vascular regression can cause further exacerbation in the inflammatory response (Mazzone et al., 2009). This is the cases in many diseases such as, atherosclerosis, rheumatoid arthritis and psoriasis, in which the decision between sustained inflammation or tissue repair is significantly influenced by the composition and turnover of the ECM (Jackson et al., 1997, Costa et al., 2007, Arroyo and Iruela-Arispe, 2010). This may suggest that mice can restore their homeostatic control providing vascular regression during tissue repair after injury, whilst rats may not be able to restore vascular regression efficiently thus

further exacerbation of the inflammatory response occurs leading to large cavity formation.

Our mouse and rat model of inflammation indicates distinct inflammatory-induced angiogenic responses between the two species 8 dpl. Whilst zymosan caused further tissue damage and micro-cavities in the CNS environment of mice and rats, it is clear that inflammation alone is not the only mechanism that contributes to cavitation after SCI.

CHAPTER 6

GENOME WIDE ANALYSIS OF SCI-INDUCED ANGIOGENIC/WOUND HEALING-RELATED GENES IN MICE AND RATS

6.1 Introduction

6.1.1 Introduction to microarray analysis

Microarray analysis is a 2D array that can assess large amounts of biological material and therefore as a research tool, has become popular in recent years due to various analyses that can be carried out post array. These include variation detection within the gene sequence of a given sample, sequence determination, gene mapping and most importantly gene expression or genetic variation analysis. There are many different microarrays available on the market that include, DNA microarray, protein microarray and tissue microarray amongst many more. There are two types of microarrays based on the fluorescent dyes used known as one-colour or two colour microarrays. Cyanine 3 (Cy3) and Cyanine 5 (Cy5) are the two dyes commonly used that label the cDNA from the samples tested, Cy3 is detected at a wavelength of 570nm (green section of the light spectrum), whilst Cy5 is detected at 670nm (red section of the light spectrum). The advantages of using one-colour microarray is that each array chip is exposed to only one sample thereby reducing sample contamination and the ease of data comparison between different experiments. However, the disadvantage when compared to a two-colour microarray is double the amount of microarrays are needed to compare samples within a given experiment. Using one-colour microarray reduces the cost by 50% and results in 94% genes correctly annotated compared to the 98% using the two-colour microarray, therefore resulting in only a moderate decrease in overall specificity and sensitivity (Schwarz et al., 2010).

The first large-scale gene expression study in acute SCI in rats revealed changes in mRNA levels associated with inflammatory signals and neuronal loss,

with *in vivo* studies in rats at early time points showing increased transcription, neurotransmitter dysfunction, ionic imbalance and changes in genes that may play a role in tissue damage or repair after SCI (Carmel et al., 2001, Song et al., 2001, Nesic et al., 2002, Tachibana et al., 2002, Xiao et al., 2005, Velardo et al., 2004).

6.1.2 Angiogenesis and wound healing

Wound healing is a dynamic process like angiogenesis, by which the damaged skin/organ-tissue repairs itself after injury. Haemostasis, inflammation, proliferation and tissue remodelling and resolution are the four main overlapping, precisely programmed phases that occur after injury in order for successful wound healing to occur (Guo and Dipietro, 2010, Gosain and DiPietro, 2004). Haemostasis is induced immediately after injury to stop the initial bleeding at the site of injury by vascular constriction and platelet aggregation to form a clot. The damaged tissue and clot release pro-inflammatory factors causing infiltration of neutrophils, monocytes and lymphocytes to remove the cellular debris. Followed closely after the inflammatory phase is the proliferative phase, mainly characterised by re-epithelialisation (epithelial proliferation), angiogenesis (blood vessel capillary growth), collagen synthesis and ECM formation. Finally the remodelling phase is a critical phase allowing collagen remodelling, vascular maturation and regression of newly formed capillaries.

There are various factors that can affect wound healing and therefore result in impaired tissue repair (Guo and Dipietro, 2010). Local factors such as oxygenation and infection are factors that directly influence the characteristics of the wound, whilst systemic factors such as age, gender, medications, obesity and alcohol for example,

are factors that affect the individual's ability to heal. Angiogenesis plays an important role in wound healing and therefore impaired angiogenesis can affect and potentially delay wound healing (Zhou et al., 2004, Echtermeyer et al., 2001, Swift et al., 1999, Lee et al., 1999). In SCI aberrant inflammatory angiogenesis that occurs as a consequence of secondary damage can impair wound healing, and that using an anti-pathoangiogenic polysaccharide can inhibit the impaired angiogenesis and accelerate the rate of wound healing (Nanney et al., 2001).

In our study, we performed intricate analysis combing the use of microarray, q-PCR and immunohistochemical analysis to characterise the genome wide expression profile changes focussing on angiogenic/wound healing-related genes induced after acute SCI in mouse and rat 8 dpl.

6.2 Rationale

Previous research has demonstrated that mice and rats exhibit differences in wound healing, scarring and inflammatory responses after SCI. Furthermore, our model of T8 sub-acute SCI supports the differential wound cavitation and inflammatory responses between the two species but also demonstrates differential angiogenic protein expression and localisation as well as acute functional differences. This led us propose that other angiogenic/wound healing-related genes may be involved in the robust wound healing response seen in mice after SCI compared to rats. Therefore using 8 dpl as a time point that has previously shown the greatest differences between the two species, to investigate genome wide known and unknown early angiogenic/wound healing-related genes using microarray analysis.

6.3 Hypothesis

Mice have a robust wound healing response compared to rats after SCI which enable them to present a cavity free response that coincides with increased angiogenic expression. Known angiogenic/wound healing-related genes may be involved the early stages in preventing cavitation after SCI in mice that will be detected using microarray gene expression and thus contribute to the sparing of axons from damage.

6.4 Aims

- To compare mouse and rat control (0 dpl) and injured (8 dpl) spinal cord samples using microarray analysis.
- To compare the raw data of each species compared to controls using 'Statistical analysis of microarray' software (SAM) and IPA Ingenuity software.
- To determine all angiogenic/wound healing-related genes that are up- or downregulated after T8 DC crush in mice and rats compared to species matched controls.
- Search through the genes that are unique to mouse and rat and identify any that are angiogenic/wound healing-related.
- Validate a number of angiogenic/wound healing-related genes that are mapped and differentially regulated between mouse and rat after SCI using qPCR, and immunohistochemistry.

6.5 Materials and Methods

6.5.1 Experimental design

Type of analysis	N -numbers	End-points (days)
Microarray analysis	4 per species/group	0, 8
Validation by qPCR	3 per species/group	0, 8
Angiogenic/wound healing immunohistochemistry	3 per species/group	0,8

Table 6.1 Experimental design to assess angiogenic/wound healing-related genes by microarray analysis, qPCR and immunohistochemistry.

6.5.2 RNA Extraction (Performed by Stephen Kissane)

Please refer to Materials and Methods section 2.4 RNA extraction for standard protocol used. Once RNA was extracted from control and injured mouse and rat samples (n = 8 (4 control and 4 injured) per species), they were the tested on a Bioanalyzer (Agilent) to ensure RNA Integrity Number (RIN) values were above 7 before continuing to ensure repeatability of experiments (Appendix 1.1 and Appendix 1.2). Samples were then analysed individually through microarray analysis that resulted in 16 arrays in total and the quadruplets were then analysed in SAM software.

6.5.3 Real-time polymerase chain reaction (qPCR)

Please refer to Materials and Methods section 2.8.2 Real-time quantitative polymerase chain reaction for standard protocol used. The genes chosen from microarray analysis were only considered if they were more than 2-fold upregulated or downregulated for validation of gene expression by qPCR (Table 6.2 and 6.3).

Gene	Log ratio	Comments
Alpha-2-Adrenergic receptor beta (α_{2B}-AR)	3.317 (Rat)	An angiogenic gene that was shown to be regulated after SCI in rat only.
Annexin A3 (ANXA3)	-1.93 (Mouse) -5.119 (Rat)	An angiogenic gene that was shown to be regulated in both species after SCI.
CD44	-3.608 (Mouse) -6.069 (Rat)	An angiogenic/wound healing gene that was shown to be regulated in both species after SCI.
H2.0-like homeobox (HLX-1)	-10.707 (Rat)	An angiogenic gene that was shown to be regulated after SCI in rat only.
Integrin beta 2 (ITGβ2)	-4.437 (Rat)	An angiogenic/wound healing gene that was shown to be regulated after SCI in rat only.
Metallothionein (MTIH)	-11.075 (Rat)	A wound healing gene that was shown the regulated after SCI in rat only.
Protein kinase C-eta (PRKCH)	-4.797 (Rat)	A wound healing gene that was shown the regulated after SCI in rat only.
Retinoic acid receptor beta (RARβ)	3.136 (Mouse)	An angiogenic gene that was shown to be regulated after SCI in mouse only.
Transforming growth factor beta receptor 1 (TGFβR1)	-2.202 (Mouse) -2.745 (Rat)	An angiogenic/wound healing gene that was shown to be regulated in both species after SCI.

Table 6.2 The angiogenic/wound healing-related genes chosen for validation from the raw microarray data.

Gene	Probe No.	Forward primer	Reverse primer	Reference number
Mus musculus (mouse)				
Alpha-2-Adrenergic receptor beta (α_{2B}-AR)	#83	gtggccaaggctgattagaa	aagcctgcctgttggctta	NM_009633.3
Annexin A3 (ANXA3)	#17	gcagtaccaagcagcgtatg	gccagagagatcacccttca	NM_013470.2
CD44	#49	tccttctttatccggagcac	cctggagtccttggatgagt	M27130.1
H2.0-like homeobox (HLX-1)	#85	ccttaagctccaacccaaga	tggcatggtgtccttagtga	NM_008250.2
Integrin beta 2 (ITGβ2)	#32	cccagtgtgagtgtcagtgc	tcccaatgtagccagactca	NM_008404.4
Metallothionein (MTIH)	#18	caagtgcacctcctgcaa	ttcgtcacatcaggcacag	NM_013602.3

Protein kinase C-eta (PRKCH)	#52	ccacagggatcc tcaagtct	aaagggtgtctc aggatctcat	NM_008856.3
Retinoic acid receptor beta (RARβ)	#69	caccggcatact gctcaa	caaacgaagca gggcttg	NM_011243.1
Transforming growth factor beta receptor 1 (TGFβR1)	#70	gcagctcctcatc gtgttg	agaggtggcag aaacactgtaat	NM_009370.2
Rattus (rat)				
Alpha-2-Adrenergic receptor beta (α_{2B}-AR)	#60	gagagagagcg ccttttcg	tgcaggacgcac agaact	NM_138505.2
Annexin A3 (ANXA3)	#62	ggagaattatctg ggcattttg	ggggtgttcctcg tacagc	NM_012823.2
CD44	#75	gagaaaactgg acccaggaac	ttaggatctgccc aggttgt	NM_012924.2
H2.0-like homeobox (HLX-1)	#85	caacatcaattcc aagacacg	ttgtacgtctgtgg catggt	NM_001077674.1
Integrin beta 2 (ITGβ2)	#66	tccacaaaaagt gacccttaact	cgtcggaaagtc acattgaa	NM_001037780.2
Metallothionein (MTIH)	#15	caccagatctcg gaatggac	aggagcagcag ctcttcttg	NM_138826.4
Protein kinase C (PRKCH)	#84	aaccacccttc ctcacc	actccatgacaa agaacagacg	NM_031085.2
Retinoic acid receptor beta (RARβ)	#70	agcaccggcata ctgctc	cagacgaagca gggcttg	NM_031529.1
Transforming growth factor beta receptor 1 (TGFβR1)	#53	aaggccaaatat tcccaaca	attttggccatcac tctcaag	NM_012775.2

Table 6.3 The angiogenic/wound healing-related genes chosen from microarray analysis gene lists that were either 2-fold upregulated/downregulated for validation by qPCR for mouse and rat, the probe number, forward and reverse primer sequences and their reference number.

6.5.4 Fluorescent immunohistochemistry

Please refer to Materials and Methods section 2.3.2 Fluorescent immunohistochemistry for standard protocol used to assess the localisation of chosen known angiogenic/wound healing-related proteins. Primary antibodies used; retinoic acid receptor beta (1:500, rabbit polyclonal, Abcam, ab53161, Cambridge, MA, USA), PKC (1:100, rabbit polyclonal, Abcam, ab4134), Annexin A3 (1:100, rabbit polyclonal, Abcam, ab127924), integrin β2 (1:100, rabbit polyclonal, Santa Cruz

Biotechnology, SC-28661, Dallas, Texas, USA); HLX-1 (1:100, rabbit polyclonal, Santa Cruz Biotechnology, SC-133657); α_{2B}-AR (1:100, rabbit polyclonal, Santa Cruz Biotechnology, SC-10723).

6.6 Results

6.6.1 Microarray data analysis

Following microarray analysis on mouse and rat control and injured samples after T8 sub-acute SCI, 55821 probes in the mouse (Appendix 2.1) and 30507 probes in the rat (Appendix 2.2) were expressed at 8 dpl. Multiclass analysis was then performed in SAM on the raw data files to reduce the amount of false positives that may be detected using a false discovery rate (FDR) at <10% and significance level set at <0.025 for any genes to be deemed as significant (Figure 6.1A and B). This resulted in 1090 genes showing significant regulation in mice and 1616 genes in rats. Pathway analysis was then performed using IPA Ingenuity software to interrogate this data further. We determined genes that were: (1), differentially expressed in mouse/rat control versus mouse/rat injured tissues; (2) mapped and differentially regulated genes (874 and 721 genes, respectively) in mouse versus rat; and (3) unmapped genes that were differentially regulated in mouse and rat (388 and 98 genes, respectively) (Figure 6.1C). Separate to this, the whole array of gene expression was analysed and we found 562 genes that were unique to the mouse and 689 that were unique to the rat.

From the raw data files for mouse and rat, a full list of genes that were common (Appendix 2.3), mapped (Appendix 2.4 and Appendix 2.5), un-mapped (Appendix 2.6) and unique (Appendix 2.7 and Appendix 2.8) were extracted. We

determined that 31 genes were common between mouse and rat, 670 and 795 genes, respectively, that were mapped in mouse and rat, 388 and 97 genes, respectively, that were un-mapped in mouse and rat and 562 and 689 genes, respectively, that were unique to either mouse or rat only. Further to this a full list of known angiogenic and wound healing genes (Appendix 2.9) to date was used to extract angiogenic (Appendix 2.10) and wound healing (Appendix 2.11) genes that are expressed after SCI in the mouse and rat from these lists and those that were either 2-fold upregulated or downregulated were deemed as significant. From this data 9 angiogenic/wound healing genes were selected based on expression levels for further validation by qPCR.

Raw microarray data was also analysed using cluster analysis and results viewed with TreeView software (Figure 6.2). Cluster analysis allows genes to be grouped together into the same family of molecules with similar functions and to show how they are regulated after SCI. Figure 6.2 shows the known angiogenic/wound healing genes in the mouse and rat, and genes that are red are upregulated and those in green are downregulated. The higher intensity of the colour represents higher expression of those genes. Following IPA analysis genes that were mapped and differentially expressed were grouped into similar functions for both mouse (Figure 6.3) and rat (Figure 6.4).

A

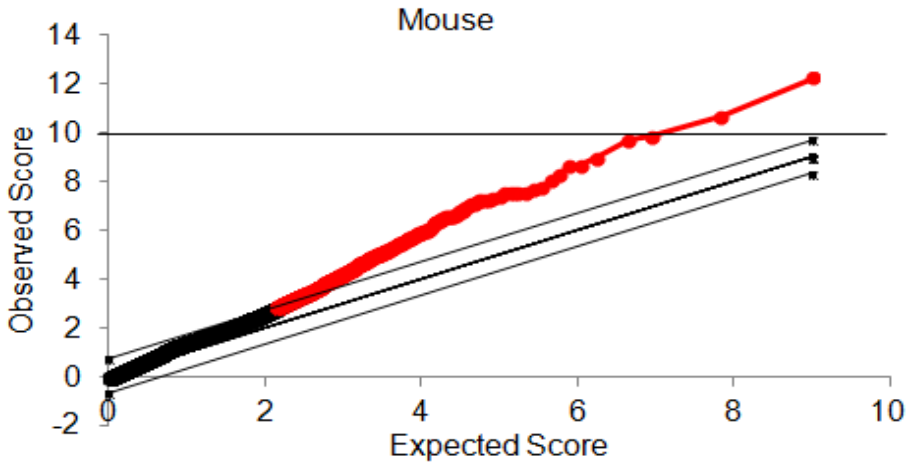

B

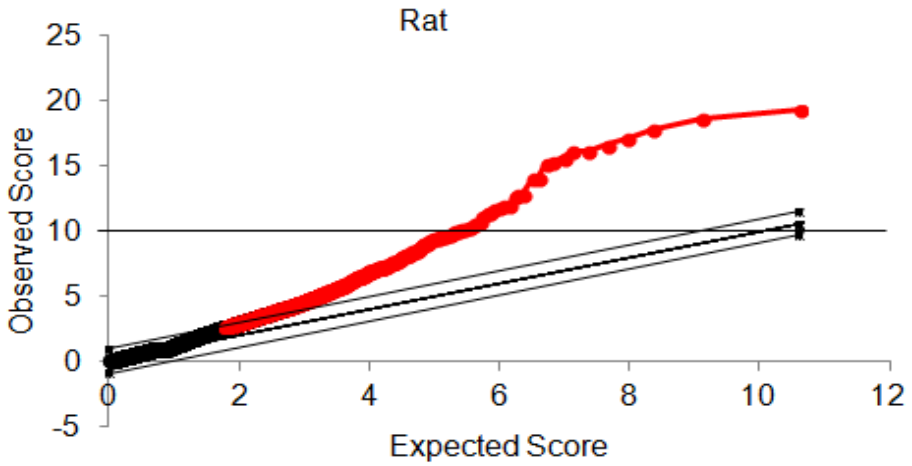

C

Genes	Mouse	Rat
Unique	562	689
Mapped and differentially regulated	874	721
Unmapped	388	98

Figure 6.1 Multiclass analysis in SAM software produced q-values that had a false discovery rate of <10% and p-value of 0.025 resulting in 1090 genes in mice **(A)** and 1616 genes in rat **(B)**. IPA analysis of these q-values revealed genes that were unique, mapped and unmapped between mouse and rat **(C)**.

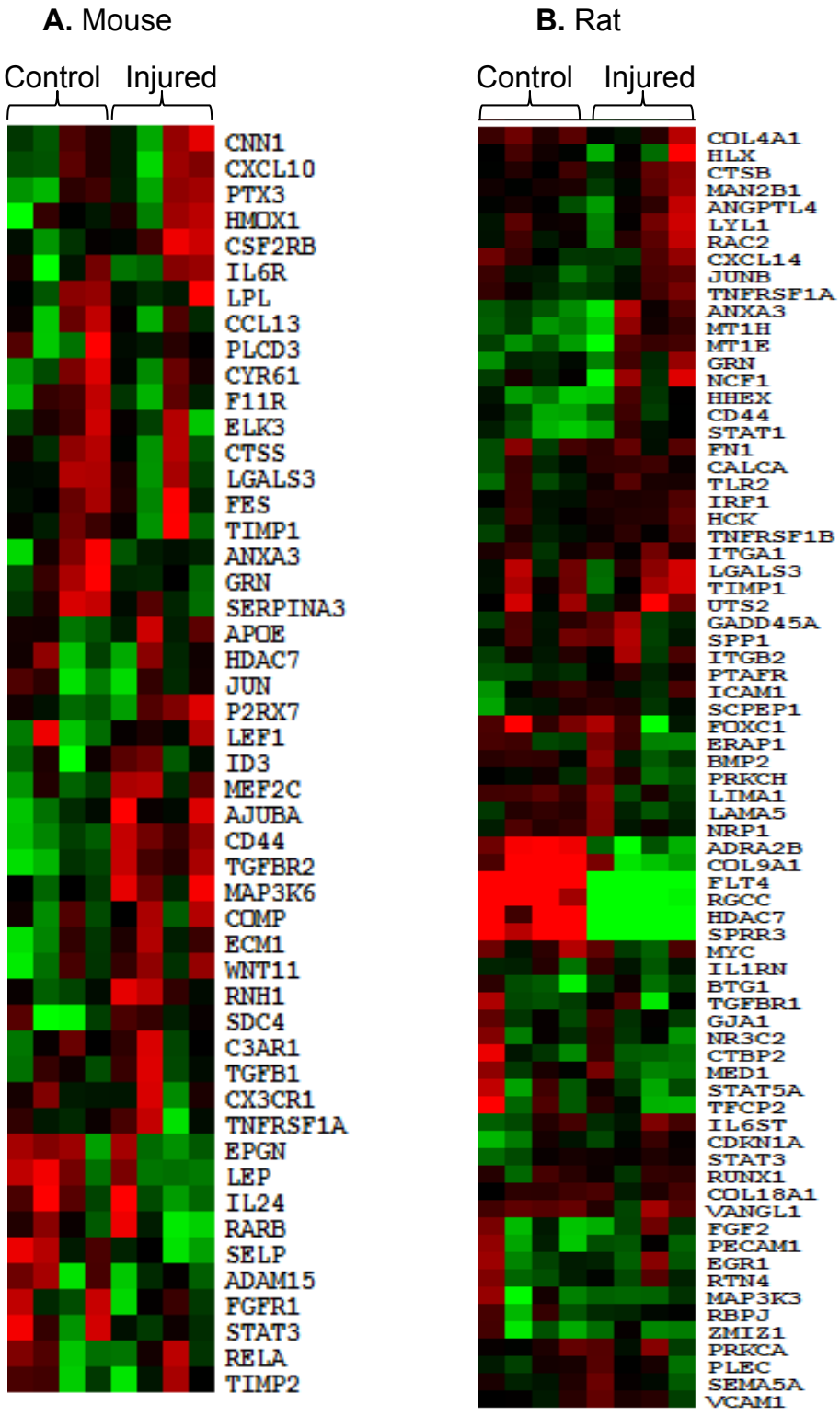

Figure 6.2 Heat maps for angiogenic/wound healing genes expressed in mouse **(A)** and rat **(B)** control (0 dpl) and injured (8 dpl) samples, generated using Cluster and TreeView analysis.

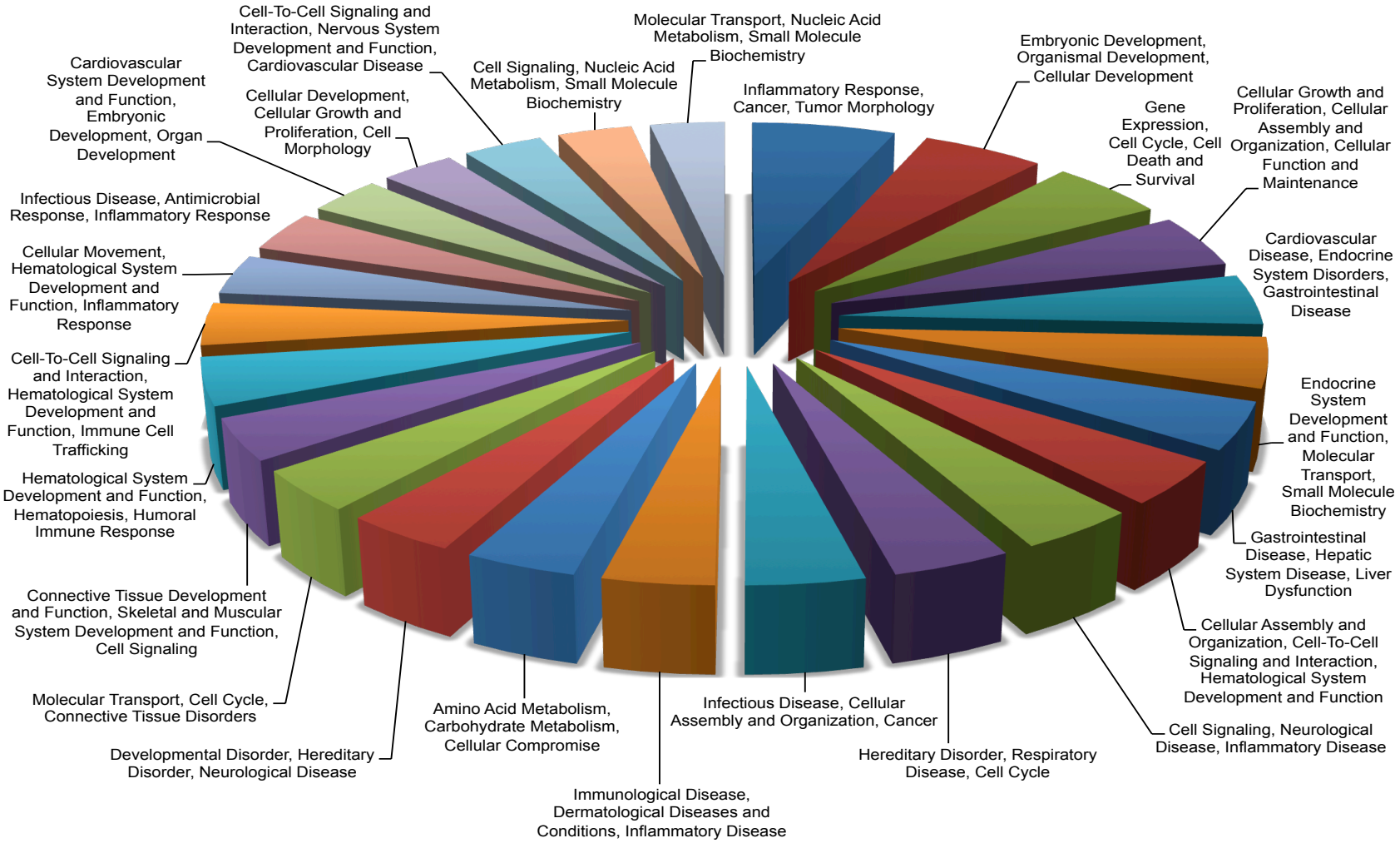

Figure 6.3 The molecular functions of mapped and differentially regulated genes expressed in mice after DC lesion at 8dpl following multiclass analysis using SAM software.

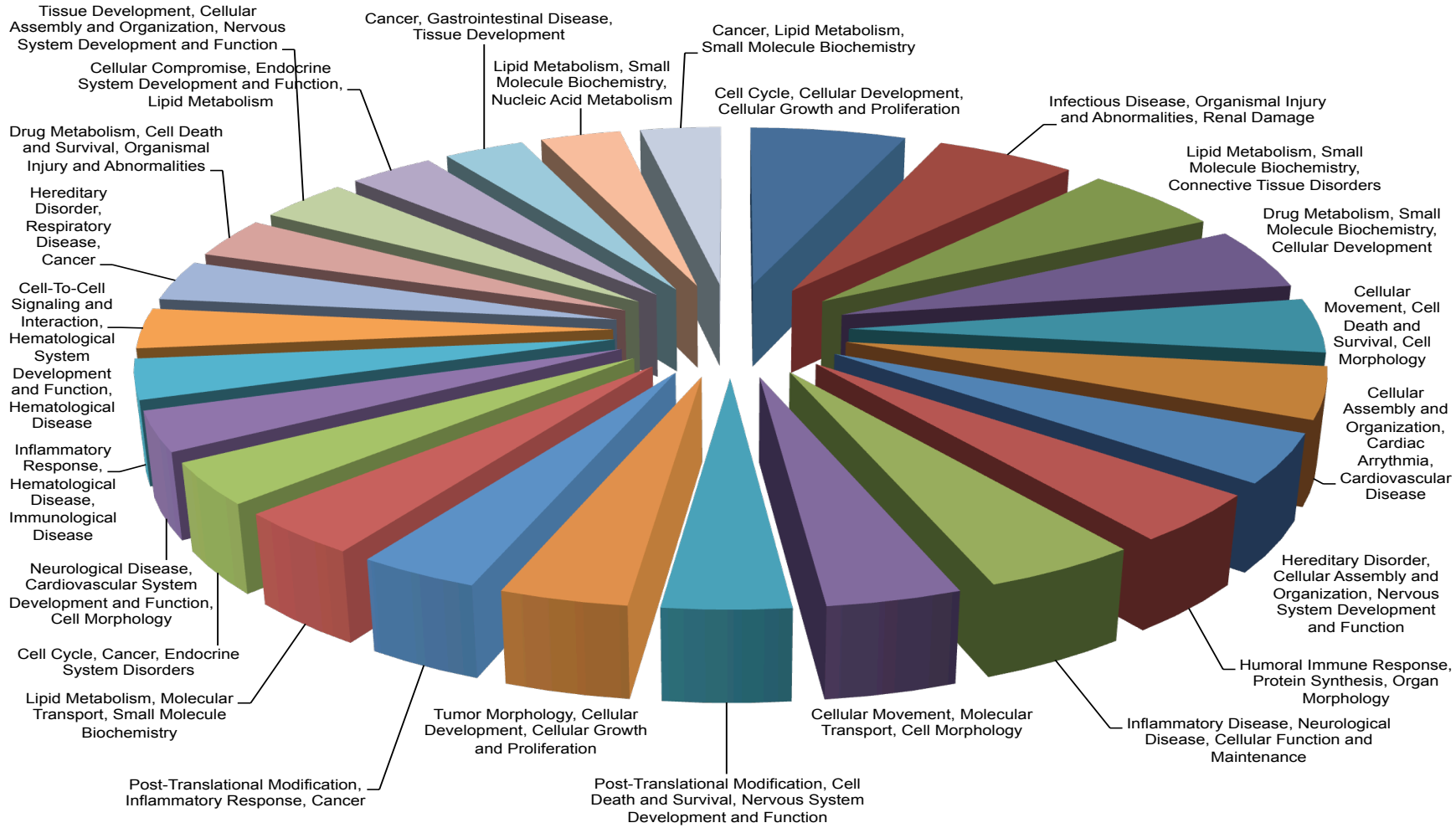

Figure 6.4 The molecular functions of mapped and differentially regulated genes expressed in rats after DC lesion at 8dpl following multiclass analysis using SAM software.

6.6.2 Known canonical pathways after SCI

IPA Ingenuity software was used to assess known canonical pathways between mice and rats after sub-acute SCI at 8 dpl using the Molecular Activity Predictor (MAP) (Figure 6.5A and B for key legend). The IL8 signalling pathway demonstrated key changes between mice and rats after SCI (Figure 6.6 and 6.7, respectively). Mice demonstrated a predicted activation of cadherin E through the highly inhibited cytokine CXCR1/R2 that leads to cell adherence, however, in rats this same relationship is inconsistent with the state of the downstream molecule. Moreover, angiogenic molecules such as VEGF, EGFR and MMP2 are highly inhibited through the IL8 pathway in mice after SCI (Figure 6.6). Whilst in rats it is predicted that IL8 leads to slight activation of these angiogenic molecules suggesting that after SCI there is abnormal upregulation of angiogenesis (Figure 6.7).

The NGF signalling pathway which plays a role in neurite outgrowth and differentiation displayed specific differences between mice and rats after SCI (Figure 6.8 and 6.9, respectively). In mice there is inhibition of NF-$_k$B presumably due to the predicted slight downregulation of TRAF6 and thus inhibits neurite outgrowth and differentiation after SCI, whilst no change was seen in molecules that are responsible for apoptosis (Figure 6.8). However, in rats there is a slight predicted upregulation of P75 that further causes the predicted activation of molecules such as BAX and p53 that lead to apoptosis after SCI (Figure 6.9). There is a highly predicted upregulation of NF-$_k$B that ultimately leads to neurite outgrowth and differentiation in rats after SCI. this however, could be counteracted by the aberrant upregulation of apoptosis after SCI as seen in the predicted MAP pathway.

PDGF plays a role in cell proliferation and cell survival in angiogenesis particularly in the later stages of the angiogenic process and after SCI there are key differences between mice and rats (Figure 6.10 and 6.11, respectively). In mice the predicted effect of the relationships between PDGF molecules and the molecules that lead to cell proliferation and mitogenesis are not predicted in this instance (Figure 6.10). However there is slight upregulation of P13K phosphatase and a slight down regulation of the CRK complex in mice after sub-acute SCI. However, various predicted relationships resulted from the activation of PDGF receptor; PDGFR are highly activated in rats compared to mice after SCI (Figure 6.11). These relationships include activation of mitogenesis through the CRK complex and cell proliferation via STAT1 and STAT3 transcription regulators. This could again be a result of aberrant upregulation of various molecules of the PDGF signalling pathway that result in the detrimental effects such as cavitation seen in rats after SCI compared to mice.

Finally, the VEGF signalling pathway demonstrated specific differences in the hypoxic and angiogenic responses between mice and rats after sub-acute SCI (Figure 6.12 and 6.13, respectively). In mice there is slight upregulation of P13K and Bcl-2 that lead to cell survival and angiogenesis after injury with no effect on hypoxic VEGF and HIF-1α molecules (Figure 6.12). However, in rats there is upregulation and activation of the VEGF receptor; VEGFR but this has little effect on the activation of its downstream molecules like Bcl-2 and P13k that result in cell survival, angiogenesis, cell proliferation and cell migration. More over there is a strong prediction in the activation of HIF-1α that leads to the activation of slight upregulated VEGF mRNA as a result of the hypoxic environment and therefore causing VEGF to activate its receptor VEGFR after SCI (Figure 6.13). However in the results already

seen in the previous chapters i.e. downregulation of angiogenic markers after sub-acute SCI in rats, these results could indicate that the mechanism for an increase of angiogenesis is present after injury but aberrant upregulation could lead to the detrimental effects seen after SCI in rats.

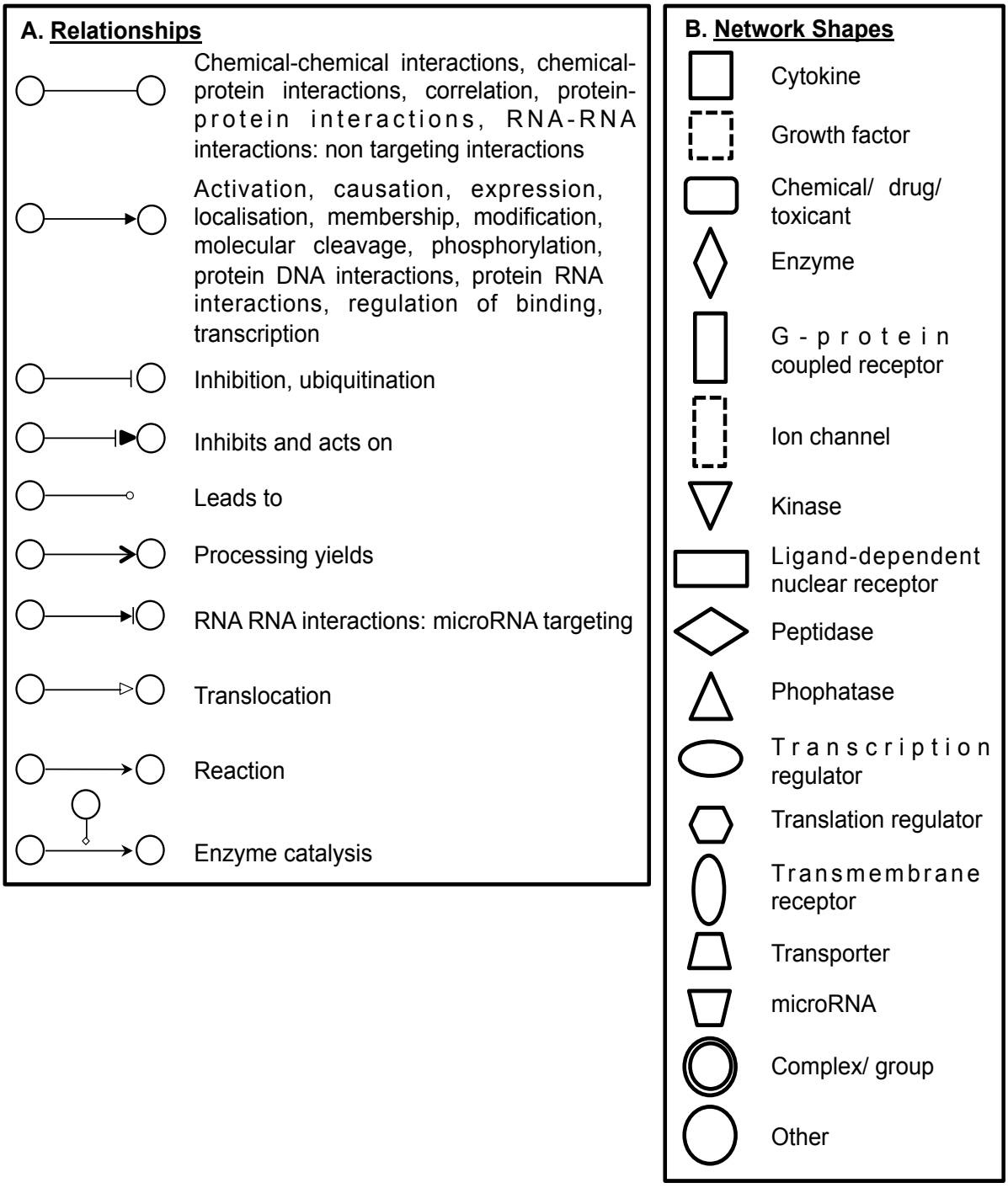

Figure 6.5 IPA legend for Molecule Activity Predictor (MAP) that allows the prediction of upstream and/or downstream effects of activation or inhibition and allows for interactions and relationships between molecules **(A)** and the network shapes used in canonical pathways **(B)** (Legend adapted from Ingenuity Pathway Analysis).

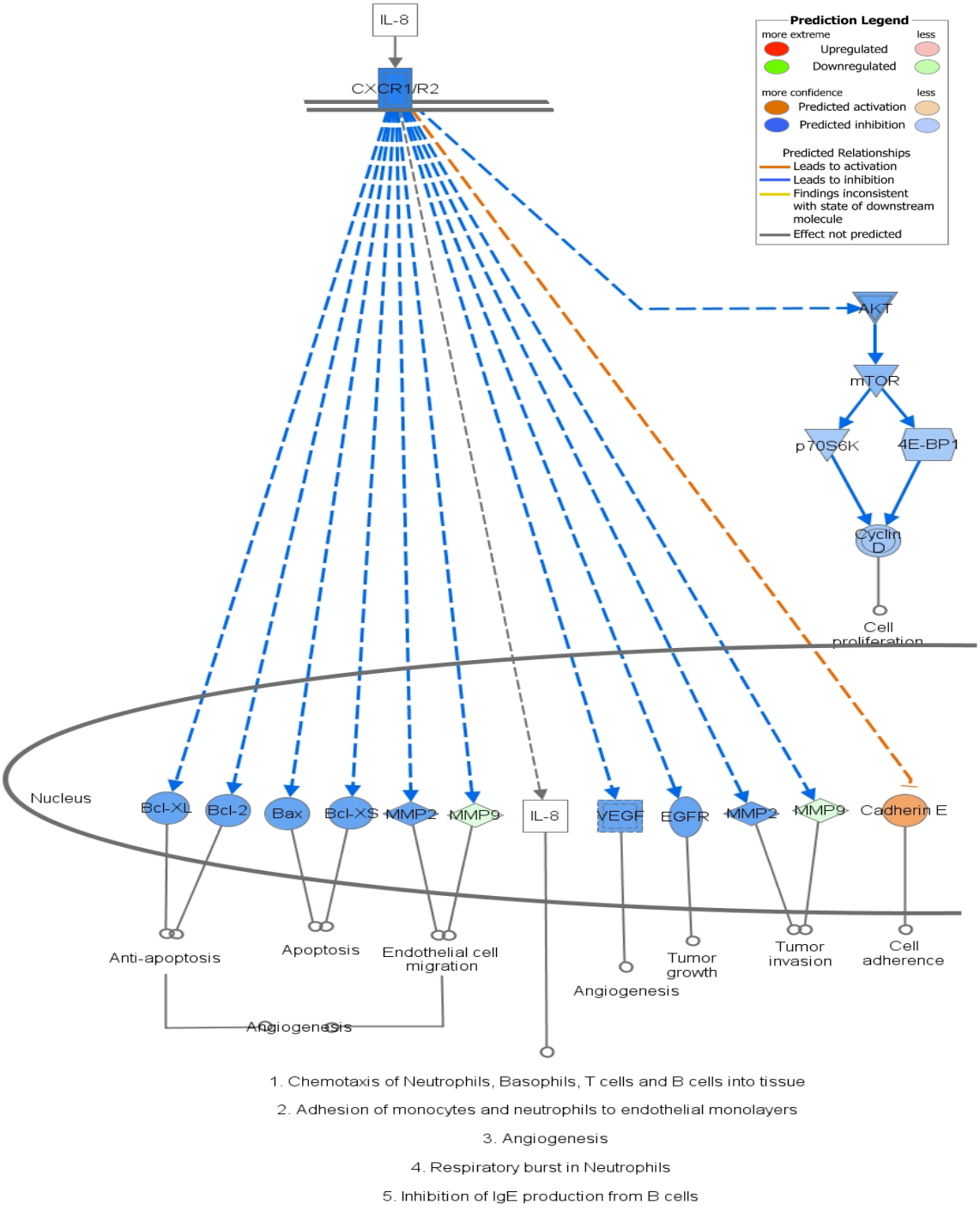

Figure 6.6 Molecular Activity Predicator (MAP) using IPA analysis of IL8 mediated regulation of angiogenesis and tumour growth canonical pathway in mice after T8 sub-acute SCI 8 dpl. The predicted activation of cadherin E and its predicted relationship is inhibited by complex CXCR1/R2 in the IL8 pathway (MAP Prediction Legend adapted from Ingenuity Pathway Analysis).

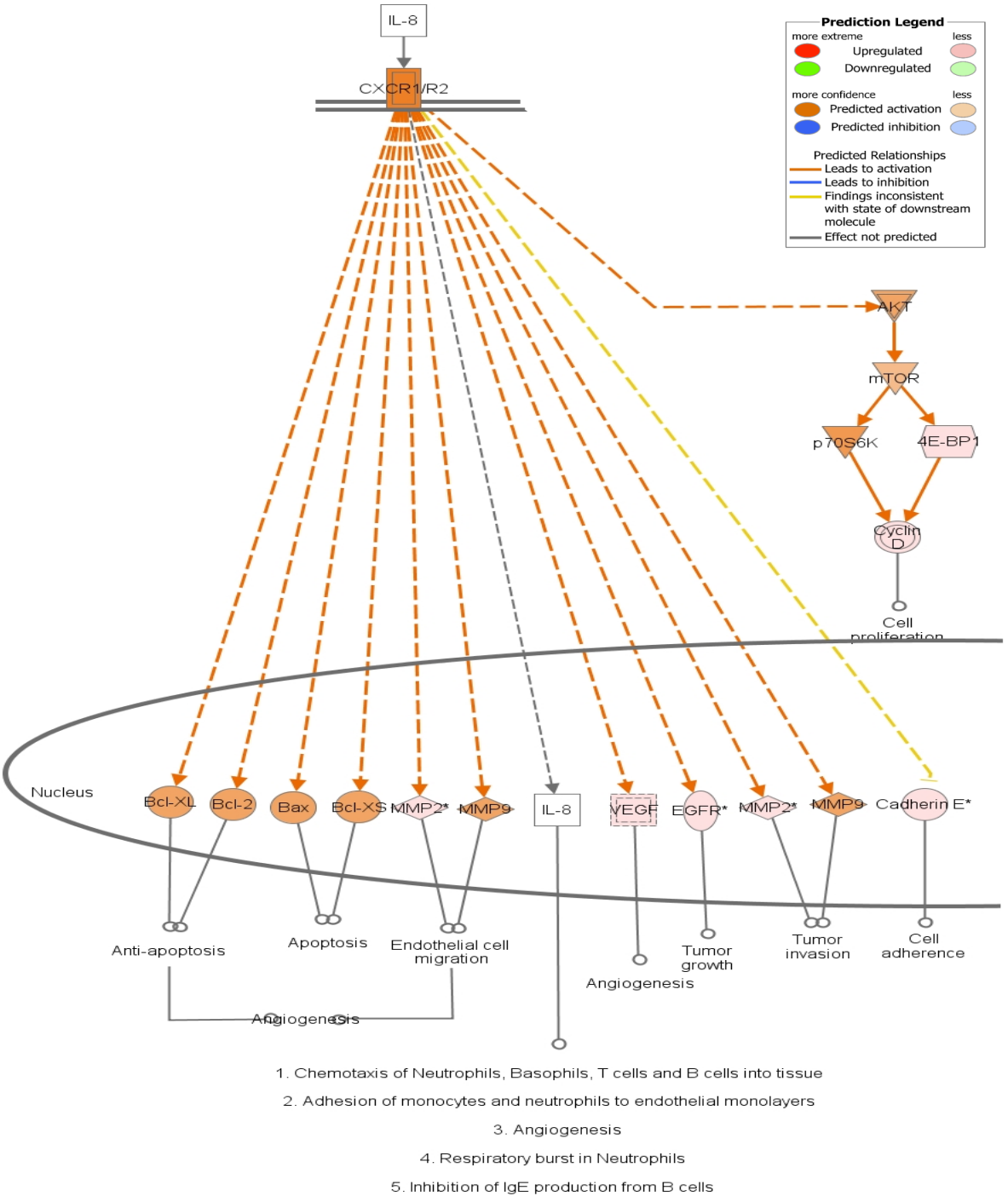

Figure 6.7 Molecular Activity Predicator (MAP) using IPA analysis of IL8 mediated regulation of angiogenesis and tumour growth canonical pathway in rats after T8 sub-acute SCI 8 dpl. The predicted relationship between complex CXCR1/R2 demonstrates inconsistent findings with the state of the downstream molecule in the IL8 pathway (MAP Prediction Legend adapted from Ingenuity Pathway Analysis).

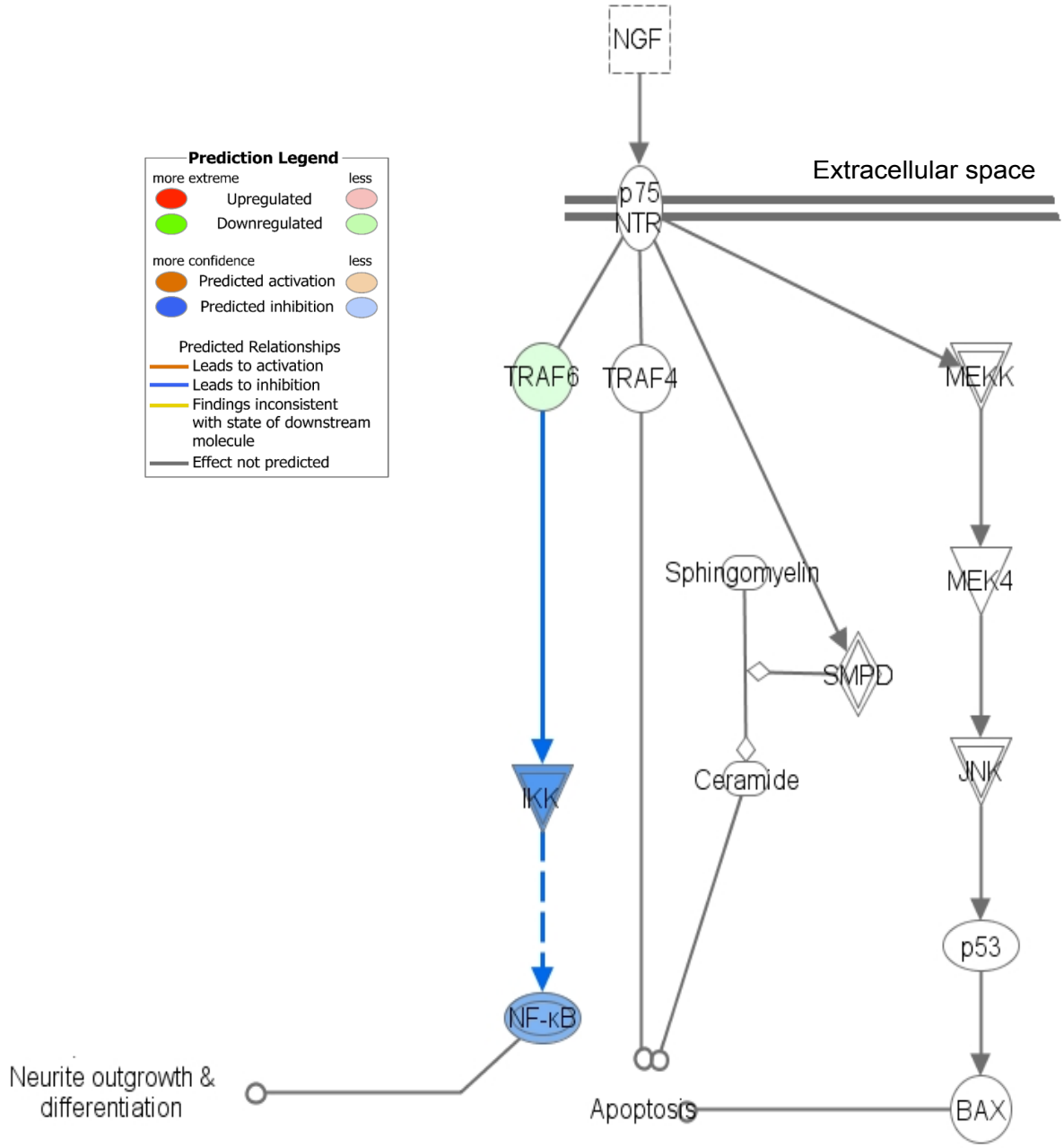

Figure 6.8 Molecular Activity Predicator (MAP) using IPA analysis of NGF signalling for neurite outgrowth and differentiation canonical pathway in mice after T8 sub-acute SCI 8 dpl. The NGF pathway causes a slight downregulation of TRAF6 that result in the highly predicted inhibition of NF-kB and thus neurite outgrowth and differentiation (MAP Prediction Legend adapted from Ingenuity Pathway Analysis).

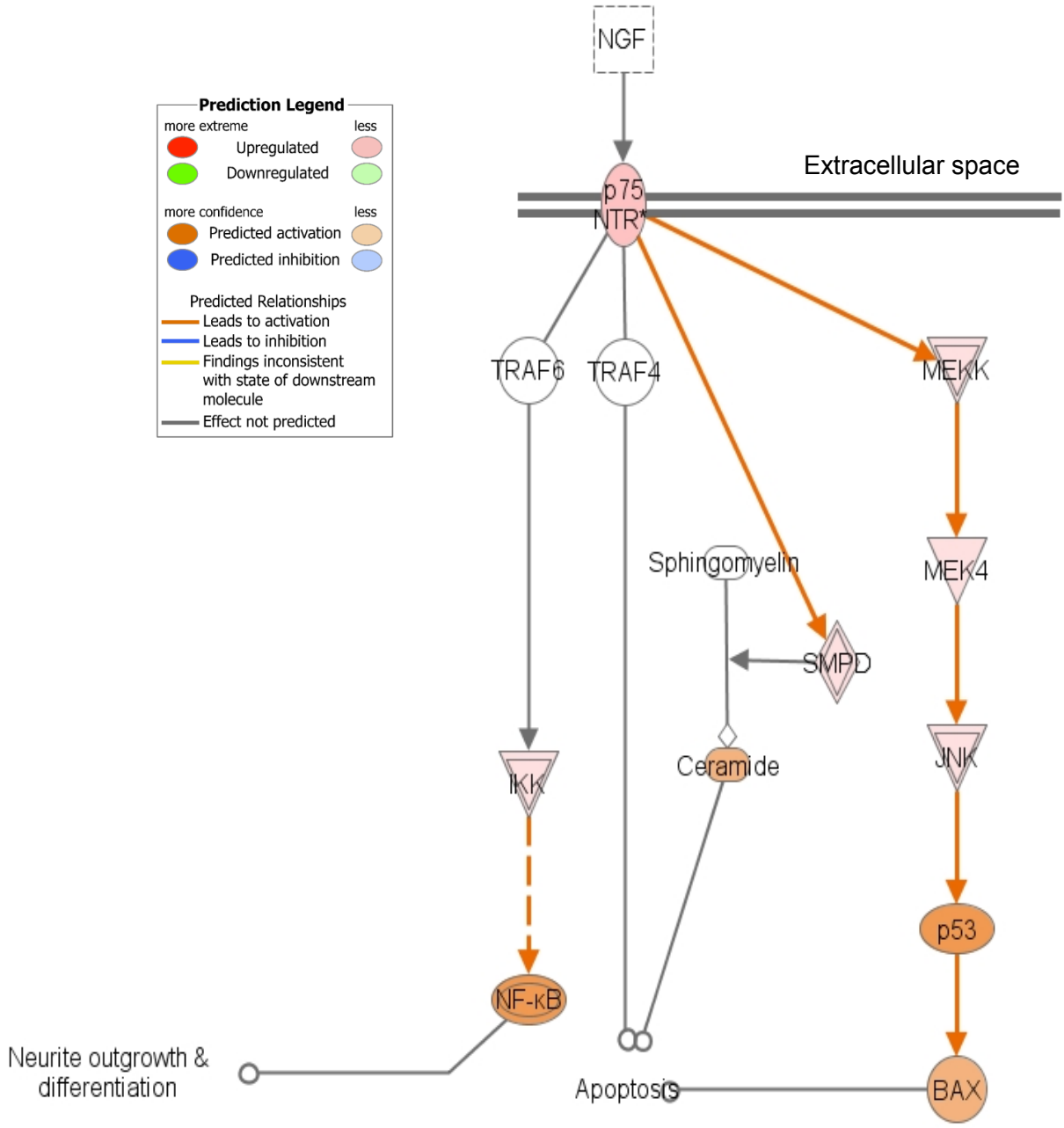

Figure 6.9 Molecular Activity Predicator (MAP) using IPA analysis of NGF signalling for neurite outgrowth and differentiation canonical pathway in rats after T8 sub-acute SCI 8 dpl. NGF causes the predicted upregulation of p53 and BAX; two molecules that play a part in apoptosis particularly in rats after SCI potentially aiding to the detrimental secondary pathology seen after injury (MAP Prediction Legend adapted from Ingenuity Pathway Analysis).

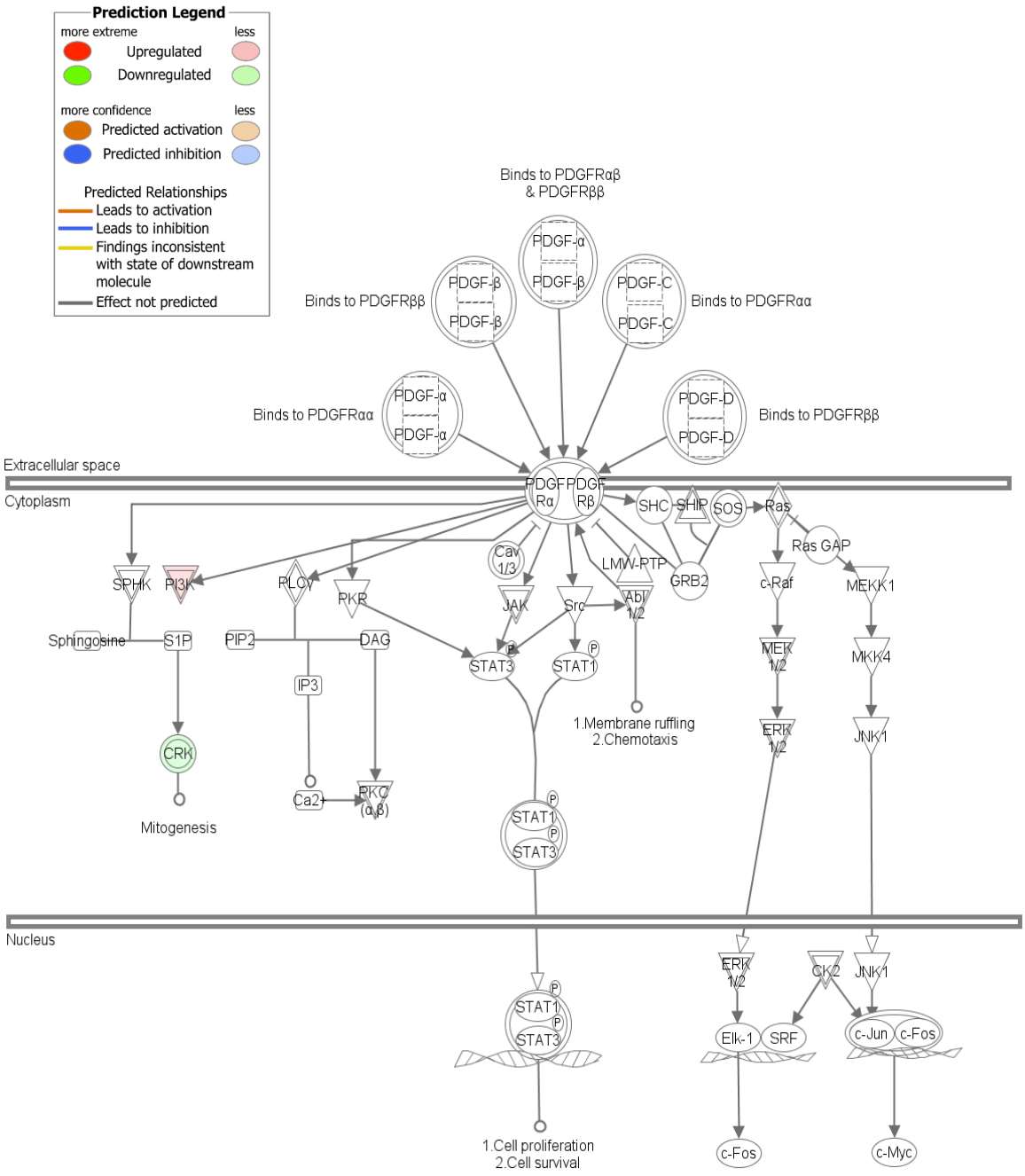

Figure 6.10 Molecular Activity Predicator (MAP) using IPA analysis of PDGF signalling for cell proliferation and survival canonical pathway in mice after T8 sub-acute SCI 8 dpl. After SCI not many changes are seen in the PDGF pathway in mice, however there was a slight activation in PI3K and a slight downregulation of complex CRK. Moreover no predicted effects on the relationships were observed in this instance (MAP Prediction Legend adapted from Ingenuity Pathway Analysis).

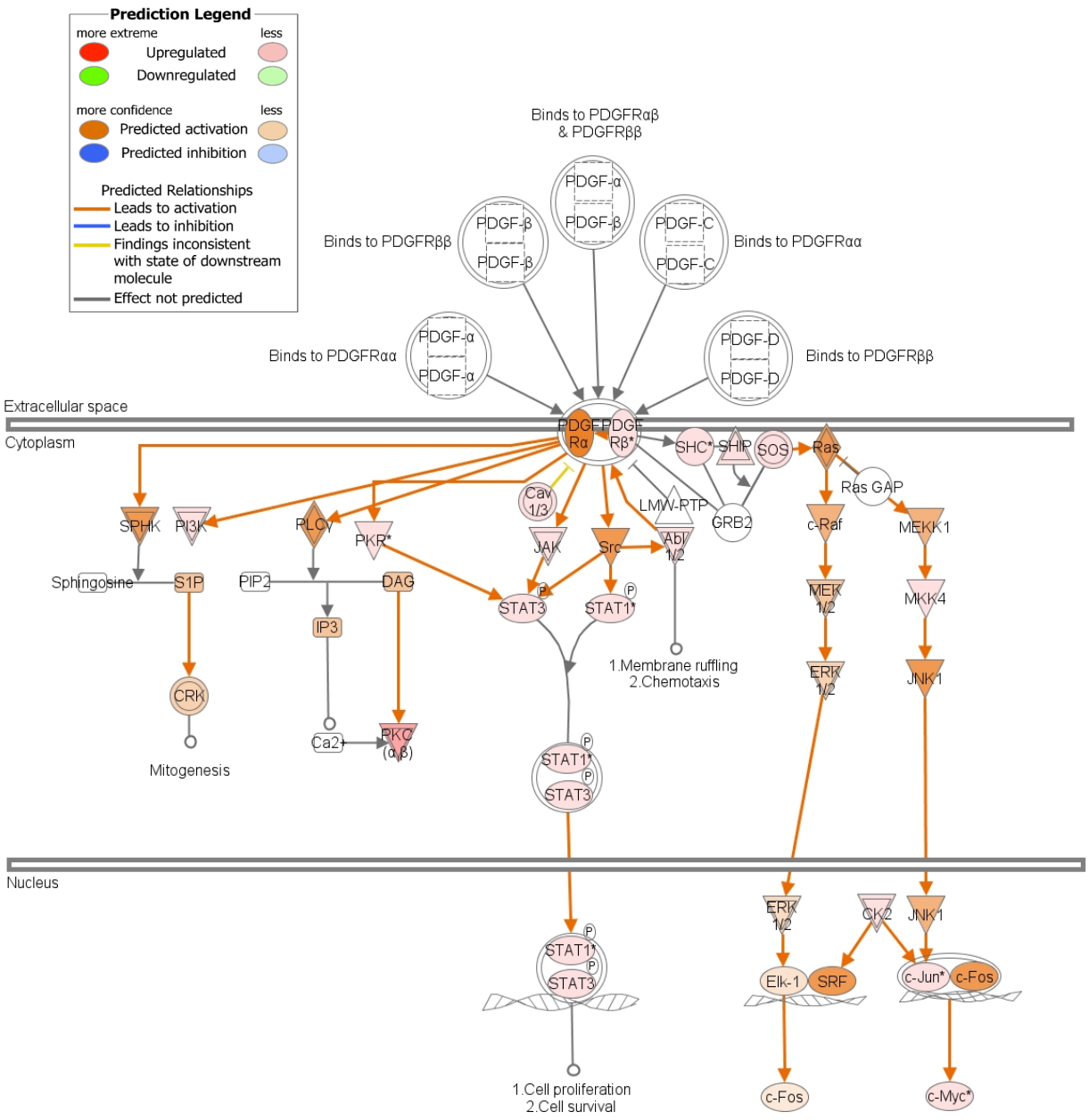

Figure 6.11 Molecular Activity Predicator (MAP) using IPA analysis of PDGF signalling for cell proliferation and survival canonical pathway in rats after T8 sub-acute SCI 8 dpl. After SCI the PDGF receptor; PDGFR, are strongly activated causing a vast amount of other downstream molecules to become activated that play a role in cell proliferation and survival and mitogenesis (MAP Prediction Legend adapted from Ingenuity Pathway Analysis).

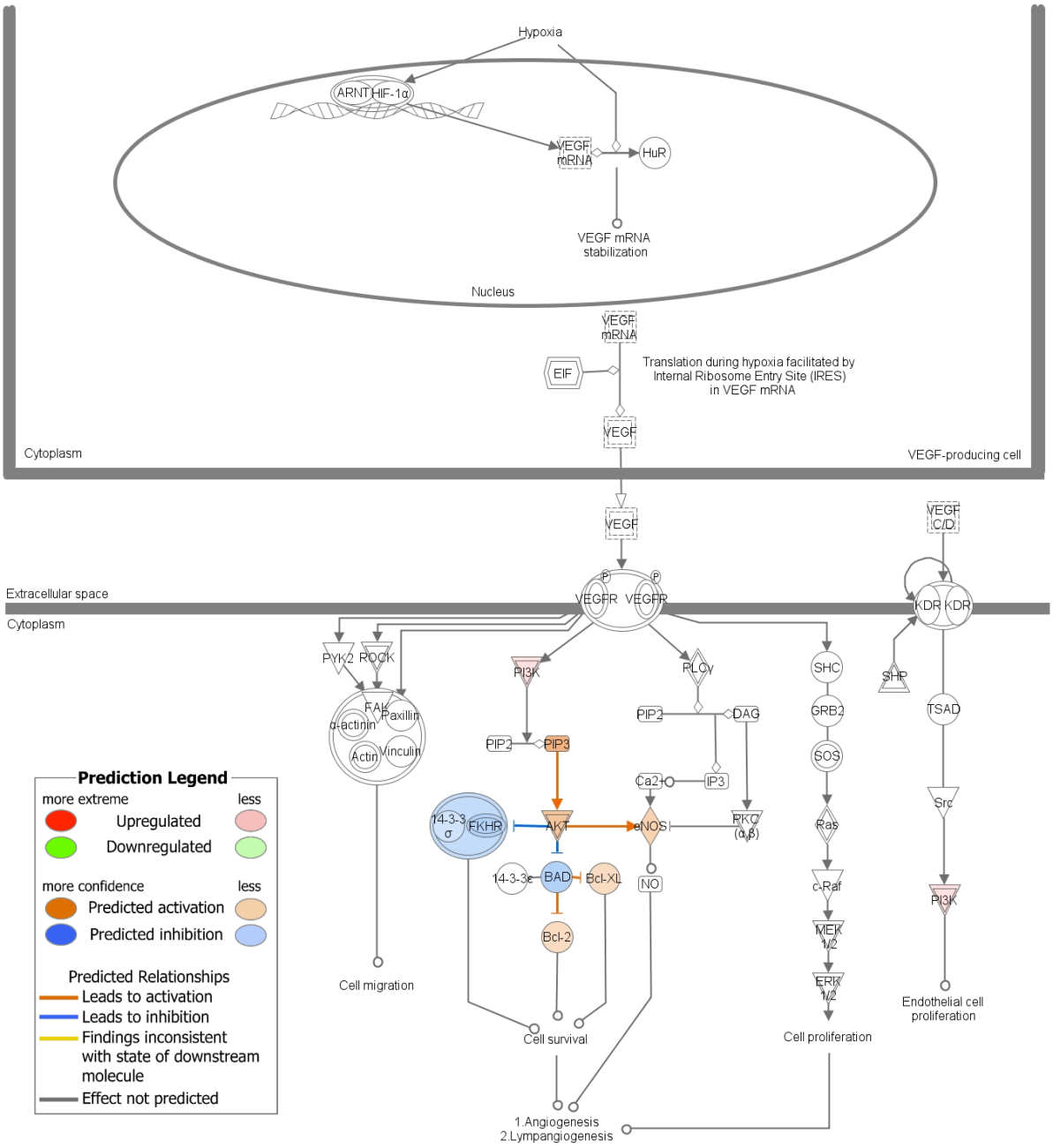

Figure 6.12 Molecular Activity Predicator (MAP) using IPA analysis of VEGF signalling for hypoxia and angiogenesis canonical pathway in mice after T8 sub-acute SCI 8 dpl. After SCI in mice there is no predicted effect on the relationship between hypoxia and angiogenic VEGF (MAP Prediction Legend adapted from Ingenuity Pathway Analysis).

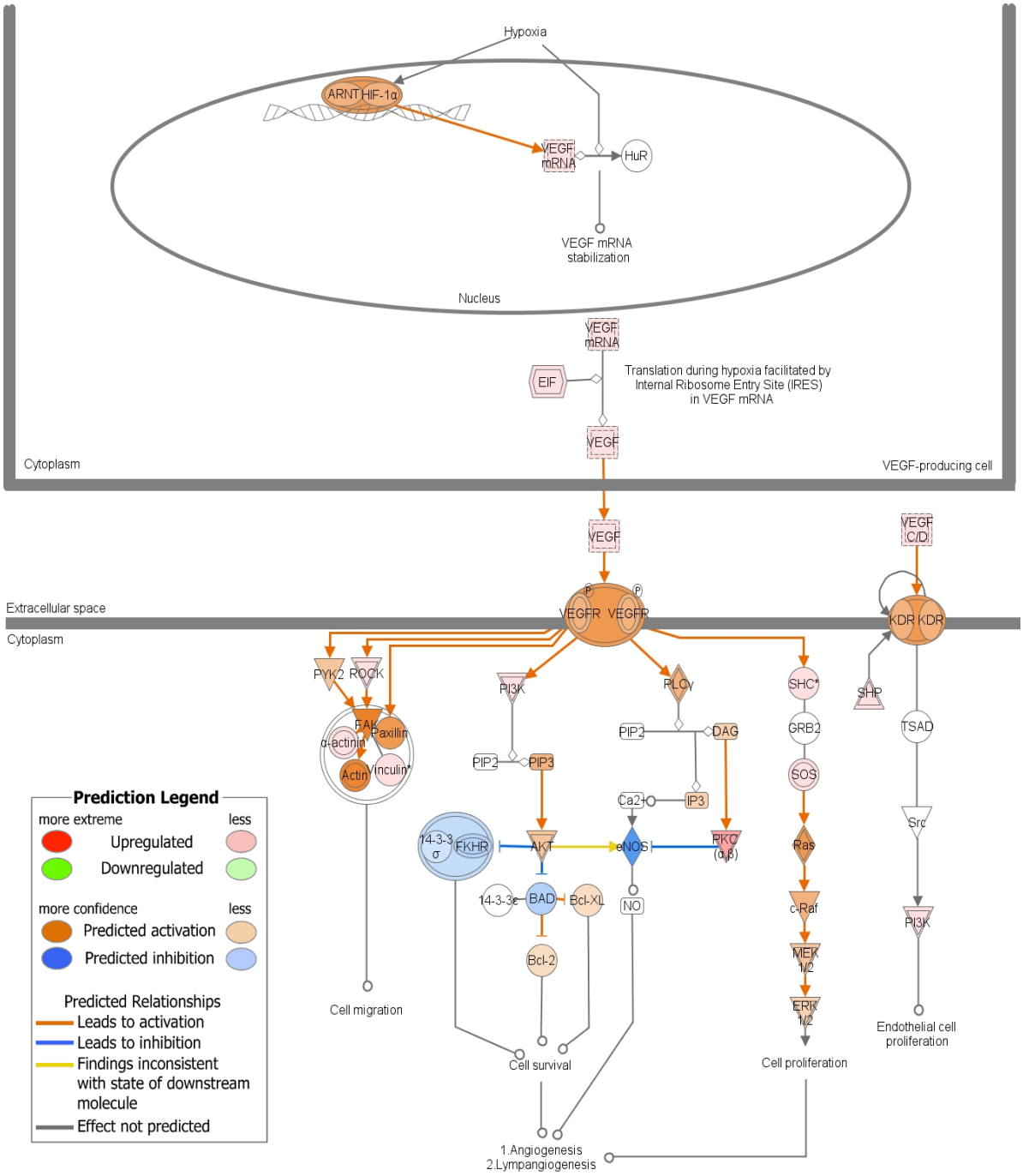

Figure 6.13 Molecular Activity Predicator (MAP) using IPA analysis of VEGF signalling for hypoxia and angiogenesis canonical pathway in rats after T8 sub-acute SCI 8 dpl. After SCI in rats HIF-1α is strongly upregulated where it dimerises with ARNT under hypoxic conditions to further cause an increase in VEGF mRNA (MAP Prediction Legend adapted from Ingenuity Pathway Analysis).

6.6.3 Screening of angiogenic/wound healing genes by qPCR

qPCR was conducted to determine whether angiogenic/wound healing-related α_{2B}-AR (Figure 6.14A), ANXA3 (Figure 6.14B), CD44 (Figure 6.14C), HLX-1 (Figure 6.18A), ITGβ2 (Figure 6.18B), MT1H (Figure 6.18C), PRKCH (Figure 6.22A), RARβ (Figure 6.22B) and TGFβR1 (Figure 6.22C) genes are truly expressed in mice and rats after T8 sub-acute SCI at 8 dpl. The representative data and standard curve for each gene and treatment group are shown in α_{2B}-AR (Figure 6.15), ANXA3 (Figure 6.16), CD44 (Figure 6.17), HLX-1 (Figure 6.19), ITGβ2 (Figure 6.20), MT1H (Figure 6.21), PRKCH (Figure 6.23), RARβ (Figure 6.24) and TGFβR1 (Figure 6.25). All expression values were normalised to mouse control 1 to show true biological variability between different treatment groups. In this instance α_{2B}-AR was upregulated after SCI in mice compared to control and when compared to injured rats but no change was observed between normal and injured rat (Figure 6.14A). This same pattern was also seen in ANXA3 (Figure 6.14B), CD44 (Figure 6.14C), MT1H (Figure 6.18C), PRKCH (Figure 6.22A) and RARβ (Figure 6.22B). The expression of HLX-1 was slightly increased after SCI in mice but in rats it was decreased after injury, and when comparing injured species, the expression of HLX-1 was slightly increased in mice compared to rats (Figure 6.18A). The expression of ITGβ2 gene was increased after SCI in both species but on a whole was higher in rats compared to mice after injury (Figure 6.18B). The expression of TGFβR1 was upregulated in rats after injury compared to control whilst no change was seen in the mouse after injury compared to control, but as a whole the expression of TGFβR1 was higher in rats compared to mice after injury (Figure 6.22C). Whilst some groups showed significant differences (Table 6.4, highlighted in bold) only ANXA3, CD44 and

PRKCH showed an overall significance with the variability highly dependent on treatment and species.

Angiogenic gene	NM vs. IM	NR vs. IR	NM vs. NR	IM vs. IR	Overall significance and variability
α_{2B}-AR	0.127	0.246	0.127	0.653	0.147; 49%
ANXA3	0.184	1.000	**0.046**	0.072	**0.037; 77%**
CD44	0.127	**0.034**	**0.037**	0.637	**0.028; 83%**
HLX-1	0.513	**0.037**	0.658	**0.037**	0.080; 61%
ITGβ2	0.827	0.050	0.050	0.275	0.077; 62%
MT1H	0.513	0.121	**0.037**	0.050	**0.027; 84%**
PRKCH	0.513	0.184	0.050	0.275	0.110; 55%
RARβ	0.127	0.513	0.275	0.513	0.376; 28%
TGFβR1	0.827	0.050	0.050	0.513	0.108; 55%

Table 6.4 Significance of gene expression between groups was determined using non-parametric Kruskal-Wallis method. The variability means that the overall values are dependent on species and treatment (P value = < 0.05).

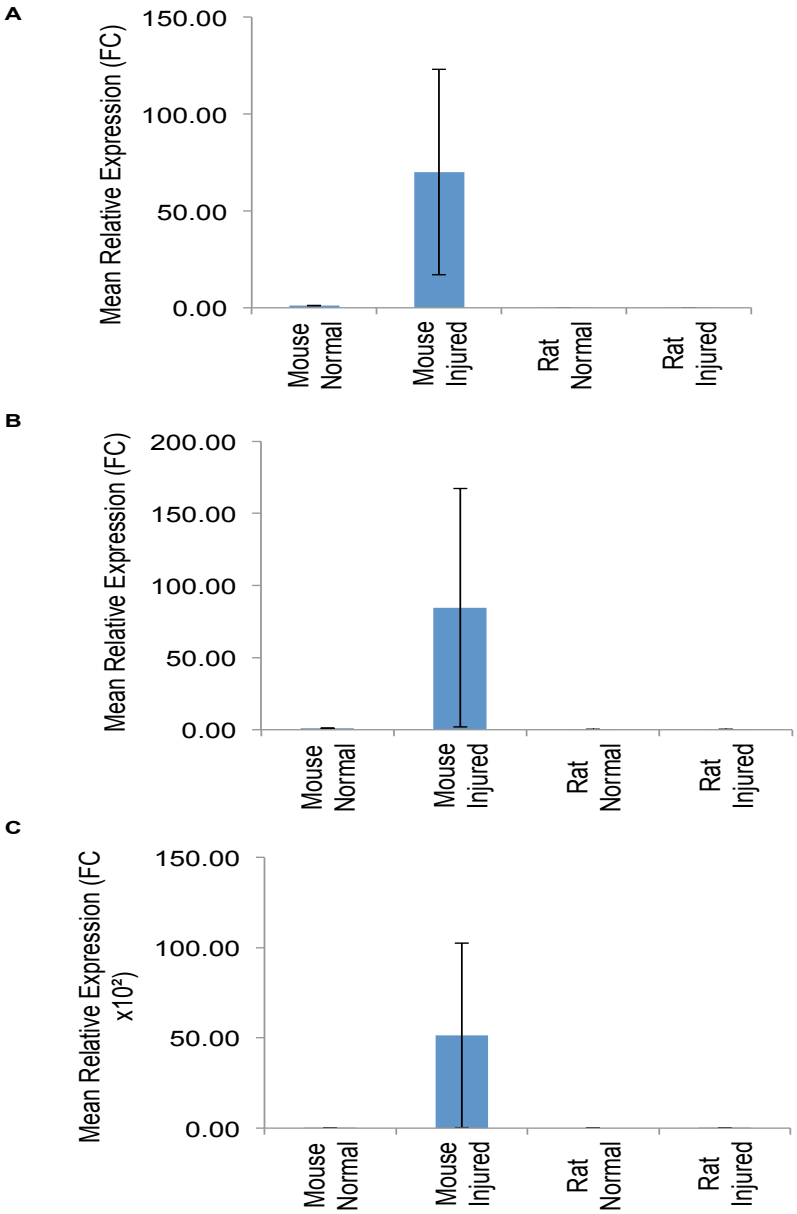

Figure 6.14 The expression of alpha-2-adrenergic receptor beta was validated by qPCR revealing that its expression was high in injured mice compared to normal mouse, whilst in rats the expression did not alter much **(A)**. The expression of annexin A3 revealed that its expression was high in injured mice compared to normal mouse, whilst in rats the expression did not alter much **(B)**. The expression of CD44 revealed that its expression was high in injured mice compared to normal mouse, whilst in rats the expression did not alter much **(C)**.

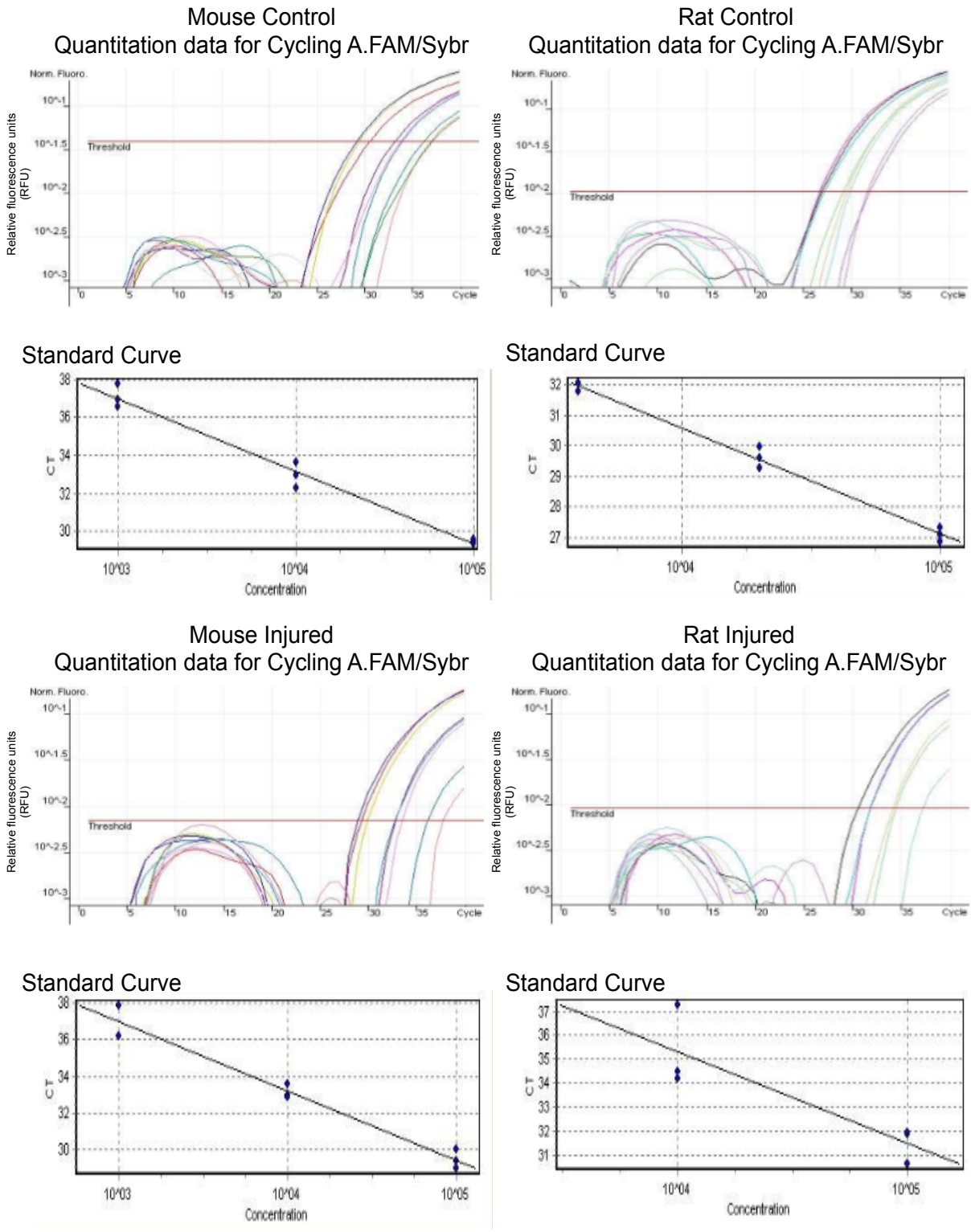

Figure 6.15 A representative quantification data and standard curve from each treatment group for alpha-2-adrenergic receptor beta gene.

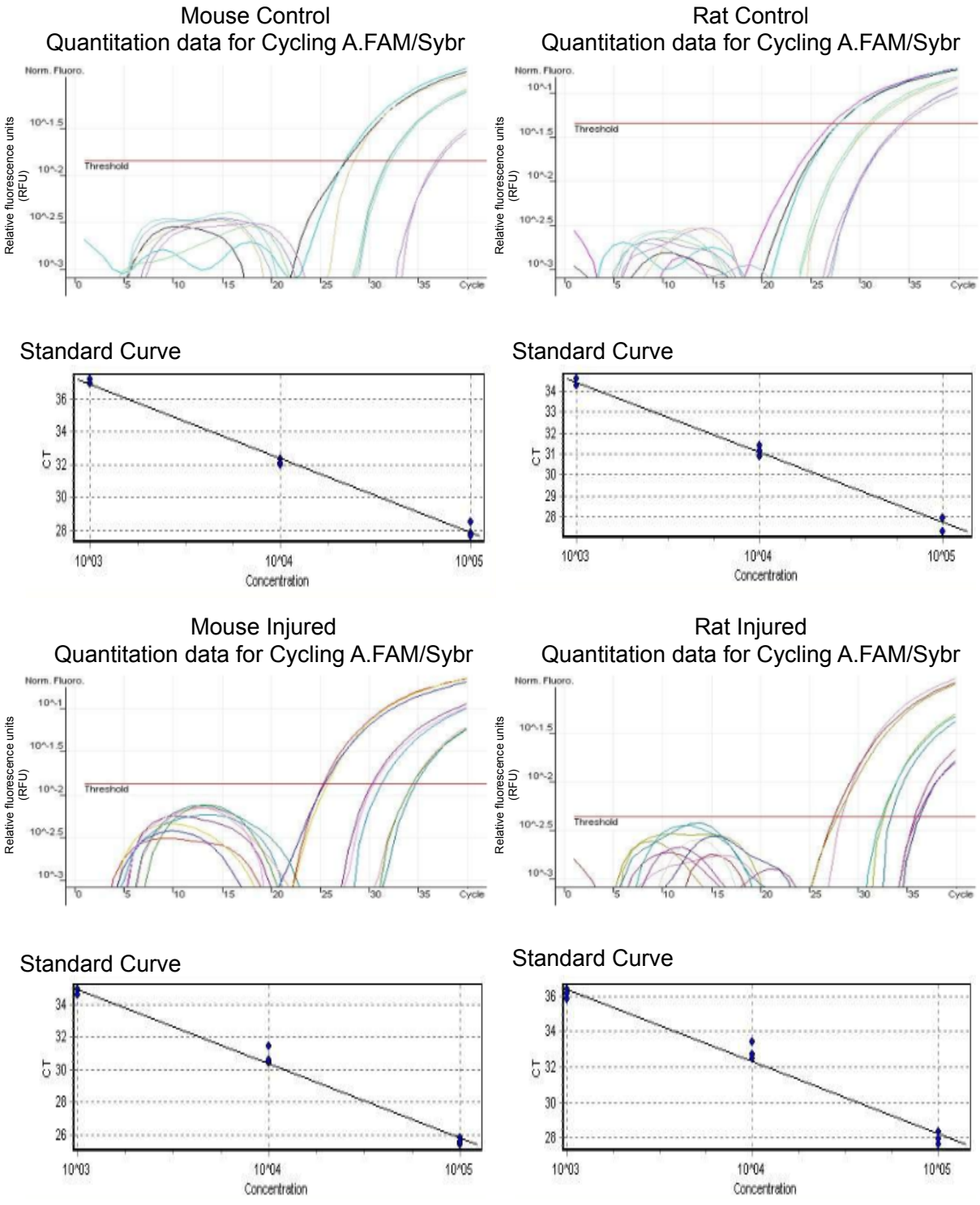

Figure 6.16 A representative quantification data and standard curve from each treatment group for annexin A3 gene.

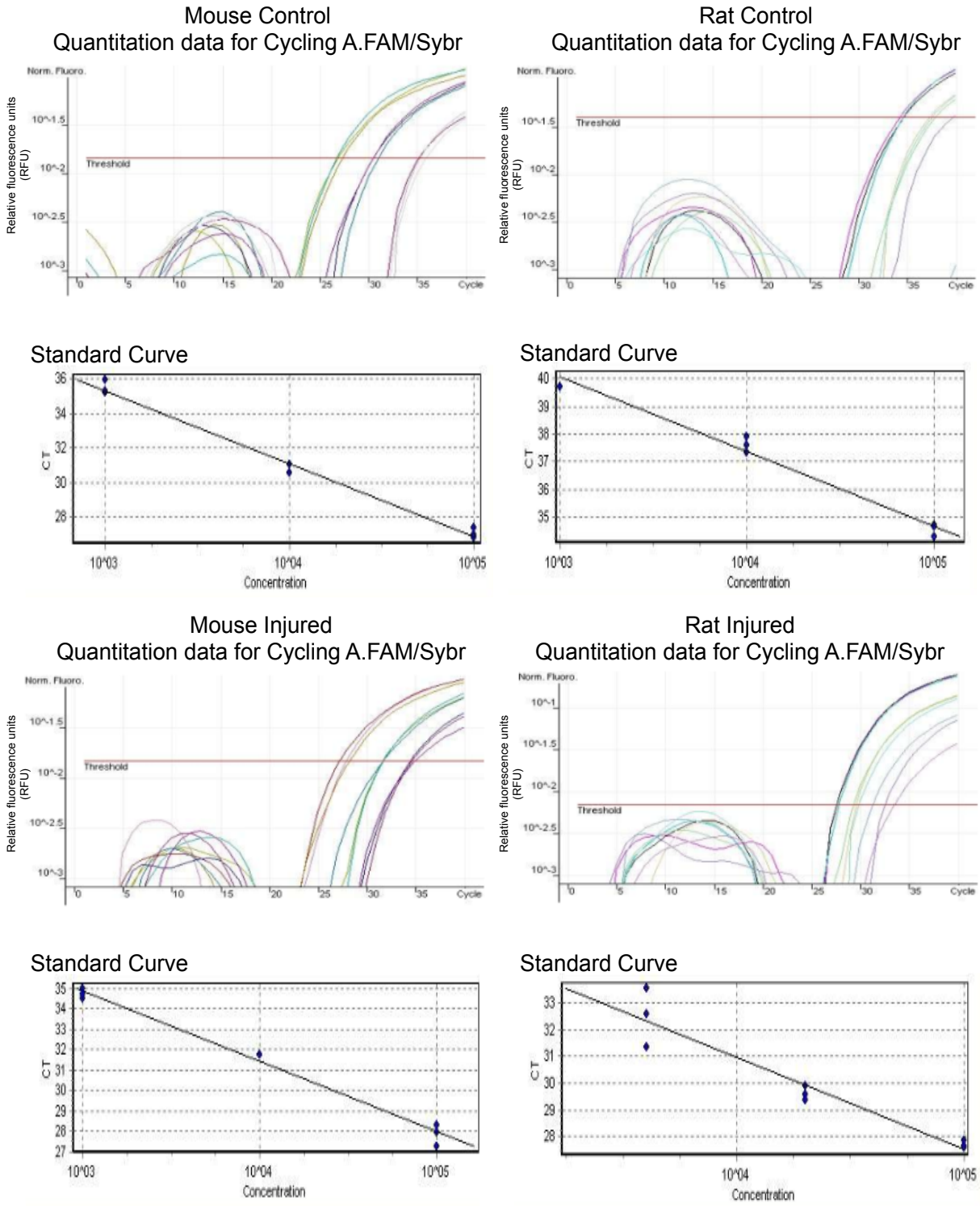

Figure 6.17 A representative quantification data and standard curve from each treatment group for CD44 gene.

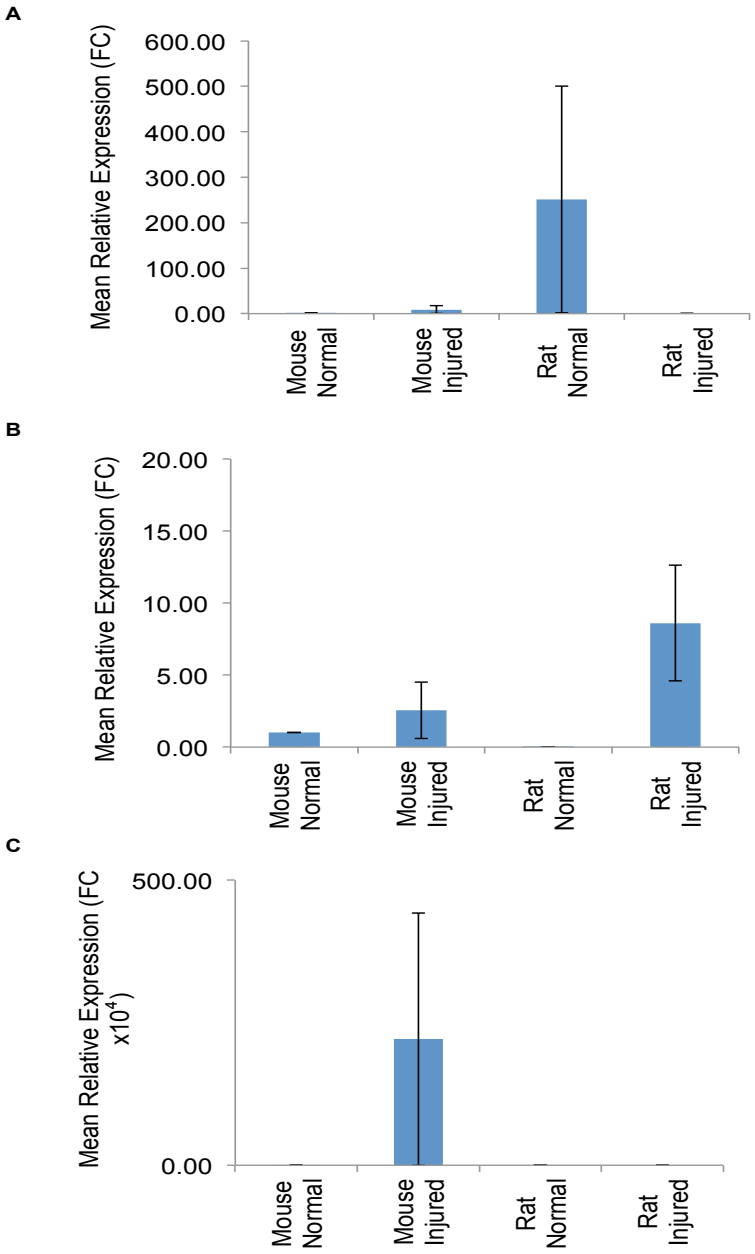

Figure 6.18 The expression of HLX-1 was validated by qPCR revealing that its expression was slightly higher in injured mouse compared to normal mouse, whilst in rats the expression decreased after injury **(A)**. The expression of integrin beta 2 revealed that its expression was higher in injured mice compared to normal mouse, whilst in rats the expression was higher compared to normal rat **(B)**. The expression of metallothionein 1H revealed that its expression was high in injured mice compared to normal mouse, whilst in rats the expression did not alter much **(C)**.

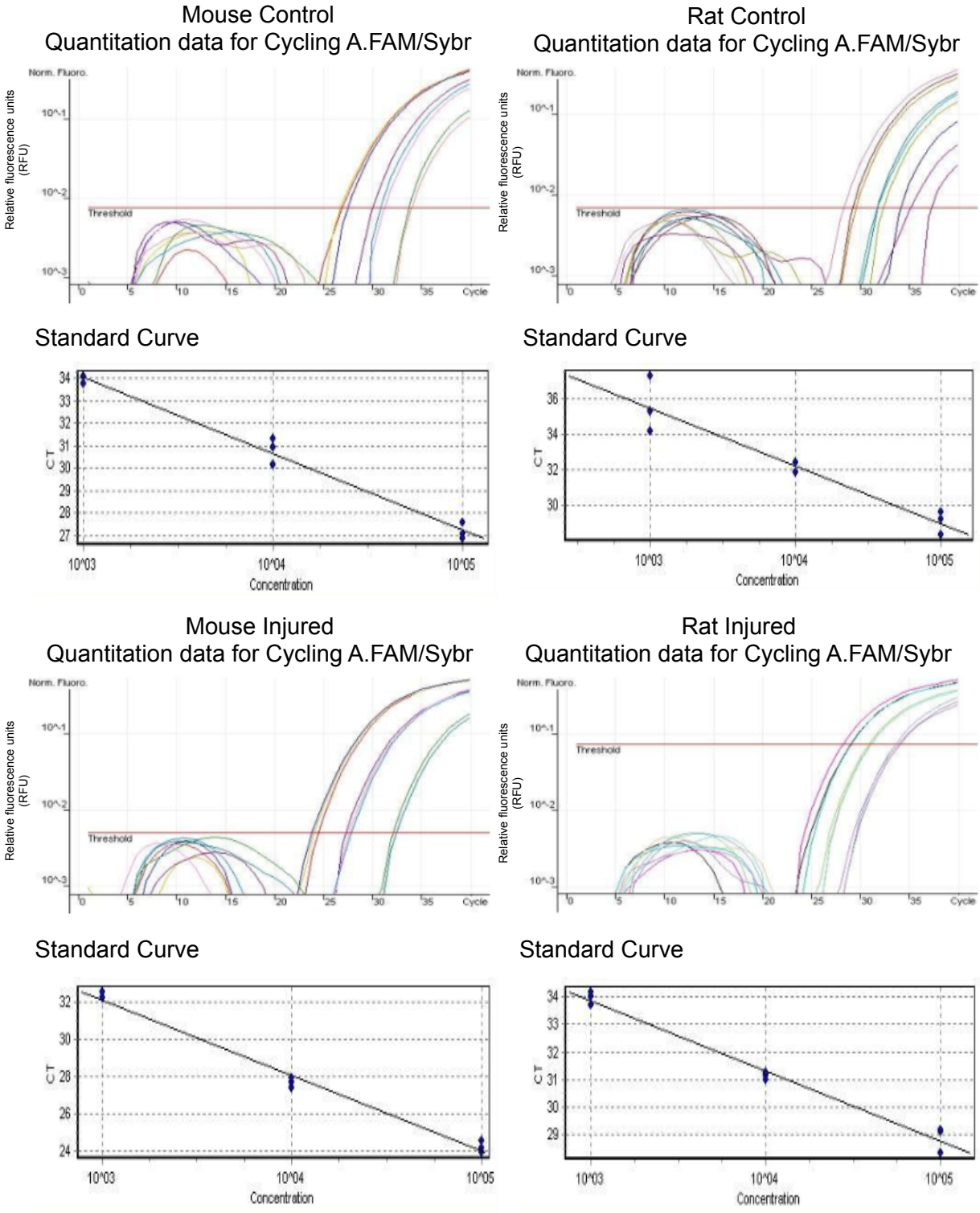

Figure 6.19 A representative quantification data and standard curve from each treatment group HLX-1 gene.

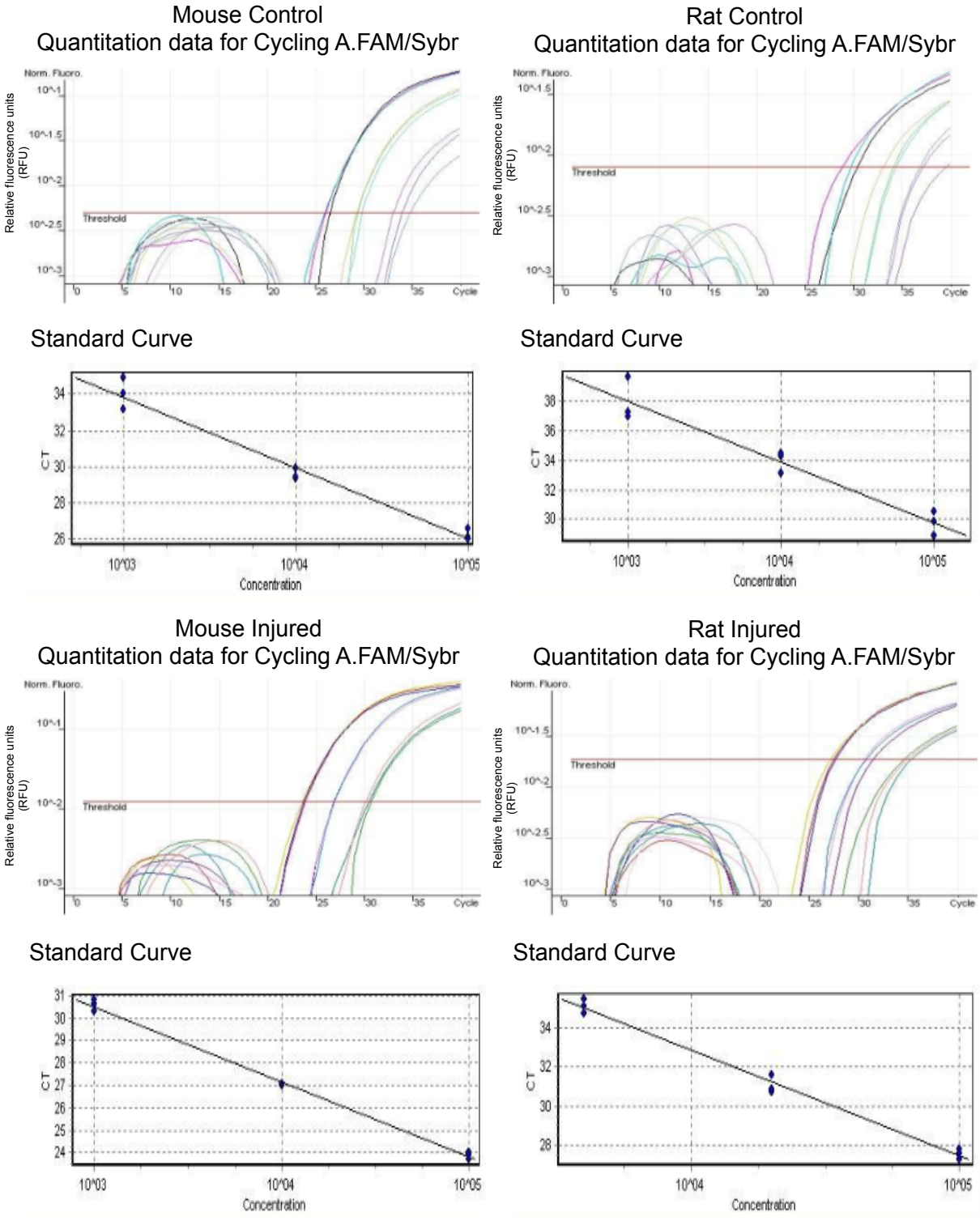

Figure 6.20 A representative quantification data and standard curve from each treatment group integrin beta 2.

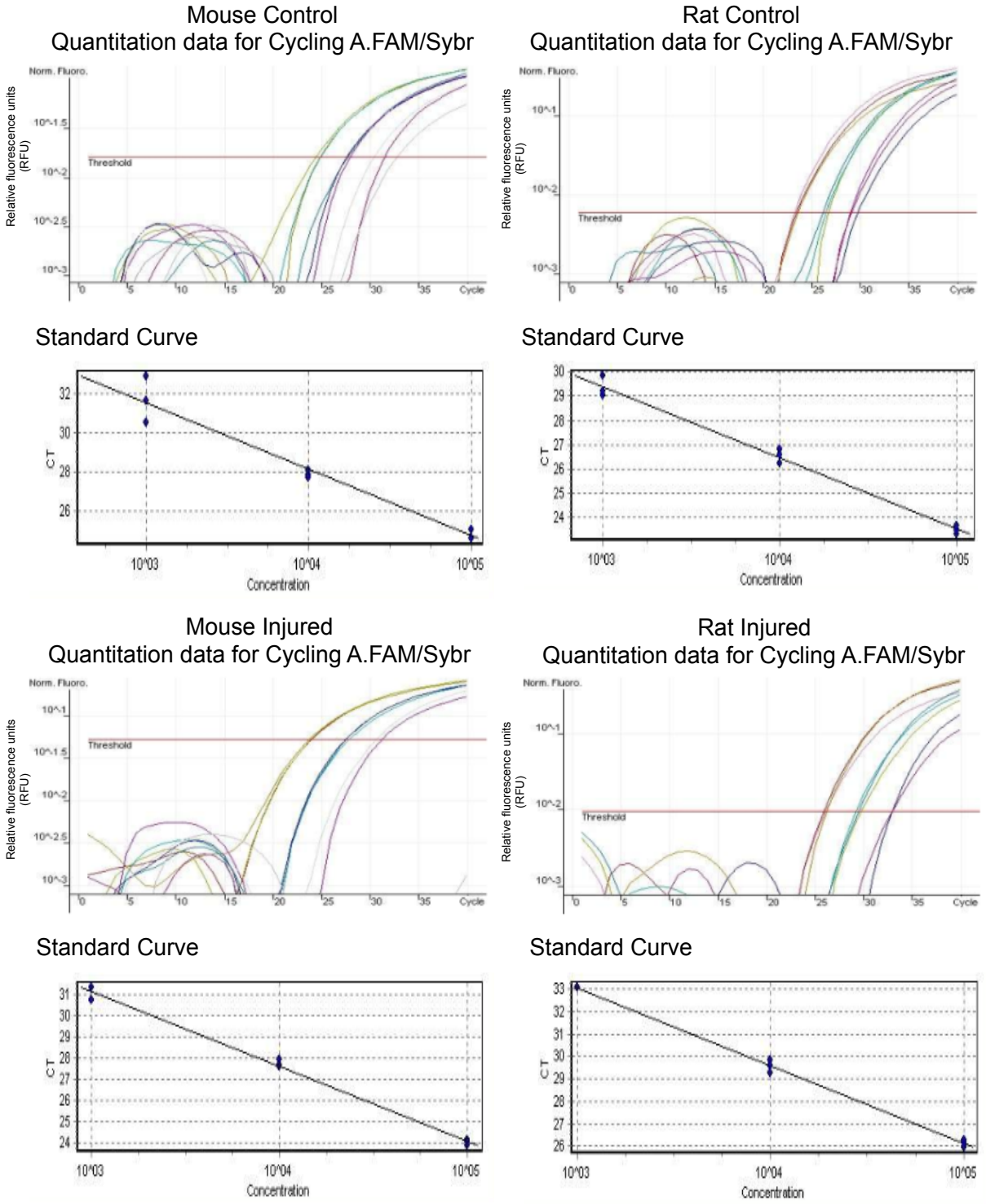

Figure 6.21 A representative quantification data and standard curve from each treatment group metallothionein 1H gene.

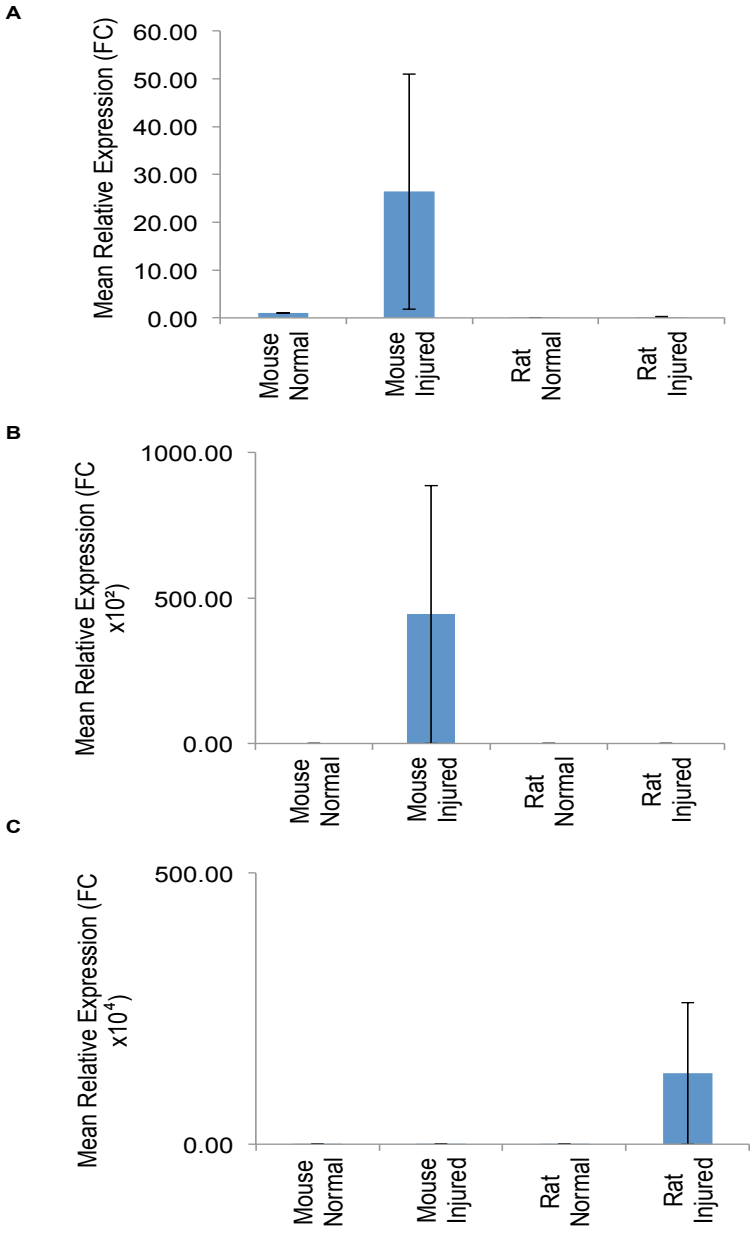

Figure 6.22 The expression of protein kinase C-eta was validated by qPCR revealing that its expression was high in injured mice compared to normal mouse, whilst in rats the expression did not alter much **(A)**. The expression of retinoic acid receptor beta revealed that its expression was high in injured mice compared to normal mouse, whilst in rats the expression did not alter much **(B)**. The expression of transforming growth factor beta receptor 1 revealed that its expression did not alter between normal and injured mouse, whilst in rats the expression increased after injury **(C)**.

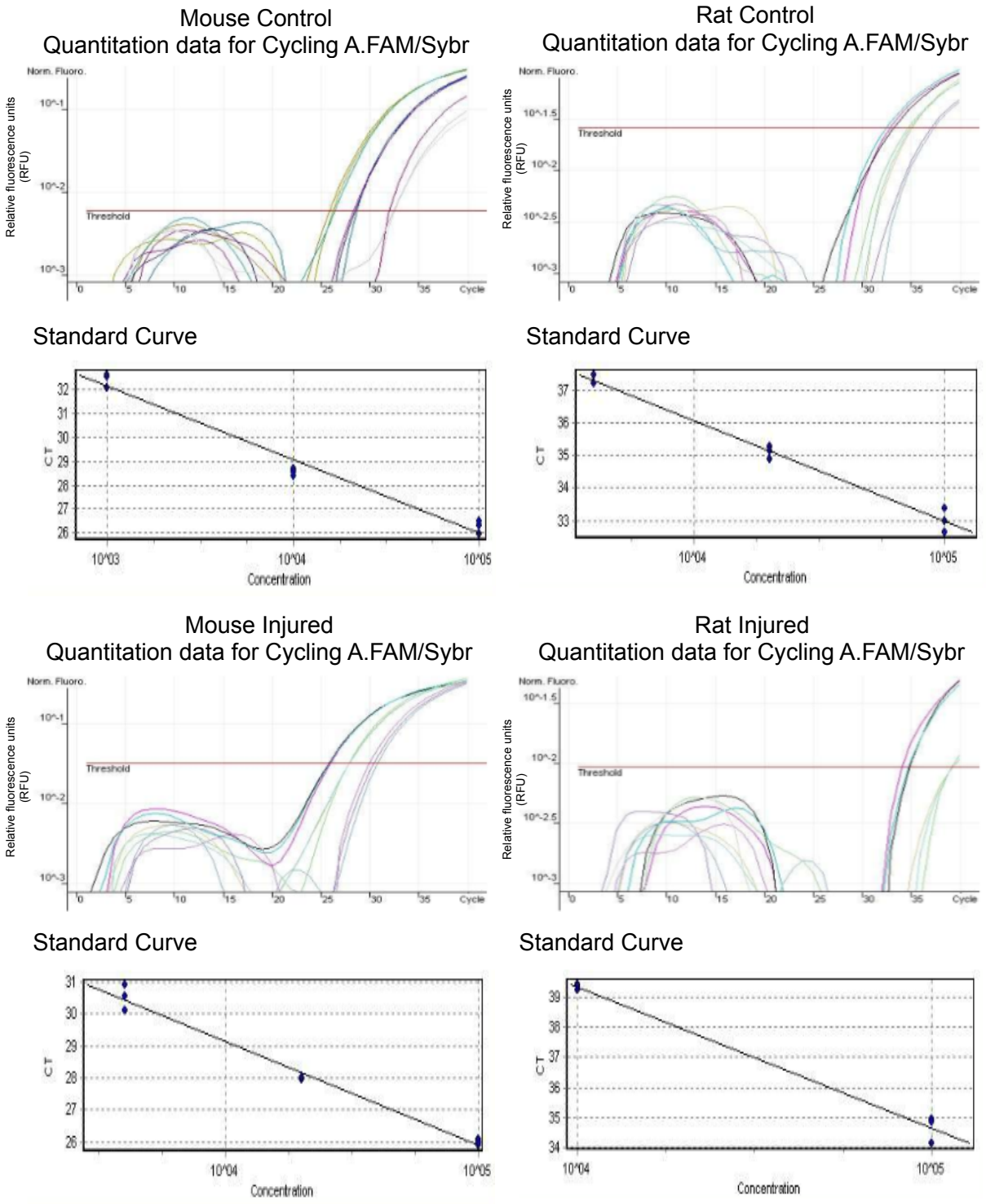

Figure 6.23 A representative quantification data and standard curve from each treatment group for protein kinase C-eta gene.

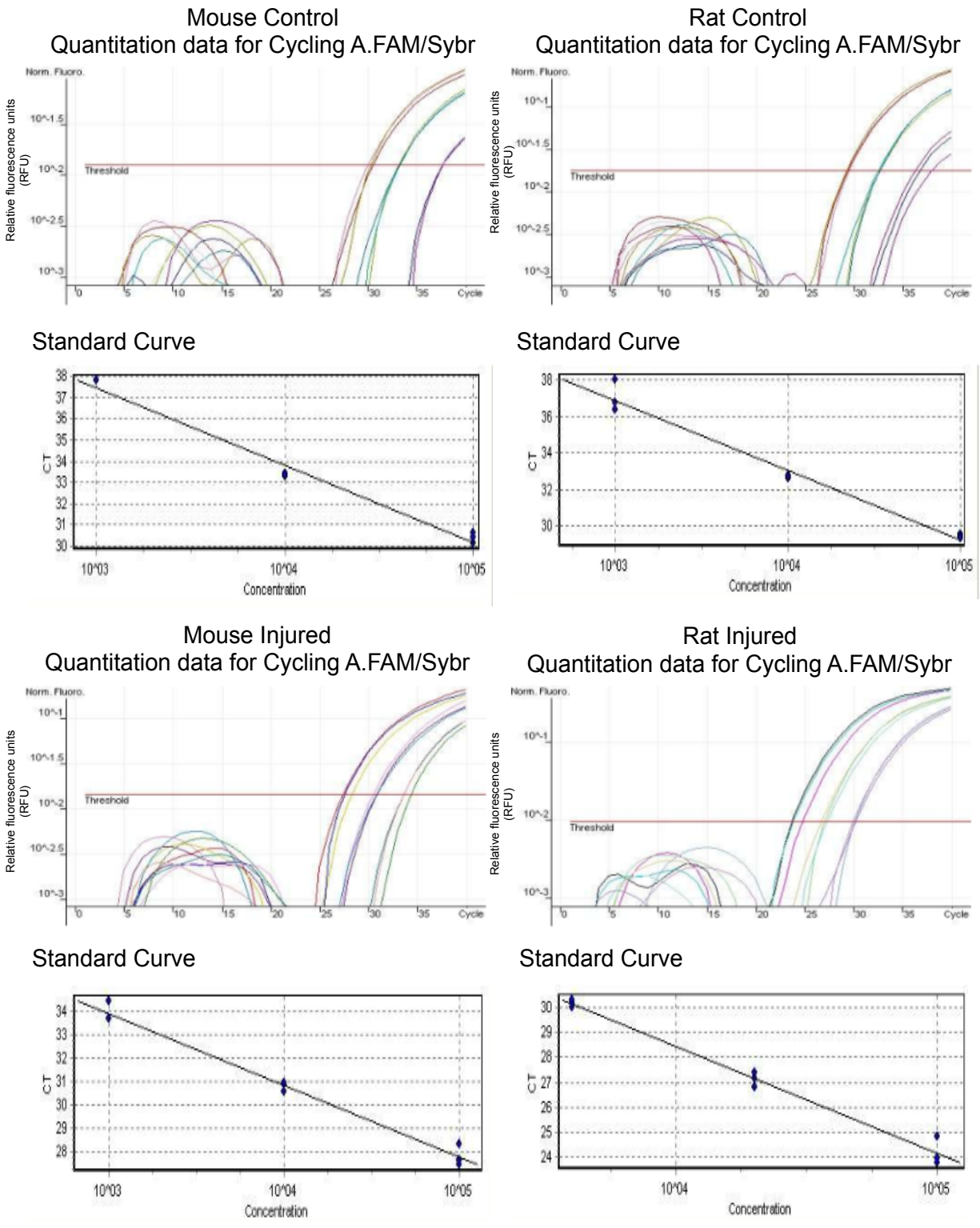

Figure 6.24 A representative quantification data and standard curve from each treatment group for retinoic acid receptor beta gene.

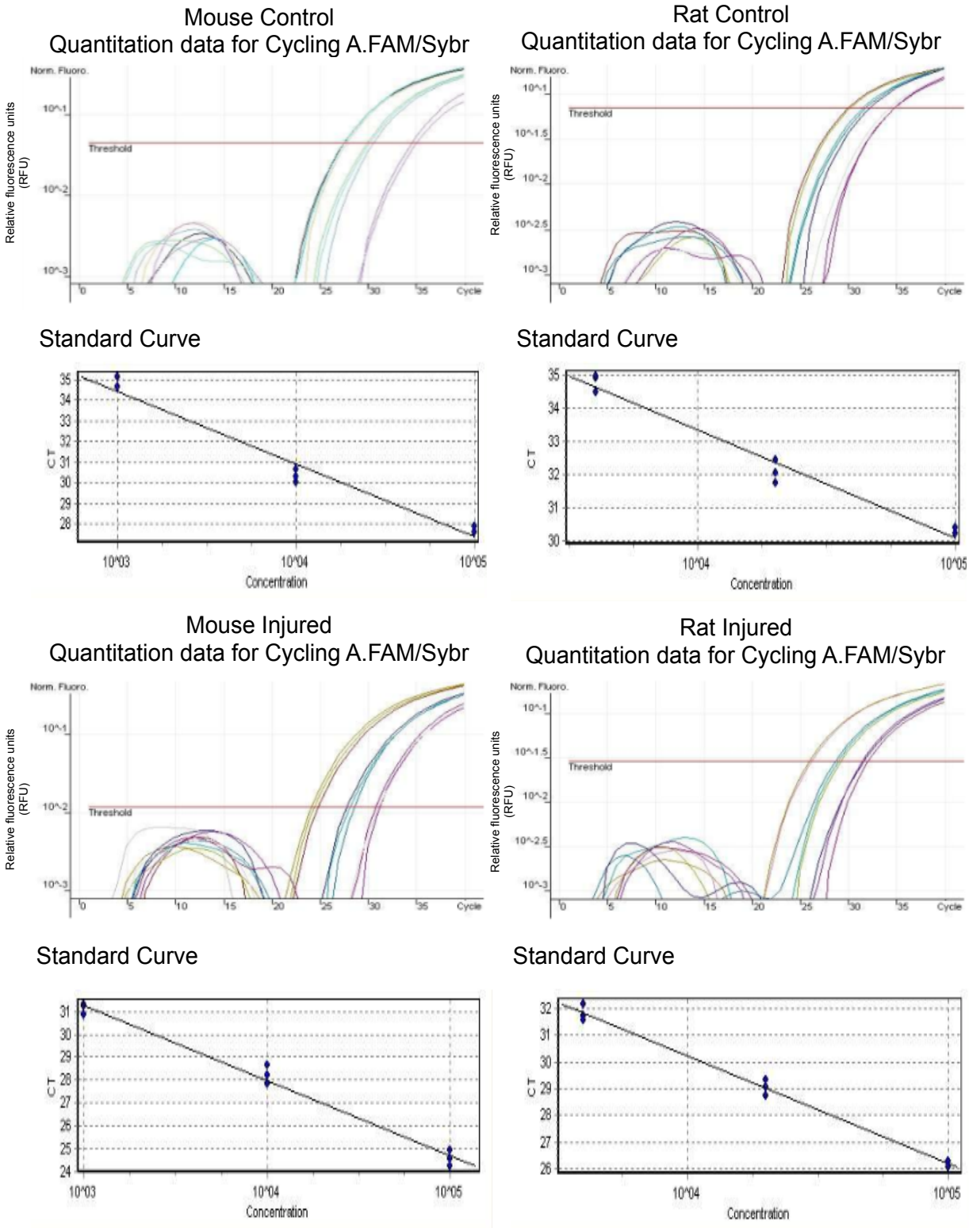

Figure 6.25 A representative quantification data and standard curve from each treatment group for transforming growth factor beta receptor 1 gene.

6.6.4 Localisation of angiogenic/wound healing-related genes

The localisation of angiogenic/wound healing-related proteins was determined by fluorescent immunohistochemistry (Figure 6.26 and 6.27). The localisation of α_{2B}-AR in normal mouse tissue displayed base line levels before injury in mice (Figure 6.26A) and after SCI there is an increase in α_{2B}-AR particularly around the lesioned area (Figure 6.26B). This same phenomenon was observed with ANXA3 (Figure 6.26C and D), HLX-1 (Figure 6.26E and F), ITGβ2 (Figure 6.26G and H) and PRKCH (Figure 6.26I and J) which all coincided with gene expression results. However, the gene expression of RARβ was increased after SCI in mice but immunoreactivity did not represent this expression (Figure 6.26K and L). This could be due to biological variability between samples of the same species.

Whilst in rats there was no comparable change seen in the immunoreactivity of α_{2B}-AR between control and injured animals (Figure 6.27A and B), and this same pattern was also observed for ANXA3 (Figure 6.27C and D), HLX-1 (Figure 6.27E and F) and RARβ (Figure 6.27K and L) which matched the gene expression results. However, this could not be said about ITGβ2 (Figure 6.27G and H) and PRKCH (figure 6.27I and J). The immunoreactivity of ITGβ2 was decreased after SCI and therefore did not match the gene expression results that showed increased gene expression. The expression of PRKCH showed no comparable change before and after injury, but the immunoreactivity levels of PRKCH was increased. Again these variations in data could be accounted for by the biological variation between samples of the same species.

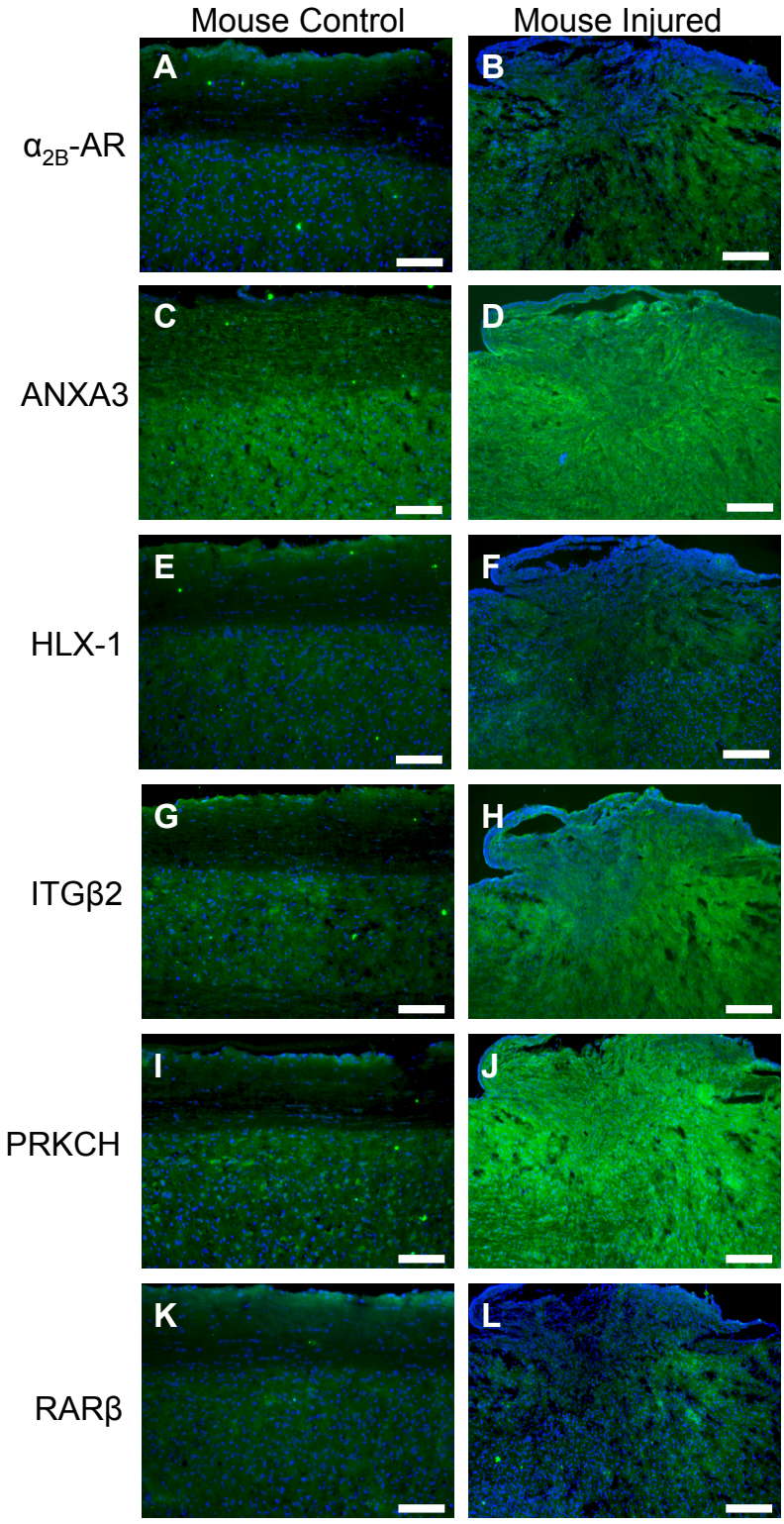

Figure 6.26 The localisation of angiogenic/wound healing-related proteins using fluorescent immunohistochemistry at 8 days after DC lesion. Pictures taken in AxionVision (x100 magnification) (n=3/group/antibody). Scale bars in A-L = 100μm.

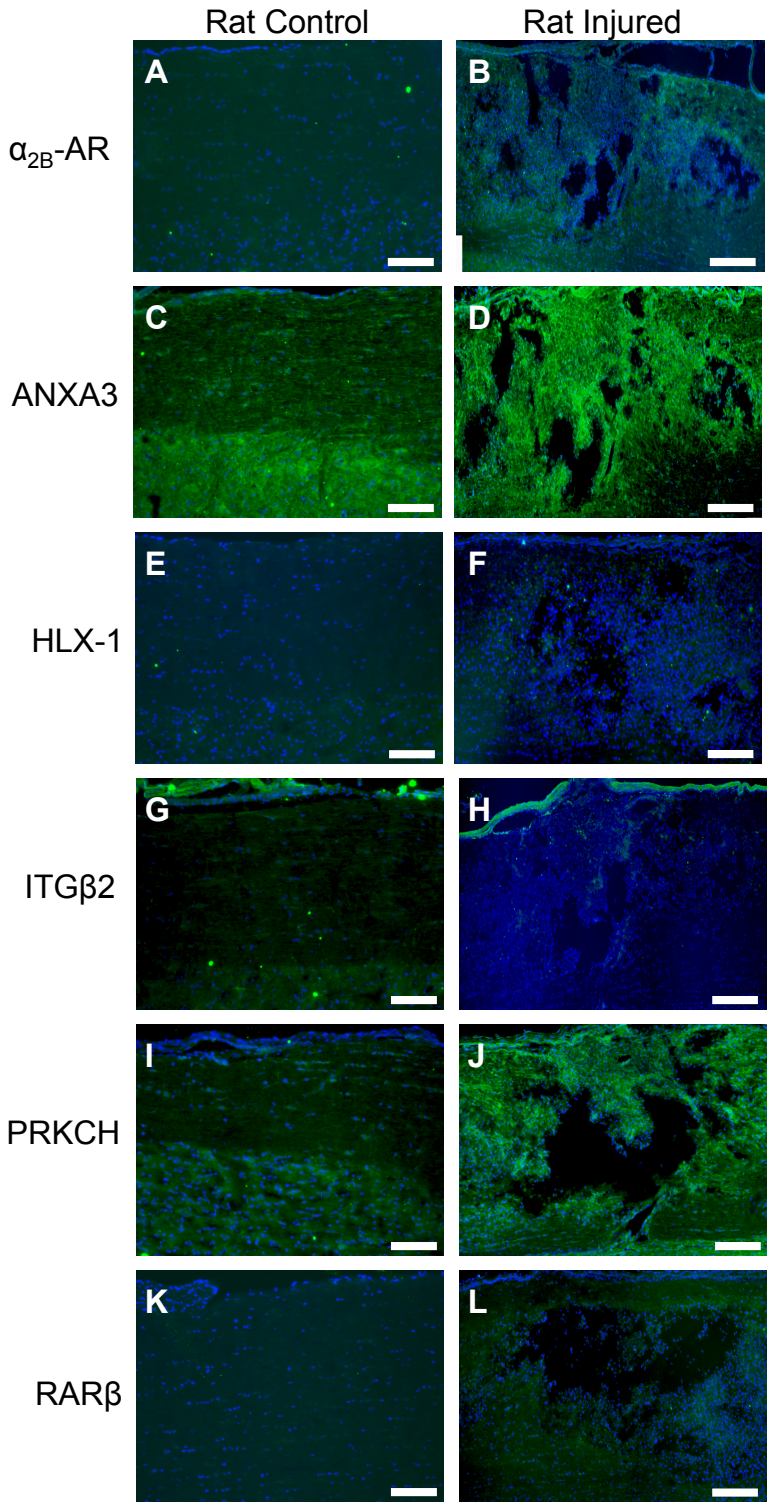

Figure 6.27 The localisation of angiogenic/wound healing-related proteins using fluorescent immunohistochemistry at 8 days after DC lesion. Pictures taken in AxionVision (x100 magnification) (n=3/group/antibody). Scale bars in A-L = 100μm.

6.6.5 Genome wide normalisation

Biological variation is one of the main pitfalls of comparing two species against one another and whilst microarray analysis provides average gene expression in the samples, the qPCR validation resulted in huge error bars indicating that not all samples express a specific gene at the same level. To confirm the biological variation the raw data was analysed in Linear Models for Microarray Data (LIMMA) which is a statistical package that allows the analysis of microarray data. It uses linear models to assess differential expression in the designed experiment and thus, each injured mouse and rat sample can be compared to their representative control samples using various codes within the package for global normalisation (Figure 6.28 and Appendix 3). The genes validated by qPCR were assessed in this manner to establish huge variation between samples of the same species and in this instance both mouse and rat showed marked variation in genes HLX1, ITGβ2 and TGFβR1, whilst MT1H and PRKCH was only variable in rat and mouse, respectively (Table 6.5). The top 20 and 20 bottom genes expressed in both mouse (Table 6.6) and rat was analysed (Table 6.7) to determine if any genes were expressed on the same level. In this manner Gpnmb, Serpina3n, Ccl3 and cd68 genes were in the top 20 genes that were highly expressed in the treated samples compared to control in both species. However, there were no genes that were in the bottom 20 that were common in both species.

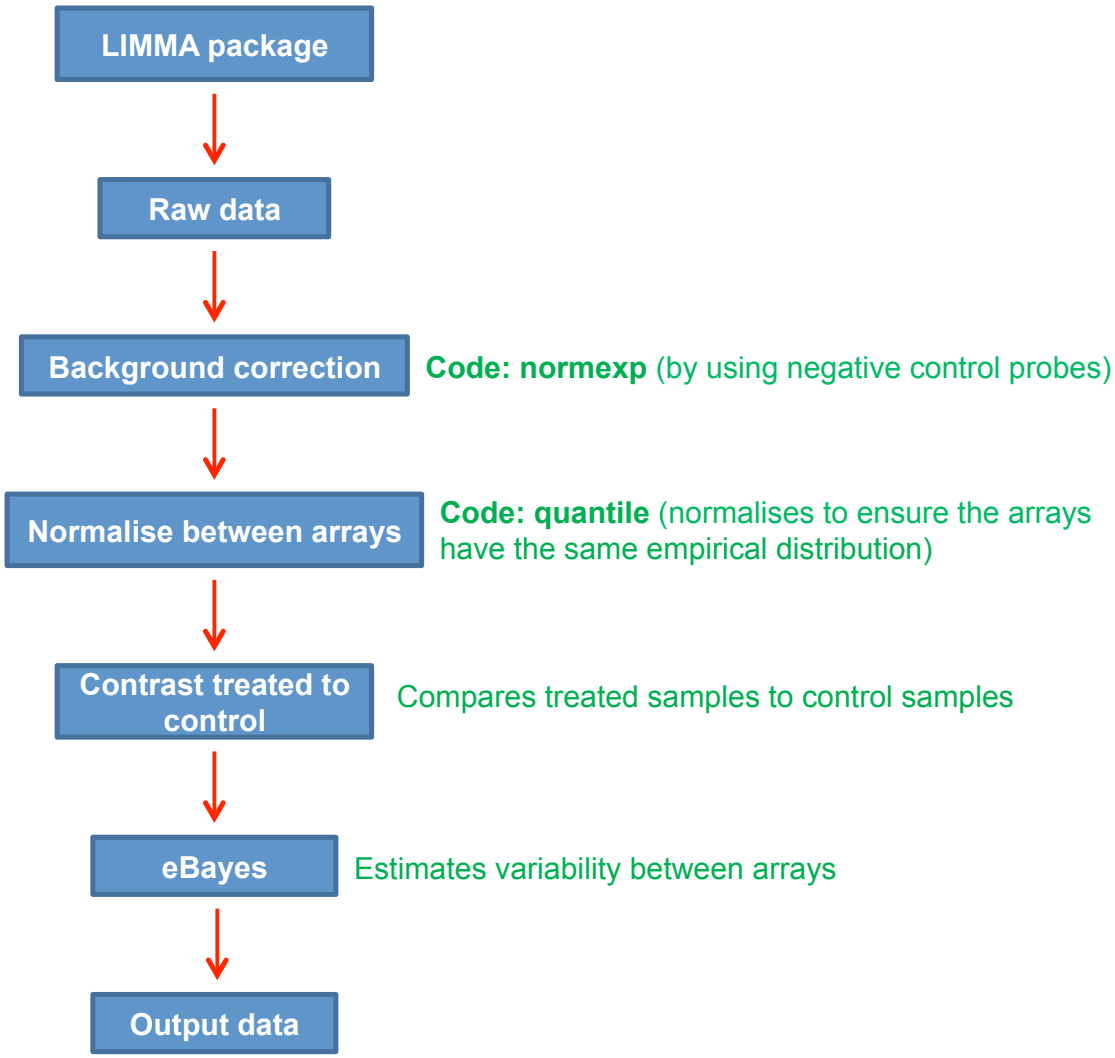

Figure 6.28 A flow diagram representation of the commands and codes used in the LIMMA package to assess the raw microarray data to estimate the variability between the arrays.

Number	Probe number	Gene symbol	Sample 1 logFC	Sample 2 logFC	Sample 3 logFC	Sample 4 logFC	Sample mean logFC
			Mus musculus (mouse)				
1	A_55_P1994027	Alpha-2-Adrenergic receptor beta	-1.23390972	-0.17175395	-0.38623904	-0.26532275	-0.520083727
2	A_55_P2056325	annexin A3	2.56079809	2.53740130	2.15727629	2.20185159	2.407680747
3	A_55_P2064043	CD44	0.40792437	0.85920411	1.15568355	0.52691227	0.735762741
4	A_51_P179701	H2.0-like homeobox	-1.88933495	0.06036528	-1.10351221	-0.66534948	-0.887394054
5	A_51_P262208	Integrin beta 2	1.32069049	1.56898064	2.32291897	1.63846431	1.725674778
6	A_66_P111660	Metallothionein	-0.00557403	-0.10017106	0.21036148	0.33741974	0.117770373
7	A_51_P355852	Protein kinase C-eta	1.16996187	1.36053779	-0.20682296	-0.03805165	0.625270584
8	A_55_P2084807	Retinoic acid receptor beta	0.08773170	0.16002007	-0.54127186	0.13814893	-0.004963839
9	A_55_P2137211	Transforming growth factor beta receptor 1	1.82474528	0.83875293	0.18243684	1.27208182	1.114244834
			Rattus (rat)				
10	A_64_P138008	Alpha-2-Adrenergic receptor beta	-0.56471	-0.83458	-0.80746	-0.57817	-0.693340228
11	A_44_P325508	annexin A3	1.367028	0.711145	1.055104	1.553076	1.166203155
12	A_64_P080817	CD44	0.718257	0.921977	0.677076	1.44472	0.927787969
13	A_42_P460351	H2.0-like homeobox	0.750358	0.530825	1.677066	2.545135	1.34657912
14	A_42_P591344	Integrin beta 2	1.80609	0.998719	2.960178	1.958429	1.910085321
15	A_64_P123603	Metallothionein	1.238768	0.530675	3.106903	2.327902	1.751289343
16	A_64_P019638	Protein kinase C-eta	0.615275	0.499325	0.91402	0.94893	0.735108794
17	A_64_P016249	Retinoic acid receptor beta	-0.18279	0.04831	0.439737	0.739502	0.20735347

18	A_64_P045651	Transforming growth factor beta receptor 1	0.346688	0.649364	0.4809	0.959905	0.601934197

Table 6.5 A list of the chosen genes validated by qPCR and the individual expression values for each sample compared to their representative controls and the average of those values for both mouse and rat.

Number	Probe number	Gene symbol / Target ID	Mouse 1 logFC	Mouse 2 logFC	Mouse 3 logFC	Mouse 4 logFC	Mouse mean logFC
1	A_51_P438967	Gpnmb	5.89198506	5.70245996	7.04679567	6.58607612	6.346912445
2	A_51_P137419	Cst7	5.18645776	5.28253262	6.21365721	4.58712959	5.344085985
3	A_51_P139678	Sprr1a	4.31786049	4.70115880	6.02285310	4.66825812	4.967096054
4	A_51_P205779	Cd5l	4.80519630	3.84617646	6.24002043	3.40562024	4.589421311
5	A_51_P246653	Clec7a	4.22027374	4.38594099	6.10922248	3.67233205	4.578915286
6	A_55_P1957459	Lilrb4	3.97648500	3.57444249	5.92867472	4.56533732	4.52666022
7	A_51_P303424	Itgax	4.50650332	4.17068552	5.41352796	3.77876176	4.514777894
8	A_55_P1958165	Ms4a7	3.72280098	3.24972728	6.33393221	3.37125409	4.130264913
9	A_55_P2171116	Lgals3	3.82387252	3.71153291	5.31750148	3.48317787	4.049111794
10	A_55_P2008987	Ch25h	3.99581439	3.46650580	5.04147643	3.20032468	3.969106822
11	A_51_P321150	Lyz2	4.46160685	3.42680898	4.21473631	3.70027281	3.966706352
12	A_51_P159453	Serpina3n	4.47385527	3.41767669	3.45719993	3.96586618	3.878583389
13	A_55_P1985850	Timp1	4.33356164	2.49976759	5.52239169	3.10954919	3.817485153
14	A_51_P390804	Wisp2	3.23174289	2.92092873	5.33333254	3.36409558	3.710914599
15	A_51_P140710	Ccl3	3.16714559	3.46699671	4.54943268	3.46754414	3.667707425
16	A_55_P1961943	Cd68	2.95631320	3.03324106	4.76665106	3.41986205	3.540201653
17	A_51_P509573	Ccl4	3.08088928	3.66455819	3.99111875	3.24667892	3.523629922
18	A_51_P390538	Mpeg1	3.40789024	3.28950858	4.35053542	3.00453264	3.510343718
19	A_55_P2016462	Cxcl10	3.40698882	3.59642904	4.55382287	2.33295926	3.464584124
20	A_55_P1962937	Trem2	3.36895576	3.26565512	4.06565373	2.65653662	3.338456774
21	A_30_P01019700	chr18:3003075-	-3.70394860	-2.18050164	-2.98479172	-2.29518378	-

		3016150_F					2.801454175
22	A_55_P2208682	B230334C09Rik	-3.47204997	-1.80024556	-2.54957359	-3.37048896	-2.817081071
23	A_30_P01027915	chr19:54011403-54018978_F	-3.95513763	-3.15152115	-1.85667473	-2.11191713	-2.829760602
24	A_52_P188042	Trat1	-1.04771229	-1.06196747	-9.96536217	0.35766663	-2.845310757
25	A_30_P01024761	chr5:15146475-15170100_F	-4.09403809	-3.55986540	-1.65382983	-1.89045844	-2.876934281
26	A_30_P01032085	chr10:82074600-82085425_F	-8.22497129	-1.82810194	-1.48349064	-0.95040127	-3.109743631
27	A_30_P01022919	chr18:3003075-3016150_R	-3.27326914	-2.77135806	-3.91574508	-2.65891809	-3.149356408
28	A_30_P01032775	chrX:92149320-92151107_R	-4.40636708	-2.79420035	-3.25575599	-2.42936925	-3.236106373
29	A_55_P2050747	4930557B15Rik	-3.87338472	-3.56712539	-3.47768217	-2.10791381	-3.259800879
30	A_55_P2089398	TC1709339	-4.61772973	-2.91686519	-3.30658156	-2.68433217	-3.35508493
31	A_30_P01028043	chr4:3009566-3009932_R	-3.50172909	-3.14724880	-3.30924986	-3.50737751	-3.3776035
32	A_30_P01033617	chrX:92139043-92140820_R	-4.53248666	-3.10229217	-3.62012190	-2.32714929	-3.403957091
33	A_55_P1957865	Unknown	-4.86401918	-4.59927795	-2.56706150	-2.62065037	-3.720866815
34	A_30_P01017834	chr5:15146475-15170100_F	-4.79686176	-4.82521838	-2.50539711	-3.01293501	-3.770900917
35	A_55_P2279498	4933438K21Rik	-4.68399199	-3.54177705	-3.89665981	-3.15881507	-3.841871908
36	A_30_P01029005	chr5:14943275-14944205_F	-4.73949414	-5.07511057	-2.67789485	-2.99856524	-3.859425273
37	A_30_P01023020	chr18:3003075-	-4.21080020	-4.70045875	-4.60877863	-3.61383246	-

		3016150_R					4.283062796
38	A_30_P01031842	chr5:15146475-15170100_F	-5.00549672	-5.62376375	-3.37373773	-3.80572856	-4.4290566
39	A_30_P01018533	chr5:15146475-15170100_F	-5.33960833	-5.22639512	-3.62109536	-3.82758312	-4.468591972
40	A_30_P01019442	chr5:14943275-14944205_F	5.41487528	-5.30993106	-3.80898660	-3.79752440	-4.531068753

Table 6.6 A list of the top 20 and bottom 20 genes in each mouse injured sample compared to its representative control indicating the level of expression for that particular gene.

Number	Probe number	Gene symbol / Target ID	Rat 1 logFC	Rat 2 logFC	Rat 3 logFC	Rat 4 logFC	Rat mean logFC
1	A_44_P990376	Gpnmb	4.154838	2.666411	4.521813	4.9884	4.027771723
2	A_64_P059728	TC597252	2.994824	2.278056	3.301945	4.992649	3.365957969
3	A_64_P019260	Cd68	2.930126	1.669075	2.926219	4.363112	2.931408127
4	A_44_P1023538	C3	2.290524	1.878488	3.893855	2.58147	2.616035051
5	A_42_P714311	Ccl3	2.205907	2.163499	2.376008	3.434482	2.529210581
6	A_64_P149280	Vegfb	-0.03244	4.93425	5.126778	1.287988	2.511129445
7	A_44_P1000653	Serpina3n	2.315075	2.836115	1.009049	3.42614	2.369845254
8	A_64_P119127	Unknown	1.01392	2.459927	1.426598	4.483438	2.322098839
9	A_43_P12698	Lgals3	1.981876	2.211423	2.085039	2.69779	2.23892154
10	A_42_P686879	Siglec1	1.426674	1.480708	2.231108	3.95273	2.22498532
11	A_44_P1039128	Cxcl10	1.647039	1.080097	3.944641	2.154608	2.158587681
12	A_42_P567268	Mt2A	1.966689	1.444918	2.531827	2.766486	2.142133969
13	A_64_P026316	C4a	1.267121	1.989006	2.647144	2.746835	2.122519743
14	A_44_P115116	Mpeg1	1.098664	2.86058	3.076251	1.984928	2.100357939
15	A_64_P019790	Cyp2d1	1.197507	1.887371	1.90169	3.559268	2.095199779
16	A_64_P036725	Gpr63	0.483037	2.035594	3.394641	2.62822	2.039815229
17	A_64_P001211	Cyp2d5	1.104044	1.853117	1.825171	3.479227	2.02154868

18	A_64_P058336	Ucn	1.466213	1.684027	2.431743	2.43484	1.968147628
19	A_64_P039693	Unknown	0.938036	0.956756	4.162889	1.832246	1.944354676
20	A_42_P591344	Itgb2	1.80609	0.998719	2.960178	1.958429	1.910085321
21	A_64_P049738	Unknown	-2.47931	-1.88494	-2.36692	-1.66452	-2.068562861
22	A_64_P074544	Ankrd61	-1.65037	-1.40274	-3.78067	-1.6348	-2.102764221
23	A_64_P017473	Chmp4bl1	-1.48364	-1.97589	-2.61163	-2.46863	-2.110169207
24	A_44_P552452	RT1-Bb	-3.41722	-4.86162	-0.14356	0.01438	-2.129867032
25	A_64_P089410	LOC367436	-0.52206	-0.97178	-3.60203	-3.99501	-2.173922537
26	A_64_P121091	Acoxl	-1.37307	-1.0136	-4.1215	-2.35871	-2.19689634
27	A_64_P122168	Lhx6	-1.76206	-1.31402	-3.94155	-1.76785	-2.204759175
28	A_64_P001301	Unknown	-1.31435	-1.53917	-3.7107	-2.34074	-2.226466678
29	A_64_P100669	E2f8	-2.02178	-1.30411	-3.86626	-2.07665	-2.313368742
30	A_64_P020531	TC600364	-2.37602	-1.26157	-3.86074	-1.99291	-2.338446142
31	A_64_P053411	ENSRNOT00000044462	-2.21067	-1.074	-3.48051	-2.83507	-2.353114623
32	A_64_P043546	Unknown	-1.60005	-1.34514	-4.44055	-2.24304	-2.398442543
33	A_64_P166168	ENSRNOT00000051988	-2.21085	-1.51288	-3.62255	-2.71833	-2.489797379
34	A_64_P137734	ENSRNOT00000052393	-1.556	-1.83267	-4.14567	-2.98483	-2.579600407
35	A_43_P17464	TC628549	-2.54863	-1.09049	-4.61122	-2.34216	-

							2.616442246
36	A_64_P127173	Unknown	-2.5613	-1.54302	-4.31685	-2.43696	-2.686336704
37	A_64_P080179	Unknown	-0.2428	-0.1439	0.013226	-11.8417	-2.76728462
38	A_64_P105550	Unknown	-2.58876	-1.87724	-4.24234	-2.48592	-2.805829696
39	A_64_P286599	Vwf	-4.05406	-2.17121	-5.35609	-3.482	-3.716496849
40	A_64_P015163	Unknown	-1.63945	-4.95575	-4.23493	-4.23801	-3.728893926

Table 6.7 A list of the top 20 and bottom 20 genes in each rat injured sample compared to its representative control indicating the level of expression for that particular gene.

6.7 Discussion

Multiclass analysis revealed 1090 genes in mice and 1616 genes in rats that were deemed as significantly expressed after SCI. IPA analysis on these values revealed that in mice and rats 562 and 689 genes, respectively, were unique whilst 874 and 721 genes, respectively, were mapped and differentially regulated whilst 388 and 98 genes, respectively, were un mapped after SCI. Known canonical pathways were used to assess IL8 mediated regulation of angiogenesis and tumour growth, NGF signalling for neurite outgrowth and differentiation, PDGF signalling for cell proliferation and survival and VEGF signalling for hypoxia and angiogenesis pathways that showed significant differences between mice and rats after SCI. Known angiogenic/wound healing-related genes that were either 2-fold up or down regulated after sub-acute SCI at 8 dpl were extracted from the raw data sets, and of those 9 genes were chosen to be validated by qPCR. Whilst alpha-2-adrenergic receptor beta, annexin A3, CD44, metallothionein 1H, protein kinase C-eta and retinoic acid receptor beta gene expression was increased in injured mouse compared to other treatment groups, HLX-1 gene expression was reduced in injured rat compared to other treatment groups. Integrin beta 2 and transforming growth factor beta receptor 1 gene expression was increased in injured rat compared to other treatment groups; with only annexin A3, CD44 and metallothionein 1H showed overall significance.

Whilst microarray analysis provides average gene expression in the samples, true biological variation is not accounted and therefore large variations in gene expression were observed. Each injured sample was compared to a control sample indicating that there was marked variation in HLX-1, integrin beta 2 and transforming

growth factor beta receptor 1 in both species, whilst metallothionein 1H and protein kinase C-eta in rat and mouse, respectively. The top 20 and bottom 20 genes expressed in both mouse and rat was analysed to determine if genes were expressed on the same level. In this manner Gpnmb, Serpina3n, Ccl3 and cd68 genes were in the top 20 genes that were highly expressed in the treated samples compared to control in both species. However, there were no genes that were in the bottom 20 that were common in both species.

6.7.1 Angiogenic/wound healing-related genes chosen for validation

6.7.1.1 Alpha-2-adrenergic receptor beta (α_{2B}-AR)

Catecholamines are neurotransmitters of the sympathetic nervous system that respond by binding to their adrenergic receptors (adrenoreceptors) (Figure 6.29) (Kanagy, 2005). Adrenoreceptors are members of the G protein-coupled family that is formed of a 7-transmembrane domain, typically found throughout vertebrates, that have a critical role in regulating neurotransmitter release from sympathetic nerves and from adrenergic neurones in the CNS (Aris-Brosou et al., 2009, Wang et al., 2002). Whilst there are a total of nine known isoforms, alpha-2-adrenoreceptor has 3 highly homologous isoforms; alpha2A, alpha2B and alpha2C that are expressed within the CNS, kidney, heart and vasculature (Nicholas et al., 1996, Kanagy, 2005, Bylund, 1995). Alpha-2-adrenoreceptor mRNA is expressed throughout rat CNS, predominately found in the DRG, intermediolateral cell column of the thoracic spinal cord, dorsal horn and the cerebral cortex, whilst in mice the mRNA is expressed in the brain, mainly the thalamus and purkinje layer of the cerebellum (Nicholas et al., 1996, Wang et al., 1996). The chromosomal location of alpha-2-adrenoreceptor in

humans is located on chromosome 10 whilst in mice it is located on chromosome 19 (Yang-Feng et al., 1990).

Alpha-2-adrenoreceptors play an important role not only in regulation of blood pressure but also in the regulation of noradrenergic neurotransmission in human CNS and PNS (Bawa-Khalfe et al., 2007). The long-term, chronic, paralysis that results from SCI is reversed when alpha-2-adrenoreceptor agonist, clonidine is administered in cats, resulting in “normalisation” of sensory-motor and autonomic dysfunction in preliminary experiments in humans with traumatic SCI indicating that autonomic dysreflexia and spasticity can be controlled and minimised (Naftchi, 1982). Clonidine also reduces the conditioned aversion in the central nuclei of the amygdala in the visceral pain-induced aversion in rats (Deyama et al., 2010). Early research demonstrates that alpha-2-adrenoreceptor plays a central role in the modulation of sensory inputs to the visual cortex in rats (Kolta et al., 1987). Alpha-2-adrenoreceptor agonists provide neuroprotective effects in rat optical nerve degeneration model and the loss of RGCs two weeks after injury was three times lower than that of controls and therefore reduced intraocular pressure (Yoles et al., 1999). Dormant microglia predominately express beta-2-adrenoreceptors but switch to alpha-2-adrenoreceptors under pro-inflammatory conditions, and despite differential expression of receptors, norepinephrine causes process retraction in both resting and activated microglia suggesting its role in modulating the motility of microglia (Gyoneva and Traynelis, 2013). Patients with Alzheimer’s disease were found to have 50% increase in densities of alpha-2-adrenoreceptors in cerebral microvessels compared to matched controls and thus associated with blood-brain barrier abnormalities (Harik and Kalaria, 1991). It has been reported that alpha-1 and -2

antagonists induce wound healing in rat cutaneous wounds 14 days after injury, affecting leukocyte migration, proliferation of epithelial and connective tissue and pro-MMP-9 levels, and when compared to beta-1 and-2 antagonists wound healing was not delayed (Romana-Souza et al., 2009).

6.7.1.2 Annexin A3 (ANXA3)

ANXA3 is a member of calcium-dependent phospholipid-binding protein annexin family playing a role in the regulation of cellular growth, proliferation, apoptosis and differentiation whilst also playing a role in various signal transduction pathways (Raynal and Pollard, 1994, Gerke and Moss, 2002, Gerke et al., 2005). Annexin family is made up of five major groups; A-E, that are present in humans (annexins A1-A13), animals (annexin B9-B12), fungi/moulds (annexin C1, C2 and C5), plants (annexin D1-D25) and protists (annexin E1-E3) (Gerke and Moss, 2002). ANXA3 is a 33kDa protein that is expressed in neutrophils with a 36kDa variant found in monocytes, and more recently ANXA3 mRNA and protein has been detected in zebrafish eggs and in mouse adipose tissues than any other tissues (Le Cabec and Maridonneau-Parini, 1994, Le Cabec et al., 1992, Sopkova et al., 2002, Ozerova and Minin, 2008, Watanabe et al., 2012).

In vitro observations demonstrate that ANXA3 is an angiogenic factor by inducing migration and tube formation of human umbilical vein endothelial cells (HUVECs) (Park et al., 2005). Not only was VGEF detected in the cultured medium but so was HIF-1 activity suggesting that ANXA3 induces VEGF expression through the HIF-1 pathway.

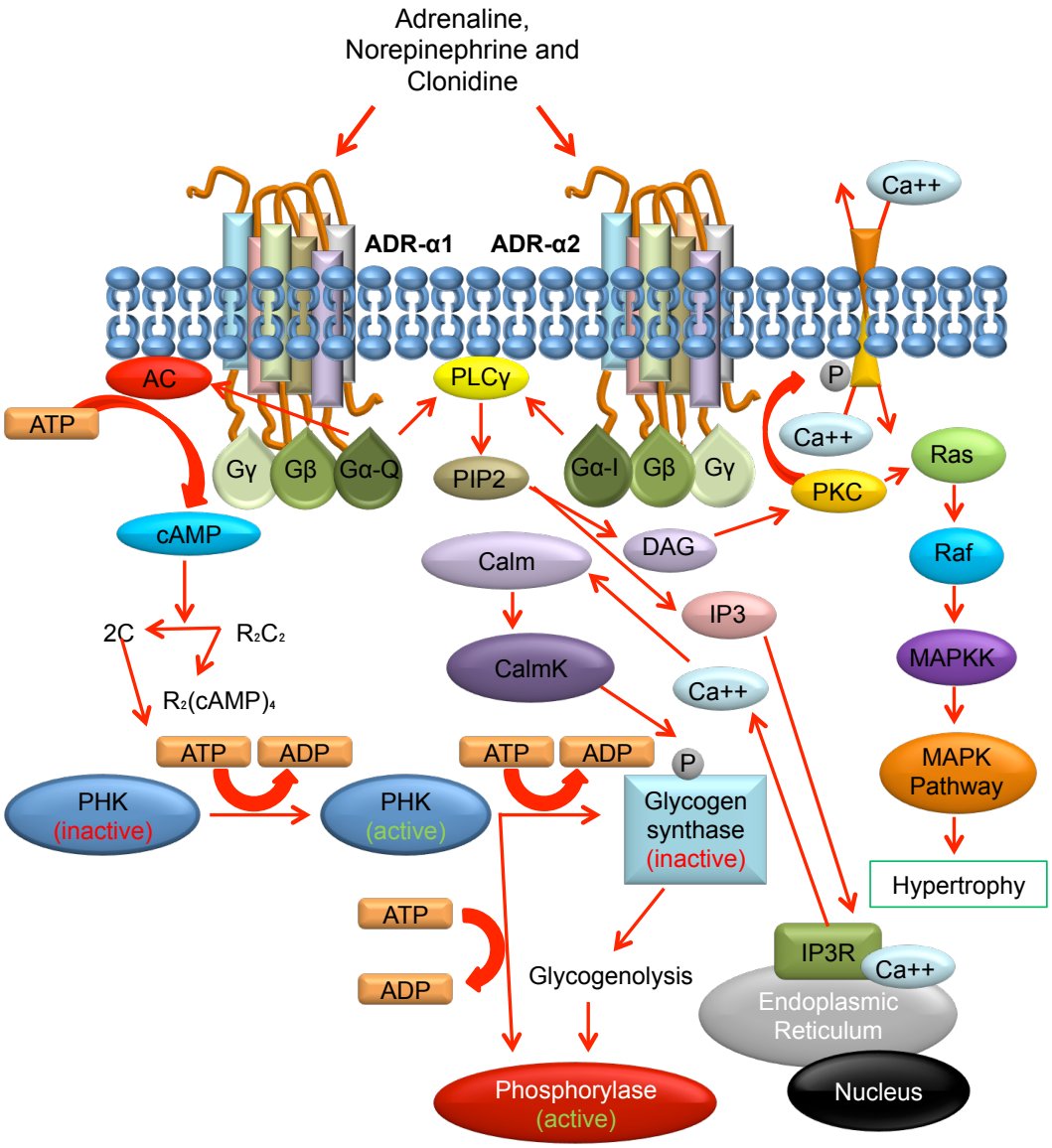

Figure 6.29 Alpha-adrenergic receptor (ADR) signalling pathway. ADR are receptors for adrenaline, norepinephrine and clonidine within the sympathetic nervous system. ADR are coupled through G-proteins that subsequently activate PLC-γ leading to the hydrolysis of membrane PIP2 producing DAG and IP3. DAG binds and activates PKC that activates the MAPK signalling pathway, whilst IP3 binds to its receptor; IP3R, located on the endoplasmic reticulum that leads to the release of calcium ions. The calcium ions activate glycogen synthase by interacting with Calm and CalmK (adapted from Qiagen).

ANXA3 has been investigated in the CNS using lactacystin; a proteasome inhibitor, that is used to stimulate ubiquitin proteasome system dysfunction in neurones to mimic pathological features of neurodegenerative disorders. Results revealed significant increases in ANXA3 in mouse and murine cortical neurones at 12-15 hours post-lactocystin treatment correlating with neuronal injury and onset of neuronal death (Chong et al., 2010). In animal models of cerebral ischemia and motor nerve injury, ANXA3 is unregulated and expressed by microglia after injury identifying it as a novel marker of brain microglial (Junker et al., 2007, Kessler et al., 2008, Konishi et al., 2006). Observed ANXA3 immunoreactivity results confirmed that ANXA3 was produced by activated microglial cells and occasionally located around neurones suggesting its role in the removal of dying neurones after stroke (Kessler et al., 2008).

6.7.1.3 CD44

CD44 is a multifunctional, cell surface glycoprotein that is involved in various cellular processes that include cell growth and adhesion during neurite outgrowth, differentiation, motility, survival, and tumor metastasis (Jones et al., 2000, Matsumoto et al., 2012). CD44; the main receptor for osteopontin and hyaluronan, has been implicated in the inflammatory processes associated with many neuronal injuries, aiding as potential biological markers for disease states, definition of disease severity and CNS metastasis (Matsumoto et al., 2012). *In vitro* experiments using RGCs suggest a novel biological function for CD44 in axon growth and that reduced CD44 expression results in the reduction of axon initiation in RGCs (Ries et al., 2007). Gliomas provide detrimental effects to the CNS, and *in vitro* and *in vivo* experiments

demonstrate that increased CD44 expression in brain tissue containing glioma in mouse models correlate with the progression of the glioma, and thus CD44 may act as a potential biomarker in gliomas (Wiranowska et al., 2006).

CD44 plays an important role in disease severity and progression and patients with neurodegenerative Alzheimer's disease displayed increased CD44 gene expression in lymphocytes compared to healthy controls (Uberti et al., 2010). In mouse models of EAE, CD44 deficient mice displayed a delayed response of onset EAE compared with wild type mice, furthermore improved symptoms, reduced demyelination and impaired CD4+ T-cell extravasation was observed in these mice, suggesting that increased expression of CD44 and other inflammatory markers are responsible for increased severity of EAE (Li et al., 2011a, Winkler et al., 2012, Sinha et al., 2011). Amyotrophic lateral sclerosis (ALS) is a motor neurone degenerative disease and in mouse models of ALS CD44 expression was not only increased with the onset of the disease but also continued to increase thereon after (Matsumoto et al., 2012). Furthermore *in vivo* and *in vitro* experiments demonstrate that CD44 expressing microglial and astrocytes play a role in the inflammatory response and thus the progression of ALS. This phenomenon was also observed after SCI in dogs where increased CD44 expression on microglia further enhanced their function in leukocyte adhesion and aggregation, and therefore contributing to the secondary injury after SCI (Boekhoff et al., 2012). After SCI in rats increased CD44 protein expression was localised to some astrocytes in the periphery lesions, majority of the inflammatory cells, vessels and myelin sheaths in the lesion core compared to sham controls suggesting that CD44 contributes to the early stages after SCI in cell adhesion and glial cell attraction (Moon et al., 2004). CD44 plays a role after injury to

both the CNS and PNS, where injury to the PNS the appearance of CD44 was localised to affected neurones, their dendrites and axons which was also seen after SCI but was abolished after spinal root transection. Non-neuronal CD44 was restricted to the sites of direct injury, confined to monocytes and granulocytes after sciatic nerve injury but after injury to the cerebral cortex immunoreactivity was localised to astrocytes and leukocytes. After optic nerve crush CD44 immunoreactivity was confined to reactive retinal astrocytes and microglia, suggesting that this molecule is important in the brain pathology in response to trauma in roles in the neuronal, glial and leukocytes cells (Jones et al., 2000). Triple negative breast cancer is uncommon and has the ability to spread to the CNS and therefore the identification of CD44+ cells have higher CNS affinity that could result in metastasis (Katakkar, 2012).

CD44 not only shows to play an important role in inflammation but also wound healing. CD44 immunoreactivity coincided with hyaluronan in the early stages of wound healing in rabbit corneal epithelial wound healing and in rat liver injury (Asari et al., 1996, Kikuchi et al., 2005). But wound healing has shown to be age dependant and in which case increases of CD44 plays a detrimental role where it is associated with delayed wound healing in aged skin rat models compared to young rats (Oriana et al., 2013). CD44 deficient mice have shown to improve healing properties after patellar tendon injury model (Ansorge et al., 2009). CD44 is also involved in pathological angiogenesis and is expressed on many cell types including endothelial cells (Pall et al., 2011). But over expression of CD44 can have detrimental effects resulting in metastatic behaviour and aid in the expansion of tumour cells (Gunthert et al., 1991, Kogerman et al., 1997). *In vitro* experiments demonstrate that CD44

expression is induced in endothelial cells cultured with angiogenic growth factors (Griffioen et al., 1997). CD44 deficient mice resulted in inhibited tumour and wound angiogenesis and this impairment may be due to the loss of endothelial CD44, and *in vitro* experiments revealed that the endothelial cells had impaired ability to form tubes although their cell proliferation, survival and wound-induced migration was not affected. These results suggest a role in the stability of endothelial tubular networks during *in vivo* angiogenesis (Cao et al., 2006).

6.7.1.4 H2.0-like homeobox 1 (HLX1)

HLX1 belongs to the H2.0 homeobox family that is located on chromosome 1q41-q42 (Kennedy et al., 1994, Nishimura et al., 1993). The human HLX1 protein shares 85.5% homology to the murine HLX gene, that is also closely linked to the human TGFβ-2 gene (Kennedy et al., 1994, Nishimura et al., 1993). HLX1 is predominately expressed by reproductive tissues and limited immune cells, where it plays a role in embryogenesis and haematopoiesis. *In vitro* experiments demonstrate that HLX1 mRNA and protein is expressed in a trophoblast cell line; HTR-8/SVneo, via hepatocyte growth factor (HGF) and that using a siRNA to HLX1 inhibited responses to HGF treatment, further reducing the growth and invasion capacities of the trophoblast cell line (Liu et al., 2012). These results suggest that HLX1 is an essential downstream signalling component of HGF that leads to the invasiveness and growth of the trophoblast cells.

The effect HLX1 has on the developing CNS has been investigated in zebrafish. Early experiments show that HLX1 is expressed at specific dorsal ventral levels along the hindbrain and spinal cord and loss-of-function (antisense

morpholino oligodendrocytes directed against HLX1) and gain-of-function (blastomeres injected with synthetic HLX1 mRNA) experiments revealed severe defects in brain morphogenesis as a result of abnormal ventricle formation when HLX1 is over-expressed (Fjose et al., 1994). Animals displayed a reduction in the size of forebrain neuronal clusters and axonal path finding. Whilst using HLX1 antisense morpholinos perturbed hindbrain morphogenesis leading to defects in the integrity of the neuroepithelium. Their results suggest various roles for HLX1 during zebrafish morphogenesis (Hjorth et al., 2002).

6.7.1.5 Integrin β2 (ITGβ2)

Integrin β2 (CD18) is part of a large family of integrins that are integral cell surface proteins composed of an alpha chain and a beta chain. These heterodimeric cell adhesion molecules mediate cell-cell and cell-ECM interactions and are involved in many processes that include wound healing, neuroprotection and the inflammatory response after injury (Hynes, 2002). In humans there are 24 different integrin molecules that each contain an extracellular region (containing α and β chains), a transmembrane domain and a cytoplasmic tail (Hynes, 2002, Suzuki and Naitoh, 1990). The beta subunit is divided into two classes; β1 and β2, in which β2 is further subdivided into four isoforms with their expression limited to mainly white blood cells and thus important in the function of leukocytes (Springer, 1990, Noti et al., 2000).

The use of anti-CD11d monoclonal antibody against the subunit of CD11d/CD18 integrin has shown many neuroprotective benefits in the CNS particularly after SCI. Early use of CD11d monoclonal antibody after SCI has shown to reduce neutrophil infiltration and delay the entry of macrophages into the injured

lesion whilst further reducing intraspinal concentration of reactive oxygen and nitrogen species. Furthermore there was evidence of reduced pain, autonomic dysreflexia and improved locomotor performance and tissue preservation (Gris et al., 2004, Bao et al., 2004). Extensive research has been carried out that display similar results after treatment with anti-CD11d monoclonal antibody after SCI where reduction in not only acute inflammation but also oxidative stress and cell death often seen after SCI enhances locomotor recovery and neurological function (Bao et al., 2005, Oatway et al., 2005, Bao et al., 2011). Furthermore microarray analysis on animals treated with anti-CD11d monoclonal antibody compared to controls revealed reduced gene expression of pro-inflammatory cytokines and increased gene expression of inflammatory mediators that promote wound healing and the expression of scar proteins predicted to improve nerve growth (Gris et al., 2009). The use of anit-CD11d monoclonal antibody has also been implemented in other CNS disorders including traumatic brain injury demonstrating the beneficial use in improving functional recovery by reducing inflammation, oxidative activity and tissue damage (Geremia et al., 2012, Bao et al., 2012).

Whilst treatment with CD11d monoclonal antibody has provided beneficial evidence to the possible treatment to SCI, it is very much dependent on the injury model produced. Contradictory to earlier reports that a significant reduction in neurological deficits is seen after treatment in spinal cord ischemia injury models, it was later demonstrated that it is not dependent on neutrophils particularly the CD18 integrin molecules (Clark et al., 1991, Forbes et al., 1994). Furthermore SCI induced by spinal cord clip compression resulted in no significant differences in motor

recovery, myelin preservation and mechanical allodynia in animals that received this treatment compared to controls (Hurtado et al., 2012).

ITGβ2 has demonstrated to play a role in wound healing and patients that suffer from mutations in ITGβ2 results in a condition called leukocyte adhesion deficiency type 1 (LAD1) that results in impaired wound healing and recurrent infections (Parvaneh et al., 2010, van de Vijver et al., 2012). In patients that suffer from SCI, reduced gene expression of CD18 contributes to the delayed wound healing to their pressure ulcers due to the reduced expression, impaired cell-cell interaction and lack of ECM protein expression (Cruse et al., 2002, Cruse et al., 2000).

6.7.1.6 Metallothionein 1H (MT1H)

Metallothioneins (MTs) are intracellular, low molecular weight, metal binding proteins that have a high content of cysteine residues, that was first isolated from horse kidney (Coyle et al., 2002, Han et al., 2013, Cherian et al., 2003, Margoshes and Vallee, 1957). Human MT genes are clustered together on a locus on chromosome 16 q13 and their neuronal receptor; LRP2 (megalin), was first identified in 1997 found on human astrocytes (Stennard et al., 1994, Cherian et al., 2003, Michael et al., 2011, El Refaey et al., 1997). These proteins are transcriptionally regulated due to their unique structural characteristics by heavy metals and glucocorticoids (Coyle et al., 2002). MTs are part of a superfamily of 15 subfamilies involved in various biological processes with four subfamilies present in mammal's; MT1-MT4. MT1 and MT2 have been shown to be involved in zinc homeostasis and provide protection against heavy metal toxicity and oxidative stress, and MT3 and

MT4 expression is mainly confined to neurones and glia, and differentiating stratified squamous epithelial cells, respectively (Carpene et al., 2007, Kagi, 1991, Vasak, 2005, Rigby Duncan and Stillman, 2006, Li et al., 2006). In the CNS MTs are released by astrocytes showing its association with neuroprotection (Michael et al., 2011).

CNS disorders such as bipolar disorder with psychotic features are closely related to schizophrenia and therefore, psychosis is an alternative phenotype. Cross-study analysis of 7 gene expression microarrays that include psychosis and non-psychosis subjects was performed and quantitative PCR validated that MT genes were upregulated that included MT1H in psychosis patients compared to controls (Choi et al., 2008). Early reports show that MT1H is essential for wound repair in the CNS and deficiencies impair neuronal survival (Penkowa et al., 1999). MTs also demonstrate a neuroprotective role in the CNS where whole genome transcriptome analysis showed increased expression of metallothionein genes that include MT1E, MT1F, MT1G, MT1H, MT1M and MT1X and MT2A found in reactive astrocytes and increased expression of its receptor LRP2 in sporadic cases of Parkinson's disease (PD) compared to non-PD controls (Michael et al., 2011). After human SCI MT's including MT1H gene expression was increased at 2 and 5 days post-SCI and protein and immunoreactivity levels were increased at 5 days post-SCI only, indicating these proteins may be early targets for degradation post-SCI (Urso et al., 2007).

6.7.1.7 Retinoic acid receptor beta (RARβ)

Retinoic acid receptor is a member of the thyroid-steroid hormone receptor superfamily of nuclear transcriptional regulators that consist of three members; alpha, beta and gamma (Evans, 1988, Green and Chambon, 1988, Geisen et al., 1997, Mendelsohn et al., 1994). Each of these members has at least two isoforms that are derived from primary transcripts, but in particular RARβ has four isoforms (RARβ1-4) with RARβ2 and 4 being confined to mainly embryonic CNS (Mendelsohn et al., 1994, Mendelsohn et al., 1991). Retinoic acid receptor binds retinoic acid, the biologically active form of vitamin A, to mediate cellular signalling in embryonic morphogenesis, cell growth, differentiation, organogenesis and neuronal development (Wilson et al., 1953, Desai et al., 2006, Bi et al., 2013). Whilst isoform RARβ2 and RARβ4 is modulated by retinoic acid RARβ1 and RARβ3 are not (Mendelsohn et al., 1994, Mendelsohn et al., 1991, Mey and Hammelmann, 2000). The adult CNS including the cerebellum and the cerebral cortex has also been shown to express RARβ2, and outside of the CNS, RARβ gene has been observed and expressed in normal lung tissue (Agudo et al., 2010, Houle et al., 1993)

Early research demonstrates that RARβ, particularly, RARβ2 is an early marker of the developing alimentary tract and the CNS in early embryonic stages in chicken (Smith, 1994). Many reports since state that RARβ plays a critical role in all areas of the CNS, particularly in inducing axonal regeneration and growth in the developing brain, eye and spinal cord (Carter et al., 2011). Loss of RARβ expression restricts axonal regeneration of adult rat RGCs, therefore indicating that there is a crucial period in the developing retina up until which the RGCs start to restrict axonal regrowth (Koriyama et al., 2013). Furthermore, using an inhibitor, trichostatin A, to

histone deacetylase (HDAC) induced axonal regeneration of RGCs via RARβ induction and thus promoted neurite outgrowth (Koriyama et al., 2014). *In vitro* over-expression of RARβ2 in adult rat DRG cultures increases neurite outgrowth, also seen *in vivo*, enabling axons to regenerate across the inhibitory dorsal root entry zone, projecting into the GM of the spinal cord and thus enhancing neuronal activity and significant improvement in sensorimotor tasks (Wong et al., 2006).

It has been demonstrated that not only does retinoic acid signal through RARβ2 to promote neurite outgrowth in the PNS in embryonic and adult DRG but also in the CNS only in mouse embryonic spinal cord, and in contrast, in the adult mouse spinal cord there is no upregulation of RARβ2 by retinoic acid and thus no neurite outgrowth (Corcoran et al., 2002). And that using a virus vector expressing RARβ2 to transduce adult rat or mouse spinal cord, neurite outgrowth occurs. *In vitro* delivery of RARβ2 using a lentiviral vector to dissociated adult cortical neurones resulted in significantly enhanced neurite outgrowth. Furthermore lentiviral-mediated transduction of corticospinal neurones resulted in robust axonal projections in the corticospinal tract of the spinal cord, and thus enhanced regeneration of descending corticospinal tract fibres and further promoting functional recovery (Yip et al., 2006). Inhibited neurite outgrowth is observed in neurones in the cerebellum that are grown in the presence of inhibitory myelin-associated glycoprotein (MAG), and that using a RARβ agonist (CD2019) activates RARβ2 in a dose-dependent manner resulting in neurite outgrowth via signalling through the PI3K pathway, and in a model of SCI RARβ agonist induces axonal outgrowth of descending corticospinal fibres thus promoting functional recovery (Agudo et al., 2010). Further supporting regenerative abilities seen in the PNS and CNS, RARβ also promotes regeneration in the tail of

adult newt using the cloned full-length sub-type RARβ2 (NvRARβ2). NvRARβ2 cDNA was significantly upregulated 2 weeks after amputation of the tail particularly in the rostral cut surface of the cord, and using an inhibitor significantly inhibited ependymal outgrowth and decreased tail regeneration length, further supporting spinal cord regeneration (Carter et al., 2011).

6.7.1.8 Protein kinase C eta (PRKCH)

Protein kinase C (PKC) is part of a mutligene family of serine/threonine-specific protein kinases that are activated by calcium and the second messenger diacyglycerol. PKC family members phosphorylate a wide variety of protein targets that are known to be involved in the diverse cellular signalling pathways including growth factor-dependent signalling (Steinberg, 2008). PKC isoforms share specific structural features; catalytic domain for ATP binding and catalysis and a regulatory domain containing a NH_2 domain that maintains the inactive protein conformation. PRKCH is located on human chromosome 14 (14q22-23) whilst in mice it is located on chromosome 12 (12C3-D2), and is highly expressed in epithelial tissues by specific activation from sulphated metabolites of cholesterol and cerebroside and cholesterol sulphate. It has been shown that over expression of PRKCH induces G1 arrest and differentiation in keratinocytes and that PRKCH-knockout mice are more sensitive to carcinogenesis suggesting that PRKCH is negatively involved in tumour promotion via keratinocyte differentiation (Kashiwagi et al., 2002).

PRKCH has been considered as a therapeutic target for the management of glioblastoma multiforme (GBM); primary CNS tumours that are currently resistant to chemotherapy/radiation methods, as PRKCH not only increases cell proliferation but

is also resistant to radiation in GBM cell lines (Martin and Hussaini, 2005). SNPs in PRKCH have also been shown to play a role in the pathogenesis of multiple sclerosis relapse via vitamin D expression (Lin et al., 2014). Over expression of atypical kinases such as PRKCH is sufficient to inhibit neurite growth in embryonic rat hippocampal neurones (Buchser et al., 2010).

PRKCH also plays a role in wound healing and tumour suppression using a PRKCH-deficient mouse model. The PRKCH-deficient mice exhibited increased susceptibility to tumor formation in skin carcinogenesis and after a punch biopsy wound healing on the dorsal surface was significantly delayed, indicating that PRKCH plays a role in the maintenance of epithelial architecture and thus wound healing *in vivo* (Chida et al., 2003).

6.7.1.9 Transforming growth factor beta type 1 receptor (TGFβR1)

As previously mentioned, the largest family of secreted growth factors in mammals is the TGFβ family. TGFβ bind to their type 1 and 2 receptors to produce a receptor complex and activate SMAD proteins to initiate signal transduction pathways (Chapter 3 Introduction and Figure 3.2) (Li et al., 2011b). TGFβR1 is one of seven type 1 receptors for TGFβ ligand (Massague, 1992, Massague, 1998). Heterozygous mutations in TGFBR1 and 2 causes Loeys-Dietz syndrome, which is an autosomal dominant aortic aneurysm syndrome with widespread systemic involvement (Loeys et al., 2006).

TGFβR1 has been shown to play a role in the CNS in an angiogenic dependant manner where outgrowth endothelial cells (OECs) from ischemic stroke patients in the colony stage rather than mature stage presented over expression of

TGFβR1 along with other angiogenic genes thus confirming that OECs demonstrate a higher level of pro-angiogenic factors at early stages of ischemic stroke (Navarro-Sobrino et al., 2013). TGFβR1 has been shown to play a role in regenerative wound healing in mouse ear punch models, where a point mutation on TGFβR1 lead to a 3-fold decrease in the diameter of the wound compared to wild-type mice (Liu et al., 2011). Contradictory to this earlier report that TGFβR1 may be beneficial in aiding in wound healing, it has further been shown that using Moxifloxacin blocked TGFβR1 and thus inhibited TGFβ-induced fibroblast to myofibroblast differentiation and thus may participate in corneal wound healing (Chen et al., 2013).

In conclusion, these data demonstrates the vast amount of differences that mice and rats exhibit during the sub-acute SCI response and the large amount of genes that play a part in the healing response. These genes and pathways could provide possible insights into the post-injury mechanisms associated with SCI and therefore could be used to establish possible therapies to reduce cavitation and thus secondary damage.

CHAPTER 7

GENERAL DISCUSSION

7.1 Summary research findings

The research presented in this thesis demonstrates that mice and rats display unique differences that may contribute to lesion cavity development that is normally observed in rats after sub-acute SCI. This therefore provides crucial evidence that may aid in potential therapeutic treatments for clinical situations. Parallel to current research, the extent of cavitation to the injured rat cord increases over time compared to mice (Inman and Steward, 2003, Sroga et al., 2003, Byrnes et al., 2010). In rats the fluid-filled cavity expands both rostrally and caudally from the lesion epicentre, however in mice the lesion areas are completely filled with ECM and thus free from cavities, a scenario which has been shown to aid in axon regeneration in the PNS (Previtali et al., 2008). Furthermore, a correlation was observed between the extent of cavity formation and the lack of laminin deposition over time. In mice after injury laminin deposition increased over time, however, in rats laminin deposition was devoid in the lesion areas and confined only to the boundaries of the cavity. This time course revealed that the biggest difference in cavity formation and laminin deposition between the two species was observed at 8 dpl. Sub-acute injury responses in mice also revealed an increase in $GFAP^+$ astrocytes and $fibronectin^+$ ECM material in the lesion core however this was not seen in rats indicating that mice have a better balance of scar deposition after SCI. This led to the hypothesis that the cavity free response seen in mice is due to an increase in angiogenesis and a better balance of scar deposition and thus mice may be conducive to wound healing after SCI. There is evidence that demonstrates a link between wound healing and functional recovery after SCI, particularly the presence of MMP-2 after injury (Hsu et al., 2006). MMP-2 not only facilitated the wound healing process but it also regulated the formation of

the glial scar and white matter sparing and thus promoted functional recovery in mice.

A range of pro-angiogenic/wound healing-related proteins were tested on mouse and rat spinal cord lesions at 8 dpl. In this manner pro-angiogenic/wound healing-related proteins such as VEGF-A, TGFβ-2, PDGF-BB, FGF2, angiogenin, angiopoietin-1, MMP-1, MMP-9 localisation and protein expression were all significantly increased in mice lesion areas compared to rats. Whilst anti-angiogenic/wound healing-related proteins such as TIMP-2 and semaphorin 3A were significantly higher in rats compared to mice, further supporting the hypothesis that the absence of cavity development in mice is due to the adequate balance of angiogenesis, wound healing and scar deposition. Differences were also observed in axonal sparing between mice and rats, demonstrating that at 8 dpl after sub-acute SCI there was a greater reduction of axonal sparing in rats compared to mice, suggesting that cavitation is detrimental to axon integrity. One would expect these results to coincide with better functional recovery in mice compared to rats after SCI. However, our results show that the presence of a large cavity in rats had no effect on mechanical allodynia but thermal allodynia was affected in both mice and rats immediately after injury, recovering to normal levels within 7 dpl demonstrating acute and transient functional deficits. Whilst our injury damages all axons within the dorsal funiculi, previous research demonstrates that behavioural deficits correlate strongly with injury depth and therefore more overt injury models are required to demonstrate functional deficits after SCI (Hill et al., 2009).

Since prior studies demonstrate that mice and rats exhibit differential inflammatory responses after SCI, the aim here was to investigate if induced

inflammation immediately after injury using zymosan would induce cavity formation in mice similar to that seen in rats after injury. Increased accumulation of micro-cavities was observed in mice and rats in those treated with zymosan compared to PBS injected controls (Sroga et al., 2003, Byrnes et al., 2010). After induced inflammation differences were observed in the inflammatory responses between mice and rats. There was no difference in the microglia response in the lesion site in mice compared to rats, however, the levels of macrophages and resident T-cells were significantly increased in rats compared to mice after zymosan injection compared to control PBS. The DC scarring response demonstrated that there was an increase in fibronectin^{+} ECM after induced inflammation in rats compared to mice and their representative PBS controls. Whilst increases were observed in angiogenic VEGF-A in mice compared to rats, MMP-1 and laminin were significantly higher in rats compared to mice, and anti-angiogenic semaphorin 3a was significantly higher in mice compared to rats after zymosan injection. Chronic inflammation results in areas of hypoxia that can cause inflammatory mediators to either directly or indirectly promote angiogenesis further contributing to prolonged inflammation, and in a model of neurodegeneration, angiogenesis induced CNS inflammation promoted neuronal remodelling (Jackson et al., 1997, Arroyo and Iruela-Arispe, 2010, Muramatsu et al., 2012). This may suggest that in rats chronic inflammation promotes angiogenesis and aims to undergo neuronal remodelling in an attempt to preserve axonal damage- a function that is disabled and results in cavitation in response to induced inflammation after sub-acute SCI.

In response to the significant difference seen between mice and rats after T8 sub-acute SCI at 8 dpl microarray analysis was carried out to assess the genome

wide response in known angiogenic/wound healing-related genes and the possibility of unknown, novel genes that may be significantly up or down regulated after SCI. This may reveal clues to the reasons why rat's cavitate and mice do not. Stringent analysis using multiclass analysis revealed 1090 genes in mice and 1616 genes in rats that were deemed as significantly expressed after SCI. IPA analysis on these values revealed that in mice and rats 562 and 689 genes, respectively, were unique whilst 874 and 721 genes, respectively, were mapped and differentially regulated whilst 388 and 98 genes, respectively, were un mapped after SCI. Known canonical pathways were used to assess IL8 mediated regulation of angiogenesis and tumour growth, NGF signalling for neurite outgrowth and differentiation, PDGF signalling for cell proliferation and survival and VEGF signalling for hypoxia and angiogenesis pathways that showed significant differences between mice and rats after SCI. Known angiogenic/wound healing-related genes that were either 2-fold up or down regulated after sub-acute SCI at 8 dpl were extracted from the raw data sets, and of those 9 genes (alpha-2-adrenergic receptor beta, annexin A3, CD44, HLX-1, integrin beta 2, metallothionein 1H, protein kinase C-eta, retinoic acid receptor beta and transforming growth factor beta receptor 1) were chosen to be validated by qPCR. Whilst alpha-2-adrenergic receptor beta, annexin A3, CD44, metallothionein 1H, protein kinase C-eta and retinoic acid receptor beta gene expression was increased in injured mouse compared to other treatment groups, HLX-1 gene expression was reduced in injured rat compared to other treatment and integrin beta 2 and transforming growth factor beta receptor 1 gene expression was increased in injured rat compared to other treatment groups only annexin A3, CD44 and metallothionein 1H showed overall significance.

Whilst microarray analysis provides average gene expression in the samples, biological variation is not accounted for therefore causing huge variation in the gene expression data. Each injured sample was compared to its relative control sample indicating that there was huge variation in HLX-1, integrin beta 2 and transforming growth factor beta receptor 1 in both species, whilst metallothionein 1H and protein kinase C-eta in rat and mouse, respectively. The top 20 and bottom genes expressed in both mouse and rat was analysed to determine if genes were expressed on the same level. In this manner Gpnmb, Serpina3n, Ccl3 and cd68 genes were in the top 20 genes that were highly expressed in the treated samples compared to control in both species. However, there were no genes that were in the bottom 20 that were common in both species. This large amount of data demonstrates that there is a large amount of genes that play a part in the healing response in mice and rats after SCI, and could be used to establish possible mechanisms to reduce cavitation and therefore secondary damage that human experience.

7.2 Advantages / disadvantages associated with the current model

In hind sight it is quite difficult to mimic clinical human SCI using animal models as the anatomical location of injury differs greatly between the two (Kundi et al., 2013). In clinical situations humans present with SCI at the cervical region but to mimic that in an experimental model could lead to potential life threatening complications to the animals and therefore SCI at the thoracic level is more commonly used (Akhtar et al., 2008). The use of laminectomy and anaesthesia also contributes largely to experimental SCI not mimicking the clinical injury presented by humans. Both of these factors can have a major impact and alter the physiological

responses to injury and therefore using a laminectomy free method such as balloon compression may mimic the human condition more accurately (Kundi et al., 2013).

Rodents and humans differ considerably in size which is factor that should be taken into consideration particularly when investigating axon regeneration as several millimetres are sufficient enough to induce functional recovery in rodents. However, in humans distances of many centimetres may be required (Nout et al., 2012). This difference in scale posses as a significant issue particularly when investigating surgically applied therapies and feasibility. Another factor to take into consideration is the difference in functional roles of axon systems between rodents and humans and a fine example of this is the corticospinal tract (CST) (Nout et al., 2012). In humans the CST is essential for fine motor control but not so essential in rats (Courtine et al., 2007, Lawrence and Kuypers, 1968, Lemon and Griffiths, 2005).

It is important to remember that while the injury induced in this study is a mild form that gives little insight to the functional recovery after injury, it still provides the pathological and physiological changes that are associated and observed after SCI.

7.3 Advances made in SCI research

Since investigating the angiogenic and lesion cavity responses between mice and rats after sub-acute SCI there has been limited, ongoing research to investigate other possible mechanisms that may be affected and differential between the two species. Platelet-derived growth factor (PDGF)-responsive neural precursors (PRP) isolated from the forebrain of fetal mice has been used to test the potential of remyelinating axons after injury (Plemel et al., 2011). PRPs transplanted 1 week after T8 spinal cord contusion in rats developed the typical phenotype of mature

oligodendrocytes 2 weeks post-transplantation, expressing the oligodendrocyte marker APC-CC1. These cells also had close association with myelin basic protein indicating mature myelin sheath formation. Furthermore transplantation of the PRPs in demyelinated Shiver mice confirmed the ability of the PRPs to produce myelin sheaths suggesting it as a novel candidate in CNS repair.

Sigma-1 receptors, localised in the nervous system, play an essential role in pain sensitisation. Recent studies show that increases in sigma-1 receptor mediates increases in spinal p38 MAPK phosphorylation that causes the induction of mechanical allodynia in mice and neuropathic pain in rats but not thermal hyperalgesia (Moon et al., 2013). More importantly sigma-1 receptor modulation of phosphorylated p38 MAPK plays an important role in the induction but not the maintenance of mechanical allodynia in neuropathic pain. Furthermore, in a rat model of neuropathic pain in the sciatic nerve, mechanical allodynia and thermal hyperalgesia was evaluated in mice and rats. Results demonstrated that spinal sigma-1 receptors modulate NAPDH oxidase 2 activation and reactive oxygen species (ROS) production in the spinal cord, contributing ultimately to sigma-1 receptor-induced pain hypersensitivity in mice and mechanical allodynia in neuropathic rats (Choi et al., 2013).

The Wnt family of proteins plays a vital role during CNS development and therefore is involved in many neurological pathologies including SCI. A recent study has demonstrated that Wnt expression in the spinal cord of adult mice is modulated by SCI and differs to previous findings described in rats (Gonzalez-Fernandez et al., 2014). These studies demonstrate that mice and rats exhibit differential responses

and mechanisms to SCI that include remyelination, neuropathic pain and Wnt signalling and could contribute to secondary damage seen after injury.

7.4 Conclusion

In conclusion, differences do exist between mice and rats in cavity formation, matrix deposition and pro-angiogenic protein levels after DC injury, indicating that mice have a more robust angiogenic and wound healing response to SCI that is associated with an absence of cavitation and axon sparing, despite acute deficits in functional recovery in mice and rats. Our results support the hypothesis that the absence of cavitation in mice is due to an adequate balance between angiogenesis, wound healing and scar deposition compared to rats which fail to lay down ECM after sub-acute SCI and thus display large cavities. These key differences between the wound healing responses in mice compared to rats warrant further investigation.

7.5 Future work

Whilst key differences have been established in the sub-acute response to SCI between mice and rats further work needs to be carried out to optimise the mechanisms that are responsible for cavitation and ultimately axonal degeneration. While advances in sub-acute SCI research have been made the aim for clinical trials is still a long way off.

7.5.1 In vitro astrocyte culture

Rat or human astrocyte cultures can be used to asses wound healing properties particularly in the CNS with an aim to assess cavitation (Fitch et al., 1999, Souza et

al., 2013). The idea would be to grow confluent adult rat astrocytes to coincide with the adult data already obtained. Once cultures are confluent a vertical scratch would be made in each of the wells and the amount of wound closure would be observed by taking pictures at 0, 24, 48 and 72 hrs (time points suggested in previous astrocyte culture studies (Yang et al., 2009, Puschmann et al., 2010, Nishio et al., 2005). The aim of using adult astrocytes would be to:

1. To assess typical wound closure after injury in a controlled environment.
2. To assess the wound closure and cavity development in the CNS after induced inflammation using zymosan compared to controls.

The idea would be to further analyse whether the in vitro studies resemble what was seen in vivo i.e. an accumulation of microcavities in response to induced inflammation after SCI.

7.5.2 In vitro knockdown/over expression

Rat or human astrocyte or endothelial cell cultures using HUVECs (human umbilical vein endothelial cells) could further be used for knockdown or over expression assays particularly to assess the angiogenic/wound healing abilities and cavity development. The microarray data revealed angiogenic/wound healing-related genes that were either significantly upregulated or downregulated after sub-acute SCI and the idea would be to pick 2-4 identified genes that were differentially regulated between mice and rats. To knockdown gene expression in culture would require the use of a siRNA to that particular gene. The idea would be to further validate the function of these genes and whether they truly play a role in angiogenesis/wound healing and more importantly cavitation and neurite outgrowth.

7.5.3 In vivo gel based therapeutics

The angiogenic process requires the activation of various angiogenic genes and therefore a combination of angiogenic/wound healing-related genes would be beneficial for gel based therapeutics to achieve maximal axon regeneration through the lesion cavity. In the Logan lab a collagen based gel has been produced and preliminary results have shown that once injected in to the injured area immediately after SCI in rats promotes axon regeneration in combination with Decorin; an anti-scarring proteoglycan. The aim would be to use 2-3 angiogenic proteins identified from microarray analysis that are ultimately involved in various stages of the angiogenic process in combination with this gel and inject it directly into the lesion area of rats and compare any possible axonal regeneration across the lesioned area and assess reduction in cavity formation in rats compared to mice.

7.5.4 Anti-viral work

Viral vectors are a method of gene based delivery that allows DNA or a drug to be delivered to a specified cell. The idea would be to prepare viral gene constructs preparation against 2-4 genes angiogenic/wound healing-related genes to reduce cavity formation in rats

References

ABDUL-MUNEER, P. M., SCHUETZ, H., WANG, F., SKOTAK, M., JONES, J., GORANTLA, S., ZIMMERMAN, M. C., CHANDRA, N. & HAORAH, J. 2013. Induction of oxidative and nitrosative damage leads to cerebrovascular inflammation in an animal model of mild traumatic brain injury induced by primary blast. *Free radical biology & medicine,* 60, 282-91.

ABRAHAM, J. A., MERGIA, A., WHANG, J. L., TUMOLO, A., FRIEDMAN, J., HJERRILD, K. A., GOSPODAROWICZ, D. & FIDDES, J. C. 1986a. Nucleotide sequence of a bovine clone encoding the angiogenic protein, basic fibroblast growth factor. *Science,* 233**,** 545-8.

ABRAHAM, J. A., WHANG, J. L., TUMOLO, A., MERGIA, A. & FIDDES, J. C. 1986b. Human basic fibroblast growth factor: nucleotide sequence, genomic organization, and expression in mammalian cells. *Cold Spring Harbor symposia on quantitative biology,* 51 Pt 1**,** 657-68.

ABRAMSSON, A., LINDBLOM, P. & BETSHOLTZ, C. 2003. Endothelial and nonendothelial sources of PDGF-B regulate pericyte recruitment and influence vascular pattern formation in tumors. *The Journal of clinical investigation,* 112**,** 1142-51.

ACEVEDO, L. M., BARILLAS, S., WEIS, S. M., GOTHERT, J. R. & CHERESH, D. A. 2008. Semaphorin 3A suppresses VEGF-mediated angiogenesis yet acts as a vascular permeability factor. *Blood,* 111**,** 2674-80.

ACKER, T., BECK, H. & PLATE, K. H. 2001. Cell type specific expression of vascular endothelial growth factor and angiopoietin-1 and -2 suggests an important role of astrocytes in cerebellar vascularization. *Mechanisms of development,* 108**,** 45-57.

ADAMKIEWICZ, A. A. 1882. Die Blutgefasse der menschlichen. 85**,** 29.

ADAMS, R. H. & ALITALO, K. 2007. Molecular regulation of angiogenesis and lymphangiogenesis. *Nature reviews. Molecular cell biology,* 8**,** 464-78.

AGUDO, M., YIP, P., DAVIES, M., BRADBURY, E., DOHERTY, P., MCMAHON, S., MADEN, M. & CORCORAN, J. P. 2010. A retinoic acid receptor beta agonist (CD2019) overcomes inhibition of axonal outgrowth via phosphoinositide 3-kinase signalling in the injured adult spinal cord. *Neurobiology of disease,* 37**,** 147-55.

AHMED, Z., BANSAL, D., TIZZARD, K., SUREY, S., ESMAEILI, M., GONZALEZ, A. M., BERRY, M. & LOGAN, A. 2014. Decorin blocks scarring and cystic cavitation in acute and induces scar dissolution in chronic spinal cord wounds. *Neurobiology of disease*. 64**,** 163-76.

AHMED, Z., READ, M. L., BERRY, M. & LOGAN, A. 2010. Satellite glia not DRG neurons constitutively activate EGFR but EGFR inactivation is not correlated with axon regeneration. *Neurobiology of disease*. 39**,** 292-300.

AHMED, Z. & BICKNELL, R. 2009. Angiogenic signalling pathways. *Methods in molecular biology,* 467**,** 3-24.

AIGNER, L. & BOGDAHN, U. 2008. TGF-beta in neural stem cells and in tumors of the central nervous system. *Cell and tissue research,* 331**,** 225-41.

AKHTAR, A. Z., PIPPIN, J. J. & SANDUSKY, C. B. 2008. Animal models in spinal cord injury: a review. *Reviews in the neurosciences,* 19**,** 47-60.

AKIYAMA, C., YUGUCHI, T., NISHIO, M., TOMISHIMA, T., FUJINAKA, T., TANIGUCHI, M., NAKAJIMA, Y., KOHMURA, E. & YOSHIMINE, T. 2004. Src

family kinase inhibitor PP1 reduces secondary damage after spinal cord compression in rats. *Journal of neurotrauma,* 21**,** 923-31.
AKUTHOTA, V., LENTO, P. & SOWA, G. 2003. Pathogenesis of lumbar spinal stenosis pain: why does an asymptomatic stenotic patient flare? *Physical medicine and rehabilitation clinics of North America,* 14**,** 17-28, v.
ALBERTS, B., JONHSON, A., LEWIS, J. & AL, E. 2002. Molecular biology of the cell. 4th edition. Helper T Cells and Lymphocyte Activation. *New York: Garland Science*.
ALLEN, A.R. 1911. Surgery of experimental lesion of spinal cord equivalent to crush injury of fracture dislocation of spinal column: A preliminary report. *Journal of American Medical Association,* 57.
ALLUIN, O., KARIMI-ABDOLREZAEE, S., DELIVET-MONGRAIN, H., LEBLOND, H., FEHLINGS, M. G. & ROSSIGNOL, S. 2011. Kinematic study of locomotor recovery after spinal cord clip compression injury in rats. *Journal of neurotrauma,* 28**,** 1963-81.
American Association of Spinal Cord Injury. 2004. Nurses standards of practice--revised 2003-2004. *SCI nursing : a publication of the American Association of Spinal Cord Injury Nurses,* 21**,** 228-32.
ANDRAE, J., GALLINI, R. & BETSHOLTZ, C. 2008. Role of platelet-derived growth factors in physiology and medicine. *Genes & development,* 22**,** 1276-312.
ANGHELESCU, N., PETRESCU, A. & ALEXANDRESCU, I. 1995. Thepay study on the experimental injury of spinal cord. IV. High doses of methyl-prednisolone. *Romanian journal of neurology and psychiatry*. 33, 241-249.
ANIK, I., KOKTURK, S., GENC, H., CABUK, B., KOC, K., YAVUZ, S., CEYLAN, S., CEYLAN, S., KAMACI, L. & ANIK, Y. 2011a. Immunohistochemical analysis of TIMP-2 and collagen types I and IV in experimental spinal cord ischemia-reperfusion injury in rats. *The journal of spinal cord medicine,* 34**,** 257-64.
ANIK, I., KOKTURK, S., GENC, H., CABUK, B., KOC, K., YAVUZ, S., CEYLAN, S., KAMACI, L. & ANIK, Y. 2011b. Immunohistochemical analysis of TIMP-2 and collagen types I and IV in experimental spinal cord ischemia-reperfusion injury in rats. *The journal of spinal cord medicine,* 34**,** 257-64.
ANSORGE, H. L., BEREDJIKLIAN, P. K. & SOSLOWSKY, L. J. 2009. CD44 deficiency improves healing tendon mechanics and increases matrix and cytokine expression in a mouse patellar tendon injury model. *Journal of orthopaedic research : official publication of the Orthopaedic Research Society,* 27**,** 1386-91.
ARIS-BROSOU, S., CHEN, X., PERRY, S. F. & MOON, T. W. 2009. Timing of the functional diversification of alpha- and beta-adrenoceptors in fish and other vertebrates. *Annals of the New York Academy of Sciences,* 1163**,** 343-7.
ARROYO, A. G. & IRUELA-ARISPE, M. L. 2010. Extracellular matrix, inflammation, and the angiogenic response. *Cardiovascular research,* 86, 226-35.
ASARI, A., MORITA, M., SEKIGUCHI, T., OKAMURA, K., HORIE, K. & MIYAUCHI, S. 1996. Hyaluronan, CD44 and fibronectin in rabbit corneal epithelial wound healing. *Japanese journal of ophthalmology,* 40**,** 18-25.
ATKINS, C. M., CEPERO, M. L., KANG, Y., LIEBL, D. J. & DIETRICH, W. D. 2013. Effects of early rolipram treatment on histopathological outcome after controlled cortical impact injury in mice. *Neuroscience letters,* 532, 1-6.
AUSTIN, J. W., AFSHAR, M. & FEHLINGS, M. G. 2012. The relationship between localized subarachnoid inflammation and parenchymal pathophysiology after spinal cord injury. *Journal of neurotrauma,* 29**,** 1838-49.

BAFFERT, F., LE, T., THURSTON, G. & MCDONALD, D. M. 2006. Angiopoietin-1 decreases plasma leakage by reducing number and size of endothelial gaps in venules. *American Journal of Physiology-Heart and Circulatory Physiology,* 290**,** H107-H118.

BAFFOUR, R., ACHANTA, K., KAUFMAN, J., BERMAN, J., GARB, J. L., RHEE, S. & FRIEDMANN, P. 1995. Synergistic effect of basic fibroblast growth factor and methylprednisolone on neurological function after experimental spinal cord injury. *Journal of neurosurgery,* 83**,** 105-10.

BALAZY, T. E. 1992. Clinical management of chronic pain in spinal cord injury. *The Clinical journal of pain,* 8**,** 102-10.

BALIKI, M., et al., 2005. Spared nerve injury rats exhibit thermal hyperalgesia on an automated operant dynamic thermal escape task. *Molecular pain*. 1**,** 18.

BALLAGI, A. E., ODIN, P., ORTHBERG-CEDERSTROM, A., SMITS, A., DUAN, W. M., LINDVALL, O. & FUNA, K. 1994. Platelet-dervived growth factor receptor expression after neural grafting in a rat model of Parkinson's disease. *Cell Transplantation,* 3, 453-460.

BAO, F., BROWN, A., DEKABAN, G. A., OMANA, V. & WEAVER, L. C. 2011. CD11d integrin blockade reduces the systemic inflammatory response syndrome after spinal cord injury. *Experimental neurology,* 231**,** 272-83.

BAO, F., CHEN, Y., DEKABAN, G. A. & WEAVER, L. C. 2004. Early anti-inflammatory treatment reduces lipid peroxidation and protein nitration after spinal cord injury in rats. *Journal of neurochemistry,* 88**,** 1335-44.

BAO, F., DEKABAN, G. A. & WEAVER, L. C. 2005. Anti-CD11d antibody treatment reduces free radical formation and cell death in the injured spinal cord of rats. *Journal of neurochemistry,* 94**,** 1361-73.

BAO, F., SHULTZ, S. R., HEPBURN, J. D., OMANA, V., WEAVER, L. C., CAIN, D. P. & BROWN, A. 2012. A CD11d monoclonal antibody treatment reduces tissue injury and improves neurological outcome after fluid percussion brain injury in rats. *Journal of neurotrauma,* 29**,** 2375-92.

BARRITT, A. W., DAVIES, M., MARCHAND, F., HARTLEY, R., GRIST, J., YIP, P., MCMAHON, S. B. & BRADBURY, E. J. 2006. Chondroitinase ABC promotes sprouting of intact and injured spinal systems after spinal cord injury. *The Journal of neuroscience : the official journal of the Society for Neuroscience,* 26**,** 10856-67.

BARTHOLDI, D., RUBIN, B. P. & SCHWAB, M. E. 1997. VEGF mRNA induction correlates with changes in the vascular architecture upon spinal cord damage in the rat. *The European journal of neuroscience,* 9**,** 2549-60.

BATTEGAY, E. J., RUPP, J., IRUELA-ARISPE, L., SAGE, E. H. & PECH, M. 1994. PDGF-BB modulates endothelial proliferation and angiogenesis in vitro via PDGF beta-receptors. *The Journal of cell biology,* 125**,** 917-28.

BASSO, D. M., BEATTIE, M. S. & BRESNAHAN, J. C. 1995. A sensitive and reliable locomotor rating scale for open field testing in rats. *Journal of neurotrauma,* 12**,** 1-21.

BASSO, D. M., BEATTIE, M. S., BRESNAHAN, J. C., ANDERSON, D. K., FADEN, A. I., GRUNER, J. A., HOLFORD, T. R., HSU, C. Y., NOBLE, L. J., NOCKELS, R., PEROT, P. L., SALZMAN, S. K. & YOUNG, W. 1996. MASCIS evaluation of open field locomotor scores: effects of experience and teamwork on reliability. Multicenter Animal Spinal Cord Injury Study. *Journal of neurotrauma,* 13**,** 343-59.

BAWA-KHALFE, T., ALTEMEMI, G. F., MANDYAM, C. D., SCHWARZ, L. A., EIKENBURG, D. C. & STANDIFER, K. M. 2007. The presence of beta2-adrenoceptors sensitizes alpha2A-adrenoceptors to desensitization after chronic epinephrine treatment. *BMC pharmacology,* 7**,** 16.

BEERS, M. H. & PORTER, R. S. 2006. *The Merck Manual of Diagnosis and Therapy 18th Edition*, Wiley and Sons.

BEHRMANN, D. L., BRESNAHAN, J. C. & BEATTIE, M. S. 1993. A comparison of YM-14673, U-50488H, and nalmefene after spinal cord injury in the rat. *Experimental neurology,* 119**,** 258-67.

BENTON, R. L., MADDIE, M. A., GRUENTHAL, M. J., HAGG, T. & WHITTEMORE, S. R. 2009. Neutralizing endogenous VEGF following traumatic spinal cord injury modulates microvascular plasticity but not tissue sparing or functional recovery. *Current neurovascular research,* 6**,** 124-31.

BENTON, R. L., MADDIE, M. A., MINNILLO, D. R., HAGG, T. & WHITTEMORE, S. R. 2008. Griffonia simplicifolia isolectin B4 identifies a specific subpopulation of angiogenic blood vessels following contusive spinal cord injury in the adult mouse. *The Journal of comparative neurology,* 507**,** 1031-52.

BENTON, R. L., MADDIE, M. A., WORTH, C. A., MAHONEY, E. T., HAGG, T. & WHITTEMORE, S. R. 2008. Transcriptomic screening of microvascular endothelial cells implicates novel molecular regulators of vascular dysfunction after spinal cord injury. *Journal of cerebral blood flow and metabolism : official journal of the International Society of Cerebral Blood Flow and Metabolism,* 28**,** 1771-85.

BENTON, R. L. & WHITTEMORE, S. R. 2003. VEGF165 therapy exacerbates secondary damage following spinal cord injury. *Neurochemical research,* 28**,** 1693-703.

BERANEK, J. T. 2005. CD68 is not a macrophage-specific antigen. *Annals of the rheumatic diseases,* 64, 342-3; author reply 343-4.

BERENS, S. A., COLVIN, D. C., YU, C. G., YEZIERSKI, R. P. & MARECI, T. H. 2005. Evaluation of the pathologic characteristics of excitotoxic spinal cord injury with MR imaging. *AJNR. American journal of neuroradiology,* 26**,** 1612-22.

BERGER, J. V., KNAEPEN, L., JANSSEN, S. P., JAKEN, R. J., MARCUS, M. A., JOOSTEN, E. A. & DEUMENS, R. 2011. Cellular and molecular insights into neuropathy-induced pain hypersensitivity for mechanism-based treatment approaches. *Brain research reviews,* 67**,** 282-310.

BERGERON, M., GIDDAY, J. M., YU, A. Y., SEMENZA, G. L., FERRIERO, D. M. & SHARP, F. R. 2000. Role of hypoxia-inducible factor-1 in hypoxia-induced ischemic tolerance in neonatal rat brain. *Annals of neurology,* 48**,** 285-96.

BERGERON, M., YU, A. Y., SOLWAY, K. E., SEMENZA, G. L. & SHARP, F. R. 1999. Induction of hypoxia-inducible factor-1 (HIF-1) and its target genes following focal ischaemia in rat brain. *The European journal of neuroscience,* 11**,** 4159-70.

BERNHARD, M., GRIES, A., KREMER, P. & BOTTIGER, B. W. 2005. Spinal cord injury (SCI)--prehospital management. *Resuscitation,* 66**,** 127-39.

BERNINI, G. P., MORETTI, A., BONADIO, A. G., MENICAGLI, M., VIACAVA, P., NACCARATO, A. G., IACCONI, P., MICCOLI, P. & SALVETTI, A. 2002. Angiogenesis in human normal and pathologic adrenal cortex. *The Journal of clinical endocrinology and metabolism,* 87**,** 4961-5.

BERRY, M., AHMED, Z., LORBER, B., DOUGLAS, M. & LOGAN, A. 2008. Regeneration of axons in the visual system. *Restorative neurology and neuroscience,* 26**,** 147-74.
BETHEA, J. R., CASTRO, M., KEANE, R. W., LEE, T. T., DIETRICH, W. D. & YEZIERSKI, R. P. 1998. Traumatic spinal cord injury induces nuclear factor-kappaB activation. *The Journal of neuroscience : the official journal of the Society for Neuroscience,* 18**,** 3251-60.
BHATOE, H. S. 2009. Posttraumatic Syringomyelia. *Indian Journal of Neurotrauma,* 6.
BI, Y., GONG, M., HE, Y., WEI, X., CHEN, J. & LI, T. 2013. Adenovirus-mediated RAR-beta over-expression enhances ATRA-induced neuronal differentiation of rat mesenchymal stem cells. *Archives of medical science : AMS,* 9**,** 314-22.
BIDDISON, W. E., TAUB, D. D., CRUIKSHANK, W. W., CENTER, D. M., CONNOR, E. W. & HONMA, K. 1997. Chemokine and matrix metalloproteinase secretion by myelin proteolipid protein-specific CD8+ T cells: potential roles in inflammation. *Journal of immunology (Baltimore, Md : 1950),* 158**,** 3046-53.
BILGEN, M., AL-HAFEZ, B., ALREFAE, T., HE, Y. Y., SMIRNOVA, I. V., ALDUR, M. M. & FESTOFF, B. W. 2007. Longitudinal magnetic resonance imaging of spinal cord injury in mouse: changes in signal patterns associated with the inflammatory response. *Magnetic resonance imaging,* 25**,** 657-64.
BIRKEDAL-HANSEN, H., MOORE, W. G., BODDEN, M. K., WINDSOR, L. J., BIRKEDAL-HANSEN, B., DECARLO, A. & ENGLER, J. A. 1993. Matrix metalloproteinases: a review. *Critical reviews in oral biology and medicine : an official publication of the American Association of Oral Biologists,* 4**,** 197-250.
BIYANI, A. & EL MASRY, W. S. 1994. Post-traumatic syringomyelia: a review of the literature. *Paraplegia,* 32**,** 723-31.
BLIGHT, A. R. 2000. Animal Models Of Spinal Cord Injury. 6**,** 13.
BLIGHT, A. R. 1994. Effects of silica on the outcome from experimental spinal cord injury: implication of macrophages in secondary tissue damage. *Neuroscience,* 60**,** 263-73.
BLIGHT, A. R. 1992. Macrophages and inflammatory damage in spinal cord injury. *Journal of neurotrauma,* 9 Suppl 1**,** S83-91.
BLIGHT, A. R., COHEN, T. I., SAITO, K. & HEYES, M. P. 1995. Quinolinic acid accumulation and functional deficits following experimental spinal cord injury. *Brain : a journal of neurology,* 118 (Pt 3)**,** 735-52.
BOEKHOFF, T. M., ENSINGER, E. M., CARLSON, R., BOCK, P., BAUMGARTNER, W., ROHN, K., TIPOLD, A. & STEIN, V. M. 2012. Microglial contribution to secondary injury evaluated in a large animal model of human spinal cord trauma. *Journal of neurotrauma,* 29**,** 1000-11.
BOILLÉE, S., VELDE, C. V. & CLEVELAND, D. W. 2006. ALS: A Dsiease of Motor Neurons and Their Nonneuronal Neighbors. *Cell Press,* 1, 39-59.
BOTTNER, M., KRIEGLSTEIN, K. & UNSICKER, K. 2000. The transforming growth factor-betas: structure, signaling, and roles in nervous system development and functions. *Journal of neurochemistry,* 75**,** 2227-40.
BOTTNER, M., UNSICKER, K. & SUTER-CRAZZOLARA, C. 1996. Expression of TGF-beta type II receptor mRNA in the CNS. *Neuroreport,* 7, 2903-7.
BOUHY, D., GHASEMLOU, N., LIVELY, S., REDENSEK, A., RATHORE, K. I., SCHLICHTER, L. C. & DAVID, S. 2011. Inhibition of the Ca(2)(+)-dependent K(+) channel, KCNN4/KCa3.1, improves tissue protection and locomotor

recovery after spinal cord injury. *The Journal of neuroscience : the official journal of the Society for Neuroscience,* 31**,** 16298-308.
BRAHMACHARI, S., FUNG, Y. K. & PAHAN, K. 2006. Induction of glial fibrillary acidic protein expression in astrocytes by nitric oxide. *The Journal of neuroscience : the official journal of the Society for Neuroscience,* 26, 4930-9.
BROOKS, A. N., KILGOUR, E. & SMITH, P. D. 2012. Molecular pathways: fibroblast growth factor signaling: a new therapeutic opportunity in cancer. *Clinical cancer research : an official journal of the American Association for Cancer Research,* 18**,** 1855-62.
BRUCE, J. C., OATWAY, M. A. & WEAVER, L. C. 2002. Chronic pain after clip-compression injury of the rat spinal cord. *Experimental neurology,* 178**,** 33-48.
BUCHSER, W. J., SLEPAK, T. I., GUTIERREZ-ARENAS, O., BIXBY, J. L. & LEMMON, V. P. 2010. Kinase/phosphatase overexpression reveals pathways regulating hippocampal neuron morphology. *Molecular systems biology,* 6**,** 391.
BULLOCK, R. & FUJISAWA, H. 1992. The role of glutamate antagonists for the treatment of CNS injury. *Journal of neurotrauma,* 9 Suppl 2**,** S443-62.
BURKE, D. A., LINDEN, R. D., ZHANG, Y. P., MAISTE, A. C. & SHIELDS, C. B. 2001. Incidence rates and populations at risk for spinal cord injury: A regional study. *Spinal cord,* 39**,** 274-8.
BUSCH, S. A., HAMILTON, J. A., HORN, K. P., CUASCUT, F. X., CUTRONE, R., LEHMAN, N., DEANS, R. J., TING, A. E., MAYS, R. W. & SILVER, J. 2011. Multipotent adult progenitor cells prevent macrophage-mediated axonal dieback and promote regrowth after spinal cord injury. *The Journal of neuroscience : the official journal of the Society for Neuroscience,* 31**,** 944-53.
BUSS, A., PECH, K., KAKULAS, B. A., MARTIN, D., SCHOENEN, J., NOTH, J. & BROOK, G. A. 2007. Matrix metalloproteinases and their inhibitors in human traumatic spinal cord injury. *BMC neurology,* 7**,** 17.
BUSS, A., PECH, K., KAKULAS, B. A., MARTIN, D., SCHOENEN, J., NOTH, J. & BROOK, G. A. 2008. TGF-beta1 and TGF-beta2 expression after traumatic human spinal cord injury. *Spinal cord,* 46**,** 364-71.
BUSS, A., PECH, K., KAKULAS, B. A., MARTIN, D., SCHOENEN, J., NOTH, J. & BROOK, G. A. 2009. NG2 and phosphacan are present in the astroglial scar after human traumatic spinal cord injury. *BMC Neurology, 9.*
BUTT, A. M., IBRAHIM, M. & BERRY, M. 1997. The relationship between developing oligodendrocyte units and maturing axons during myelinogenesis in the anterior medullary velum of neonatal rats. *Journal of Neurocytology,* 26, 327-338.
BYLUND, D. B. 1995. Pharmacological characteristics of alpha-2 adrenergic receptor subtypes. *Annals of the New York Academy of Sciences,* 763**,** 1-7.
BYRNES, K. R., FRICKE, S. T. & FADEN, A. I. 2010. Neuropathological differences between rats and mice after spinal cord injury. *Journal of magnetic resonance imaging : JMRI,* 32**,** 836-46.
CADOTTE, D. W. & FEHLINGS, M. G. 2011. Spinal cord injury: a systematic review of current treatment options. *Clinical orthopaedics and related research,* 469**,** 732-41.
CAIRNS, D. M., ADKINS, R. H. & SCOTT, M. D. 1996. Pain and depression in acute traumatic spinal cord injury: origins of chronic problematic pain? *Archives of physical medicine and rehabilitation,* 77**,** 329-35.

CAO, G., SAVANI, R. C., FEHRENBACH, M., LYONS, C., ZHANG, L., COUKOS, G. & DELISSER, H. M. 2006. Involvement of endothelial CD44 during in vivo angiogenesis. *The American journal of pathology,* 169**,** 325-36.

CAPPARUCCIA, L. & TAMAGNONE, L. 2009. Semaphorin signaling in cancer cells and in cells of the tumor microenvironment--two sides of a coin. *Journal of cell science,* 122**,** 1723-36.

CARMEL, J. B., GALANTE, A., SOTEROPOULOS, P., TOLIAS, P., RECCE, M., YOUNG, W. & HART, R. P. 2001. Gene expression profiling of acute spinal cord injury reveals spreading inflammatory signals and neuron loss. *Physiological genomics,* 7**,** 201-13.

CARMELIET, P. 2005. Angiogenesis in life, disease and medicine. *Nature,* 438**,** 932-6.

CARPENE, E., ANDREANI, G. & ISANI, G. 2007. Metallothionein functions and structural characteristics. *Journal of trace elements in medicine and biology : organ of the Society for Minerals and Trace Elements,* 21 Suppl 1**,** 35-9.

CARTER, C., CLARK, A., SPENCER, G. & CARLONE, R. 2011. Cloning and expression of a retinoic acid receptor beta2 subtype from the adult newt: evidence for an early role in tail and caudal spinal cord regeneration. *Developmental dynamics : an official publication of the American Association of Anatomists,* 240**,** 2613-25.

CASAZZA, A., FU, X., JOHANSSON, I., CAPPARUCCIA, L., ANDERSSON, F., GIUSTACCHINI, A., SQUADRITO, M. L., VENNERI, M. A., MAZZONE, M., LARSSON, E., CARMELIET, P., DE PALMA, M., NALDINI, L., TAMAGNONE, L. & ROLNY, C. 2011. Systemic and targeted delivery of semaphorin 3A inhibits tumor angiogenesis and progression in mouse tumor models. *Arteriosclerosis, thrombosis, and vascular biology,* 31**,** 741-9.

CASELLA, G. T., BUNGE, M. B. & WOOD, P. M. 2006. Endothelial cell loss is not a major cause of neuronal and glial cell death following contusion injury of the spinal cord. *Experimental neurology,* 202**,** 8-20.

CASELLA, G. T., MARCILLO, A., BUNGE, M. B. & WOOD, P. M. 2002. New vascular tissue rapidly replaces neural parenchyma and vessels destroyed by a contusion injury to the rat spinal cord. *Experimental neurology,* 173**,** 63-76.

CASSADA, D. C., TRIBBLE, C. G., LONG, S. M., LAUBACH, V. E., KAZA, A. K., LINDEN, J., NGUYEN, B. N., RIEGER, J. M., FISER, S. M., KRON, I. L. & KERN, J. A. 2002. Adenosine A2A analogue ATL-146e reduces systemic tumor necrosing factor-alpha and spinal cord capillary platelet-endothelial cell adhesion molecule-1 expression after spinal cord ischemia. *Journal of vascular surgery,* 35**,** 994-8.

CELLUCCI, T., TYRRELL, P. N., PULLENAYEGUM, E. & BENSELER, S. M. 2012. von Willebrand factor antigen--a possible biomarker of disease activity in childhood central nervous system vasculitis? *Rheumatology,* 51**,** 1838-45.CHEN, K. B., UCHIDA, K. & NAKAJIMA, H. 2011. Tumor necrosis factor-α antagonist reduces apoptosis of neurons and oligodendroglia in rat spinal cord injury. *Spine,* 36, 1350-1358.

CHEN, T. C., CHANG, S. W. & WANG, T. Y. 2013. Moxifloxacin modifies corneal fibroblast-to-myofibroblast differentiation. *British journal of pharmacology,* 168**,** 1341-54.

CHEN, Z. L & STRICKLAND, S. 2003. Laminin ϒ1 is critical fro Schwann cell differentiation, axon myelination, and regeneration in the peripheral nerve. *The Journal of Cell Biology*, 163, 889-899.

CHENG, Y. S., CHAMPLIAUD, M. F., BURGESON, R. E., MARINKOVICH, M. P. & YURCHENCO, P. D. 1997. Self-assembly of laminin isoforms. *The Journal of biological chemistry,* 272**,** 31525-32.

CHERIAN, M. G., JAYASURYA, A. & BAY, B. H. 2003. Metallothioneins in human tumors and potential roles in carcinogenesis. *Mutation research,* 533**,** 201-9.

CHESNEY, J. & BUCALA, R. 1997. Peripheral blood fibrocytes: novel fibroblast-like cells that present antigen and mediate tissue repair. *Biochemical Society transactions,* 25**,** 520-4.

CHIDA, K., HARA, T., HIRAI, T., KONISHI, C., NAKAMURA, K., NAKAO, K., AIBA, A., KATSUKI, M. & KUROKI, T. 2003. Disruption of protein kinase Ceta results in impairment of wound healing and enhancement of tumor formation in mouse skin carcinogenesis. *Cancer research,* 63**,** 2404-8.

CHOI, K. H., ELASHOFF, M., HIGGS, B. W., SONG, J., KIM, S., SABUNCIYAN, S., DIGLISIC, S., YOLKEN, R. H., KNABLE, M. B., TORREY, E. F. & WEBSTER, M. J. 2008. Putative psychosis genes in the prefrontal cortex: combined analysis of gene expression microarrays. *BMC psychiatry,* 8**,** 87.

CHOI, S. R., ROH, D. H., YOON, S. Y., KANG, S. Y., MOON, J. Y., KWON, S. G., CHOI, H. S., HAN, H. J., BEITZ, A. J., OH, S. B. & LEE, J. H. 2013. Spinal sigma-1 receptors activate NADPH oxidase 2 leading to the induction of pain hypersensitivity in mice and mechanical allodynia in neuropathic rats. *Pharmacological research : the official journal of the Italian Pharmacological Society,* 74**,** 56-67.

CHONG, K. W., CHEN, M. J., KOAY, E. S., WONG, B. S., LEE, A. Y., RUSSO-MARIE, F. & CHEUNG, N. S. 2010. Annexin A3 is associated with cell death in lactacystin-mediated neuronal injury. *Neuroscience letters,* 485**,** 129-33.

CHRISTENSEN, M. D. & HULSEBOSCH, C. E. 1997. Chronic central pain after spinal cord injury. *Journal of neurotrauma,* 14**,** 517-37.

CHUNG, A. S. & FERRARA, N. 2010. The Extracellular Matrix & Angiogenesis: Role of the Extracellular Matrix in Developing Vessels and Tumor Angiogenesis.

CHUNG, A. S., LEE, J. & FERRARA, N. 2010. Targeting the tumour vasculature: insights from physiological angiogenesis. *Nature reviews. Cancer,* 10**,** 505-14.

CLARK, W. M., MADDEN, K. P., ROTHLEIN, R. & ZIVIN, J. A. 1991. Reduction of central nervous system ischemic injury in rabbits using leukocyte adhesion antibody treatment. *Stroke; a journal of cerebral circulation,* 22**,** 877-83.

COHEN, J., BURNE, J. F., MCKINLAY, C. & WINTER, J. 1987. The role of laminin and the laminin/fibronectin receptor complex in the outgrowth of retinal ganglion cell axons. *Developmental biology,* 122**,** 407-18.

CORCORAN, J., SO, P. L., BARBER, R. D., VINCENT, K. J., MAZARAKIS, N. D., MITROPHANOUS, K. A., KINGSMAN, S. M. & MADEN, M. 2002. Retinoic acid receptor beta2 and neurite outgrowth in the adult mouse spinal cord in vitro. *Journal of cell science,* 115**,** 3779-86.

CORNBROOKS, C. J., CAREY, D. J., MCDONALD, J. A., TIMPL, R. & BUNGE, R. P. 1983. In vivo and in vitro observations on laminin production by Schwann cells. *Proceedings of the National Academy of Sciences of the United States of America,* 80**,** 3850-4.

COSTA, C., INCIO, J. & SOARES, R. 2007. Angiogenesis and chronic inflammation: cause or consequence? *Angiogenesis,* 10, 149-66.

COUMANS, J. V., LIN, T. T., DAI, H. N., MACARTHUR, L., MCATEE, M., NASH, C. & BREGMAN, B. S. 2001. Axonal regeneration and functional recovery after

complete spinal cord transection in rats by delayed treatment with tranplants and neurotrophins. *The journal of neuroscience.* 21, 9334-9344.

COURTINE, G., BUNGE, M. B, FAWCETT, J. W., GROSSMAN, R. G., KAAS, J. H., LEMON, R., MAIER, I., MARTIN, J., NUDO, R. J., RAMON-CUETO, A., ROUILLER, E. M., SCHNELL, L., WANNIER, T., SCHWAB, M. E. & EDGERTON, V. R. 2007. Can experiments in nonhuman primates expedite that translation of treatments for spinal cord injury in humans? *Nature Medicine,* 13, 561-566.

COYLE, P., PHILCOX, J. C., CAREY, L. C. & ROFE, A. M. 2002. Metallothionein: the multipurpose protein. *Cellular and molecular life sciences : CMLS,* 59**,** 627-47.

CRABB, S. J., PATSIOS, D., SAUERBREI, E., ELLIS, P. M., ARNOLD, A., GOSS, G., LEIGHL, N. B., SHEPHERD, F. A., POWERS, J., SEYMOUR, L. & LAURIE, S. A. 2009. Tumor cavitation: impact on objective response evaluation in trials of angiogenesis inhibitors in non-small-cell lung cancer. *Journal of clinical oncology : official journal of the American Society of Clinical Oncology,* 27**,** 404-10.

CRABTREE, B., THIYAGARAJAN, N., PRIOR, S. H., WILSON, P., IYER, S., FERNS, T., SHAPIRO, R., BREW, K., SUBRAMANIAN, V. & ACHARYA, K. R. 2007. Characterization of human angiogenin variants implicated in amyotrophic lateral sclerosis. *Biochemistry,* 46**,** 11810-8.

CROCK, H. V. & YOSHIZAWA, H. 1977. The blood supply of the vertebral column and spinal cord in man. Springer.

CROCKER, S. J., PAGENSTECHER, A. & CAMPBELL, I. L. 2004. The TIMPs tango with MMPs and more in the central nervous system. *Journal of neuroscience research,* 75**,** 1-11.

CROSS, M. J. & CLAESSON-WELSH, L. 2001. FGF and VEGF function in angiogenesis: signalling pathways, biological responses and therapeutic inhibition. *Trends in pharmacological sciences,* 22**,** 201-7.

CRUZ-ALMEIDA, Y., et al., 2012. Decreased spinothalamic and dorsal column medial lemniscus-mediated function is associated with neuropathic pain after spinal cord injury. *Journal of neurotrauma*. 29**,** 2706-15.

CUI, W. & ACKHURST, R. J. 1996. Transforming growth factor Bs: Biochemistry and biological activities *in vivo* and *in vitro*. . *In Growth Factors in Health and Disease,* 1B**,** 319-356.

CULHACI, N., SAGOL, O., KARADEMIR, S., ASTARCIOGLU, H., ASTARCIOGLU, I., SOYTURK, M., OZTOP, I. & OBUZ, F. 2005. Expression of transforming growth factor-beta-1 and p27Kip1 in pancreatic adenocarcinomas: relation with cell-cycle-associated proteins and clinicopathologic characteristics. *BMC cancer,* 5**,** 98.

CURRAN, T. P., SHAPIRO, R., RIORDAN, J. F. & VALLEE, B. L. 1993. Modulation of the activity of angiogenin by mutagenesis at Asp-116. *Biochimica et biophysica acta,* 1202**,** 281-6.

CUZNER, M. L., GVERIC, D., STRAND, C., LOUGHLIN, A. J., PAEMEN, L., OPDENAKKER, G. & NEWCOMBE, J. 1996. The expression of tissue-type plasminogen activator, matrix metalloproteases and endogenous inhibitors in the central nervous system in multiple sclerosis: comparison of stages in lesion evolution. *Journal of neuropathology and experimental neurology,* 55**,** 1194-204.

D'ONOFRIO, P. M., THAYAPARARAJAH, M., LYSKO, M. D., MAGHARIOUS, M., SPRATT, S. K., LEE, G., ANDO, D., SUROSKY, R., FEHLINGS, M. G. & KOEBERLE, P. D. 2011. Gene therapy for traumatic central nervous system injury and stroke using an engineered zinc finger protein that upregulates VEGF-A. *Journal of neurotrauma,* 28**,** 1863-79.

DAVIS, S., ALDRICH, T. H., JONES, P. F., ACHESON, A., COMPTON, D. L., JAIN, V., RYAN, T. E., BRUNO, J., RADZIEJEWSKI, C., MAISONPIERRE, P. C. & YANCOPOULOS, G. D. 1996. Isolation of angiopoietin-1, a ligand for the TIE2 receptor, by secretion-trap expression cloning. *Cell,* 87**,** 1161-9.

DAVOODY, L., QUITON, R. L., LUCAS, J. M., JI, Y., KELLER, A. & MASRI, R. 2011. Conditioned place preference reveals tonic pain in an animal model of central pain. *The journal of pain : official journal of the American Pain Society,* 12**,** 868-74.

DE CAESTECKER, M. P., PIEK, E. & ROBERTS, A. B. 2000. Role of transforming growth factor-beta signaling in cancer. *Journal of the National Cancer Institute,* 92**,** 1388-402.

DE LAPORTE, L., DES RIEUX, A., TUINSTRA, H. M., ZELIVYANSKAYA, M. L., DE CLERCK, N. M., POSTNOV, A. A., PREAT, V. & SHEA, L. D. 2011. Vascular endothelial growth factor and fibroblast growth factor 2 delivery from spinal cord bridges to enhance angiogenesis following injury. *Journal of biomedical materials research. Part A,* 98**,** 372-82.

DE WINTER, F., OUDEGA, M., LANKHORST, A. J., HAMERS, F. P., BLITS, B., RUITENBERG, M. J., PASTERKAMP, R. J., GISPEN, W. H. & VERHAAGEN, J. 2002. Injury-induced class 3 semaphorin expression in the rat spinal cord. *Experimental neurology,* 175**,** 61-75.

DE THE, H., CHOMIENNE, C., LANOTTE, M., DEGOS, L. & DEJEAN, A. 1990. The t(15;17) translocation of acute promyelocytic leukaemia fuses the retinoic acid receptor alpha gene to a novel transcribed locus. *Nature,* 347**,** 558-61.

DESAI, T. J., CHEN, F., LU, J., QIAN, J., NIEDERREITHER, K., DOLLE, P., CHAMBON, P. & CARDOSO, W. V. 2006. Distinct roles for retinoic acid receptors alpha and beta in early lung morphogenesis. *Developmental biology,* 291**,** 12-24.

DETLOFF, M. R., et al., 2012. Acute and chronic tactile sensory testing after spinal cord injury in rats. Journal of visualized experiments : *JoVE*. e3247.

DETLOFF, M. R., CLARK, L. M., HUTCHINSON, K. J., KLOOS, A. D., FISHER, L. C. & BASSO, D. M. 2010. Validity of acute and chronic tactile sensory testing after spinal cord injury in rats. *Experimental neurology,* 225**,** 366-76.

DEUMENS, R., JOOSTEN, E. A., WAXMAN, S. G. & HAINS, B. C. 2008. Locomotor dysfunction and pain: the scylla and charybdis of fiber sprouting after spinal cord injury. *Molecular neurobiology,* 37**,** 52-63.

DEUMENS, R., KOOPMANS, G. C. & JOOSTEN, E. A. 2005. Regeneration of descending axon tracts after spinal cord injury. *Progress in neurobiology,* 77**,** 57-89.

DEYAMA, S., TAKISHITA, A., TANIMOTO, S., IDE, S., NAKAGAWA, T., SATOH, M. & MINAMI, M. 2010. Roles of beta- and alpha2-adrenoceptors within the central nucleus of the amygdala in the visceral pain-induced aversion in rats. *Journal of pharmacological sciences,* 114**,** 123-6.

DI GIROLAMO, N., TEDLA, N., LLOYD, A. & WAKEFIELD, D. 1998. Expression of matrix metalloproteinases by human plasma cells and B lymphocytes. *European journal of immunology,* 28**,** 1773-84.

DIETZ, V. 2002. Do human bipeds use quadrupedal coordination? *Trends in neurosciences,* 25**,** 462-7.
DIETZ, V. 2006. G. Heiner Sell memorial lecture: neuronal plasticity after spinal cord injury: significance for present and future treatments. *The journal of spinal cord medicine,* 29**,** 481-8.
DING, T., LUO, Z. J., ZHENG, Y., HU, X. Y. & YE, Z. X. 2010. Rapid repair and regeneration of damaged rabbit sciatic nerves by tissue-engineered scaffold made from nano-silver and collagen type I. *Injury,* 41**,** 522-7.
DOCHERTY, A. J., LYONS, A., SMITH, B. J., WRIGHT, E. M., STEPHENS, P. E., HARRIS, T. J., MURPHY, G. & REYNOLDS, J. J. 1985. Sequence of human tissue inhibitor of metalloproteinases and its identity to erythroid-potentiating activity. *Nature,* 318**,** 66-9.
DOHRMANN, G. J., WAGNER, F. C., JR. & BUCY, P. C. 1972. Transitory traumatic paraplegia: electron microscopy of early alterations in myelinated nerve fibers. *Journal of neurosurgery,* 36**,** 407-15.
DOMMISSE, G. F. 1975. The arteries and veins for the human spinal cord from birth. New York: Churchhill Livingstone.
DONO, R. 2003. Fibroblast growth factors as regulators of central nervous system development and function. *American journal of physiology. Regulatory, integrative and comparative physiology,* 284**,** R867-81.
DUCKER, T. B. & ASSENMACHER, D. R. 1969. Microvascular response to experimental spinal cord trauma. *Surgical forum,* 20**,** 428-30.
DURHAM-LEE, J. C., WU, Y., MOKKAPATI, V. U., PAULUCCI-HOLTHAUZEN, A. A. & NESIC, O. 2012. Induction of angiopoietin-2 after spinal cord injury. *Neuroscience,* 202**,** 454-64.
ECKENSTEIN, F. P., SHIPLEY, G. D. & NISHI, R. 1991. Acidic and basic fibroblast growth factors in the nervous system: distribution and differential alteration of levels after injury of central versus peripheral nerve. *The Journal of neuroscience : the official journal of the Society for Neuroscience,* 11**,** 412-9.
ECHTERMEYER, F., STREIT, M., WILCOX-ADELMAN, S., SAONCELLA, S., DENHEZ, F., DETMAR, M. & GOETINCK, P. 2001. Delayed wound repair and impaired angiogenesis in mice lacking syndecan-4. *The Journal of clinical investigation,* 107**,** R9-R14.
EDGAR, R. & QUAIL, P. 1994. Progressive post-traumatic cystic and non-cystic myelopathy. *British journal of neurosurgery,* 8**,** 7-22.
EDGERTON, V. R. & ROY, R. R. 2002. Paralysis recovery in humans and model systems. *Current opinion in neurobiology,* 12**,** 658-67.
EKBLOM, M., FALK, M., SALMIVIRTA, K., DURBEEJ, M. & EKBLOM, P. 1998. Laminin isoforms and epithelial development. *Annals of the New York Academy of Sciences,* 857**,** 194-211.
EL REFAEY, H., EBADI, M., KUSZYNSKI, C. A., SWEENEY, J., HAMADA, F. M. & HAMED, A. 1997. Identification of metallothionein receptors in human astrocytes. *Neuroscience letters,* 231**,** 131-4.
EUGENIN, E. A., GAMSS, R., BUCKNER, C., BUONO, D., KLEIN, R. S., SCHOENBAUM, E. E., CALDERON, T. M. & BERMAN, J. W. 2006. Shedding of PECAM-1 during HIV infection: a potential role for soluble PECAM-1 in the pathogenesis of NeuroAIDS. *Journal of leukocyte biology,* 79**,** 444-52.
EVANS, R. M. 1988. The steroid and thyroid hormone receptor superfamily. *Science,* 240**,** 889-95.

FAIRBANKS, C. A., SCHREIBER, K. L., BREWER, K. L., YU, C. G., STONE, L. S., KITTO, K. F., NGUYEN, H. O., GROCHOLSKI, B. M., SHOEMAN, D. W., KEHL, L. J., REGUNATHAN, S., REIS, D. J., YEZIERSKI, R. P. & WILCOX, G. L. 2000. Agmatine reverses pain induced by inflammation, neuropathy, and spinal cord injury. *Proceedings of the National Academy of Sciences of the United States of America,* 97**,** 10584-9.

FAN, J., ZHANG, H., HE, J., XIAO, Z., CHEN, B., XIAODAN, J., DAI, J. & XU, R. 2011. Neural regrowth induced by PLGA nerve conduits and neurotrophin-3 in rats with complete spinal cord transection. *Journal of biomedical materials research. Part B, Applied biomaterials,* 97**,** 271-7.

FANG, B., LI, X. M., SUN, X. J., BAO, N. R., REN, X. Y., LV, H. W. & MA, H. 2013a. Ischemic Preconditioning Protects against Spinal Cord Ischemia-Reperfusion Injury in Rabbits by Attenuating Blood Spinal Cord Barrier Disruption. *International journal of molecular sciences,* 14**,** 10343-54.

FANG, B., WANG, H., SUN, X. J., LI, X. Q., AI, C. Y., TAN, W. F., WHITE, P. F. & MA, H. 2013b. Intrathecal transplantation of bone marrow stromal cells attenuates blood-spinal cord barrier disruption induced by spinal cord ischemia-reperfusion injury in rabbits. *Journal of vascular surgery*.

FAROOQUE, M. 2000. Spinal cord compression injury in the mouse: presentation of a model including assessment of motor dysfunction. *Acta neuropathologica,* 100**,** 13-22.

FASSBENDER, J. M., WHITTEMORE, S. R. & HAGG, T. 2011. Targeting microvasculature for neuroprotection after SCI. *Neurotherapeutics : the journal of the American Society for Experimental NeuroTherapeutics,* 8**,** 240-51.

FAULKNER, J. R., HERRMANN, J. E., WOO, M. J., TANSEY, K. E., DOAN, N. B. & SOFRONIEW, M. V. 2004. Reactive astrocytes protect tissue and preserve function after spinal cord injury. *The Journal of neuroscience : the official journal of the Society for Neuroscience,* 24**,** 2143-55.

FEHLINGS, M. & ROBINS-STEELE, S. 2012. The delayed post-injury administration of soluble Fas receptor attenuates post-traumatic neural degeneration and enhances functional recovery after traumatic cervical spinal cord injury. *Journal of neurotrauma*.

FETT, J. W., STRYDOM, D. J., LOBB, R. R., ALDERMAN, E. M., BETHUNE, J. L., RIORDAN, J. F. & VALLEE, B. L. 1985. Isolation and characterization of angiogenin, an angiogenic protein from human carcinoma cells. *Biochemistry,* 24**,** 5480-6.

FIGLEY, S. A., KHOSRAVI, R., LEGASTO, J. M., TSENG, Y. F. & FEHLINGS, M. G. 2014. Characterization of vascular disruption and blood-spinal cord barrier permeability following traumatic spinal cord injury. *Journal of neurotrauma,* 31**,** 541-52.

FILHO, T. E. & MOLINA, A. E. 2007. Analysis of the Sensitivity and Reproducibility of The Basso, Beattie, Bresnahan (BBB) Scale in Wistar Rats. *Clinics,* 63**,** 6.

FINNERUP, N. B., SORENSEN, L., BIERING-SORENSEN, F., JOHANNESEN, I. L. & JENSEN, T. S. 2007. Segmental hypersensitivity and spinothalamic function in spinal cord injury pain. *Experimental neurology,* 207**,** 139-49.

FINNERUP, N. B., JOHANNESEN, I. L., SINDRUP, S. H., BACH, F. W. & JENSEN, T. S. 2001. Pain and dysesthesia in patients with spinal cord injury: A postal survey. *Spinal cord,* 39**,** 256-62.

FITCH, M. T., DOLLER, C., COMBS, C. K., LANDRETH, G. E. & SILVER, J. 1999. Cellular and molecular mechanisms of glial scarring and progressive cavitation: in vivo and in vitro analysis of inflammation-induced secondary injury after CNS trauma. *The Journal of neuroscience : the official journal of the Society for Neuroscience,* 19**,** 8182-98.

FJOSE, A., IZPISUA-BELMONTE, J. C., FROMENTAL-RAMAIN, C. & DUBOULE, D. 1994. Expression of the zebrafish gene hlx-1 in the prechordal plate and during CNS development. *Development,* 120**,** 71-81.

FLEMING, J. C., NORENBERG, M. D., RAMSAY, D. A., DEKABAN, G. A., MARCILLO, A. E., SAENZ, A. D., PASQUALE-STYLES, M., DIETRICH, W. D. & WEAVER, L. C. 2006. The cellular inflammatory response in human spinal cords after injury. *Brain : a journal of neurology,* 129**,** 3249-69.

FORBES, A. D., SLIMP, J. C., WINN, R. K. & VERRIER, E. D. 1994. Inhibition of neutrophil adhesion does not prevent ischemic spinal cord injury. *The Annals of thoracic surgery,* 58**,** 1064-8.

FOLLESA, P., WRATHALL, J. R. & MOCCHETTI, I. 1994. Increased basic fibroblast growth factor mRNA following contusive spinal cord injury. *Brain research. Molecular brain research,* 22**,** 1-8.

FORD-HOLEVINSKI, T. S., HOPKINS, J. M., MCCOY, J. P. & AGRANOFF, B. W. 1986. Laminin supports neurite outgrowth from explants of axotomized adult rat retinal neurons. *Brain research,* 393**,** 121-6.

FORSBERG-NILSSON, K., BEHAR, T. N., AFRAKHTE, M., BARKER, J. L. & MCKAY, R. D. 1998. Platelet-derived growth factor induces chemotaxis of neuroepithelial stem cells. *Journal of neuroscience research,* 53**,** 521-30.

FRAUTSCHY, S. A., WALICKE, P. A. & BAIRD, A. 1991. Localization of basic fibroblast growth factor and its mRNA after CNS injury. *Brain research,* 553**,** 291-9.

FREDRIKSSON, L., LI, H. & ERIKSSON, U. 2004. The PDGF family: four gene products form five dimeric isoforms. *Cytokine & growth factor reviews,* 15**,** 197-204.

FROLICHSTHAL-SCHOELLER, P., VESCOVI, A. L., KREKOSKI, C. A., MURPHY, G., EDWARDS, D. R. & FORSYTH, P. 1999. Expression and modulation of matrix metalloproteinase-2 and tissue inhibitors of metalloproteinases in human embryonic CNS stem cells. *Neuroreport,* 10**,** 345-51.

FUJII, Y., MAMMEN, E. F., FARAG, A., MUZ, J., SALCICCIOLI, G. G. & WEINGARDEN, S. T. 1992. Thrombosis in spinal cord injury. *Thrombosis research,* 68**,** 357-68.

FUNA, K. & SASAHARA, M. 2014. The roles of PDGF in Development and During Neurogenesis in the Normal and Diseased Nervous System. *Journal of Neuroimmune Pharamacology,* 9, 168-181.

FURLAN, J. C., SAKAKIBARA, B. M., MILLER, W. C. & KRASSIOUKOV, A. V. 2013. Global incidence and prevalence of traumatic spinal cord injury. *The Canadian journal of neurological sciences. Le journal canadien des sciences neurologiques,* 40**,** 456-64.

FURUKAWA, S. & FURUKAWA, Y. 2007. [FGF-2-treatment improves locomotor function via axonal regeneration in the transected rat spinal cord]. *Brain and nerve = Shinkei kenkyu no shinpo,* 59**,** 1333-9.

FUXE, J., TABRUYN, S., COLTON, K., ZAID, H., ADAMS, A., BALUK, P., LASHNITS, E., MORISADA, T., LE, T., O'BRIEN, S., EPSTEIN, D. M., KOH, G. Y. & MCDONALD, D. M. 2011. Pericyte requirement for anti-leak action of

angiopoietin-1 and vascular remodeling in sustained inflammation. *The American journal of pathology,* 178**,** 2897-909.
GAMBLE, J. R., DREW, J., TREZISE, L., UNDERWOOD, A., PARSONS, M., KASMINKAS, L., RUDGE, J., YANCOPOULOS, G. & VADAS, M. A. 2000. Angiopoietin-1 is an antipermeability and anti-inflammatory agent in vitro and targets cell junctions. *Circulation research,* 87**,** 603-7.
GAO, X. & XU, Z. 2008. Mechanisms of action of angiogenin. *Acta Biochim Biophys Sin,* 40, 619-624.
GASSON, J. C., GOLDE, D. W., KAUFMAN, S. E., WESTBROOK, C. A., HEWICK, R. M., KAUFMAN, R. J., WONG, G. G., TEMPLE, P. A., LEARY, A. C., BROWN, E. L. & ET AL. 1985. Molecular characterization and expression of the gene encoding human erythroid-potentiating activity. *Nature,* 315**,** 768-71.
GAVIRIA, M., HATON, H., SANDILLON, F. & PRIVAT, A. 2002. A mouse model of acute ischemic spinal cord injury. *Journal of neurotrauma,* 19**,** 205-21.
GENSEL, C. J., DONNELLY, D. J. & POPOVICH, P. G. 2011. Spinal cord injury therapies in humans: an overview of current clinical trials and their potential effects on intrinsic CNS macrophages. *Expert Opinion on Therapeutic Targets,* 15, 505-518.
GEORGE, M. L., ECCLES, S. A., TUTTON, M. G., ABULAFI, A. M. & SWIFT, R. I. 2000. Correlation of plasma and serum vascular endothelial growth factor levels with platelet count in colorectal cancer: clinical evidence of platelet scavenging? *Clinical cancer research : an official journal of the American Association for Cancer Research,* 6**,** 3147-52.
GEREMIA, N. M., BAO, F., ROSENZWEIG, T. E., HRYCIW, T., WEAVER, L., DEKABAN, G. A. & BROWN, A. 2012. CD11d Antibody Treatment Improves Recovery in Spinal Cord-Injured Mice. *Journal of neurotrauma,* 29**,** 539-50.
GERHARDT, H., GOLDING, M., FRUTTIGER, M., RUHRBERG, C., LUNDKVIST, A., ABRAMSSON, A., JELTSCH, M., MITCHELL, C., ALITALO, K., SHIMA, D. & BETSHOLTZ, C. 2003. VEGF guides angiogenic sprouting utilizing endothelial tip cell filopodia. *The Journal of cell biology,* 161**,** 1163-77.
GERKE, V., CREUTZ, C. E. & MOSS, S. E. 2005. Annexins: linking Ca2+ signalling to membrane dynamics. *Nature reviews Molecular cell biology,* 6**,** 449-61.
GERKE, V. & MOSS, S. E. 2002. Annexins: from structure to function. *Physiological reviews,* 82**,** 331-71.
GIULIAN, D. & ROBERTSON, C. 1990. Inhibition of mononuclear phagocytes reduces ischemic injury in the spinal cord. *Annals of neurology,* 27**,** 33-42.
GLASER, J., GONZALEZ, R., SADR, E. & KEIRSTEAD, H. S. 2006. Neutralization of the chemokine CXCL10 reduces apoptosis and increases axon sprouting after spinal cord injury. *Journal of neuroscience research,* 84, 724-34.
GONZALEZ-FERNANDEZ, C., FERNANDEZ-MARTOS, C. M., SHIELDS, S. D., ARENAS, E. & JAVIER RODRIGUEZ, F. 2014. Wnts are expressed in the spinal cord of adult mice and are differentially induced after injury. *Journal of neurotrauma,* 31**,** 565-81.
GONZALEZ-LARA, L. E., XU, X., HOFSTETROVA, K., PNIAK, A., BROWN, A. & FOSTER, P. J. 2009. In vivo magnetic resonance imaging of spinal cord injury in the mouse. *Journal of neurotrauma,* 26, 753-62.
GOSAIN, A. & DIPIETRO, L. A. 2004. Aging and wound healing. *World journal of surgery,* 28**,** 321-6.
GOUSSEV, S., HSU, J. Y., LIN, Y., TJOA, T., MAIDA, N., WERB, Z. & NOBLE-HAEUSSLEIN, L. J. 2003. Differential temporal expression of matrix

metalloproteinases after spinal cord injury: relationship to revascularization and wound healing. *Journal of neurosurgery,* 99**,** 188-97.
GRAESSER, D., SOLOWIEJ, A., BRUCKNER, M., OSTERWEIL, E., JUEDES, A., DAVIS, S., RUDDLE, N. H., ENGELHARDT, B. & MADRI, J. A. 2002. Altered vascular permeability and early onset of experimental autoimmune encephalomyelitis in PECAM-1-deficient mice. *The Journal of clinical investigation,* 109**,** 383-92.
GRANGER, D. N. & SENCHENKOVA, E. 2010. *Inflammation and the Microcirculation.* San Rafael (CA).
GRAUMANN, U., RITZ, M. F. & HAUSMANN, O. 2011. Necessity for re-vascularization after spinal cord injury and the search for potential therapeutic options. *Current neurovascular research,* 8**,** 334-41.
GREEN, D. 1991. Prevention of thromboembolism after spinal cord injury. *Seminars in thrombosis and hemostasis,* 17**,** 347-50.
GREEN, S. & CHAMBON, P. 1988. Nuclear receptors enhance our understanding of transcription regulation. *Trends in genetics : TIG,* 4**,** 309-14.
GREENE, J., WANG, M., LIU, Y. E., RAYMOND, L. A., ROSEN, C. & SHI, Y. E. 1996. Molecular cloning and characterization of human tissue inhibitor of metalloproteinase 4. *The Journal of biological chemistry,* 271**,** 30375-80.
GREENWAY, M. J., ANDERSEN, P. M., RUSS, C., ENNIS, S., CASHMAN, S., DONAGHY, C., PATTERSON, V., SWINGLER, R., KIERAN, D., PREHN, J., MORRISON, K. E., GREEN, A., ACHARYA, K. R., BROWN, R. H., JR. & HARDIMAN, O. 2006. ANG mutations segregate with familial and 'sporadic' amyotrophic lateral sclerosis. *Nature genetics,* 38**,** 411-3.
GRIFFIOEN, A. W., COENEN, M. J., DAMEN, C. A., HELLWIG, S. M., VAN WEERING, D. H., VOOYS, W., BLIJHAM, G. H. & GROENEWEGEN, G. 1997. CD44 is involved in tumor angiogenesis; an activation antigen on human endothelial cells. *Blood,* 90**,** 1150-9.
GRIMPE, B., DONG, S., DOLLER, C., TEMPLE, K., MALOUF, A. T. & SILVER, J. 2002. *The critical role of basement membrane-independent laminin Y1 chain during axon regneration in the CNS*. The Journal of Neuroscience, 22, 3144-3180.
GRIS, D., MARSH, D. R., OATWAY, M. A., CHEN, Y., HAMILTON, E. F., DEKABAN, G. A. & WEAVER, L. C. 2004. Transient blockade of the CD11d/CD18 integrin reduces secondary damage after spinal cord injury, improving sensory, autonomic, and motor function. *The Journal of neuroscience : the official journal of the Society for Neuroscience,* 24**,** 4043-51.
GRIS, P., TIGHE, A., THAWER, S., HEMPHILL, A., OATWAY, M., WEAVER, L., DEKABAN, G. A. & BROWN, A. 2009. Gene expression profiling in anti-CD11d mAb-treated spinal cord-injured rats. *Journal of neuroimmunology,* 209**,** 104-13.
GRUNER, J. A. 1992. A monitored contusion model of spinal cord injury in the rat. *Journal of neurotrauma,* 9**,** 123-6; discussion 126-8.
GUEST, J. D., HIESTER, E. D. & BUNGE, R. P. 2005. Demyelination and Schwann cell responses adjacent to injury epicenter cavities following chronic human spinal cord injury. *Experimental neurology,* 192**,** 384-93.
GUEYE, Y., FERHAT, L., SBAI, O., BIANCO, J., OULD-YAHOUI, A., BERNARD, A., CHARRAT, E., CHAUVIN, J. P., RISSO, J. J., FERON, F., RIVERA, S. & KHRESTCHATISKY, M. 2011. Trafficking and secretion of matrix

metalloproteinase-2 in olfactory ensheathing glial cells: A role in cell migration? *Glia,* 59**,** 750-70.
GUIZAR-SAHAGUN, G., GRIJALVA, I., HERNANDEZ-GODINEZ, B., FRANCO-BOURLAND, R. E., CRUZ-ANTONIO, L., MARTINEZ-CRUZ, A., IBANEZ-CONTRERAS, A. & MADRAZO, I. 2011. New approach for graded compression spinal cord injuries in Rhesus macaque: method feasibility and preliminary observations. *Journal of medical primatology,* 40**,** 401-13.
GUNTHERT, U., HOFMANN, M., RUDY, W., REBER, S., ZOLLER, M., HAUSSMANN, I., MATZKU, S., WENZEL, A., PONTA, H. & HERRLICH, P. 1991. A new variant of glycoprotein CD44 confers metastatic potential to rat carcinoma cells. *Cell,* 65**,** 13-24.
GUO, S. & DIPIETRO, L. A. 2010. Factors affecting wound healing. *Journal of dental research,* 89**,** 219-29.
GUO, X., ZAHIR, T., MOTHE, A., SHOICHET, M. S., MORSHEAD, C. M., KATAYAMA, Y. & TATOR, C. H. 2012. The Effect of Growth Factors and Soluble Nogo66 Receptor Protein on Transplanted Neural Stem/Progenitor Survival and Axonal Regeneration after Complete Transection of Rat Spinal Cord. *Cell transplantation*.
GUTH, L., ZHANG, Z., DIPROSPERO, N. A., JOUBIN, K. & FITCH, M. T. 1994. Spinal cord injury in the rat: treatment with bacterial lipopolysaccharide and indomethacin enhances cellular repair and locomotor function. *Experimental neurology,* 126**,** 76-87.
GYONEVA, S. & TRAYNELIS, S. F. 2013. Norepinephrine modulates the motility of resting and activated microglia via different adrenergic receptors. *The Journal of biological chemistry,* 288**,** 15291-302.
HAAS, T. L. 2005. Endothelial cell regulation of matrix metalloproteinases. *Canadian journal of physiology and pharmacology,* 83**,** 1-7.
HAGG, T. & OUDEGA, M. 2006. Degenerative and spontaneous regenerative processes after spinal cord injury. *Journal of neurotrauma,* 23**,** 264-80.
HAINS, B. C. & WAXMAN, S. G. 2006. Activated microglia contribute tot eh maintance of chronuic pain after spinal cord injury. *Journal of Neuroscience,* 26, 4308-4317.
HALEY, P. J. 2003. Species differences in the structure and fucntion of the immune system. *Toxicology,* 188, 49-71.
HALL, E. D. 1992. The neuroprotective pharmacology of methylprednisolone. *Journal of neurosurgery,* 76**,** 13-22.
HALL, E. D. & BRAUGHLER, J. M. 1982. Glucocorticoid mechanisms in acute spinal cord injury: a review and therapeutic rationale. *Surgical neurology,* 18**,** 320-7.
HALLMANN, R., HORN, N., SELG, M., WENDLER, O., PAUSCH, F. & SOROKIN, L. M. 2005. Expression and function of laminins in the embryonic and mature vasculature. *Physiological reviews,* 85**,** 979-1000.
HAMILL, C. E., GOLDSHMIDT, A., NICOLE, O., MCKEON, R. J., BRAT, D. J. & TRAYNELIS, S. F. 2005. Special lecture: glial reactivity after damage: implications for scar formation and neuronal recovery. *Clinical neurosurgery,* 52**,** 29-44.
HAN, S., ARNOLD, S. A., SITHU, S. D., MAHONEY, E. T., GERALDS, J. T., TRAN, P., BENTON, R. L., MADDIE, M. A., D'SOUZA, S. E., WHITTEMORE, S. R. & HAGG, T. 2010. Rescuing vasculature with intravenous angiopoietin-1 and alpha v beta 3 integrin peptide is protective after spinal cord injury. *Brain : a journal of neurology,* 133**,** 1026-42.

HANSEN, C. N., FISHER, L. C., DEIBERT, R. J., JAKEMAN, L. B., ZHANG, H., NOBLE-HAEUSSLEIN, L., WHITE, S. & BASSO, D. M. 2013. Elevated mmp-9 in the lumbar cord early after thoracic spinal cord injury impedes motor relearning in mice. *The Journal of neuroscience : the official journal of the Society for Neuroscience,* 33**,** 13101-11.

HANSEN, T. M., MOSS, A. J. & BRINDLE, N. P. 2008. Vascular endothelial growth factor and angiopoietins in neurovascular regeneration and protection following stroke. *Current neurovascular research,* 5**,** 236-45.

HAO, J. X., XU, X. J., ALDSKOGIUS, H., SEIGER, A. & WIESENFELD-HALLIN, Z. 1991. Allodynia-like effects in rat after ischaemic spinal cord injury photochemically induced by laser irradiation. *Pain,* 45**,** 175-85.

HARGREAVES, K., et al., 1988. A new and sensitive method for measuring thermal nociception in cutaneous hyperalgesia. *Pain*. 32**,** 77-88.

HARIK, S. I. & KALARIA, R. N. 1991. Blood-brain barrier abnormalities in Alzheimer's disease. *Annals of the New York Academy of Sciences,* 640**,** 47-52.

HARKNESS, A. K., ADAMSON, P., SUSSMAN, J. D., DAVIES-JONES, G. A. B., GREENWOOD, J. & WOODROOFE, M. N. 1999. Dexamethasone regulation of matrix metalloproteinase expression in CNS vascular endothelium. *Brain : a journal of neurology,* 123.

HARKNESS, K. A., ADAMSON, P., SUSSMAN, J. D., DAVIES-JONES, G. A., GREENWOOD, J. & WOODROOFE, M. N. 2000. Dexamethasone regulation of matrix metalloproteinase expression in CNS vascular endothelium. *Brain : a journal of neurology,* 123 (Pt 4)**,** 698-709.

HARRIS, J. E., NUTTALL, R. K., ELKINGTON, P. T., GREEN, J. A., HORNCASTLE, D. E., GRAEBER, M. B., EDWARDS, D. R. & FRIEDLAND, J. S. 2007. Monocyte-astrocyte networks regulate matrix metalloproteinase gene expression and secretion in central nervous system tuberculosis in vitro and in vivo. *Journal of immunology,* 178**,** 1199-207.

HASHIMOTO, M., INO, H., KODA, M., MURAKAMI, M., YOSHINAGA, K., YAMAZAKI, M. & MORIYA, H. 2004. Regulation of semaphorin 3A expression in neurons of the rat spinal cord and cerebral cortex after transection injury. *Acta neuropathologica,* 107**,** 250-6.

HATTORI, Y., MIYAKE, A., MIKAMI, T., OHTA, M. & ITOH, N. 1997a. Transient expression of FGF-5 mRNA in the rat cerebellar cortex during post-natal development. *Brain research. Molecular brain research,* 47**,** 262-6.

HATTORI, Y., YAMASAKI, M., KONISHI, M. & ITOH, N. 1997b. Spatially restricted expression of fibroblast growth factor-10 mRNA in the rat brain. *Brain research. Molecular brain research,* 47**,** 139-46.

HE, X., et al., 2012. Promotion of spinal cord regeneration by neural stem cell-secreted trimerized cell adhesion molecule L1. *PloS one*. 7**,** e46223.

HERRERA, J. J., NESIC, O. & NARAYANA, P. A. 2009. Reduced vascular endothelial growth factor expression in contusive spinal cord injury. *Journal of neurotrauma,* 26**,** 995-1003.

HERRERA, J. J., SUNDBERG, L. M., ZENTILIN, L., GIACCA, M. & NARAYANA, P. A. 2010. Sustained expression of vascular endothelial growth factor and angiopoietin-1 improves blood-spinal cord barrier integrity and functional recovery after spinal cord injury. *Journal of neurotrauma,* 27**,** 2067-76.

HILL, R. L., ZHANG, Y. P., BURKE, D. A., DEVRIES, W. H., ZHANG, Y., MAGNUSON, D. S., WHITTEMORE, S. R. & SHIELDS, C. B. 2009.

Anatomical and functional outcomes following a precise, graded, dorsal laceration spinal cord injury in C57BL/6 mice. *Journal of neurotrauma,* 26**,** 1-15.
HIRAOKA, N., ALLEN, E., APEL, I. J., GYETKO, M. R. & WEISS, S. J. 1998. Matrix metalloproteinases regulate neovascularization by acting as pericellular fibrinolysins. *Cell,* 95**,** 365-77.
HIRSCHI, K. K. & D'AMORE, P. A. 1996. Pericytes in the microvasculature. *Cardiovascular Research,* 32, 687-698.
HJORTH, J. T., CONNOR, R. M. & KEY, B. 2002. Role of hlx1 in zebrafish brain morphogenesis. *The International journal of developmental biology,* 46**,** 583-96.
HO, C., SASAKI, C. T. & PRASAD, M. L. 2013. Crystalloid granulomas of the parotid gland mimicking tumor: a case report with review of the literature. *International journal of surgical pathology,* 21, 282-6.
HOLNESS, C. L. & SIMMONS, D. L. 1993. Molecular cloning of CD68, a human macrophage marker related to lysosomal glycoproteins. *Blood,* 81, 1607-13.
HOOSHMAND, M. J., SONTAG, C. J., UCHIDA, N., TAMAKI, S., ANDERSON, A. J. & CUMMINGS, B. J. 2009. Analysis of host-mediated repair mechanisms after human CNS-stem cell transplantation for spinal cord injury: correlation of engraftment with recovery. *PloS one,* 4**,** e5871.
HORI, S., OHTSUKI, S., HOSOYA, K., NAKASHIMA, E. & TERASAKI, T. 2004. A pericyte-derived angiopoietin-1 multimeric complex induces occludin gene expression in brain capillary endothelial cells through Tie-2 activation in vitro. *Journal of neurochemistry,* 89**,** 503-13.
HOSSAIN, M. A., FIELDING, K. E., TRESCHER, W. H., HO, T., WILSON, M. A. & LATERRA, J. 1998. Human FGF-1 gene delivery protects against quinolinate-induced striatal and hippocampal injury in neonatal rats. *The European journal of neuroscience,* 10**,** 2490-9.
HURTADO, A., MARCILLO, A., FRYDEL, B., BUNGE, M. B., BRAMLETT, H. M. & DIETRICH, W. D. 2012. Anti-CD11d monoclonal antibody treatment for rat spinal cord compression injury. *Experimental neurology,* 233**,** 606-11.
HOUWELING, D. A., LANKHORST, A. J., GISPEN, W. H., BAR, P. R. & JOOSTEN, E. A. 1998a. Collagen containing neurotrophin-3 (NT-3) attracts regrowing injured corticospinal axons in the adult rat spinal cord and promotes partial functional recovery. *Experimental neurology,* 153**,** 49-59.
HOUWELING, D. A., VAN ASSELDONK, J. T., LANKHORST, A. J., HAMERS, F. P., MARTIN, D., BAR, P. R. & JOOSTEN, E. A. 1998b. Local application of collagen containing brain-derived neurotrophic factor decreases the loss of function after spinal cord injury in the adult rat. *Neuroscience letters,* 251**,** 193-6.
HSU, J. Y., MCKEON, R., GOUSSEV, S., WERB, Z., LEE, J. U., TRIVEDI, A. & NOBLE-HAEUSSLEIN, L. J. 2006. Matrix metalloproteinase-2 facilitates wound healing events that promote functional recovery after spinal cord injury. *The Journal of Neuroscience,* 26, 9841-50.
HSU, J. Y., BOURGUIGNON, L. Y., ADAMS, C. M., PEYROLLIER, K., ZHANG, H., FANDEL, T., CUN, C. L., WERB, Z. & NOBLE-HAEUSSLEIN, L. J. 2008. Matrix metalloproteinase-9 facilitates glial scar formation in the injured spinal cord. *The Journal of Neuroscience,* 28, 13467-77.
HSU, Y. C., LEE, D. C., CHEN, S. L., LIAO, W. C., LIN, J. W., CHIU, W. T. & CHIU, I. M. 2009. Brain-specific 1B promoter of FGF1 gene facilitates the isolation of

neural stem/progenitor cells with self-renewal and multipotent capacities. *Developmental dynamics : an official publication of the American Association of Anatomists,* 238**,** 302-14.

HU, G., RIORDAN, J. F. & VALLEE, B. L. 1994. Angiogenin promotes invasiveness of cultured endothelial cells by stimulation of cell-associated proteolytic activities. *Proceedings of the National Academy of Sciences of the United States of America,* 91**,** 12096-100.

HU, G. F., CHANG, S. I., RIORDAN, J. F. & VALLEE, B. L. 1991. An angiogenin-binding protein from endothelial cells. *Proceedings of the National Academy of Sciences of the United States of America,* 88**,** 2227-31.

HU, G. F., RIORDAN, J. F. & VALLEE, B. L. 1997. A putative angiogenin receptor in angiogenin-responsive human endothelial cells. *Proceedings of the National Academy of Sciences of the United States of America,* 94**,** 2204-9.

HU, G. F., STRYDOM, D. J., FETT, J. W., RIORDAN, J. F. & VALLEE, B. L. 1993. Actin is a binding protein for angiogenin. *Proceedings of the National Academy of Sciences of the United States of America,* 90**,** 1217-21.

HUANG, S. S. & HUANG, J. S. 2005. TGF-beta control of cell proliferation. *Journal of cellular biochemistry,* 96**,** 447-62.

HUANG, W. C., KUO, H. S., TSAI, M. J., MA, H., CHIU, C. W., HUANG, M. C., YANG, L. H., CHANG, P. T., LIN, Y. L., KUO, W. C., LEE, M. J., LIU, J. C. & CHENG, H. 2011. Adeno-associated virus-mediated human acidic fibroblast growth factor expression promotes functional recovery of spinal cord-contused rats. *The journal of gene medicine,* 13**,** 283-9.

HUGENHOLTZ, H. 2003. Methylprednisolone for acute spinal cord injury: not a standard of care. *CMAJ : Canadian Medical Association journal = journal de l'Association medicale canadienne,* 168**,** 1145-6.

HUGHES, C. C. 2008. Endothelial-stromal interactions in angiogenesis. *Current opinion in hematology,* 15**,** 204-9.

HUGHES, D. P., MARRON, M. B. & BRINDLE, N. P. 2003. The antiinflammatory endothelial tyrosine kinase Tie2 interacts with a novel nuclear factor-kappaB inhibitor ABIN-2. *Circulation research,* 92**,** 630-6.

HUNT, D., COFFIN, R. S. & ANDERSON, P. N. 2002. The Nogo receptor, its ligands and axonal regeneration in the spinal cord; a review. *Journal of neurocytology,* 31**,** 93-120.

HURLBERT, R. J. 2000. Methylprednisolone for acute spinal cord injury: an inappropriate standard of care. *Journal of neurosurgery,* 93**,** 1-7.

HYNES, R. O. 2002. Integrins: bidirectional, allosteric signaling machines. *Cell,* 110**,** 673-87.

INMAN, D. M. & STEWARD, O. 2003. Physical size does not determine the unique histopathological response seen in the injured mouse spinal cord. *Journal of neurotrauma,* 20**,** 33-42.

IANNOTTI, C., ZHANG, Y. P., SHIELDS, L. B., HAN, Y., BURKE, D. A., XU, X. M. & SHIELDS, C. B. 2006. Dural repair reduces connective tissue scar invasion and cystic cavity formation after acute spinal cord laceration injury in adult rats. *Journal of neurotrauma,* 23, 853-65.

IIHARA, K., HASIMOTO, N., TSUKAHARA, T., SAKATA, M., YANAMOTO, H. & TANGIGUCHI, T. 1997. Platelet-derived growth factor-BB, but not-AA, prevents delayed neuronal death after forebrain ischemia in rats. *Journal of Cerebral Blood Flow & Metabolism,* 17, 1097-1106.

INMAN, D. M. & STEWARD, O. 2003. Physical size does not determine the unique histopathological response seen in the injured mouse spinal cord. *Journal of neurotrauma,* 20, 33-42.
ITO, T., OHTORI, S., INOUE, G., KOSHI, T., DOYA, H., OZAWA, T., SAITO, T., MORIYA, H. & TAKAHASHI, K. 2007. Glial phosphorylated p38 MAP kinase mediates pain in a rat model of lumbar disc herniation and induces motor dysfunction in a rat model of lumbar spinal canal stenosis. *Spine,* 32**,** 159-67.
ITO, T. K., ISHII, G., CHIBA, H. & OCHIAI, A. 2007. The VEGF angiogenic switch of fibroblasts is regulated by MMP-7 from cancer cells. *Oncogene,* 26**,** 7194-203.
ITO, Y., WATANABE, T., NAGATOMO, S., SEKI, T., NIIMI, S. & ARIGA, T. 2007. Annexin A3-expressing cellular phenotypes emerge from necrotic lesion in the pericentral area in 2-acetylaminofluoren/carbon tetrachloride-treated rat livers. *Bioscience, biotechnology, and biochemistry,* 71**,** 3082-9.
IWASAKI, M., WILCOX, J. T., NISHIMURA, Y., ZWECKBERGER, K., SUZUKI, H., WANG, J., LIU, Y., KARADIMAS, S. K. & FEHLINGS, M. G. 2014. Synergistic effects of self-assembling peptide and neural stem/progenitor cells to promote tissue repair and forelimb functional recovery in cervical spinal cord injury. *Biomaterials*.
JACKSON, A. B., DIJKERS, M., DEVIVO, M. J. & POCZATEK, R. B. 2004. A demographic profile of new traumatic spinal cord injuries: change and stability over 30 years. *Archives of physical medicine and rehabilitation,* 85**,** 1740-8.
JACKSON, J. R., SEED, M. P., KIRCHER, C. H., WILLOUGHBY, D. A. & WINKLER, J. D. 1997. The codependence of angiogenesis and chronic inflammation. *FASEB journal : official publication of the Federation of American Societies for Experimental Biology,* 11, 457-65.
JACQUE, C. M., VINNER, C., KUJAS, M., RAOUL, M., RACADOT, J. & BAUMANN, N. A. 1978. Determination of glial fibrillary acidic protein (GFAP) in human brain tumors. *Journal of the neurological sciences,* 35, 147-55.
JAKEMAN, L. B., GUAN, Z., WEI, P., PONNAPPAN, R., DZWONCZYK, R., POPOVICH, P. G. & STOKES, B. T. 2000. Traumatic spinal cord injury produced by controlled contusion in mouse. *Journal of neurotrauma,* 17**,** 299-319.
JAMES, N. D., BARTUS, K., GRIST, J., BENNETT, D. L. H., MCMAHON, S. B. & BRADBURY, E. J. 2011. Conduction failure following spinal cord injury: functional and anatomical changes from acute to chronic stages. *The Journal of neuroscience : the official journal of the Society for Neuroscience,* 31**,** 18543-55.
JANG, J. W., LEE, J. K. & KIM, S. H. 2011. Activation of matrix metalloproteinases-9 after photothrombotic spinal cord injury model in rats. *Journal of Korean Neurosurgical Society,* 50**,** 288-92.
JAWORSKI, D. M. 2000. Differential regulation of tissue inhibitor of metalloproteinase mRNA expression in response to intracranial injury. *Glia,* 30**,** 199-208.
JAWORSKI, D. M., SOLOWAY, P., CATERINA, J. & FALLS, W. A. 2006. Tissue inhibitor of metalloproteinase-2(TIMP-2)-deficient mice display motor deficits. *Journal of neurobiology,* 66**,** 82-94.
JAUHIAINEN, S., HAKKINEN, S-K., TOIVANEN, P. I., HEINONEN, S. E., JYRKKANEN, H-K., KANSANEN, E., LEINONEN, H., LEVONEN, A-L. & YLA-HERTTUALA, S. 2011. Vascular endothelial growth factor (VEGF)-D

stimulates VEGF-A, Stanniocalcin-1, and Neuropilin-2 and has potent angiogenic effects. *Cell Biology/Signaling,* 31, 1617-1624.
JI, K. & TSIRKA, S. E. 2012. Inflammation modulates expression of laminin in the central nervous system following ischemic injury. *Journal of neuroinflammation,* 9**,** 159.
JIMENEZ HAMANN, M. C., TATOR, C. H. & SHOICHET, M. S. 2005. Injectable intrathecal delivery system for localized administration of EGF and FGF-2 to the injured rat spinal cord. *Experimental neurology,* 194**,** 106-19.
JIN, K. L., MAO, X. O. & GREENBERG, D. A. 2000. Vascular endothelial growth factor: direct neuroprotective effect in in vitro ischemia. *Proceedings of the National Academy of Sciences of the United States of America,* 97**,** 10242-7.
JOHNSON, D. H., FEHRENBACHER, L., NOVOTNY, W. F., HERBST, R. S., NEMUNAITIS, J. J., JABLONS, D. M., LANGER, C. J., DEVORE, R. F., 3RD, GAUDREAULT, J., DAMICO, L. A., HOLMGREN, E. & KABBINAVAR, F. 2004. Randomized phase II trial comparing bevacizumab plus carboplatin and paclitaxel with carboplatin and paclitaxel alone in previously untreated locally advanced or metastatic non-small-cell lung cancer. *Journal of clinical oncology : official journal of the American Society of Clinical Oncology,* 22**,** 2184-91.
JONES, L. L., LIU, Z., SHEN, J., WERNER, A., KREUTZBERG, G. W. & RAIVICH, G. 2000. Regulation of the cell adhesion molecule CD44 after nerve transection and direct trauma to the mouse brain. *The Journal of comparative neurology,* 426**,** 468-92.
JUNG, E. J., MOON, H. G., PARK, S. T., CHO, B. I., LEE, S. M., JEONG, C. Y., JU, Y. T., JEONG, S. H., LEE, Y. J., CHOI, S. K., HA, W. S., LEE, J. S., KANG, K. R. & HONG, S. C. 2010. Decreased annexin A3 expression correlates with tumor progression in papillary thyroid cancer. *Proteomics. Clinical applications,* 4**,** 528-37.
JUNKER, H., SUOFU, Y., VENZ, S., SASCAU, M., HERNDON, J. G., KESSLER, C., WALTHER, R. & POPA-WAGNER, A. 2007. Proteomic identification of an upregulated isoform of annexin A3 in the rat brain following reversible cerebral ischemia. *Glia,* 55**,** 1630-7.
JONKER, J. W., SUH, J. M., ATKINS, A. R., AHMADIAN, M., LI, P., WHYTE, J., HE, M., JUGUILON, H., YIN, Y. Q., PHILLIPS, C. T., YU, R. T., OLEFSKY, J. M., HENRY, R. R., DOWNES, M. & EVANS, R. M. 2012. A PPARgamma-FGF1 axis is required for adaptive adipose remodelling and metabolic homeostasis. *Nature,* 485**,** 391-4.
JOOSTEN, E. A., BAR, P. R. & GISPEN, W. H. 1995. Directional regrowth of lesioned corticospinal tract axons in adult rat spinal cord. *Neuroscience,* 69**,** 619-26.
KAGI, J. H. 1991. Overview of metallothionein. *Methods in enzymology,* 205**,** 613-26.
KALIL, K. & REH, T. 1979. Regrowth of severed axons in the neonatal central nervous system: establishment of normal connections. *Science,* 205**,** 1158-61.
KANEKO, S., IWANAMI, A., NAKAMURA, M., KISHINO, A., KIKUCHI, K., SHIBATA, S., OKANO, H. J., IKEGAMI, T., MORIYA, A., KONISHI, O., NAKAYAMA, C., KUMAGAI, K., KIMURA, T., SATO, Y., GOSHIMA, Y., TANIGUCHI, M., ITO, M., HE, Z., TOYAMA, Y. & OKANO, H. 2006. A selective Sema3A inhibitor enhances regenerative responses and functional recovery of the injured spinal cord. *Nature medicine,* 12**,** 1380-9.

KANG, K. N., LEE, J. Y., KIM DA, Y., LEE, B. N., AHN, H. H., LEE, B., KHANG, G., PARK, S. R., MIN, B. H., KIM, J. H., LEE, H. B. & KIM, M. S. 2011. Regeneration of completely transected spinal cord using scaffold of poly(D,L-lactide-co-glycolide)/small intestinal submucosa seeded with rat bone marrow stem cells. *Tissue engineering. Part A,* 17**,** 2143-52.

KAO, C. C., CHANG, L. W. & BLOODWORTH, J. M., JR. 1977. The mechanism of spinal cord cavitation follwing spinal cord transection. Part 2. Electron microscopic observations. *Journal of neurosurgery,* 46**,** 745-56.

KARÉN, J. 2010, The role of microvascular pericytes in the generation of pro-fibrotic connective tissue cells. Investigations *in vitro* and in reactive tissues *in vivo*. *Digital Comprehensive Summaries of Uppsala Dissertations from the Faculty of Medicine,* 6183 38pp.

KASHIWAGI, M., OHBA, M., CHIDA, K. & KUROKI, T. 2002. Protein kinase C eta (PKC eta): its involvement in keratinocyte differentiation. *Journal of biochemistry,* 132**,** 853-7.

KASTIN, A. J., AKERSTROM, V., HACKLER, L. & PAN, W. 2003. Different mechanisms influencing permeation of PDGF-AA and PDGF-BB across the blood-brain barrier. *Journal of neurochemistry,* 87**,** 7-12.

KATAKKAR, S. B. 2012. A triple negative breast cancer: what it is not! *Breast cancer,* 4**,** 21-3.

KAWASAKI, Y., XU, Z. Z., WANG, X., PARK, J. Y., ZHUANG, Z. Y., TAN, P. H., GAO, Y. J., ROY, K., CORFAS, G., LO, E. H. & JI, R. R. 2008. Distinct roles of matrix metalloproteases in the early- and late-phase development of neuropathic pain. *Nature medicine,* 14**,** 331-6.

KENNEDY, M. A., RAYNER, J. C. & MORRIS, C. M. 1994. Genomic structure, promoter sequence, and revised translation of human homeobox gene HLX1. *Genomics,* 22**,** 348-55.

KESSLER, C., JUNKER, H., BALSEANU, T. A., OPREA, B., PIRICI, D., MOGOANTA, L. & POPA-WAGNER, A. 2008. Annexin A3 expression after stroke in the aged rat brain. *Romanian journal of morphology and embryology = Revue roumaine de morphologie et embryologie,* 49**,** 27-35.

KHAIBULLINA, A. A., ROSENSTEIN, J. M. & KRUM, J. M. 2004. Vascular endothelial growth factor promotes neurite maturation in primary CNS neuronal cultures. *Brain research. Developmental brain research,* 148**,** 59-68.

KHALIL, N. 1999. TGF-beta: from latent to active. *Microbes and infection / Institut Pasteur,* 1**,** 1255-63.

KHALIL, N., BEREZNAY, O., SPORN, M. & GREENBERG, A. H. 1989. Macrophage production of transforming growth factor beta and fibroblast collagen synthesis in chronic pulmonary inflammation. *The Journal of experimental medicine,* 170**,** 727-37.

KIERAN, D., SEBASTIA, J., GREENWAY, M. J., KING, M. A., CONNAUGHTON, D., CONCANNON, C. G., FENNER, B., HARDIMAN, O. & PREHN, J. H. 2008. Control of motoneuron survival by angiogenin. *The Journal of neuroscience : the official journal of the Society for Neuroscience,* 28**,** 14056-61.

KIGERL, K. A., GENSEL, C. J., ANKENY, D. P., ALEXANDER, J. K., DONNELLY, D. J. & POPOVICH, P. G. 2009. Identification of two distinct macrophage subsets with divergent effects causing either neurotoxicity in the injured mouse spinal cord. *The Journal of Neuroscience,* 29, 13435-13444.

KIKUCHI, S., GRIFFIN, C. T., WANG, S. S. & BISSELL, D. M. 2005. Role of CD44 in epithelial wound repair: migration of rat hepatic stellate cells utilizes

hyaluronic acid and CD44v6. *The Journal of biological chemistry,* 280**,** 15398-404.
KIM, H., LEE, J. M., PARK, J. S., JO, S. A., KIM, Y. O., KIM, C. W. & JO, I. 2008. Dexamethasone coordinately regulates angiopoietin-1 and VEGF: a mechanism of glucocorticoid-induced stabilization of blood-brain barrier. *Biochemical and biophysical research communications,* 372**,** 243-8.
KIM, H. M., HWANG, D. H., LEE, J. E., KIM, S. U. & KIM, B. G. 2009. Ex vivo VEGF delivery by neural stem cells enhances proliferation of glial progenitors, angiogenesis, and tissue sparing after spinal cord injury. *PloS one,* 4**,** e4987.
KIM, H. M., KANG, D. K., KIM, H. Y., KANG, S. S. & CHANG, S. I. 2007. Angiogenin-induced protein kinase B/Akt activation is necessary for angiogenesis but is independent of nuclear translocation of angiogenin in HUVE cells. *Biochemical and biophysical research communications,* 352**,** 509-13.
KIM, I., KIM, H. G., SO, J. N., KIM, J. H., KWAK, H. J. & KOH, G. Y. 2000. Angiopoietin-1 regulates endothelial cell survival through the phosphatidylinositol 3'-Kinase/Akt signal transduction pathway. *Circulation research,* 86**,** 24-9.
KIM, I., MOON, S. O., PARK, S. K., CHAE, S. W. & KOH, G. Y. 2001. Angiopoietin-1 reduces VEGF-stimulated leukocyte adhesion to endothelial cells by reducing ICAM-1, VCAM-1, and E-selectin expression. *Circulation research,* 89**,** 477-9.
KIM, Y. J., KIM DO, Y., SEO, J. W., LEE, S. A., HWANG, J. J., KIM, H. J. & LEE, K. Y. 2013. A Case of Congenital Cystic Adenomatoid Malformation Infected with Mycobacterium avium-intracellulare Complex. *Tuberculosis and respiratory diseases,* 74, 28-31.
KISHIKAWA, H., WU, D. & HU, G. F. 2008. Targeting angiogenin in therapy of amyotropic lateral sclerosis. *Expert opinion on therapeutic targets,* 12**,** 1229-42.
KISHIMOTO, K., LIU, S., TSUJI, T., OLSON, K. A. & HU, G. F. 2005. Endogenous angiogenin in endothelial cells is a general requirement for cell proliferation and angiogenesis. *Oncogene,* 24**,** 445-56.
KLOSTERMANN, A., LOHRUM, M., ADAMS, R. H. & PUSCHEL, A. W. 1998. The chemorepulsive activity of the axonal guidance signal semaphorin D requires dimerization. *The Journal of biological chemistry,* 273**,** 7326-31.
KOCH, A. E., POLVERINI, P. J. & LEIBOVICH, S. J. 1986. Induction of neovascularization by activated human monocytes. *Journal of leukocyte biology,* 39, 233-8.
KOCH, M., OLSON, P. F., ALBUS, A., JIN, W., HUNTER, D. D., BRUNKEN, W. J., BURGESON, R. E. & CHAMPLIAUD, M. F. 1999. Characterization and expression of the laminin gamma3 chain: a novel, non-basement membrane-associated, laminin chain. *The Journal of cell biology,* 145**,** 605-18.
KOGERMAN, P., SY, M. S. & CULP, L. A. 1997. Counter-selection for over-expressed human CD44s in primary tumors versus lung metastases in a mouse fibrosarcoma model. *Oncogene,* 15**,** 1407-16.
KOHTA, M., KOHMURA, E. & YAMASHITA, T. 2009. Inhibition of TGF-beta1 promotes functional recovery after spinal cord injury. *Neuroscience research,* 65**,** 393-401.
KOLLERMANN, J., SCHLOMM, T., BANG, H., SCHWALL, G. P., VON EICHEL-STREIBER, C., SIMON, R., SCHOSTAK, M., HULAND, H., BERG, W., SAUTER, G., KLOCKER, H. & SCHRATTENHOLZ, A. 2008. Expression and

prognostic relevance of annexin A3 in prostate cancer. *European urology,* 54**,** 1314-23.
KOLODKIN, A. L., MATTHES, D. J. & GOODMAN, C. S. 1993. The semaphorin genes encode a family of transmembrane and secreted growth cone guidance molecules. *Cell,* 75**,** 1389-99.
KOLTA, A., DIOP, L. & READER, T. A. 1987. Noradrenergic effects on rat visual cortex: single-cell microiontophoretic studies of alpha-2 adrenergic receptors. *Life sciences,* 41**,** 281-9.
KONISHI, H., NAMIKAWA, K. & KIYAMA, H. 2006. Annexin III implicated in the microglial response to motor nerve injury. *Glia,* 53**,** 723-32.
KONYA, D., GERCEK, A., AKAKIN, A., AKAKIN, D., TURAL, S., CETINEL, S., OZGEN, S. & PAMIR, M. N. 2008. The effects of inflammatory response associated with traumatic spinal cord injury in cutaneous wound healing and on expression of transforming growth factor-beta1 (TGF-beta1) and platelet-derived growth factor (PDGF)-A at the wound site in rats. *Growth factors,* 26**,** 74-9.
KOPPEL, A. M. & RAPER, J. A. 1998. Collapsin-1 covalently dimerizes, and dimerization is necessary for collapsing activity. *The Journal of biological chemistry,* 273**,** 15708-13.
KORIYAMA, Y., SUGITANI, K., OGAI, K. & KATO, S. 2014. Neuritogenic Activity of Trichostatin A in Adult Rat Retinal Ganglion Cells Through Acetylation of Histone H3 Lysine 9 and RARbeta Induction. *Journal of pharmacological sciences,* 124**,** 112-6.
KORIYAMA, Y., TAKAGI, Y., CHIBA, K., YAMAZAKI, M., SUGITANI, K., ARAI, K., SUZUKI, H. & KATO, S. 2013. Requirement of retinoic acid receptor beta for genipin derivative-induced optic nerve regeneration in adult rat retina. *PloS one,* 8**,** e71252.
KOUTROUBAKIS, I. E., TSIOLAKIDOU, G., KARMIRIS, K. & KOUROUMALIS, E. A. 2006. Role of angiogenesis in inflammatory bowel disease. *Inflammatory bowel diseases,* 12, 515-23.
KRAJACIC, A., WEISHAUPT, N., GIRGIS, J., TETZLAFF, W. & FOUAD, K. 2010. Training-induced plasticity in rats with cervical spinal cord injury: effects and side effects. *Behavioural brain research,* 214**,** 323-31.
KRASSIOUKOV, A. V., FURLAN, J. C. & FEHLINGS, M. G. 2003. Autonomic dysreflexia in acute spinal cord injury: an under-recognized clinical entity. *Journal of neurotrauma,* 20**,** 707-16.
KRITIS, A., KAPOUKRANIDOU, D., MICHAILIDOU, B., HATZISOTIRIOU, A. & ALBANI, M. 2010. Sciatic nerve crush evokes a biphasic TGF-beta and decorin modulation in the rat spinal cord. *Hippokratia,* 14**,** 37-41.
KRUPINSKI, J., ISSA, R., BUJNY, T., SLEVIN, M., KUMAR, P., KUMAR, S. & KALUZA, J. 1997. A putative role for platelet-derived growth factor in angiogenesis and neuroprotection after ischemic stroke in humans. *Stroke; a journal of cerebral circulation,* 28**,** 564-73.
KUNDI, S., BICKNELL, R. & AHMED, Z. 2013a. The role of angiogenic and wound-healing factors after spinal cord injury in mammals. *Neuroscience research,* 76**,** 1-9.
KUNDI, S., BICKNELL, R. & AHMED, Z. 2013b. The role of angiogenic and wound-healing factors after spinal cord injury in mammals. *Neuroscience research,* 76**,** 1-9.

KUNZ-SCHUGHART, L. A., WEBER, A., REHLI, M., GOTTFRIED, E., BROCKHOFF, G., KRAUSE, S. W., ANDREESEN, R. & KREUTZ, M. 2003. [The "classical" macrophage marker CD68 is strongly expressed in primary human fibroblasts]. *Verhandlungen der Deutschen Gesellschaft fur Pathologie,* 87, 215-23.

KURACHI, K., DAVIE, E. W., STRYDOM, D. J., RIORDAN, J. F. & VALLEE, B. L. 1985. Sequence of the cDNA and gene for angiogenin, a human angiogenesis factor. *Biochemistry,* 24**,** 5494-9.

LAGORD, C., BERRY, M. & LOGAN, A. 2002. Expression of TGFbeta2 but not TGFbeta1 correlates with the deposition of scar tissue in the lesioned spinal cord. *Molecular and cellular neurosciences,* 20**,** 69-92.

LAM, S., BATZDORF, U. & BERGSNEIDER, M. 2008. Thecal shunt placement for treatment of obstructive primary syringomyelia. *Journal of Neurosurgery-Spine,* 9**,** 581-588.

LAWRENCE, D. G. & KUYPERS, H. G. 1968. The functional organization of the motor system in the monkey. I. The effects of bilateral pyramidal lesions. *Brain,* 91, 1-14.

LE CABEC, V. & MARIDONNEAU-PARINI, I. 1994. Annexin 3 is associated with cytoplasmic granules in neutrophils and monocytes and translocates to the plasma membrane in activated cells. *The Biochemical journal,* 303 (Pt 2)**,** 481-7.

LE CABEC, V., RUSSO-MARIE, F. & MARIDONNEAU-PARINI, I. 1992. Differential expression of two forms of annexin 3 in human neutrophils and monocytes and along their differentiation. *Biochemical and biophysical research communications,* 189**,** 1471-6.

LEE, B. B., CRIPPS, R. A., FITZHARRIS, M. & WING, P. C. 2014. The global map for traumatic spinal cord injury epidemiology: update 2011, global incidence rate. *Spinal cord,* 52**,** 110-6.

LEE, J. H., CHOI, C. B., CHUNG, D. J., KANG, E. H., CHANG, H. S., HWANG, S. H., HAN, H., CHOE, B. Y., SUR, J. H., LEE, S. Y. & KIM, H. Y. 2008. Development of an improved canine model of percutaneous spinal cord compression injury by balloon catheter. *Journal of neuroscience methods,* 167**,** 310-6.

LEE, J. Y., KIM, H. S., CHOI, H. Y., OH, T. H., JU, B. G. & YUNE, T. Y. 2012. Valproic acid attenuates blood-spinal cord barrier disruption by inhibiting matrix metalloprotease-9 activity and improves functional recovery after spinal cord injury. *Journal of neurochemistry,* 121**,** 818-29.

LEE, J. Y., KIM, H. S., OH, T. H. & YUNE, T. Y. 2010. Ethanol Extract of Bupleurum falcatum Improves Functional Recovery by Inhibiting Matrix Metalloproteinases-2 and -9 Activation and Inflammation after Spinal Cord Injury. *Experimental neurobiology,* 19**,** 146-54.

LEE, M. A., PALACE, J., STABLER, G., FORD, J., GEARING, A. & MILLER, K. 1999. Serum gelatinase B, TIMP-1 and TIMP-2 levels in multiple sclerosis. A longitudinal clinical and MRI study. *Brain : a journal of neurology,* 122 (Pt 2)**,** 191-7.

LEE, M. J., CHEN, C. J., HUANG, W. C., HUANG, M. C., CHANG, W. C., KUO, H. S., TSAI, M. J., LIN, Y. L. & CHENG, H. 2011. Regulation of chondroitin sulphate proteoglycan and reactive gliosis after spinal cord transection: effects of peripheral nerve graft and fibroblast growth factor 1. *Neuropathology and applied neurobiology,* 37**,** 585-99.

LEE, P. C., SALYAPONGSE, A. N., BRAGDON, G. A., SHEARS, L. L., 2ND, WATKINS, S. C., EDINGTON, H. D. & BILLIAR, T. R. 1999. Impaired wound healing and angiogenesis in eNOS-deficient mice. *The American journal of physiology,* 277**,** H1600-8.

LEE, S. I., JEONG, S. R., KANG, Y. M., HAN, D. H., JIN, B. K., NAMGUNG, U. & KIM, B. G. 2010. Endogenous expression of interleukin-4 regulates macrophage activation and confines cavity formation after traumatic spinal cord injury. *Journal of neuroscience research,* 88, 2409-19.

LEE, S. W., KIM, W. J., JUN, H. O., CHOI, Y. K. & KIM, K. W. 2009. Angiopoietin-1 reduces vascular endothelial growth factor-induced brain endothelial permeability via upregulation of ZO-2. *International journal of molecular medicine,* 23**,** 279-84.

LEMON, R. N. & GRIFFITHS, J. 2005. Comparing the function of the corticospinal system in different species: organizational differences for motor specialization? *Muscle Nerve,* 32, 261-279.

LETELLIER, E., KUMAR, S., SANCHO-MARTINEZ, I., KRAUTH, S., FUNKE-KAISER, A., LAUDENKLOS, S., KONECKI, K., KLUSSMANN, S., CORSINI, N. S., KLEBER, S., DROST, N., NEUMANN, A., LEVI-STRAUSS, M., BRORS, B., GRETZ, N., EDLER, L., FISCHER, C., HILL, O., THIEMANN, M., BIGLARI, B., KARRAY, S. & MARTIN-VILLALBA, A. 2010. CD95-ligand on peripheral myeloid cells activates Syk kinase to trigger their recruitment to the inflammatory site. *Immunity,* 32**,** 240-52.

LEVITZKI, A. 2004. PDGF receptor kinase inhibitors for the treatment of PDGF driven diseases. *Cytokine & growth factor reviews,* 15**,** 229-35.

LEVY, A. P. 1998. Hypoxic regulation of VEGF mRNA stability by RNA-binding proteins. *Trends in cardiovascular medicine,* 8**,** 246-50.

LI, H., NOURBAKHSH, B., SAFAVI, F., LI, K., XU, H., CULLIMORE, M., ZHOU, F., ZHANG, G. & ROSTAMI, A. 2011a. Kit (W-sh) mice develop earlier and more severe experimental autoimmune encephalomyelitis due to absence of immune suppression. *Journal of immunology,* 187**,** 274-82.

LI, J., LUO, M., XU, X. & SHENG, W. 2012. Association between 1425G/A SNP in PRKCH and ischemic stroke among Chinese and Japanese populations: a meta-analysis including 3686 cases and 4589 controls. *Neuroscience letters,* 506**,** 55-8.

LI, Q., AGNO, J. E., EDSON, M. A., NAGARAJA, A. K., NAGASHIMA, T. & MATZUK, M. M. 2011b. Transforming growth factor beta receptor type 1 is essential for female reproductive tract integrity and function. *PLoS genetics,* 7**,** e1002320.

LI, Y., KIMURA, T., LAITY, J. H. & ANDREWS, G. K. 2006. The zinc-sensing mechanism of mouse MTF-1 involves linker peptides between the zinc fingers. *Molecular and cellular biology,* 26**,** 5580-7.

LIESI, P., KAAKKOLA, S., DAHL, D. & VAHERI, A. 1984. Laminin is induced in astrocytes of adult brain by injury. *The EMBO journal,* 3**,** 683-6.

LIM, J. H., JUNG, C. S., BYEON, Y. E., KIM, W. H., YOON, J. H., KANG, K. S. & KWEON, O. K. 2007. Establishment of a canine spinal cord injury model induced by epidural balloon compression. *Journal of veterinary science,* 8**,** 89-94.

LIN, R., TAYLOR, B. V., SIMPSON, S., JR., CHARLESWORTH, J., PONSONBY, A. L., PITTAS, F., DWYER, T. & VAN DER MEI, I. A. 2014. Novel modulating effects of PKC family genes on the relationship between serum vitamin D and

relapse in multiple sclerosis. *Journal of neurology, neurosurgery, and psychiatry,* 85**,** 399-404.
LINDHOLM, T., SKOLD, M. K., SUNESON, A., CARLSTEDT, T., CULLHEIM, S. & RISLING, M. 2004. Semaphorin and neuropilin expression in motoneurons after intraspinal motoneuron axotomy. *Neuroreport,* 15**,** 649-54.
LINDSEY, A. E., et al., 2000. An analysis of changes in sensory thresholds to mild tactile and cold stimuli after experimental spinal cord injury in the rat. *Neurorehabilitation and neural repair*. 14**,** 287-300.
LIOU, J. T., SUM, D. C., LIU, F. C., MAO, C. C., LAI, Y. S. & DAY, Y. J. 2013. Spatial and temporal analysis of nociception-related spinal cord matrix metalloproteinase expression in a murine neuropathic pain model. *Journal of the Chinese Medical Association : JCMA,* 76**,** 201-10.
LIU, H., KATO, Y., ERZINGER, S. A., KIRIAKOVA, G. M., QIAN, Y., PALMIERI, D., STEEG, P. S. & PRICE, J. E. 2012. The role of MMP-1 in breast cancer growth and metastasis to the brain in a xenograft model. *BMC cancer,* 12**,** 583.
LIU, H. & SHUBAYEV, V. I. 2011. Matrix metalloproteinase-9 controls proliferation of NG2+ progenitor cells immediately after spinal cord injury. *Experimental neurology,* 231**,** 236-46.
LIU, H. Y., JIA, X. Q., GAO, L. X. & MA, Y. Y. 2012. Hepatocyte growth factor regulates HLX1 gene expression to modulate HTR-8/SVneo trophoblast cells. *Reproductive biology and endocrinology : RB&E,* 10**,** 83.
LIU, J., JOHNSON, K., LI, J., PIAMONTE, V., STEFFY, B. M., HSIEH, M. H., NG, N., ZHANG, J., WALKER, J. R., DING, S., MUNEOKA, K., WU, X., GLYNNE, R. & SCHULTZ, P. G. 2011a. Regenerative phenotype in mice with a point mutation in transforming growth factor beta type I receptor (TGFBR1). *Proceedings of the National Academy of Sciences of the United States of America,* 108**,** 14560-5.
LIU, X., NUGOLI, M., LAFERRIERE, J., SALEH, S. M., RODRIGUE-GERVAIS, I. G., SALEH, M., PARK, M., HALLETT, M. T., MULLER, W. J. & GIGUERE, V. 2011b. Stromal retinoic acid receptor beta promotes mammary gland tumorigenesis. *Proceedings of the National Academy of Sciences of the United States of America,* 108**,** 774-9.
LIU, X., BOLTEUS, A. J., BALKIN, D. M., HENSCHEL, O. & BORDEY, A. 2006. GFAP-expressing cells in the postnatal subventricular zone display a unique glial phenotype intermediate between radial glia and astrocytes. *Glia,* 54, 394-410.
LIU, X., SHAN, Y. & XUE, B. 2013. Int7G24A polymorphism (rs334354) and cancer risk. *Archives of medical science : AMS,* 9**,** 3-7.
LIU, Y. F., XIAO, Z. Q., LI, M. X., LI, M. Y., ZHANG, P. F., LI, C., LI, F., CHEN, Y. H., YI, H., YAO, H. X. & CHEN, Z. C. 2009. Quantitative proteome analysis reveals annexin A3 as a novel biomarker in lung adenocarcinoma. *The Journal of pathology,* 217**,** 54-64.
LIU, S., YU, D., XU, Z. P., RIORDAN, J. F. & HU, G. F. 2001. Angiogenin activates Erk1/2 in human umbilical vein endothelial cells. *Biochemical and biophysical research communications,* 287**,** 305-10.
LIU, W. G., WANG, Z. Y. & HUANG, Z. S. 2011. Bone marrow-derived mesenchymal stem cells expressing the bFGF transgene promote axon regeneration and functional recovery after spinal cord injury in rats. *Neurological research,* 33**,** 686-93.

LIU, Y., FIGLEY, S., SPRATT, S. K., LEE, G., ANDO, D., SUROSKY, R. & FEHLINGS, M. G. 2010. An engineered transcription factor which activates VEGF-A enhances recovery after spinal cord injury. *Neurobiology of Disease,* 37**,** 384-393.

LO, T. P., JR., CHO, K. S., GARG, M. S., LYNCH, M. P., MARCILLO, A. E., KOIVISTO, D. L., STAGG, M., ABRIL, R. M., PATEL, S., DIETRICH, W. D. & PEARSE, D. D. 2009. Systemic hypothermia improves histological and functional outcome after cervical spinal cord contusion in rats. *The Journal of comparative neurology,* 514**,** 433-48.

LODISH, H., BERK, A., ZIPURSKY, S. & AL., E. 2000. Molecular Cell Biology. 4th edition. *New York: W. H. Freeman*.

LOEYS, B. L., SCHWARZE, U., HOLM, T., CALLEWAERT, B. L., THOMAS, G. H., PANNU, H., DE BACKER, J. F., OSWALD, G. L., SYMOENS, S., MANOUVRIER, S., ROBERTS, A. E., FARAVELLI, F., GRECO, M. A., PYERITZ, R. E., MILEWICZ, D. M., COUCKE, P. J., CAMERON, D. E., BRAVERMAN, A. C., BYERS, P. H., DE PAEPE, A. M. & DIETZ, H. C. 2006. Aneurysm syndromes caused by mutations in the TGF-beta receptor. *The New England journal of medicine,* 355**,** 788-98.

LOPEZ, S., PRIVAT, A., BERNARD, N., OHANNA, F., VERGNES, C. & CAPDEVILA, X. 2004. Intrathecal bupivacaine protects against extension of lesions in an acute photochemical spinal cord injury model. *Canadian journal of anaesthesia = Journal canadien d'anesthesie,* 51**,** 364-72.

LOSSINSKY, A. S., WISNIEWSKI, H. M., DAMBSKA, M. & MOSSAKOWSKI, M. J. 1997. Ultrastructural studies of PECAM-1/CD31 expression in the developing mouse blood-brain barrier with the application of a pre-embedding technique. *Folia neuropathologica / Association of Polish Neuropathologists and Medical Research Centre, Polish Academy of Sciences,* 35**,** 163-70.

LOY, D. N., CRAWFORD, C. H., DARNALL, J. B., BURKE, D. A., ONIFER, S. M. & WHITTEMORE, S. R. 2002. Temporal progression of angiogenesis and basal lamina deposition after contusive spinal cord injury in the adult rat. *The Journal of comparative neurology,* 445**,** 308-24.

LUCKHEERAM, R. V., ZHOU, R., VERMA, A. D. & XIA, B. 2012. CD4(+)T cells: differentiation and functions. *Clinical & developmental immunology,* 2012, 925135.

LUO, Y., RAIBLE, D. & RAPER, J. A. 1993. Collapsin: a protein in brain that induces the collapse and paralysis of neuronal growth cones. *Cell,* 75**,** 217-27.

LUTTON, C., YOUNG, Y. W., WILLIAMS, R., MEEDENIYA, A. C., MACKAY-SIM, A. & GOSS, B. 2012. Combined VEGF and PDGF treatment reduces secondary degeneration after spinal cord injury. *Journal of neurotrauma,* 29**,** 957-70.

MA, M., BASSO, D. M., WALTERS, P., STOKES, B. T. & JAKEMAN, L. B. 2001. Behavioral and histological outcomes following graded spinal cord contusion injury in the C57Bl/6 mouse. *Experimental neurology,* 169**,** 239-54.

MA, W., FITZGERALD, W., LIU, Q. Y., O'SHAUGHNESSY, T. J., MARIC, D., LIN, H. J., ALKON, D. L. & BARKER, J. L. 2004. CNS stem and progenitor cell differentiation into functional neuronal circuits in three-dimensional collagen gels. *Experimental neurology,* 190**,** 276-88.

MADIAI, F. & HACKSHAW, K. 2002. Expression of the mouse FGF-1 and FGF-1.A mRNAs during embryonic development and in the aging heart. *Research communications in molecular pathology and pharmacology,* 112**,** 139-44.

MAHARAJ, A. S., SAINT-GENIEZ, M., MALDONADO, A. E. & D'AMORE, P. A. 2006. Vascular endothelial growth factor localization in the adult. *The American journal of pathology,* 168**,** 639-48.

MAHLKNECHT, P., STEMBERGER, S., SPRENGER, F., RAINER, J., HAMETNER, E., KIRCHMAIR, R., GRABMER, C., SCHERFLER, C., WENNING, G. K., SEPPI, K., POEWE, W. & REINDL, M. 2012. An antibody microarray analysis of serum cytokines in neurodegenerative Parkinsonian syndromes. *Proteome science,* 10**,** 71.

MAISONPIERRE, P. C., SURI, C., JONES, P. F., BARTUNKOVA, S., WIEGAND, S. J., RADZIEJEWSKI, C., COMPTON, D., MCCLAIN, J., ALDRICH, T. H., PAPADOPOULOS, N., DALY, T. J., DAVIS, S., SATO, T. N. & YANCOPOULOS, G. D. 1997. Angiopoietin-2, a natural antagonist for Tie2 that disrupts in vivo angiogenesis. *Science,* 277**,** 55-60.

MAJCZYNSKI, H. & SLAWINSKA, U. 2007. Locomotor recovery after thoracic spinal cord lesions in cats, rats and humans. *Acta neurobiologiae experimentalis,* 67**,** 235-57.

MAMMEN, E. F. 1992. Pathogenesis of venous thrombosis. *Chest,* 102**,** 640S-644S.

MANDRIOTA, S. J. & PEPPER, M. S. 1998. Regulation of angiopoietin-2 mRNA levels in bovine microvascular endothelial cells by cytokines and hypoxia. *Circulation research,* 83**,** 852-9.

MANI, N., KHAIBULLINA, A., KRUM, J. M. & ROSENSTEIN, J. M. 2005. Astrocyte growth effects of vascular endothelial growth factor (VEGF) application to perinatal neocortical explants: receptor mediation and signal transduction pathways. *Experimental neurology,* 192**,** 394-406.

MANTONVANI, A., SICA, A., SOZZANI, S., ALLAVENA, P., VECCHI, A. & LOCATI, M. 2004. The chemokine system in diverse forms of macrophage activation and polarization. *Trends in Immunology,* 28, 677-686.

MAO, L., WANG, H., QIAO, L. & WANG, X. 2010a. Disruption of Nrf2 enhances the upregulation of nuclear factor-kappaB activity, tumor necrosis factor-alpha, and matrix metalloproteinase-9 after spinal cord injury in mice. *Mediators of inflammation,* 2010**,** 238321.

MAO, L., WANG, H. D., WANG, X. L., QIAO, L. & YIN, H. X. 2010b. [Influence of nuclear factor erythroid 2-related factor 2 genotype on tumor necrosis factor-alpha and metalloproteinase-9 expression in spinal cord after spinal cord injury in mice]. *Zhonghua wai ke za zhi [Chinese journal of surgery],* 48**,** 1569-72.

MAO, L., WANG, H. D., WANG, X. L., QIAO, L. & YIN, H. X. 2010c. Sulforaphane attenuates matrix metalloproteinase-9 expression following spinal cord injury in mice. *Annals of clinical and laboratory science,* 40**,** 354-60.

MAHARAJ, A. S. R., WALSHE, T. E., SAINT-GENIEZ, M., VENKATESHA, S., MALDONADO, A. E., HIMES, N. C., MATHARU, K. S., KARUMANCHI, S. A. D'AMORE, P. A. 2008. VEGF and TGF-β are required for the maintenance of the choroid plexus and ependyma. *Journal of Experimental Medicine*, 205, 491-501.

MARGOLIS, D. J., MORRIS, L. M., PAPADOPOULOS, M., WEINBERG, L., FILIP, J. C., STEPHANIE, A. L., VAIKUNTH, S. S. & CROMBLEHOLME, T. M. 2009. Phase 1 Study of H5.020CMV.PDGF-β to Treat Leg Ulcer Disease. *Molecular Therapy,* 17, 1822-1829.

MARGOSHES, M. & VALLEE, B. L. 1957. A Cadmium Protein from Equine Kidney Cortex. *Journal of the American Chemical Society,* 79**,** 4813-4814.

MAROM, E. M., MARTINEZ, C. H., TRUONG, M. T., LEI, X., SABLOFF, B. S., MUNDEN, R. F., GLADISH, G. W., HERBST, R. S., MORICE, R. C., STEWART, D. J., JIMENEZ, C. A., BLUMENSCHEIN, G. R., JR. & ONN, A. 2008. Tumor cavitation during therapy with antiangiogenesis agents in patients with lung cancer. *Journal of thoracic oncology : official publication of the International Association for the Study of Lung Cancer,* 3**,** 351-7.

MARSH, D. R., WONG, S. T., MEAKIN, S. O., MACDONALD, J. I., HAMILTON, E. F. & WEAVER, L. C. 2002. Neutralizing intraspinal nerve growth factor with a trkA-IgG fusion protein blocks the development of autonomic dysreflexia in a clip-compression model of spinal cord injury. *Journal of neurotrauma,* 19**,** 1531-41.

MARTEAU, L., PACARY, E., VALABLE, S., BERNAUDIN, M., GUILLEMOT, F. & PETIT, E. 2011. Angiopoietin-2 regulates cortical neurogenesis in the developing telencephalon. *Cerebral cortex,* 21**,** 1695-702.

MARTI, H. J., BERNAUDIN, M., BELLAIL, A., SCHOCH, H., EULER, M., PETIT, E. & RISAU, W. 2000. Hypoxia-induced vascular endothelial growth factor expression precedes neovascularization after cerebral ischemia. *The American journal of pathology,* 156**,** 965-76.

MARTIN, P. M. & HUSSAINI, I. M. 2005. PKC eta as a therapeutic target in glioblastoma multiforme. *Expert opinion on therapeutic targets,* 9**,** 299-313.

MASSAGUE, J., BLAIN, S. W. & LO, R. S. 2000. TGFbeta signaling in growth control, cancer, and heritable disorders. *Cell,* 103**,** 295-309.

MASSAGUE, J. 1992. Receptors for the TGF-beta family. *Cell,* 69**,** 1067-70.

MASSAGUE, J. 1998. TGF-beta signal transduction. *Annual review of biochemistry,* 67**,** 753-91.

MATSUMOTO, T., IMAGAMA, S., HIRANO, K., OHGOMORI, T., NATORI, T., KOBAYASHI, K., MURAMOTO, A., ISHIGURO, N. & KADOMATSU, K. 2012. CD44 expression in astrocytes and microglia is associated with ALS progression in a mouse model. *Neuroscience letters,* 520**,** 115-20.

MATSUZAKI, H., TAMATANI, M., YAMAGUCHI, A., NAMIKAWA, K., KIYAMA, H., VITEK, M. P., MITSUDA, N. & TOHYAMA, M. 2001. Vascular endothelial growth factor rescues hippocampal neurons from glutamate-induced toxicity: signal transduction cascades. *FASEB journal : official publication of the Federation of American Societies for Experimental Biology,* 15**,** 1218-20.

MAUTES, A. E., WEINZIERL, M. R., DONOVAN, F. & NOBLE, L. J. 2000. Vascular events after spinal cord injury: contribution to secondary pathogenesis. *Physical therapy,* 80**,** 673-87.

MAZZONE, M., DETTORI, D., LEITE DE OLIVEIRA, R., LOGES, S., SCHMIDT, T., JONCKX, B., TIAN, Y. M., LANAHAN, A. A., POLLARD, P., RUIZ DE ALMODOVAR, C., DE SMET, F., VINCKIER, S., ARAGONES, J., DEBACKERE, K., LUTTUN, A., WYNS, S., JORDAN, B., PISACANE, A., GALLEZ, B., LAMPUGNANI, M. G., DEJANA, E., SIMONS, M., RATCLIFFE, P., MAXWELL, P. & CARMELIET, P. 2009. Heterozygous deficiency of PHD2 restores tumor oxygenation and inhibits metastasis via endothelial normalization. *Cell,* 136, 839-51.

MCTIGUE, D. M., POPOVICH, P. G., MORGAN, T. E. & STOKES, B. T. 2000. Localization of transforming growth factor-beta1 and receptor mRNA after experimental spinal cord injury. *Experimental neurology,* 163**,** 220-30.

MELAND, M. N., HERNDON, M. E. & STIPP, C. S. 2010. Expression of alpha5 integrin rescues fibronectin responsiveness in NT2N CNS neuronal cells. *Journal of neuroscience research,* 88, 222-32.

MELZER, N. & MEUTH, S. G. 2014. Disease-modifying therapy in multiple sclerosis and chronic inflammatory deymeylinating polyradiculoneuropathy: common and divergent current and future strategies. *Clinical and Experimental Immunology.* 175, 359-72.

MENDELSOHN, C., LARKIN, S., MARK, M., LEMEUR, M., CLIFFORD, J., ZELENT, A. & CHAMBON, P. 1994. RAR beta isoforms: distinct transcriptional control by retinoic acid and specific spatial patterns of promoter activity during mouse embryonic development. *Mechanisms of development,* 45**,** 227-41.

MENDELSOHN, C., RUBERTE, E., LEMEUR, M., MORRISS-KAY, G. & CHAMBON, P. 1991. Developmental analysis of the retinoic acid-inducible RAR-beta 2 promoter in transgenic animals. *Development,* 113**,** 723-34.

MENEZES, K., DE MENEZES, J. R., NASCIMENTO, M. A., SANTOS RDE, S. & COELHO-SAMPAIO, T. 2010. Polylaminin, a polymeric form of laminin, promotes regeneration after spinal cord injury. *FASEB journal : official publication of the Federation of American Societies for Experimental Biology,* 24**,** 4513-22.

MESTAS, J. & HUGHES, C. W. 2004. Of mice and not men: Differences between Mouse and Human Immunology. *The Journal of Immunology,* 172, 2731-2738.

MEY, J. & HAMMELMANN, S. 2000. OLN-93 oligodendrocytes synthesize all-trans-retinoic acid in vitro. *Cell and tissue research,* 302**,** 49-58.

MICHAEL, G. J., ESMAILZADEH, S., MORAN, L. B., CHRISTIAN, L., PEARCE, R. K. & GRAEBER, M. B. 2011. Up-regulation of metallothionein gene expression in parkinsonian astrocytes. *Neurogenetics,* 12**,** 295-305.

MILLS, C. D. & HULSEBOSCH, C. E. 2002. Increased expression of metabotropic glutamate receptor subtype 1 on spinothalamic tract neurons following spinal cord injury in the rat. *Neuroscience letters,* 319**,** 59-62.

MOCCHETTI, I., RABIN, S. J., COLANGELO, A. M., WHITTEMORE, S. R. & WRATHALL, J. R. 1996. Increased basic fibroblast growth factor expression following contusive spinal cord injury. *Experimental neurology,* 141**,** 154-64.

MOENNER, M., GUSSE, M., HATZI, E. & BADET, J. 1994. The widespread expression of angiogenin in different human cells suggests a biological function not only related to angiogenesis. *European journal of biochemistry / FEBS,* 226**,** 483-90.

MOON, C., HEO, S., SIM, K. B. & SHIN, T. 2004. Upregulation of CD44 expression in the spinal cords of rats with clip compression injury. *Neuroscience letters,* 367**,** 133-6.

MOON, J. Y., ROH, D. H., YOON, S. Y., KANG, S. Y., CHOI, S. R., KWON, S. G., CHOI, H. S., HAN, H. J., BEITZ, A. J. & LEE, J. H. 2013. Sigma-1 receptor-mediated increase in spinal p38 MAPK phosphorylation leads to the induction of mechanical allodynia in mice and neuropathic rats. *Experimental neurology,* 247**,** 383-91.

MONTEIRO, M. R., SHAPIRO, S. S., TAKAFUTA, T., MENEZES, D. W. & MURPHY, G. F. 1999. Von Willebrand factor receptor GPIb alpha is expressed by human factor XIIIa-positive dermal dendrocytes and is upregulated by mast cell degranulation. *The Journal of investigative dermatology,* 113**,** 272-6.

MOROIANU, J. & RIORDAN, J. F. 1994. Nuclear translocation of angiogenin in proliferating endothelial cells is essential to its angiogenic activity. *Proceedings of the National Academy of Sciences of the United States of America,* 91**,** 1677-81.
MOSSER, D. M. & EDWARDS, J. P. 2008. Exploring the full spectrum of macrophage activation. *Nature Reviews,* 8, 958-969.
MOYER, J. A., WOOD, A., ZALESKA, M. M., AY, I., FINKLESTEIN, S. P. & PROTTER, A. A. 1998. Basic fibroblast growth factor: a potential therapeutic agent for the treatment of acute neurodegenerative disorders and vascular insufficiency. *Expert Opinion on Therapeutic Patents,* 8**,** 1425-1445.
MUIR, G. D. & WHISHAW, I. Q. 2000. Red nucleus lesions impair overground locomotion in rats: a kinetic analysis. *The European journal of neuroscience,* 12**,** 1113-22.
MUNSHI, H. G., WU, Y. I., MUKHOPADHYAY, S., OTTAVIANO, A. J., SASSANO, A., KOBLINSKI, J. E., PLATANIAS, L. C. & STACK, M. S. 2004. Differential regulation of membrane type 1-matrix metalloproteinase activity by ERK 1/2- and p38 MAPK-modulated tissue inhibitor of metalloproteinases 2 expression controls transforming growth factor-beta1-induced pericellular collagenolysis. *The Journal of biological chemistry,* 279**,** 39042-50.
MURAMATSU, R., TAKAHASHI, C., MIYAKE, S., FUJIMURA, H., MOCHIZUKI, H. & YAMASHITA, T. 2012. Angiogenesis induced by CNS inflammation promotes neuronal remodeling through vessel-derived prostacyclin. *Nature medicine,* 18, 1658-64.
MURPHY, G. 2011. Tissue inhibitors of metalloproteinases. *Genome biology,* 12**,** 233.
MURRAY, P. J. & WYNN, T. A. 2011. Protective and pathogenic functions of macrophage subsets. *Nature Reviews Immunology,* 11, 723-737.
MYERS, S. A., DEVRIES, W. H., ANDRES, K. R., GRUENTHAL, M. J., BENTON, R. L., HOYING, J. B., HAGG, T. & WHITTEMORE, S. R. 2011a. CD47 knockout mice exhibit improved recovery from spinal cord injury. *Neurobiology of disease,* 42**,** 21-34.
MYERS, S. A., DEVRIES, W. H., GRUENTHAL, M. J., ANDRES, K. R., HAGG, T. & WHITTEMORE, S. R. 2011b. Sildenafil Improves Epicenter Vascular Perfusion but not Hindlimb Functional Recovery after Contusive Spinal Cord Injury in Mice. *Journal of neurotrauma*.
NAFTCHI, N. E. 1982. Functional restoration of the traumatically injured spinal cord in cats by clonidine. *Science,* 217**,** 1042-4.
NAG, S., PAPNEJA, T., VENUGOPALAN, R. & STEWART, D. J. 2005. Increased angiopoietin2 expression is associated with endothelial apoptosis and blood-brain barrier breakdown. *Laboratory investigation; a journal of technical methods and pathology,* 85**,** 1189-98.
NAGY, J. A., BENJAMIN, L., ZENG, H., DVORAK, A. M. & DVORAK, H. F. 2008. Vascular permeability, vascular hyperpermeability and angiogenesis. *Angiogenesis,* 11, 109-19.
NAKAE, A., NAKAI, K., YANO, K., HOSOKAWA, K., SHIBATA, M. & MASHIMO, T. 2011. The animal model of spinal cord injury as an experimental pain model. *Journal of biomedicine & biotechnology,* 2011**,** 939023.
NAKAMURA, M., YAMABE, H., OSAWA, H., NAKAMURA, N., SHIMADA, M., KUMASAKA, R., MURAKAMI, R., FUJITA, T., OSANAI, T. & OKUMURA, K. 2006. Hypoxic conditions stimulate the production of angiogenin and vascular

endothelial growth factor by human renal proximal tubular epithelial cells in culture. *Nephrology, dialysis, transplantation : official publication of the European Dialysis and Transplant Association - European Renal Association,* 21**,** 1489-95.

NALDINI, A. & CARRARO, F. 2005. Role of inflammatory mediators in angiogenesis. *Current drug targets. Inflammation and allergy,* 4, 3-8.

NANNEY, L. B., WAMIL, B. D., WHITSITT, J., CARDWELL, N. L., DAVIDSON, J. M., YAN, H. P. & HELLERQVIST, C. G. 2001. CM101 stimulates cutaneous wound healing through an anti-angiogenic mechanism. *Angiogenesis,* 4**,** 61-70.

NATHAN, C. 2002. Points of control in inflammation. *Nature,* 420, 846-52.

NAVARRO-SOBRINO, M., HERNANDEZ-GUILLAMON, M., FERNANDEZ-CADENAS, I., RIBO, M., ROMERO, I. A., COURAUD, P. O., WEKSLER, B. B., MONTANER, J. & ROSELL, A. 2013. The angiogenic gene profile of circulating endothelial progenitor cells from ischemic stroke patients. *Vascular cell,* 5**,** 3.

NESIC, O., SVRAKIC, N. M., XU, G. Y., MCADOO, D., WESTLUND, K. N., HULSEBOSCH, C. E., YE, Z., GALANTE, A., SOTEROPOULOS, P., TOLIAS, P., YOUNG, W., HART, R. P. & PEREZ-POLO, J. R. 2002. DNA microarray analysis of the contused spinal cord: effect of NMDA receptor inhibition. *Journal of neuroscience research,* 68**,** 406-23.

NEUFELD, G., SHRAGA-HELED, N., LANGE, T., GUTTMANN-RAVIV, N., HERZOG, Y. & KESSLER, O. 2005. Semaphorins in cancer. *Frontiers in bioscience : a journal and virtual library,* 10**,** 751-60.

NEWMAN, P. J. 1997. The biology of PECAM-1. *The Journal of clinical investigation,* 99**,** 3-8.

NEWMAN, P. J., BERNDT, M. C., GORSKI, J., WHITE, G. C., 2ND, LYMAN, S., PADDOCK, C. & MULLER, W. A. 1990. PECAM-1 (CD31) cloning and relation to adhesion molecules of the immunoglobulin gene superfamily. *Science,* 247**,** 1219-22.

NEWMAN, P. J., DOERS, M. P. & GORSKI, J. 1987. Molecular cloning of a 130 kD membrane glycoprotein expressed on human platelets, umbilical vein endothelial cells, and human erythroleukemia (HEL) cells. *Journal of Cell Biology,* 105.

NEWMAN, P. J. & NEWMAN, D. K. 2003. Signal transduction pathways mediated by PECAM-1: new roles for an old molecule in platelet and vascular cell biology. *Arteriosclerosis, thrombosis, and vascular biology,* 23**,** 953-64.

NG, M. T., STAMMERS, A. T. & KWON, B. K. 2011. Vascular Disruption and the Role of Angiogenic Proteins After Spinal Cord Injury. *Translational stroke research,* 2**,** 474-491.

NICHOLAS, A. P., HOKFELT, T. & PIERIBONE, V. A. 1996. The distribution and significance of CNS adrenoceptors examined with in situ hybridization. *Trends in pharmacological sciences,* 17**,** 245-55.

NICLOU, S. P., FRANSSEN, E. H., EHLERT, E. M., TANIGUCHI, M. & VERHAAGEN, J. 2003. Meningeal cell-derived semaphorin 3A inhibits neurite outgrowth. *Molecular and cellular neurosciences,* 24**,** 902-12.

NISHIMURA, D. Y., PURCHIO, A. F. & MURRAY, J. C. 1993. Linkage localization of TGFB2 and the human homeobox gene HLX1 to chromosome 1q. *Genomics,* 15**,** 357-64.

NISHIO, T., KAWAGUCHI, S., YAMAMOTO, M., ISEDA, T., KAWASAKI, T. & HASE, T. 2005. Tenascin-C regulates proliferation and migration of cultured astrocytes in a scratch wound assay. *Neuroscience,* 132**,** 87-102.

NOBLE, L. J., DONOVAN, F., IGARASHI, T., GOUSSEV, S. & WERB, Z. 2002. Matrix metalloproteinases limit functional recovery after spinal cord injury by modulation of early vascular events. *The Journal of neuroscience : the official journal of the Society for Neuroscience,* 22**,** 7526-35.

NOBLE, L. J., MAUTES, A. E. & HALL, J. J. 1996. Characterization of the microvascular glycocalyx in normal and injured spinal cord in the rat. *The Journal of comparative neurology,* 376**,** 542-56.

NOBLE, L. J. & WRATHALL, J. R. 1985. Spinal cord contusion in the rat: morphometric analyses of alterations in the spinal cord. *Experimental neurology,* 88**,** 135-49.

NOBLE, L. J. & WRATHALL, J. R. 1989a. Correlative analyses of lesion development and functional status after graded spinal cord contusive injuries in the rat. *Experimental neurology,* 103**,** 34-40.

NOBLE, L. J. & WRATHALL, J. R. 1989b. Distribution and time course of protein extravasation in the rat spinal cord after contusive injury. *Brain research,* 482**,** 57-66.

NOGRADI, A. & VRBOVA, G. 2000. Anatomy and physiology of the spinal cord. In: Madame Curie Bioscience Database [Internet]. Austin (TX): Landes Bioscience.

NORDAL, R. A., NAGY, A., PINTILIE, M. & WONG, C. S. 2004. Hypoxia and hypoxia-inducible factor-1 target genes in central nervous system radiation injury: a role for vascular endothelial growth factor. *Clinical cancer research : an official journal of the American Association for Cancer Research,* 10**,** 3342-53.

NORDBLOM, J., PERSSON, J. K., ABERG, J., BLOM, H., ENGQVIST, H., BRISMAR, H., SJODAHL, J., JOSEPHSON, A., FROSTELL, A., THAMS, S., BRUNDIN, L., SVENSSON, M. & MATTSSON, P. 2012. FGF1 containing biodegradable device with peripheral nerve grafts induces corticospinal tract regeneration and motor evoked potentials after spinal cord resection. *Restorative neurology and neuroscience,* 30**,** 91-102.

NOTI, J. D., JOHNSON, A. K. & DILLON, J. D. 2000. Structural and functional characterization of the leukocyte integrin gene CD11d. Essential role of Sp1 and Sp3. *The Journal of biological chemistry,* 275**,** 8959-69.

NOUT, Y. S., ROSENZWEIG, E. S., BROCK, J. H., STRAND, S. C., MOSEANKO, R., HAWBECKER, S., ZDUNOWSKI, S., NIELSON, J. L., ROY, R. R., COURTINE, G., FERGUSON, A. R., EDGERTON, V. R., BEATTIE, M. S., BRESNAHAN, J. C. & TUSZYNSKI, M. H. 2012. Animal models of neurologic disorders: A nonhuman primate model of spinal cord injury. *Neurotherapeutics,* 9, 380-392.

NSCISC. 2013. *Spinal Injury Network* [Online].

OATWAY, M. A., CHEN, Y., BRUCE, J. C., DEKABAN, G. A. & WEAVER, L. C. 2005. Anti-CD11d integrin antibody treatment restores normal serotonergic projections to the dorsal, intermediate, and ventral horns of the injured spinal cord. *The Journal of neuroscience : the official journal of the Society for Neuroscience,* 25**,** 637-47.

OEHLER, M. K. BICKNELL, R. 2000. The promise of anti-angiogenic cancer therapy. *British Journal of Cnacer*, 82.

OH, J. S., PARK, I. S., KIM, K. N., YOON DO, H., KIM, S. H. & HA, Y. 2012. Transplantation of an adipose stem cell cluster in a spinal cord injury. *Neuroreport,* 23**,** 277-82.

OHNO, M., SASAHARA, M., NARUMIYA, S., TANAKA, N., YAMANO, T., SHIMADA, M. & HAZAMA, F. 1999. Expression of platelet-derived growth factor B-chain and beta-receptor in hypoxic/ischemic encephalopathy of neonatal rats. *Journal of Neuroscience,* 90, 643-651.

OKADA, M., MIYAMOTO, O., SHIBUYA, S., ZHANG, X., YAMAMOTO, T. & ITANO, T. 2007. Expression and role of type I collagen in a rat spinal cord contusion injury model. *Neuroscience research,* 58**,** 371-7.

OLSSON, A. K., DIMBERG, A., KREUGER, J. & CLAESSON-WELSH, L. 2006. VEGF receptor signalling - in control of vascular function. *Nature reviews. Molecular cell biology,* 7**,** 359-71.

ONDARZA, A. B., YE, Z. & HULSEBOSCH, C. E. 2003. Direct evidence of primary afferent sprouting in distant segments following spinal cord injury in the rat: colocalization of GAP-43 and CGRP. *Experimental neurology,* 184**,** 373-80.

ONO, M. 2008. Molecular links between tumor angiogenesis and inflammation: inflammatory stimuli of macrophages and cancer cells as targets for therapeutic strategy. *Cancer science,* 99, 1501-6.

ORIANA, S., GUENDALINA, L., OSCAR, C., ANTONIO, Z., FIORENZA, O., MAURO, P., ROBERTO, D. P., ANDREA, G. & ANNAMARIA, O. 2013. Delayed wound healing in aged skin rat models after thermal injury is associated with an increased MMP-9, K6 and CD44 expression. *Burns : journal of the International Society for Burn Injuries,* 39**,** 776-87.

ORNITZ, D. M. & ITOH, N. 2001. Fibroblast growth factors. *Genome biology,* 2**,** REVIEWS3005.

OZEROVA, S. G. & MININ, A. A. 2008. [A study of proteins of annexin group in early fish development. IV. Identification of calcium-binding proteins in zebrafish egg by mass spectrometry]. *Ontogenez,* 39**,** 222-6.

PAGE-MCCAW, A., EWALD, A. J. & WERB, Z. 2007. Matrix metalloproteinases and the regulation of tissue remodelling. *Nature reviews. Molecular cell biology,* 8**,** 221-33.

PAHL, M. V., VAZIRI, N. D. & GONZALES, E. 1994. Coagulation profile in persons with long-standing spinal cord injury. *The Journal of the American Paraplegia Society,* 17**,** 133-5.

PALL, T., PINK, A., KASAK, L., TURKINA, M., ANDERSON, W., VALKNA, A. & KOGERMAN, P. 2011. Soluble CD44 interacts with intermediate filament protein vimentin on endothelial cell surface. *PloS one,* 6**,** e29305.

PANITCH, H. S., HIRSCH, R. L., HALEY, A. S. & JOHNSON, K. P. 1987. Exacerbations of multiple sclerosis in patients treated with gamma interferon. *Lancet,* 1.

PARK, J. E., LEE, D. H., LEE, J. A., PARK, S. G., KIM, N. S., PARK, B. C. & CHO, S. 2005. Annexin A3 is a potential angiogenic mediator. *Biochemical and biophysical research communications,* 337**,** 1283-7.

PASINELLI, P. & BROWN, R. H. 2006. Molecular biology of amyotrophic lateral sclerosis: insights from genetics. *Nature reviews. Neuroscience,* 7**,** 710-23.

PASTERKAMP, R. J., ANDERSON, P. N. & VERHAAGEN, J. 2001. Peripheral nerve injury fails to induce growth of lesioned ascending dorsal column axons into spinal cord scar tissue expressing the axon repellent Semaphorin3A. *The European journal of neuroscience,* 13**,** 457-71.

PATHAK, N. N., BALAGANUR, V., LINGARAJU, M. C., MORE, A. S., KANT, V., KUMAR, D. & TANDAN, S. K. 2013. Antihyperalgesic and Anti-inflammatory Effects of Atorvastatin in Chronic Constriction Injury-Induced Neuropathic Pain in Rats. *Inflammation*.

PAVLOFF, N., STASKUS, P. W., KISHNANI, N. S. & HAWKES, S. P. 1992. A new inhibitor of metalloproteinases from chicken: ChIMP-3. A third member of the TIMP family. *The Journal of biological chemistry,* 267**,** 17321-6.

PELA, I. R., FERREIRA, M. E., MELO, M. C., SILVA, C. A., COELHO, M. M. & VALENZUELA, C. F. 2000. Evidence that platelet-derived growth factor may be a novel endogenous pyrogen in the central nervous system. *American journal of physiology. Regulatory, integrative and comparative physiology,* 278**,** R1275-81.

PENKOWA, M., CARRASCO, J., GIRALT, M., MOOS, T. & HIDALGO, J. 1999. CNS wound healing is severely depressed in metallothionein I- and II-deficient mice. *The Journal of neuroscience : the official journal of the Society for Neuroscience,* 19**,** 2535-45.

PEREGO, C., FUMAGALLI, S. & DE SIMONI, M. G. 2011. Temporal pattern of expression and colocalization of microglia/macrophage phenotype markers following brain ischemic injury in mice. *Journal of neuroinflammation,* 8, 174.

PEREZ, R. L., RIVERA-MARRERO, C. A. & ROMAN, J. 2003. Pulmonary granulomatous inflammation: From sarcoidosis to tuberculosis. *Seminars in respiratory infections,* 18, 23-32.

PERRY, H. & HOLMES, C. 2014. Microglia priming in neurodegenerative disease. *Nature Reviews Neurology,* 10, 217-24.

PETAJA, J., MYLLYNEN, P., ROKKANEN, P. & NOKELAINEN, M. 1989. Fibrinolysis and spinal injury. Relationship to post-traumatic deep vein thrombosis. *Acta chirurgica Scandinavica,* 155**,** 241-6.

PIAO, M. S., LEE, J. K., JANG, J. W., KIM, S. H. & KIM, H. S. 2009. A mouse model of photochemically induced spinal cord injury. *Journal of Korean Neurosurgical Society,* 46**,** 479-83.

PIATON, G., AIGROT, M. S., WILLIAMS, A., MOYON, S., TEPAVCEVIC, V., MOUTKINE, I., GRAS, J., MATHO, K. S., SCHMITT, A., SOELLNER, H., HUBER, A. B., RAVASSARD, P. & LUBETZKI, C. 2011. Class 3 semaphorins influence oligodendrocyte precursor recruitment and remyelination in adult central nervous system. *Brain : a journal of neurology,* 134**,** 1156-67.

PIERCE, G. F., TARPLEY, J. E., TSENG, J., BREADY, J., CHANG, D., KENNEY, W. C., RUDOLPH, R., ROBSON, M. C., VANDE BERG, J., REID, P. & ET AL. 1995. Detection of platelet-derived growth factor (PDGF)-AA in actively healing human wounds treated with recombinant PDGF-BB and absence of PDGF in chronic nonhealing wounds. *The Journal of clinical investigation,* 96**,** 1336-50.

PLANAS, A. M., SOLE, S. & JUSTICIA, C. 2001. Expression and activation of matrix metalloproteinase-2 and -9 in rat brain after transient focal cerebral ischemia. *Neurobiology of disease,* 8**,** 834-46.

PLEMEL, J. R., CHOJNACKI, A., SPARLING, J. S., LIU, J., PLUNET, W., DUNCAN, G. J., PARK, S. E., WEISS, S. & TETZLAFF, W. 2011. Platelet-derived growth factor-responsive neural precursors give rise to myelinating oligodendrocytes after transplantation into the spinal cords of contused rats and dysmyelinated mice. *Glia,* 59**,** 1891-910.

POON, P. C., GUPTA, D., SHOICHET, M. S. & TATOR, C. H. 2007. Clip compression model is useful for thoracic spinal cord injuries: histologic and functional correlates. *Spine,* 32**,** 2853-9.

POPOVICH, P. G., GUAN, Z., WEI, P., HUITINGA, I., VAN ROOIJEN, N. & STOKES, B. T. 1999. Depletion of hematogenous macrophages promotes partial hindlimb recovery and neuroanatomical repair after experimental spinal cord injury. *Experimental neurology,* 158**,** 351-65.

POPOVICH, P. G., HORNER, P. J., MULLIN, B. B. & STOKES, B. T. 1996. A quantitative spatial analysis of the blood-spinal cord barrier. I. Permeability changes after experimental spinal contusion injury. *Experimental neurology,* 142**,** 258-75.

PREVITALI, S. C., MALAGUTI, M. C., RIVA, N., SCARLATO, M., DACCI, P., DINA, G., TRIOLO, D., PORRELLO, E., LORENZETTI, I., FAZIO, R., COMI, G., BOLINO, A. & QUATTRINI, A. 2008. The extracellular matrix affects axonal regeneration in peripheral neuropathies. *Neurology,* 71**,** 322-31.

PROCOPIO, W. N., PELAVIN, P. I., LEE, W. M. & YEILDING, N. M. 1999. Angiopoietin-1 and -2 coiled coil domains mediate distinct homo-oligomerization patterns, but fibrinogen-like domains mediate ligand activity. *The Journal of biological chemistry,* 274**,** 30196-201.

PUFE, T., PETERSEN, W. J., MENTLEIN, R. & TILLMANN, B. N. 2005. The role of vasculature and angiogenesis for the pathogenesis of degenerative tendons disease. *Scandinavian journal of medicine & science in sports,* 15**,** 211-22.

PURVES, D., AUGUSTINE, G. J. & FITZPATRICK, D. 2001. Neuroscience. 2nd edition. Central Pain Pathways: The Spinothalamic Tract. *Sunderland (MA),* Sinauer Associates.

PUSCHMANN, T. B., DIXON, K. J. & TURNLEY, A. M. 2010. Species differences in reactivity of mouse and rat astrocytes in vitro. *Neuro-Signals,* 18**,** 152-63.

QING, Z., SANDOR, M., RADVANY, Z., SEWELL, D., FALUS, A., POTTHOFF, D., MULLER, W. A. & FABRY, Z. 2001. Inhibition of antigen-specific T cell trafficking into the central nervous system via blocking PECAM1/CD31 molecule. *Journal of neuropathology and experimental neurology,* 60**,** 798-807.

RAMADHANI, D., TSUKADA, T., FUJIWARA, K., HORIGUCHI, K., KIKUCHI, M. & YASHIRO, T. 2012. Laminin isoforms and laminin-producing cells in rat anterior pituitary. *Acta histochemica et cytochemica,* 45**,** 309-15.

RAYNAL, P. & POLLARD, H. B. 1994. Annexins: the problem of assessing the biological role for a gene family of multifunctional calcium- and phospholipid-binding proteins. *Biochimica et biophysica acta,* 1197**,** 63-93.

REESE, T. S. & KARNOVSKY, M. J. 1967. Fine structural localization of a blood-brain barrier to exogenous peroxidase. *The Journal of cell biology,* 34**,** 207-17.

REININGER, A. J. 2008. Function of von Willebrand factor in haemostasis and thrombosis. *Haemophilia : the official journal of the World Federation of Hemophilia,* 14 Suppl 5**,** 11-26.

SPINAL RESEARCH. 2011. *Facts and Figures* [Online]. Available: http://www.spinal-reseatch.org.

REUSS, B. & VON BOHLEN UND HALBACH, O. 2003. Fibroblast growth factors and their receptors in the central nervous system. *Cell and tissue research,* 313**,** 139-57.

RICCIOTTI, E. & FITZGERALD, G. A. 2011. Prostaglandins and inflammation. *Arteriosclerosis, thrombosis, and vascular biology,* 31, 986-1000.
RIES, A., GOLDBERG, J. L. & GRIMPE, B. 2007. A novel biological function for CD44 in axon growth of retinal ganglion cells identified by a bioinformatics approach. *Journal of neurochemistry,* 103**,** 1491-505.
RIGBY DUNCAN, K. E. & STILLMAN, M. J. 2006. Metal-dependent protein folding: metallation of metallothionein. *Journal of inorganic biochemistry,* 100**,** 2101-7.
RINTALA, D. H., LOUBSER, P. G., CASTRO, J., HART, K. A. & FUHRER, M. J. 1998. Chronic pain in a community-based sample of men with spinal cord injury: prevalence, severity, and relationship with impairment, disability, handicap, and subjective well-being. *Archives of physical medicine and rehabilitation,* 79**,** 604-14.
RITZ, M. F., GRAUMANN, U., GUTIERREZ, B. & HAUSMANN, O. 2010. Traumatic spinal cord injury alters angiogenic factors and TGF-beta1 that may affect vascular recovery. *Current neurovascular research,* 7**,** 301-10.
ROBINSON, C. J. & STRINGER, S. E. 2001. The splice variants of vascular endothelial growth factor (VEGF) and their receptors. *Journal of cell science,* 114**,** 853-65.
ROESSMANN, U., VELASCO, M. E., SINDELY, S. D. & GAMBETTI, P. 1980. Glial fibrillary acidic protein (GFAP) in ependymal cells during development. An immunocytochemical study. *Brain research,* 200, 13-21.
ROGERS, S. L., EDSON, K. J., LETOURNEAU, P. C. & MCLOON, S. C. 1986. Distribution of laminin in the developing peripheral nervous system of the chick. *Developmental biology,* 113**,** 429-35.
ROJIANI, M. V., ALIDINA, J., ESPOSITO, N. & ROJIANI, A. M. 2010. Expression of MMP-2 correlates with increased angiogenesis in CNS metastasis of lung carcinoma. *International journal of clinical and experimental pathology,* 3**,** 775-81.
ROMANA-SOUZA, B., SANTOS, J. S. & MONTE-ALTO-COSTA, A. 2009. beta-1 and beta-2, but not alpha-1 and alpha-2, adrenoceptor blockade delays rat cutaneous wound healing. *Wound repair and regeneration : official publication of the Wound Healing Society [and] the European Tissue Repair Society,* 17**,** 230-9.
ROMANIC, A. M., WHITE, R. F., ARLETH, A. J., OHLSTEIN, E. H. & BARONE, F. C. 1998. Matrix metalloproteinase expression increases after cerebral focal ischemia in rats: inhibition of matrix metalloproteinase-9 reduces infarct size. *Stroke; a journal of cerebral circulation,* 29**,** 1020-30.
ROSENBERG, G. A., ESTRADA, E. Y. & DENCOFF, J. E. 1998. Matrix metalloproteinases and TIMPs are associated with blood-brain barrier opening after reperfusion in rat brain. *Stroke; a journal of cerebral circulation,* 29**,** 2189-95.
ROSENBERG, G. A., SULLIVAN, N. & ESIRI, M. M. 2001. White matter damage is associated with matrix metalloproteinases in vascular dementia. *Stroke; a journal of cerebral circulation,* 32**,** 1162-8.
ROSENSTEIN, J. M. & KRUM, J. M. 2004. New roles for VEGF in nervous tissue--beyond blood vessels. *Experimental neurology,* 187**,** 246-53.
ROSENZWEIG, S., RAZ-PRAG, D., NITZAN, A., GALRON, R., PAZ, M., JESERICH, G., NEUFELD, G., BARZILAI, A. & SOLOMON, A. S. 2010. Sema-3A indirectly disrupts the regeneration process of goldfish optic nerve after controlled injury. *Graefe's archive for clinical and experimental ophthalmology*

= *Albrecht von Graefes Archiv fur klinische und experimentelle Ophthalmologie,* 248**,** 1423-35.
ROY, A., FUNG, Y. K., LIU, X. & PAHAN, K. 2006. Up-regulation of microglial CD11b expression by nitric oxide. *The Journal of biological chemistry,* 281, 14971-80.
RUHRBERG, C., GERHARDT, H., GOLDING, M., WATSON, R., IOANNIDOU, S., FUJISAWA, H., BETSHOLTZ, C. & SHIMA, D. T. 2002. Spatially restricted patterning cues provided by heparin-binding VEGF-A control blood vessel branching morphogenesis. *Genes & development,* 16**,** 2684-98.
SAHIN, B., EMIRZEOGLU, M., UZUN, A., INCESU, L., BEK, Y., BILGIC, S. & KAPLAN, S. 2003. Unbiased estimation of the liver volume by the Cavalieri principle using magnetic resonance images. *European journal of radiology,* 47**,** 164-70.
SAITO, N. & SHIRAI, Y. 2002. Protein kinase C gamma (PKC gamma): function of neuron specific isotype. *Journal of biochemistry,* 132**,** 683-7.
SANDVIG, A., BERRY, M., BARRETT, L. B., BUTT, A. & LOGAN, A. 2004. Myelin-, reactive glia-, and scar-derived CNS axon growth inhibitors: expression, receptor signaling, and correlation with axon regeneration. *Glia,* 46**,** 225-51.
SAUNDERS, W. B., BOHNSACK, B. L., FASKE, J. B., ANTHIS, N. J., BAYLESS, K. J., HIRSCHI, K. K. & DAVIS, G. E. 2006. Coregulation of vascular tube stabilization by endothelial cell TIMP-2 and pericyte TIMP-3. *The Journal of cell biology,* 175**,** 179-91.
SCHLOSSHAUER, B. 1993. The blood-brain barrier: morphology, molecules, and neurothelin. *BioEssays : news and reviews in molecular, cellular and developmental biology,* 15**,** 341-6.
SCHOSTAK, M., SCHWALL, G. P., POZNANOVIC, S., GROEBE, K., MULLER, M., MESSINGER, D., MILLER, K., KRAUSE, H., PELZER, A., HORNINGER, W., KLOCKER, H., HENNENLOTTER, J., FEYERABEND, S., STENZL, A. & SCHRATTENHOLZ, A. 2009. Annexin A3 in urine: a highly specific noninvasive marker for prostate cancer early detection. *The Journal of urology,* 181**,** 343-53.
SCHWARTZ, E. D., YEZIERSKI, R. P., PATTANY, P. M., QUENCER, R. M. & WEAVER, R. G. 1999. Diffusion-weighted MR imaging in a rat model of syringomyelia after excitotoxic spinal cord injury. *AJNR. American journal of neuroradiology,* 20**,** 1422-8.
SCHWARZ, R., JOSEPH, B., GERLACH, G., SCHRAMM-GLUCK, A., ENGELHARD, K., FROSCH, M., MULLER, T. & SCHOEN, C. 2010. Evaluation of one- and two-color gene expression arrays for microbial comparative genome hybridization analyses in routine applications. *Journal of clinical microbiology,* 48**,** 3105-10.
SEBASTIA, J., KIERAN, D., BREEN, B., KING, M. A., NETTELAND, D. F., JOYCE, D., FITZPATRICK, S. F., TAYLOR, C. T. & PREHN, J. H. 2009. Angiogenin protects motoneurons against hypoxic injury. *Cell death and differentiation,* 16**,** 1238-47.
SEGAL, J. L., GONZALES, E., YOUSEFI, S., JAMSHIDIPOUR, L. & BRUNNEMANN, S. R. 1997. Circulating levels of IL-2R, ICAM-1, and IL-6 in spinal cord injuries. *Archives of physical medicine and rehabilitation,* 78**,** 44-7.
SEGATORE, M. 1994. Understanding chronic pain after spinal cord injury. *The Journal of neuroscience nursing : journal of the American Association of Neuroscience Nurses,* 26**,** 230-6.

SEKHON, L. H. & FEHLINGS, M. G. 2001. Epidemiology, demographics, and pathophysiology of acute spinal cord injury. *Spine,* 26**,** S2-12.
SEKI, T., HIDA, K., TADA, M., KOYANAGI, I. & IWASAKI, Y. 2002. Graded contusion model of the mouse spinal cord using a pneumatic impact device. *Neurosurgery,* 50**,** 1075-81; discussion 1081-2.
SEKIDO, N., JYORAKU, A., OKADA, H., WAKAMATSU, D., MATSUYA, H. & NISHIYAMA, H. 2012. A novel animal model of underactive bladder: analysis of lower urinary tract function in a rat lumbar canal stenosis model. *Neurourology and urodynamics,* 31**,** 1190-6.
SEKIGUCHI, M., KIKUCHI, S. & MYERS, R. R. 2004. Experimental spinal stenosis: relationship between degree of cauda equina compression, neuropathology, and pain. *Spine,* 29**,** 1105-11.
SEMPLE-ROWLAND, S. L., MAHATME, A., POPOVICH, P. G., GREEN, D. A., HASSLER, G., JR., STOKES, B. T. & STREIT, W. J. 1995. Analysis of TGF-beta 1 gene expression in contused rat spinal cord using quantitative RT-PCR. *Journal of neurotrauma,* 12**,** 1003-14.
SENGER, D. R., GALLI, S. J., DVORAK, A. M., PERRUZZI, C. A., HARVEY, V. S. & DVORAK, H. F. 1983. Tumor cells secrete a vascular permeability factor that promotes accumulation of ascites fluid. *Science,* 219**,** 983-5.
SENTER, H. J. & VENES, J. L. 1978. Altered blood flow and secondary injury in experimental spinal cord trauma. *Journal of neurosurgery,* 49**,** 569-78.
SHAH, M., FOREMAN, D. M. & FERGUSON, M. W. 1995. Neutralisation of TGF-beta 1 and TGF-beta 2 or exogenous addition of TGF-beta 3 to cutaneous rat wounds reduces scarring. *Journal of cell science,* 108 (Pt 3)**,** 985-1002.
SHAIMARDANOVA, G. F., MUKHAMEDSHINA IA, O., ARKHIPOVA, S. S., SALAFUTDINOV, II, RIZVANOV, A. A. & CHELYSHEV IU, A. 2011. [Posttraumatic changes of rat spinal cord after transplantation of human umbilical cord blood mononuclear cells transfected with VEGF and FGF2 genes]. *Morfologiia,* 140**,** 36-42.
SHECHTER, R., MILLER, O. & YOVEL, G. 2013. Recruitment of beneficial M2 macrophages to injured spinal cord is orchestrated by remote brain choroid plexus. *Immunity,* 30, 555-569.
SHEPHERD, F. A. & SRIDHAR, S. S. 2003. Angiogenesis inhibitors under study for the treatment of lung cancer. *Lung Cancer,* 41.
SHIMADA, Y. 1995. Experimental study on effects of omental transposition in cats with spinal cord injury (article in japanese). *No To Shinkei Brain and Nerve journal*. 47, 863-873.
SHAMIR, M. H., SHAHAR, R. & AIZENBERG, I. 1997. Subarachnoid cyst in a cat. *Journal of the American Animal Hospital Association*. 33, 123-125.
SHERK, H. H., PASQUARIELLO, P. S., RORKE, L. B. & SCHUT, L. 1984. The pathogenesis of progressive cavitation of the spinal cord. *Developmental medicine and child neurology,* 26**,** 514-9.
SHOULDERS, M. D. & RAINES, R. T. 2009. Collagen structure and stability. *Annual review of biochemistry,* 78**,** 929-58.
SIDDALL, P. J., MCCLELLAND, J. M., RUTKOWSKI, S. B. & COUSINS, M. J. 2003. A longitudinal study of the prevalence and characteristics of pain in the first 5 years following spinal cord injury. *Pain,* 103**,** 249-57.
SIDDIQ, I., PARK, E., LIU, E., SPRATT, S. K., SUROSKY, R., LEE, G., ANDO, D., GIEDLIN, M., HARE, G. M., FEHLINGS, M. G. & BAKER, A. J. 2012.

Treatment of traumatic brain injury using zinc-finger protein gene therapy targeting VEGF-A. *Journal of neurotrauma,* 29**,** 2647-59.
SILER, U., SEIFFERT, M., PUCH, S., RICHARDS, A., TOROK-STORB, B., MULLER, C. A., SOROKIN, L. & KLEIN, G. 2000. Characterization and functional analysis of laminin isoforms in human bone marrow. *Blood,* 96**,** 4194-203.
SINGER, A. J. & CLARK, R. A. 1999. Cutaneous wound healing. *The New England journal of medicine,* 341, 738-46.
SINGH, S., KUSHWAH, A. S., SINGH, R., FARSWAN, M. & KAUR, R. 2012. Current therapeutic strategy in Alzheimer's disease. *European review for medical and pharmacological sciences,* 16**,** 1651-64.
SINGH, R., SHARMA, S. C., MITTAL, R. & SHARMA, A. 2003. Traumatic spinal cord injuries in Haryana: A epidemiological study. *Indian journal of community medicine,* 28, 184-186.
SINHA, S., MILLER, L. M., SUBRAMANIAN, S., BURROWS, G. G., VANDENBARK, A. A. & OFFNER, H. 2011. RTL551 treatment of EAE reduces CD226 and T-bet+ CD4 T cells in periphery and prevents infiltration of T-bet+ IL-17, IFN-gamma producing T cells into CNS. *PloS one,* 6**,** e21868.
SKOLD, M., CULLHEIM, S., HAMMARBERG, H., PIEHL, F., SUNESON, A., LAKE, S., SJOGREN, A., WALUM, E. & RISLING, M. 2000. Induction of VEGF and VEGF receptors in the spinal cord after mechanical spinal injury and prostaglandin administration. *The European journal of neuroscience,* 12**,** 3675-86.
SMITH, S. M. 1994. Retinoic acid receptor isoform beta 2 is an early marker for alimentary tract and central nervous system positional specification in the chicken. *Developmental dynamics : an official publication of the American Association of Anatomists,* 200**,** 14-25.
SODERBLOM, C., LUO, X., BLUMENTHAL, E., BRAY, E., LYAPICHEV, K., RAMOS, J., KRISHNAN, V., LAI-HSU, C., PARK, K. K., TSOULFAS, P. & LEE, J. K. 2013. Perivascular fibroblasts form the fibrotic scar after contusive spinal cord injury. *The Journal of neuroscience : the official journal of the Society for Neuroscience,* 33**,** 13882-7.
SOKER, S., MIAO, H.-Q., NOMI, M., TAKASHIMA, S. & KLAGSBRUN, M. 2002. VEGF165 mediates formation of complexes containing VEGFR-2 and neuropilin-1 that enhance VEGF165-receptor binding. *Journal of cellular biochemistry,* 85**,** 357-68.
SONDELL, M., LUNDBORG, G. & KANJE, M. 1999. Vascular endothelial growth factor has neurotrophic activity and stimulates axonal outgrowth, enhancing cell survival and Schwann cell proliferation in the peripheral nervous system. *The Journal of neuroscience : the official journal of the Society for Neuroscience,* 19**,** 5731-40.
SONG, G., CECHVALA, C., RESNICK, D. K., DEMPSEY, R. J. & RAO, V. L. 2001. GeneChip analysis after acute spinal cord injury in rat. *Journal of neurochemistry,* 79**,** 804-15.
SONMEZ, O. F., UNAL, B., INALOZ, S., SAHIN, B., YILMAZ, M., AYDIN, A. & KAPLAN, S. 2002. Therapeutic effects of intracarotid infusion of spermine/nitric oxide complex on cerebral vasospasm. *Acta neurochirurgica,* 144**,** 921-8; discussion 928.
SOPKOVA, J., RAGUENES-NICOL, C., VINCENT, M., CHEVALIER, A., LEWIT-BENTLEY, A., RUSSO-MARIE, F. & GALLAY, J. 2002. Ca(2+) and

membrane binding to annexin 3 modulate the structure and dynamics of its N terminus and domain III. *Protein science : a publication of the Protein Society,* 11**,** 1613-25.
SOSALE, A., ROBSON, J. A. & STELZNER, D. J. 1988. Laminin distribution during corticospinal tract development and after spinal cord injury. *Experimental neurology,* 102**,** 14-22.
SOUZA, D. G., BELLAVER, B., SOUZA, D. O. & QUINCOZES-SANTOS, A. 2013. Characterization of adult rat astrocyte cultures. *PloS one,* 8**,** e60282.
SPRINGER, T. A. 1990. Adhesion receptors of the immune system. *Nature,* 346**,** 425-34.
SROGA, J. M., JONES, T. B., KIGERL, K. A., MCGAUGHY, V. M. & POPOVICH, P. G. 2003. Rats and mice exhibit distinct inflammatory reactions after spinal cord injury. *The Journal of comparative neurology,* 462**,** 223-40.
STEINBERG, S. F. 2008. Structural basis of protein kinase C isoform function. *Physiological reviews,* 88**,** 1341-78.
STENNARD, F. A., HOLLOWAY, A. F., HAMILTON, J. & WEST, A. K. 1994. Characterization of 6 Additional Human Metallothionein Genes. *Biochimica Et Biophysica Acta-Gene Structure and Expression,* 1218**,** 357-365.
STERNLICHT, M. D. & WERB, Z. 2001. How matrix metalloproteinases regulate cell behavior. *Annual review of cell and developmental biology,* 17**,** 463-516.
STETLER-STEVENSON, W. G., BROWN, P. D., ONISTO, M., LEVY, A. T. & LIOTTA, L. A. 1990. Tissue inhibitor of metalloproteinases-2 (TIMP-2) mRNA expression in tumor cell lines and human tumor tissues. *The Journal of biological chemistry,* 265**,** 13933-8.
STETLER-STEVENSON, W. G., KRUTZSCH, H. C. & LIOTTA, L. A. 1989. Tissue inhibitor of metalloproteinase (TIMP-2). A new member of the metalloproteinase inhibitor family. *The Journal of biological chemistry,* 264**,** 17374-8.
STIRLING, D. P., KHADARAHMI, K., LIU, J., MCPHAIL, L. T., MCBRIDE, C. B., STEEVES, J. D., RAMER, M. S. & TETZLAFF, W. 2004. Minocycline treatment reduces delayed oligodendrocyte death, attenuates axonal dieback, and improves functional outcome after spinal cord injury. *Journal of Neuroscience,* 24, 2182-2190.
STOCKHAMMER, G., OBWEGESER, A., KOSTRON, H., SCHUMACHER, P., MUIGG, A., FELBER, S., MAIER, H., SLAVC, I., GUNSIIUS, E. & GASTI, G. 2000. Vascular endothelial growth factor (VEGF) is elevated in brain tumor cysts and correlates with tumor progression. *Acta Neuropathologica,* 100, 101-5.
STOKES, B. T. & JAKEMAN, L. B. 2002. Experimental modelling of human spinal cord injury: a model that crosses the species barrier and mimics the spectrum of human cytopathology. *Spinal cord,* 40**,** 101-9.
STOKES, B. T., NOYES, D. H. & BEHRMANN, D. L. 1992. An electromechanical spinal injury technique with dynamic sensitivity. *Journal of neurotrauma,* 9**,** 187-95.
STRAUSS, D. J., DEVIVO, M. J., PACULDO, D. R. & SHAVELLE, R. M. 2006. Trends in life expectancy after spinal cord injury. *Archives of physical medicine and rehabilitation,* 87**,** 1079-85.
STRONCEK, J. D. & REICHERT, W. M. 2008. Healing in different tissue types. In: Reichert WM, editor. Indwelling neural implants: strategies for contending with

the in vivo enviornment. *Boca Raton (FL): CRC Press*, Chapter 1. Available from: http://www.ncbi.nlm.nih.gov/books/NBK3938.
STRYDOM, D. J., FETT, J. W., LOBB, R. R., ALDERMAN, E. M., BETHUNE, J. L., RIORDAN, J. F. & VALLEE, B. L. 1985. Amino acid sequence of human tumor derived angiogenin. *Biochemistry,* 24**,** 5486-94.
SUBRAMANIAN, V., CRABTREE, B. & ACHARYA, K. R. 2008. Human angiogenin is a neuroprotective factor and amyotrophic lateral sclerosis associated angiogenin variants affect neurite extension/pathfinding and survival of motor neurons. *Human molecular genetics,* 17**,** 130-49.
SUBRAMANIAN, V. & FENG, Y. 2007. A new role for angiogenin in neurite growth and pathfinding: implications for amyotrophic lateral sclerosis. *Human molecular genetics,* 16**,** 1445-53.
SUIDAN, G. L., BRILL, A., DE MEYER, S. F., VOORHEES, J. R., CIFUNI, S. M., CABRAL, J. E. & WAGNER, D. D. 2013. Endothelial von Willebrand factor promotes blood-brain barrier flexibility and provides protection from hypoxia and seizures in mice. *Arteriosclerosis, thrombosis, and vascular biology,* 33**,** 2112-20.
SULIK, A. & CHYCZEWSKI, L. 2008. Immunohistochemical analysis of MMP-9, MMP-2 and TIMP-1, TIMP-2 expression in the central nervous system following infection with viral and bacterial meningitis. *Folia histochemica et cytobiologica / Polish Academy of Sciences, Polish Histochemical and Cytochemical Society,* 46**,** 437-42.
SUME, S. S., KANTARCI, A., LEE, A., HASTURK, H. & TRACKMAN, P. C. 2010. Epithelial to mesenchymal transition in gingival overgrowth. *The American journal of pathology,* 177, 208-18.
SUNAMI, E., TSUNO, N., OSADA, T., SAITO, S., KITAYAMA, J., TOMOZAWA, S., TSURUO, T., SHIBATA, Y., MUTO, T. & NAGAWA, H. 2000. MMP-1 is a prognostic marker for hematogenous metastasis of colorectal cancer. *The oncologist,* 5**,** 108-14.
SUNDBERG, C., KOWANETZ, M., BROWN, L. F., DETMAR, M. & DVORAK, H. F. 2002. Stable expression of angiopoietin-1 and other markers by cultured pericytes: phenotypic similarities to a subpopulation of cells in maturing vessels during later stages of angiogenesis in vivo. *Laboratory investigation; a journal of technical methods and pathology,* 82**,** 387-401.
SUNDBERG, L. M., HERRERA, J. J. & NARAYANA, P. A. 2011. Effect of vascular endothelial growth factor treatment in experimental traumatic spinal cord injury: in vivo longitudinal assessment. *Journal of neurotrauma,* 28**,** 565-78.
SUNDERKOTTER, C., STEINBRINK, K., GOEBELER, M., BHARDWAJ, R. & SORG, C. 1994. Macrophages and angiogenesis. *Journal of leukocyte biology,* 55, 410-22.
SUTTERWALA, F. S., NOEL, G. J., CLYNES, R. & MOSSER D. M. 1997. Selective suppression of interleukin-12 induction after macrophage receptor ligation. *Journal of Experimental Medicine,* 185, 1997-1985.
SUTTERWALA, F. S., NOEL, G. J., CLYNES, R. & MOSSER D. M. 1998. Reversal of proinflammatory responses by ligating macrophage Fcgamma receptor type I. *Journal of Experimental Medicine,* 188, 217-222.
SUZUKI, S. & NAITOH, Y. 1990. Amino acid sequence of a novel integrin beta 4 subunit and primary expression of the mRNA in epithelial cells. *The EMBO journal,* 9**,** 757-63.

SWIFT, M. E., KLEINMAN, H. K. & DIPIETRO, L. A. 1999. Impaired wound repair and delayed angiogenesis in aged mice. *Laboratory investigation; a journal of technical methods and pathology,* 79**,** 1479-87.

SYED, Y. A., HAND, E., MOBIUS, W., ZHAO, C., HOFER, M., NAVE, K. A. & KOTTER, M. R. 2011. Inhibition of CNS remyelination by the presence of semaphorin 3A. *The Journal of neuroscience : the official journal of the Society for Neuroscience,* 31**,** 3719-28.

TACHIBANA, T., NOGUCHI, K. & RUDA, M. A. 2002. Analysis of gene expression following spinal cord injury in rat using complementary DNA microarray. *Neuroscience letters,* 327**,** 133-7.

TAGUCHI, T., et al., 2005. Muscular mechanical hyperalgesia revealed by behavioural pain test and c-Fos expression in the spinal dorsal horn after eccentric contraction in rats. *The Journal of physiology*. 564**,** 259-68.

TALAC, R., FRIEDMAN, J. A., MOORE, M. J., LU, L., JABBARI, E., WINDEBANK, A. J., CURRIER, B. L. & YASZEMSKI, M. J. 2004. Animal models of spinal cord injury for evaluation of tissue engineering treatment strategies.

TAMAGNONE, L., ARTIGIANI, S., CHEN, H., HE, Z., MING, G. I., SONG, H., CHEDOTAL, A., WINBERG, M. L., GOODMAN, C. S., POO, M., TESSIER-LAVIGNE, M. & COMOGLIO, P. M. 1999. Plexins are a large family of receptors for transmembrane, secreted, and GPI-anchored semaphorins in vertebrates. *Cell,* 99**,** 71-80.

TAN, Y., MENG, H. & TENG, F. 2010. Effect of miRNA interference to AnnexinA3 gene on growth of human gallbladder cencer cells. *China Hepatobiliary Surgery,* 16**,** 3.

TASSONE, E., MARAN, C., MASOLA, V., BARDASCHIA, A., GARBISA, S. & ONISTO, M. 2011. Antidepressant hyperforin up-regulates VEGF in CNS tumour cells. *Pharmalogical Research,* 63, 37-43.

TENG, Y. D., MOCCHETTI, I. & WRATHALL, J. R. 1998. Basic and acidic fibroblast growth factors protect spinal motor neurones in vivo after experimental spinal cord injury. *The European journal of neuroscience,* 10**,** 798-802.

THOMAS, M. & AUGUSTIN, H. G. 2009. The role of the Angiopoietins in vascular morphogenesis. *Angiogenesis,* 12**,** 125-37.

THRON, A. 1988. Vascular anatomy of the spinal cord: Neurological investigations and clinical syndromes. New York: Springer-Verlag Wein.

THURET, S., MOON, L. D. & GAGE, F. H. 2006. Therapeutic interventions after spinal cord injury. *Nature reviews. Neuroscience,* 7**,** 628-43.

TORRES, D., BAUSO TOSELLI, L., VECCHI, E., LEIGUARDA, R., DOCTOROVICH, D., MERELLO, M., GUEVARA, J. & NOGUES, M. 1993. [Spinal arachnoiditis as a complication of peridural anesthesia]. *Medicina,* 53, 391-6.

TURNER, J. A., CARDENAS, D. D., WARMS, C. A. & MCCLELLAN, C. B. 2001. Chronic pain associated with spinal cord injuries: a community survey. *Archives of physical medicine and rehabilitation,* 82**,** 501-9.

THURSTON, G., RUDGE, J. S., IOFFE, E., ZHOU, H., ROSS, L., CROLL, S. D., GLAZER, N., HOLASH, J., MCDONALD, D. M. & YANCOPOULOS, G. D. 2000. Angiopoietin-1 protects the adult vasculature against plasma leakage. *Nature medicine,* 6**,** 460-3.

THURSTON, G., WANG, Q., BAFFERT, F., RUDGE, J., PAPADOPOULOS, N., JEAN-GUILLAUME, D., WIEGAND, S., YANCOPOULOS, G. D. & MCDONALD, D. M. 2005. Angiopoietin 1 causes vessel enlargement, without

angiogenic sprouting, during a critical developmental period. *Development (Cambridge, England),* 132**,** 3317-26.
TSUJI, T., SUN, Y., KISHIMOTO, K., OLSON, K. A., LIU, S., HIRUKAWA, S. & HU, G. F. 2005. Angiogenin is translocated to the nucleus of HeLa cells and is involved in ribosomal RNA transcription and cell proliferation. *Cancer research,* 65**,** 1352-60.
TYOR, W. R., AVGEROPOULOS, N., OHLANDT, G. & HOGAN, E. L. 2002. Treatment of spinal cord impact injury in the rat with transforming growth factor-beta. *Journal of the neurological sciences,* 200**,** 33-41.
UBERTI, D., CENINI, G., BONINI, S. A., BARCIKOWSKA, M., STYCZYNSKA, M., SZYBINSKA, A. & MEMO, M. 2010. Increased CD44 gene expression in lymphocytes derived from Alzheimer disease patients. *Neuro-degenerative diseases,* 7**,** 143-7.
UNSICKER, K., FLANDERS, K. C., CISSEL, D. S., LAFYATIS, R. & SPORN, M. B. 1991. Transforming growth factor beta isoforms in the adult rat central and peripheral nervous system. *Neuroscience,* 44**,** 613-25.
URSO, M. L., CHEN, Y. W., SCRIMGEOUR, A. G., LEE, P. C., LEE, K. F. & CLARKSON, P. M. 2007. Alterations in mRNA expression and protein products following spinal cord injury in humans. *The Journal of physiology,* 579**,** 877-92.
VALABLE, S., MONTANER, J., BELLAIL, A., BEREZOWSKI, V., BRILLAULT, J., CECCHELLI, R., DIVOUX, D., MACKENZIE, E. T., BERNAUDIN, M., ROUSSEL, S. & PETIT, E. 2005. VEGF-induced BBB permeability is associated with an MMP-9 activity increase in cerebral ischemia: both effects decreased by Ang-1. *Journal of cerebral blood flow and metabolism : official journal of the International Society of Cerebral Blood Flow and Metabolism,* 25**,** 1491-504.
VALENTE, P., FASSINA, G., MELCHIORI, A., MASIELLO, L., CILLI, M., VACCA, A., ONISTO, M., SANTI, L., STETLER-STEVENSON, W. G. & ALBINI, A. 1998. TIMP-2 over-expression reduces invasion and angiogenesis and protects B16F10 melanoma cells from apoptosis. *International journal of cancer. Journal international du cancer,* 75**,** 246-53.
VALENZUELA, D. M., GRIFFITHS, J. A., ROJAS, J., ALDRICH, T. H., JONES, P. F., ZHOU, H., MCCLAIN, J., COPELAND, N. G., GILBERT, D. J., JENKINS, N. A., HUANG, T., PAPADOPOULOS, N., MAISONPIERRE, P. C., DAVIS, S. & YANCOPOULOS, G. D. 1999. Angiopoietins 3 and 4: diverging gene counterparts in mice and humans. *Proceedings of the National Academy of Sciences of the United States of America,* 96**,** 1904-9.
VAN GALEN, K. P., TUINENBURG, A., SMEETS, E. M. & SCHUTGENS, R. E. 2012. Von Willebrand factor deficiency and atherosclerosis. *Blood reviews,* 26**,** 189-96.
VAN NEERVEN, S., JOOSTEN, E. A., BROOK, G. A., LAMBERT, C. A., MEY, J., WEIS, J., MARCUS, M. A., STEINBUSCH, H. W., VAN KLEEF, M., PATIJN, J. & DEUMENS, R. 2010. Repetitive intrathecal VEGF(165) treatment has limited therapeutic effects after spinal cord injury in the rat. *Journal of neurotrauma,* 27**,** 1781-91.
VASAK, M. 2005. Advances in metallothionein structure and functions. *Journal of trace elements in medicine and biology : organ of the Society for Minerals and Trace Elements,* 19**,** 13-7.

VAQUERO, J., ZURITA, M., DE OYA, S. & COCA, S. 1999. Vascular endothelial growth/permeability factor in spinal cord injury. *Journal of neurosurgery,* 90**,** 220-3.

VELARDO, M. J., BURGER, C., WILLIAMS, P. R., BAKER, H. V., LOPEZ, M. C., MARECI, T. H., WHITE, T. E., MUZYCZKA, N. & REIER, P. J. 2004. Patterns of gene expression reveal a temporally orchestrated wound healing response in the injured spinal cord. *The Journal of neuroscience : the official journal of the Society for Neuroscience,* 24**,** 8562-76.

VINK, R., NOBLE, L. J., KNOBLACH, S. M., BENDALL, M. R. & FADEN, A. L. 1989. Metabolic changes in rabbit spinal cord after trauma: magnetic resonance spectroscopy studies. *Annals of Neurology*, 25, 26-31.

VIVIEN, D., BER4NAUDIN, M., BUISSON, A., DIVOUX, D., MACKENZIE, E. T. & NOUVELOT, A. 1998. Evidence of type I and type II transforming growth factor-beta receptors in central nervous tissues: changes induced by focal cerebral ischemia. *Journal of Neurochemistry,* 70, 2296-304.

VOURC'H, P. & ANDRES, C. 2004. Oligodendrocyte myelin glycoprotein (OMgp): evolution, structure and function. *Brain research. Brain research reviews,* 45**,** 115-24.

WALLQUIST, W., PATARROYO, M., THAMS, S., CARLSTEDT, T., STARK, B. & CULLHEIM, S. 2002. *Laminin chains in rat and human peripheral nerve: dirtibution and regulation during development and fater axonal injury*. Journal of Comparative Neurology, 454, 284-293.

WAMIL, A. W., WAMIL, B. D. & HELLERQVIST, C. G. 1998. CM101-mediated recovery of walking ability in adult mice paralyzed by spinal cord injury. *Proceedings of the National Academy of Sciences of the United States of America,* 95**,** 13188-93.

WANG, H. & KEISER, J. A. 1998. Vascular endothelial growth factor upregulates the expression of matrix metalloproteinases in vascular smooth muscle cells: role of flt-1. *Circulation research,* 83**,** 832-40.

WANG, G. & THOMPSON, S. M. 2008. Maladaptive homeostatic plasticity in a rodent model of central pain syndrome: thalamic hyperexcitability after spinothalamic tract lesions. *The Journal of neuroscience : the official journal of the Society for Neuroscience,* 28**,** 11959-69.

WANG, G. S., CHANG, N. C., WU, S. C. & CHANG, A. C. 2002. Regulated expression of alpha2B adrenoceptor during development. *Developmental dynamics : an official publication of the American Association of Anatomists,* 225**,** 142-52.

WANG, R., MACMILLAN, L. B., FREMEAU, R. T., JR., MAGNUSON, M. A., LINDNER, J. & LIMBIRD, L. E. 1996. Expression of alpha 2-adrenergic receptor subtypes in the mouse brain: evaluation of spatial and temporal information imparted by 3 kb of 5' regulatory sequence for the alpha 2A AR-receptor gene in transgenic animals. *Neuroscience,* 74**,** 199-218.

WANG, X., CHEN, W., LIU, W., WU, J., SHAO, Y. & ZHANG, X. 2009. The role of thrombospondin-1 and transforming growth factor-beta after spinal cord injury in the rat. *Journal of clinical neuroscience : official journal of the Neurosurgical Society of Australasia,* 16**,** 818-21.

WANG, X., LUO, C. & LI, W. 2013. Effect of infliximab combined with methylprednisolone on expressions of NF-kappaB, TRADD and FADD in rat acute spinal cord injury. *Spine,* 38, E861-E8E9.

WARD, N. L. & LAMANNA, J. C. 2004. The neurovascular unit and its growth factors: coordinated response in the vascular and nervous systems. *Neurological research,* 26**,** 870-83.
WATANABE, K., NAKAMURA, M., IWANAMI, A., FUJITA, Y., KANEMURA, Y., TOYAMA, Y. & OKANO, H. 2004. Comparison between fetal spinal-cord- and forebrain-derived neural stem/progenitor cells as a source of transplantation for spinal cord injury. *Developmental neuroscience,* 26**,** 275-87.
WATANABE, K., NAKAMURA, M., OKANO, H. & TOYAMA, Y. 2007. Establishment of three-dimensional culture of neural stem/progenitor cells in collagen Type-1 Gel. *Restorative neurology and neuroscience,* 25**,** 109-17.
WATANABE, T., ITO, Y., SATO, A., HOSONO, T., NIIMI, S., ARIGA, T. & SEKI, T. 2012. Annexin A3 as a negative regulator of adipocyte differentiation. *Journal of biochemistry,* 152**,** 355-63.
WATSON, B. D., PRADO, R., DIETRICH, W. D., GINSBERG, M. D. & GREEN, B. A. 1986. Photochemically induced spinal cord injury in the rat. *Brain research,* 367**,** 296-300.
WEI, Y. T., HE, Y., XU, C. L., WANG, Y., LIU, B. F., WANG, X. M., SUN, X. D., CUI, F. Z. & XU, Q. Y. 2010. Hyaluronic acid hydrogel modified with nogo-66 receptor antibody and poly-L-lysine to promote axon regrowth after spinal cord injury. *Journal of biomedical materials research. Part B, Applied biomaterials,* 95**,** 110-7.
WHETSTONE, W. D., HSU, J.-Y. C., EISENBERG, M., WERB, Z. & NOBLE-HAEUSSLEIN, L. J. 2003a. Blood-spinal cord barrier after spinal cord injury: relation to revascularization and wound healing. *Journal of neuroscience research,* 74**,** 227-39.
WHETSTONE, W. D., HSU, J. Y., EISENBERG, M., WERB, Z. & NOBLE-HAEUSSLEIN, L. J. 2003b. Blood-spinal cord barrier after spinal cord injury: relation to revascularization and wound healing. *Journal of neuroscience research,* 74**,** 227-39.
WIDENFALK, J., LIPSON, A., JUBRAN, M., HOFSTETTER, C., EBENDAL, T., CAO, Y. & OLSON, L. 2003. Vascular endothelial growth factor improves functional outcome and decreases secondary degeneration in experimental spinal cord contusion injury. *Neuroscience,* 120**,** 951-60.
WILCOX, J. N. & DERYNCK, R. 1988. Localization of cells synthesizing transforming growth factor-alpha mRNA in the mouse brain. *The Journal of neuroscience : the official journal of the Society for Neuroscience,* 8**,** 1901-4.
WILLIAMS, K. C., ZHAO, R. W., UENO, K. & HICKEY, W. F. 1996. PECAM-1 (CD31) expression in the central nervous system and its role in experimental allergic encephalomyelitis in the rat. *Journal of neuroscience research,* 45**,** 747-57.
WILSON, D. J. 2004. Soft tissue and joint infection. *European radiology,* 14 Suppl 3, E64-71.
WILSON, J. G., ROTH, C. B. & WARKANY, J. 1953. An analysis of the syndrome of malformations induced by maternal vitamin A deficiency. Effects of restoration of vitamin A at various times during gestation. *The American journal of anatomy,* 92**,** 189-217.
WINKLER, C. W., FOSTER, S. C., MATSUMOTO, S. G., PRESTON, M. A., XING, R., BEBO, B. F., BANINE, F., BERNY-LANG, M. A., ITAKURA, A., MCCARTY, O. J. & SHERMAN, L. S. 2012. Hyaluronan anchored to activated CD44 on central nervous system vascular endothelial cells promotes

lymphocyte extravasation in experimental autoimmune encephalomyelitis. *The Journal of biological chemistry,* 287**,** 33237-51.
WIRANOWSKA, M., LADD, S., SMITH, S. R. & GOTTSCHALL, P. E. 2006. CD44 adhesion molecule and neuro-glial proteoglycan NG2 as invasive markers of glioma. *Brain cell biology,* 35**,** 159-72.
WONG, A. L., HAROON, Z. A., WERNER, S., DEWHIRST, M. W., GREENBERG, C. S. & PETERS, K. G. 1997. Tie2 expression and phosphorylation in angiogenic and quiescent adult tissues. *Circulation research,* 81**,** 567-74.
WONG, L. F., YIP, P. K., BATTAGLIA, A., GRIST, J., CORCORAN, J., MADEN, M., AZZOUZ, M., KINGSMAN, S. M., KINGSMAN, A. J., MAZARAKIS, N. D. & MCMAHON, S. B. 2006. Retinoic acid receptor beta2 promotes functional regeneration of sensory axons in the spinal cord. *Nature neuroscience,* 9**,** 243-50.
WOZNY, W., SCHROER, K., SCHWALL, G. P., POZNANOVIC, S., STEGMANN, W., DIETZ, K., ROGATSCH, H., SCHAEFER, G., HUEBL, H., KLOCKER, H., SCHRATTENHOLZ, A. & CAHILL, M. A. 2007. Differential radioactive quantification of protein abundance ratios between benign and malignant prostate tissues: cancer association of annexin A3. *Proteomics,* 7**,** 313-22.
WU, D., YU, W., KISHIKAWA, H., FOLKERTH, R. D., IAFRATE, A. J., SHEN, Y., XIN, W., SIMS, K. & HU, G. F. 2007. Angiogenin loss-of-function mutations in amyotrophic lateral sclerosis. *Annals of neurology,* 62**,** 609-17.
WU, E., PALMER, N., TIAN, Z., MOSEMAN, A. P., GALDZICKI, M., WANG, X., BERGER, B., ZHANG, H. & KOHANE, I. S. 2008. Comprehensive dissection of PDGF-PDGFR signaling pathways in PDGFR genetically defined cells. *PloS one,* 3**,** e3794.
WU, J. C., HUANG, W. C., CHEN, Y. C., TU, T. H., TSAI, Y. A., HUANG, S. F., HUANG, H. C. & CHENG, H. 2011. Acidic fibroblast growth factor for repair of human spinal cord injury: a clinical trial. *Journal of neurosurgery. Spine,* 15**,** 216-27.
WU, L., SHEN, Y., LIU, X., MA, X., XI, B., MI, J., LINDPAINTNER, K., TAN, X. & WANG, X. 2009. The 1425G/A SNP in PRKCH is associated with ischemic stroke and cerebral hemorrhage in a Chinese population. *Stroke; a journal of cerebral circulation,* 40**,** 2973-6.
WU, N., LIU, S., GUO, C., HOU, Z. & SUN, M. Z. 2013. The role of annexin A3 playing in cancers. *Clinical & translational oncology : official publication of the Federation of Spanish Oncology Societies and of the National Cancer Institute of Mexico,* 15**,** 106-10.
XIAO, L., MA, Z. L., LI, X., LIN, Q. X., QUE, H. P. & LIU, S. J. 2005. cDNA microarray analysis of spinal cord injury and regeneration related genes in rat. *Sheng li xue bao : [Acta physiologica Sinica],* 57**,** 705-13.
XIAOWEI, H., NINGHUI, Z., WEI, X., YIPING, T. & LINFENG, X. 2006. The experimental study of hypoxia-inducible factor-1alpha and its target genes in spinal cord injury. *Spinal cord,* 44**,** 35-43.
XIE, Y.-Q., FU, D., HE, Z.-H. & TAN, Q.-D. 2013. Prognostic value of annexin a3 in human colorectal cancer and its correlation with hypoxia-inducible factor-1aplha. 4.
XU, J., KIM, G. M., AHMED, S. H., YAN, P., XU, X. M. & HSU, C. Y. 2001a. Glucocorticoid receptor-mediated suppression of activator protein-1 activation and matrix metalloproteinase expression after spinal cord injury. *The Journal of neuroscience : the official journal of the Society for Neuroscience,* 21**,** 92-7.

XU, Z., MONTI, D. M. & HU, G. 2001b. Angiogenin activates human umbilical artery smooth muscle cells. *Biochemical and biophysical research communications,* 285**,** 909-14.
YAN, X., YIN, J., YAO, H., MAO, N., YANG, Y. & PAN, L. 2010. Increased expression of annexin A3 is a mechanism of platinum resistance in ovarian cancer. *Cancer research,* 70**,** 1616-24.
YANG-FENG, T. L., XUE, F. Y., ZHONG, W. W., COTECCHIA, S., FRIELLE, T., CARON, M. G., LEFKOWITZ, R. J. & FRANCKE, U. 1990. Chromosomal organization of adrenergic receptor genes. *Proceedings of the National Academy of Sciences of the United States of America,* 87**,** 1516-20.
YANG, G. Y., BETZ, A. L., CHENEVERT, T. L., BRUNBERG, J. A. & HOFF, J. T. 1994. Experimental intracerebral hemorrhage: relationship between brain edema, blood flow, and blood-brain barrier permeability in rats. *Journal of neurosurgery,* 81**,** 93-102.
YANG, H., CHENG, X. P., LI, J. W., YAO, Q. & JU, G. 2009. De-differentiation response of cultured astrocytes to injury induced by scratch or conditioned culture medium of scratch-insulted astrocytes. *Cellular and molecular neurobiology,* 29**,** 455-73.
YANG, J. T., LEE, T. H., LEE, I. N., CHUNG, C. Y., KUO, C. H. & WENG, H. H. 2011. Dexamethasone inhibits ICAM-1 and MMP-9 expression and reduces brain edema in intracerebral hemorrhagic rats. *Acta neurochirurgica,* 153**,** 2197-203.
YAO, H., DUAN, M., YANG, L. & BUCH, S. 2012. Platelet-derived growth factor-BB restores human immunodeficiency virus Tat-cocaine-mediated impairment of neurogenesis: role of TRPC1 channels. *The Journal of neuroscience : the official journal of the Society for Neuroscience,* 32**,** 9835-47.
YATES, S., et al., 2013. Dstfunction of the mTOR pathway is a rask factor for Alzheimer's disease. *Acta Neuropathologica Communications*. 1.
YAZDANI, U. & TERMAN, J. R. 2006. The semaphorins. *Genome biology,* 7**,** 211.
YEZIERSKI, R. P., LIU, S., RUENES, G. L., KAJANDER, K. J. & BREWER, K. L. 1998. Excitotoxic spinal cord injury: behavioral and morphological characteristics of a central pain model. *Pain,* 75**,** 141-55.
YISHENG, W., FUYING, Z., LIMIN, W., JUNWEI, L., GUOFU, P. & WEIDONG, W. 2007. First aid and treatment for cervical spinal cord injury with fracture and dislocation. *Indian journal of orthopaedics,* 41**,** 300-4.
YIN, J., YAN, X., YAO, X., ZHANG, Y., SHAN, Y., MAO, N., YANG, Y. & PAN, L. 2012. Secretion of annexin A3 from ovarian cancer cells and its association with platinum resistance in ovarian cancer patients. *Journal of cellular and molecular medicine,* 16**,** 337-48.
YIP, P. K., WONG, L.-F., PATTINSON, D., BATTAGLIA, A., GRIST, J., BRADBURY, E. J., MADEN, M., MCMAHON, S. B. & MAZARAKIS, N. D. 2006. Lentiviral vector expressing retinoic acid receptor beta2 promotes recovery of function after corticospinal tract injury in the adult rat spinal cord. *Human molecular genetics,* 15**,** 3107-18.
YOLES, E., WHEELER, L. A. & SCHWARTZ, M. 1999. Alpha2-adrenoreceptor agonists are neuroprotective in a rat model of optic nerve degeneration. *Investigative ophthalmology & visual science,* 40**,** 65-73.
YONG, V. W. 2005. Metalloproteinases: mediators of pathology and regeneration in the CNS. *Nature reviews. Neuroscience,* 6**,** 931-44.

YOO, P. S., MULKEEN, A. L. & CHA, C. H. 2006. Post-transcriptional regulation of vascular endothelial growth factor: implications for tumor angiogenesis. *World journal of gastroenterology : WJG,* 12**,** 4937-42.

YOSHII, S., ITO, S., SHIMA, M., TANIGUCHI, A. & AKAGI, M. 2009. Functional restoration of rabbit spinal cord using collagen-filament scaffold. *Journal of tissue engineering and regenerative medicine,* 3**,** 19-25.

YOUNG, W., FLAMM, E. S., DEMOPOULOS, H. B., TOMASULA, J. J. & DECRESCITO, V. 1981. Effect of naloxone on posttraumatic ischemia in experimental spinal contusion. *Journal of neurosurgery,* 55**,** 209-19.

REN, Y. & YOUNG, W. 2013. Mangaing inflammation after spinal cord injury through manipulation of macrophage function. *Neural Plasticity,* 13.

YU, D., LU, G., CAO, Y., LI, G., ZHI, X. & FAN, Z. 2011. [Effects of bone marrow mesenchymal stem cells transplantation on expression of vascular endothelial growth factor gene and angiogenesis after spinal cord injury in rats]. *Zhongguo xiu fu chong jian wai ke za zhi = Zhongguo xiufu chongjian waike zazhi = Chinese journal of reparative and reconstructive surgery,* 25**,** 837-41.

YU, R., GAO, L., JIANG, S., GUAN, P. & MAO, B. 2001. Association of HIF-1alpha expression and cell apoptosis after traumatic brain injury in the rat. *Chinese journal of traumatology = Zhonghua chuang shang za zhi / Chinese Medical Association,* 4**,** 218-21.

YU, Y. C., YANG, P. M., CHUAH, Q. Y., HUANG, Y. H., PENG, C. W., LEE, Y. J. & CHIU, S. J. 2013. Radiation-induced senescence in securin-deficient cancer cells promotes cell invasion involving the IL-6/STAT3 and PDGF-BB/PDGFR pathways. *Scientific reports,* 3**,** 1675.

ZACHAREK, A., CHEN, J., CUI, X., LI, A., LI, Y., ROBERTS, C., FENG, Y., GAO, Q. & CHOPP, M. 2007. Angiopoietin1/Tie2 and VEGF/Flk1 induced by MSC treatment amplifies angiogenesis and vascular stabilization after stroke. *Journal of cerebral blood flow and metabolism : official journal of the International Society of Cerebral Blood Flow and Metabolism,* 27**,** 1684-91.

ZEILIG, G., ENOSH, S., RUBIN-ASHER, D., LEHR, B. & DEFRIN, R. 2011. The nature and course of sensory changes following spinal cord injury: predictive properties and implications on the mechanism of central pain. *Brain : a journal of neurology*.

ZHANG, F. X. & HUTCHINS, J. B. 1997. Protein phosphorylation in response to PDGF stimulation in cultured neurons and astrocytes. *Brain research. Developmental brain research,* 99**,** 216-25.

ZHANG, H., CHANG, M., HANSEN, C. N., BASSO, D. M. & NOBLE-HAEUSSLEIN, L. J. 2011a. Role of matrix metalloproteinases and therapeutic benefits of their inhibition in spinal cord injury. *Neurotherapeutics : the journal of the American Society for Experimental NeuroTherapeutics,* 8**,** 206-20.

ZHANG, H., TRIVEDI, A., LEE, J. U., LOHELA, M., LEE, S. M., FANDEL, T. M., WERB, Z. & NOBLE-HAEUSSLEIN, L. J. 2011b. Matrix metalloproteinase-9 and stromal cell-derived factor-1 act synergistically to support migration of blood-borne monocytes into the injured spinal cord. *The Journal of neuroscience : the official journal of the Society for Neuroscience,* 31**,** 15894-903.

ZHANG, J., LI, M., WU, Y., FAN, Y., ZHOU, Y., TAN, L., SHAO, Z. & SHI, H. 2011. Methylation of RAR-beta2, RASSF1A, and CDKN2A genes induced by nickel subsulfide and nickel-carcinogenesis in rats. *Biomedical and environmental sciences : BES,* 24**,** 163-71.

ZHANG, X., BO, X., ANDERSON, P. N., LIEBERMAN, A. R. & ZHANG, Y. 2006. Distribution and expression of tissue inhibitors of metalloproteinase in dorsal root entry zone and dorsal column after dorsal root injury. *Journal of neuroscience research,* 84**,** 278-90.

ZHANG, Z. G., ZHANG, L., TSANG, W., SOLTANIAN-ZADEH, H., MORRIS, D., ZHANG, R., GOUSSEV, A., POWERS, C., YEICH, T. & CHOPP, M. 2002. Correlation of VEGF and angiopoietin expression with disruption of blood-brain barrier and angiogenesis after focal cerebral ischemia. *Journal of cerebral blood flow and metabolism : official journal of the International Society of Cerebral Blood Flow and Metabolism,* 22**,** 379-92.

ZHOU, Y., CUI, Z., XIA, X., LIU, C., ZHU, X., CAO, J., WU, Y., ZHOU, L., BEN, Z., SONG, Y., ZHANG, H. & ZHANG, D. 2014. Matrix Metalloproteinase-1 (MMP-1) Expression in Rat Spinal Cord Injury Model. *Cell and Molecular Neurobiology,* 34, 1151-63.

ZHOU, Z., WANG, J., CAO, R., MORITA, H., SOININEN, R., CHAN, K. M., LIU, B., CAO, Y. & TRYGGVASON, K. 2004. Impaired angiogenesis, delayed wound healing and retarded tumor growth in perlecan heparan sulfate-deficient mice. *Cancer research,* 64**,** 4699-702.

ZIMMER, M. B., NANTWI, K. & GOSHGARIAN, H. G. 2007. Effect of spinal cord injury on the respiratory system: basic research and current clinical treatment options. *The journal of spinal cord medicine,* 30**,** 319-30.

ZIMMERMAN, T. S., RATNOFF, O. D. & POWELL, A. E. 1971. Immunologic differentiation of classic hemophilia (factor 8 deficiency) and von Willebrand's dissase, with observations on combined deficiencies of antihemophilic factor and proaccelerin (factor V) and on an acquired circulating anticoagulant against antihemophilic factor. *The Journal of clinical investigation,* 50**,** 244-54.

ZIVIN, J. A. & DEGIROLAMI, U. 1980. Spinal cord infarction: a highly reproducible stroke model. *Stroke; a journal of cerebral circulation,* 11**,** 200-2.

Appendix 1

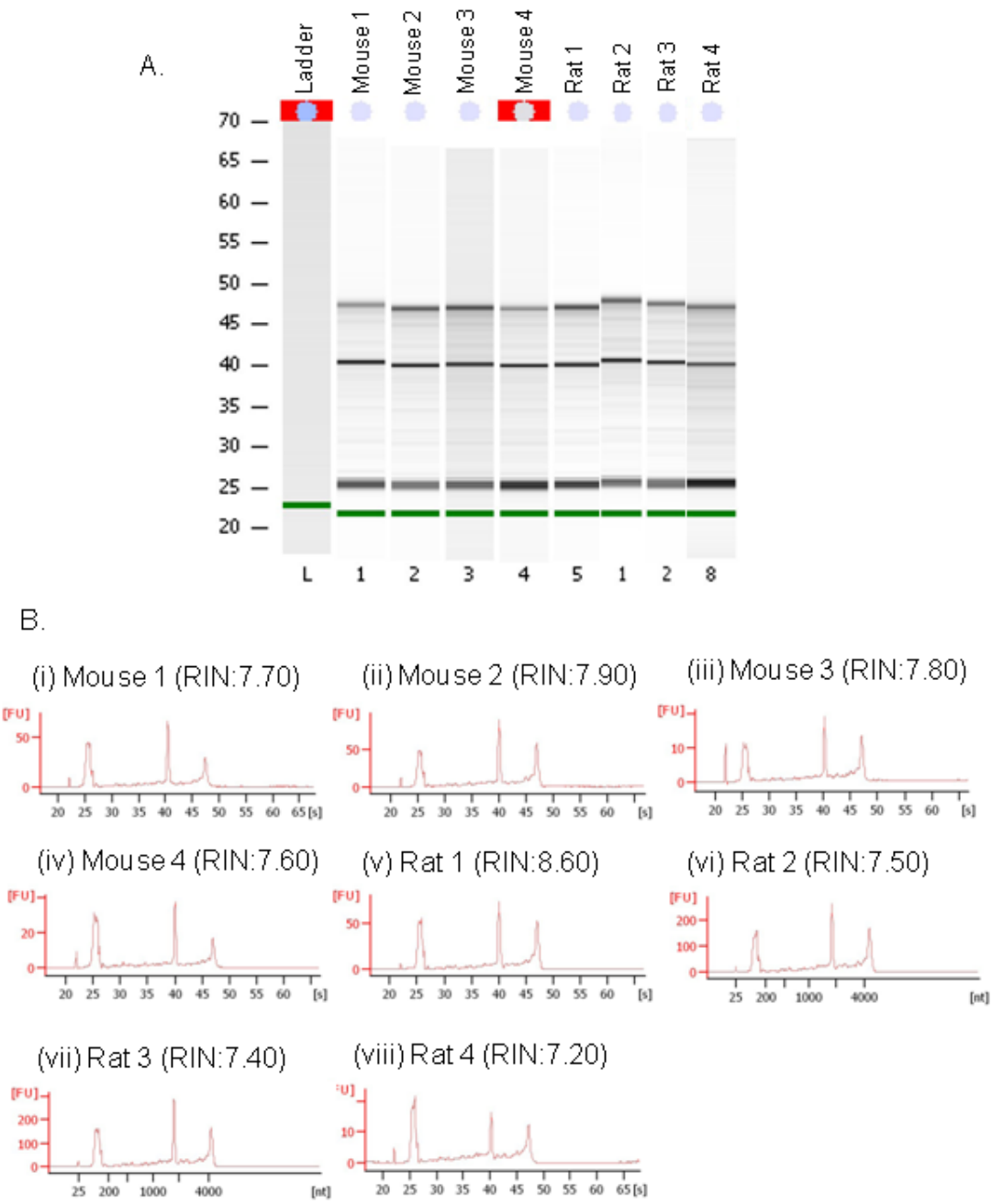

Appendix 1.1 Bioanalyzer (Agilent) analysis to determine the RNA integrity of the control rat and mouse samples extracted using TRIzol Reagent. For microarray analysis RNA integrity (RIN) values needed to be above 7.

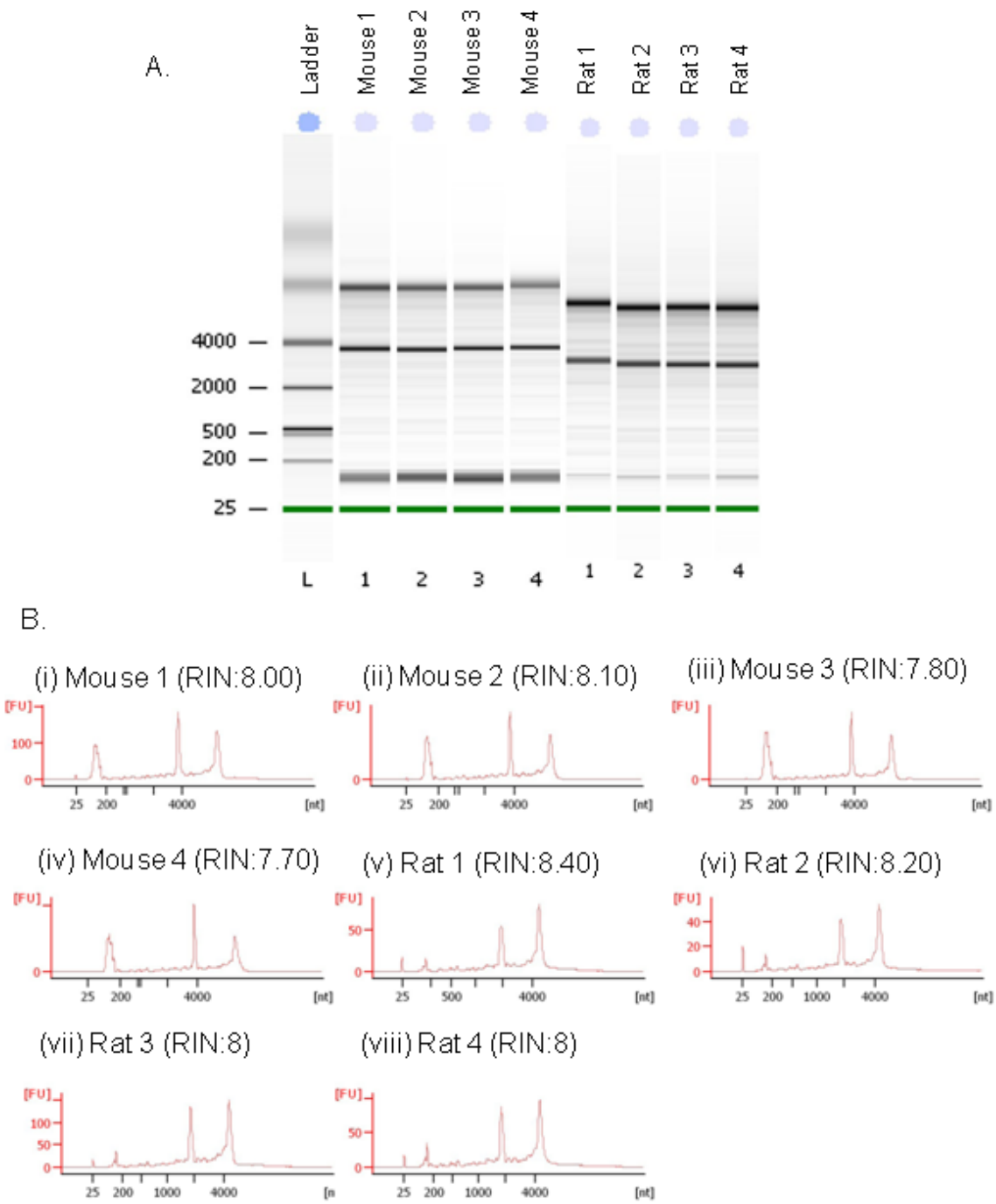

Appendix 1.2 Bioanalyzer (Agilent) analysis to determine the RNA integrity of samples from DC injured rat and mouse spinal cords extracted using TRIzol Reagent. For microarray analysis RNA integrity (RIN) values needed to be above 7.

Appendix 2

Microarray data using one-color labelling reaction on 8 x60k microarray chips on mouse vs. rat after sub-acute spinal cord injury (discs include raw data tables, and tables and information extracted from the raw data).

Appendix 3

Raw microarray data assessed in LIMMA package to show the codes that were used for analysis to show global variation.

```
> library(limma)
> setwd("~/Desktop/Microarray analysis/Both/Rat")
> targets <- readTargets("~/Desktop/Microarray analysis/Both/Rat/targets.txt")
> RG <- read.maimages(targets, path="~/Desktop/Microarray analysis/Both/Rat",
columns = list(G = "gMedianSignal", Gb = "gBGMedianSignal", R =
"gProcessedSignal",
+ Rb = "gIsPosAndSignif"), annotation = c("Row", "Col","FeatureNum",
"ControlType","ProbeName"))
> RG <- backgroundCorrect(RG, method="normexp", offset=16)
> RG$G <- normalizeBetweenArrays(RG$G, method="quantile")
> RG$G <- log2(RG$G)
> E <- new("MAList", list(targets=RG$targets, genes=RG$genes,
source=RG$source, M=RG$Gb, A=RG$G))
> E.avg <- avereps(E, ID=E$genes$ProbeName)
> f <- factor(targets$Condition, levels = unique(targets$Condition))
> design <- model.matrix(~0 + f)
> colnames(design) <- levels(f)
> fit <- lmFit(E.avg$A, design)
> contrast.matrix <- makeContrasts("treated-control", levels=design)
> fit2 <- contrasts.fit(fit, contrast.matrix)
> fit2 <- eBayes(fit2)
> output <- topTable(fit2, adjust="BH", coef="treated-control",
genelist=E.avg$genes, number=80000)
> write.table(output, file="~/Desktop/Microarray analysis/Both/Rat/Rat Mean
treated_vs_control.txt", sep="\t", quote=FALSE)
```